

Mgeni Estuary showing the three main bridges (Connaught Bridge, Athlone Bridge and Ellis Brown Viaduct), the artificial groyne and Beachwood Creek (2003, source: eThek

The Mgeni Estuary
Pre- and Post Inanda Dam Estuarine Dynamics

Neil Tinmouth

School of Geological Sciences
Faculty of Science and Agriculture
University of KwaZulu-Natal
(Westville Campus)

Submitted in fulfilment of the academic requirements for the degree of Master of Science in the
School of Geological Sciences, University of KwaZulu-Natal, Durban
October 2009

As the candidate's supervisor, I agree to the submission of this thesis.

Signed:.....Name:.....Date:.....

Abstract

The funnel-shaped Mgeni Estuary, at the mouth of the fourth largest river along the KwaZulu-Natal coast, discharges into the Indian Ocean in the northern suburbs of Durban. This system is under considerable anthropogenic stress associated with modern development and industrialisation, both adjacent to the estuary and in the catchment area. The construction of Inanda Dam in 1989, immediately upstream of the estuary, is considered to have had an irreversible impact on the system and the estuary and is addressed in this study.

A thorough analysis of available maps, aerial photographs and oblique images from 1860 to 2006, provided a record of the changes in the estuary morphology. The Pre-Inanda Dam period is characterised by the repeated re-establishment of a large central bar after major floods as evident prior to the 1987 flood. The post 1989 Inanda-Dam period, however, is characterised by the deposition of a series of side-attached bars and the development of extensive mudflats.

Sediment distribution results show a definite decrease in grain size compared to the predominant gravel fraction in 1986 towards an estuary dominated by medium to fine sand-sized sediment. A reduction in sediment grain size is also complemented by an increase in carbonate concentration throughout the estuary. This indicates an increase in marine incursion with decreased fluvial flow suggesting a shift from a river dominated estuary to a marine dominated system since the completion of Inanda Dam.

Linked to the finer grained sediment is a higher increased organic and heavy metal concentration. An analysis of the enrichment factor for 9 metals shows that the Mgeni Estuary is significantly contaminated, especially at the head of the estuary. This situation is exacerbated by decreased fluvial flow rates, an increase in the frequency of mouth closures and the reduction in flooding events effectively preventing the removal of contaminants out of the estuary.

Preface

This work was carried out in the School of Geological Sciences, University of KwaZulu-Natal, Durban, from January 2006 to December 2008, under the supervision of Dr. Ron Uken.

This study represents original work by the author. Where use has been made of the work of others it is duly acknowledged in the text.

Declaration 1 – Plagiarism

I, Neil Tinmouth, declare that:

1. The research reported in this thesis, except where otherwise indicated, is my original research.
2. This thesis does not contain other persons' data, pictures, graphs or other information, unless specifically acknowledged as being sourced from other persons.
3. This thesis does not contain other persons' writing, unless specifically acknowledged as being sourced from other researchers. Where other written sources have been quoted, then:
 - a. Their words have been re-written but the general information attributed to them has been referenced
 - b. Where their exact words have been used, then their writing has been placed in italics and inside quotation marks, and referenced.
4. This thesis does not contain text, graphics or tables copied and pasted from the Internet, unless specifically acknowledged, and the source being detailed in the thesis and in the References sections.

Signed:.....

List of Contents

Chapter 1. Introduction	1
Chapter 2. Estuary classification	5
2.1. Definitions.....	5
2.2. Classification systems.....	5
2.2.1. <i>Physiographic classification</i>	5
2.2.2. <i>Classification by tidal range</i>	7
2.2.3. <i>Evolutionary classification</i>	7
<i>Wave-dominated estuaries</i>	9
<i>Tide-dominated estuaries</i>	9
2.2.4. <i>Classification by salinity and stratification structure</i>	12
<i>Highly stratified</i>	12
<i>Partially mixed</i>	13
<i>Well-mixed or vertically homogeneous</i>	13
2.3. Morphological classification of South African estuaries	14
<i>Tide-dominated estuaries</i>	15
<i>River dominated estuaries</i>	15
Chapter 3. Regional setting	16
3.1. Catchment	16
3.2. Mgeni Estuary characteristics	18
3.3. Coastal characteristics.....	18
3.4. Climate hydrology	19
3.5. Catchment geology	20
3.6. Local geology	23
3.7. Geological development of the estuary	24
3.8. Human influences	24
3.9. Previous research on the Mgeni Estuary.....	25

Chapter 4. Historical evolution.....	28
4.1. Introduction.....	28
4.2. Methodology.....	28
4.3. Results.....	29
4.3.1. <i>Holocene evolution of the Mgeni Estuary.....</i>	29
<i>Mid 1800s to 1899 geomorphology.....</i>	31
<i>1900 to 1930.....</i>	32
<i>1931 to 1950.....</i>	34
<i>1951 to 1960.....</i>	34
<i>1961 to 1970.....</i>	35
<i>1971 to 1980.....</i>	35
<i>1981 to 1990.....</i>	38
<i>1991 to 2000.....</i>	42
<i>2001 to 2007.....</i>	42
4.4. Discussion.....	46
Chapter 5. Sedimentology.....	47
5.1. Introduction.....	47
5.2. Methodology.....	47
5.2.1. <i>Malvern Mastersizer 2000 analyzer.....</i>	49
5.2.2. <i>Sieving.....</i>	50
5.2.3. <i>Statistical parameters.....</i>	50
5.2.4. <i>Carbonate content.....</i>	52
5.2.5. <i>Organic content.....</i>	52
5.3. Results.....	53
5.3.1. <i>Particle size distribution.....</i>	53
<i>Gravel fraction.....</i>	53
<i>Sand fraction.....</i>	55
<i>Coarse to very coarse sand.....</i>	55
<i>Medium sand.....</i>	58
<i>Very fine to fine sand.....</i>	60
<i>Mud fraction.....</i>	62

5.3.2. Statistical parameters	67
Mean.....	67
Sorting (φ).....	68
Skewness.....	70
Median.....	70
5.3.3. Carbonate.....	70
5.3.4. Organic content	72
5.4. Discussion and conclusion	75
Chapter 6. Cores	76
6.1. Introduction.....	76
6.2. Methodology	76
6.3. Results.....	79
6.4. Discussion and conclusion.....	83
Chapter 7. Geochemistry	85
7.1. Introduction.....	85
7.2. Methodology	86
7.3. Results.....	88
Arsenic (As)	88
Chromium (Cr)	89
Cobalt (Co).....	91
Copper (Cu).....	92
Lead (Pb).....	94
Nickel (Ni)	95
Tin (Sn).....	97
Vanadium (V).....	98
Zinc (Zn)	98
7.4. Discussion and conclusion.....	102
Chapter 8. Conclusion	103

References	106
Appendix A	118
A.1 Sediment Sample Data.....	119
A.2 2005 versus 2006 Surface Sediment Comparison	125
A.3 Carbonate and Organics: sample distribution map	126
Appendix B	129
B. Core logs	130
Appendix C	155
C.1 Geochemistry	156
C.2 Geochemistry Enrichment Factors.....	157
C.3 Geochemistry - $\text{Fe}_2\text{O}_3/\text{Al}_2\text{O}_3$ Plots for Various Elements.....	158
C.4 Geochemistry – Various Cobalt Plots	163

Acknowledgment

The completion of this work is owed to the assistance of certain organisations and people. These organisations are thanked for input during the project duration in no particular order:

- The University of KwaZulu-Natal
- The Council for Geoscience – particularly Durban-based Marine Geoscience Unit and staff

In addition the following individuals are thanked for valuable input and assistance throughout the project:

- Dr Ron Uken - for his supervision, guidance and encouragement throughout the project.
- Mr Rio Leuci – for his supervision and assistance in the field.
- Mr Andrew Richardson – for risking life and limb to obtain those ever important samples.
- Dr Andy Green – for his patience and assistance in the field as well as sharing his knowledge of estuarine systems.
- Mr Wade Kidwell, Mr Andrew Holmwood, Mr Paul Young, Mr Charl Bosman and Ms Hayley Cawthra - for their assistance in the field.
- Dr Rochelle Wigley – her assistance in editing and research.
- Ms Dianne Vellinga – for her assistance, encouragement and support.
- And to my mother for her patience, support, and encouragement throughout the project.

CHAPTER 1

Introduction

Estuaries are coastal bodies of water where seawater mixes with fresh water resulting in diverse and productive ecosystems, essential for the health and well being of the coastal and marine environment. These systems are environmentally vulnerable, especially in developed urbanized areas where additional anthropogenic pressure is imposed on the system in various forms. This results in the need for ongoing monitoring and management of estuarine systems to ensure the optimal functioning and survival of these dynamic environments (Miller, 2000; Neal *et al.*, 2003; Cox *et al.*, 2004; Ducrotoy and Elliott, 2006; Pacheco *et al.*, 2007; Estuaries Management and Planning (2005).

The Mgeni River (also referred to as Umgeni, uMgeni or Mngeni River) with a total catchment area of 4,500 km², is the fourth largest of the 67 rivers that discharge into the Indian Ocean along the coast of KwaZulu-Natal (Orme, 1976; Begg, 1978; Badenhorst *et al.*, 1989). The Mgeni River originates in the foothills of the Drakensberg, flows some 250 km through four dams and several industrial areas before it discharges 5 km north of the Durban city centre (Figure 1.1 and Figure 1.2).

The intrinsic value of South African estuaries was recognized by the National Water Act 36 of 1998. Concerns regarding flooding, and sea-level rise in particular, resulted in additional attention concentrated on the Mgeni Estuary by the surrounding property owners, resulting in the initiation of numerous studies by various authors (Badenhorst *et al.*, 1989; Cooper, 1991; Moleko, 1998; Njoya, 2002).

Most research on the Mgeni Estuary was undertaken prior to the 1987 flood (Simpson *et al.*, 1972; Begg, 1978; Begg, 1984; Steinke and Charles, 1986; Cooper, 1986) and the completion of Inanda Dam in 1989. The need for a updated definitive study was indentified in order to understand and quantify any significant changes that may have occurred within the estuary, following on from the 1987 flood and the completion of Inanda Dam.

This present study is an expansion of previous research conducted by the author in 2005 as part of his Honours thesis (University of KwaZulu Natal) within the Mgeni Estuary (Tinmouth, 2005). The new investigation aimed to extend the research area as well as tackle issues raised by the previous research. The initial pilot study of 2005 was undertaken in order to establish 1) the current surface sediment distribution in the lower reaches of estuary and 2) to document any changes in the system that have occurred since 1989; building on the research conducted by Cooper (1986, 1991), Moleko (1998), and Njoya (2002) in order to better understand the dynamics at work within the Mgeni Estuary. The results of the 2005 study showed changes in the estuarine sedimentation characteristics compared to those identified in Cooper's (1986) study, pointing towards a shift from river-dominated to that of tide-dominated sedimentation. The cause of this shift was proposed to result from the completion of Inanda Dam. However, evidence for this argument was limited due to the two dimensional approach, with only surface sediments and recent bedform analyses available in 2005. This new quantitative study included the collection of a number of sediment cores so that a record of the changes in the estuarine environment over time could be examined in order to address these changing sediment dynamics.

The main objectives of the current study were to address the issues highlighted in the earlier study and to provide, in particular, an explanation for the significant changes observed in the surface sediments over the last 20-30 years and hence the sediment dynamics within the Mgeni estuary. This new quantitative approach was initiated with a detailed historical desktop study of aerial photography and old charts, which was undertaken to provide a framework into which all of the newly collected samples could be described and discussed. Over 100 additional surface samples were collected, in order to extend the study area from the previous study, such that a more complete and representative set of surface sediments over the entire estuary were described. In addition to the surface sediment samples, a number of vibro- and hammer cores were collected in order to provide a more detailed stratigraphic record of the estuary. The surface samples were also subject to a detailed geochemical analysis, which was undertaken to ascertain the pollution status within the estuary as well as allowing identification of flow trends and the pollutant source areas. The results of these multidisciplinary combined studies allowed for an improved understanding of the effects of urbanization and construction on the dynamics and

environmental health of the Mgeni system. As direct consequence, this study will allow a better determination of the possible future of the Mgeni Estuary and assist in the creation of plausible management procedures to help protect the estuary.

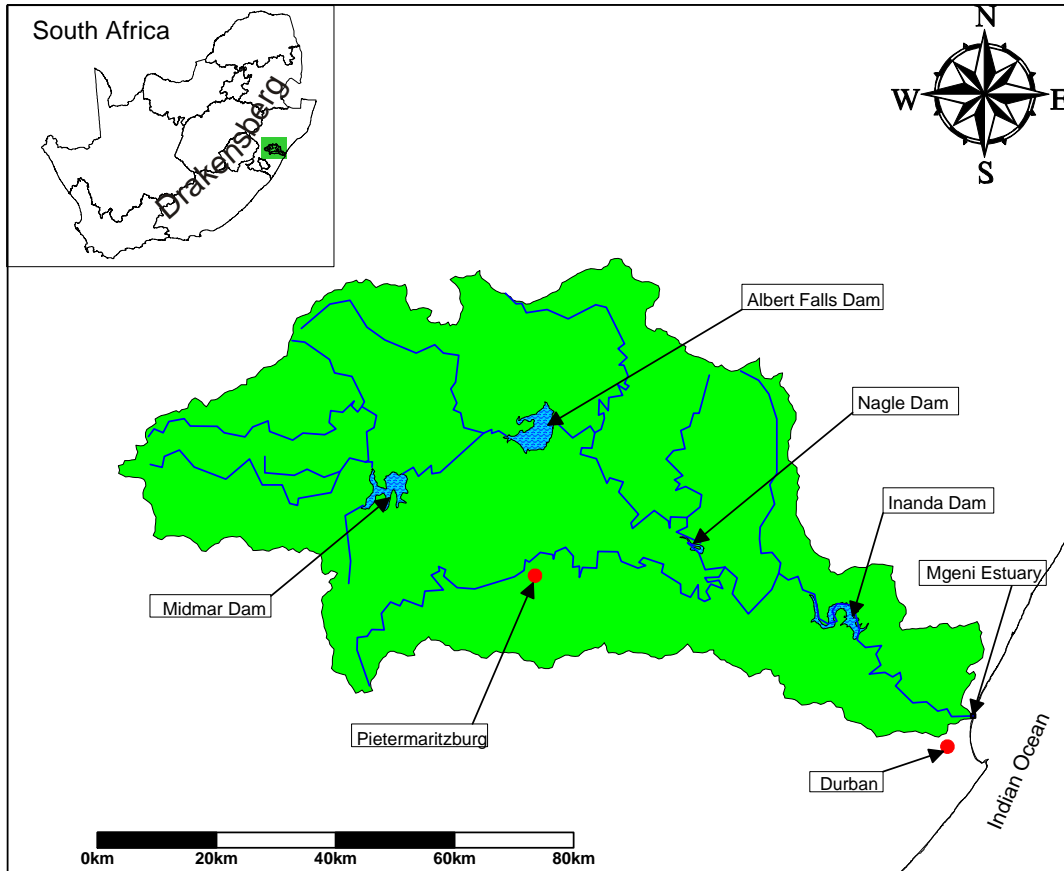


Figure 1.1 Locality of Mgeni Catchment with the four major dams (Inanda Dam, Nagle Dam, Albert Falls Dam, and Midmar Dam) upstream of the estuary.



Figure 5.1 Shows the 500 sediment sample sites distributed throughout the estuary. Blue represents the 369 samples collected during the pilot study, whilst the white represents the additional samples collected for the current study. This high sample density allowed for the creation of more precise sediment distribution maps. Sediments were analyzed for various grain sizes, statistical parameters, carbonate content and organic content.

CHAPTER 2

Estuary classification

2.1. Definitions

The word estuary originates from the Latin for tide, *aestus*. The earliest most commonly used definition of an estuary is that of Cameron and Pritchard (1963) who defined an estuary as “a semi-enclosed coastal body of water having a free connection with the open sea and within which sea water is measurably diluted with fresh water derived from land drainage”. This definition was later adapted to introduce the concept of temporarily closed estuaries by Day (1980), whereby an estuary is defined as a “semi-enclosed coastal body of water which is either permanently or periodically open to the sea and within which there is a measurable variation of salinity due to the mixture of sea water with fresh water derived from land drainage”. This definition of an estuary has become the most widely accepted and used definition of estuaries in South Africa.

2.2. Classification systems

Numerous methods and models have been used to classify estuaries based upon physiographic (Pritchard, 1952; Pritchard, 1960), tidal range (Davies, 1964; Hayes, 1975; Hayes, 1979), evolution (Dalrymple *et al.*, 1992), morphology (Davies, 1964), and salinity and stratification structure (Pritchard, 1955; Cameron and Pritchard, 1963).

2.2.1. Physiographic classification

Pritchard (1952) classified estuaries into three groups; drowned rivers, fjords and bar-built estuaries. Pritchard (1960) added a fourth category to include estuaries formed by tectonic processes. Fjords and tectonic estuaries are not present along the South African coastline and will therefore not be discussed further.

Drowned-river estuaries were formed by flooding of previously incised river valleys during the Flandrian transgression (Pritchard, 1952). Drowned river estuaries commonly occur in low to mid latitudes and typically have a funnel shape, with the cross-section increasing exponentially towards the mouth and the longitudinal profile deepening seaward (Perillo, 1995).

Bar-built estuaries are located on low relief coastlines which are characterised by both small tidal ranges (microtidal) and low river discharge. This results in the dominant processes being littoral drift and wind transport, which may lead to the development of a barrier that encloses the estuary forming a lagoon (Perillo, 1995).

Roy (1984) similarly classified estuaries along the Australian New South Wales coast into three types, based on their corresponding entrance conditions; drowned river valleys, barrier estuaries and saline coastal lakes (Figure 2.1).

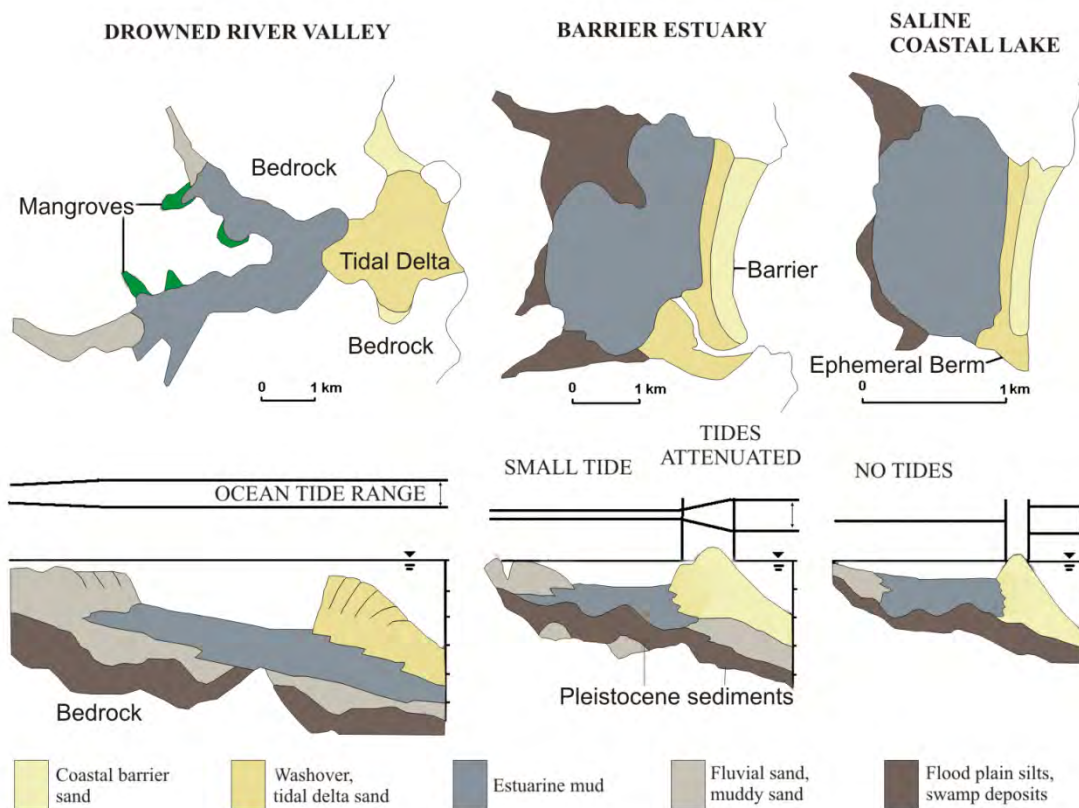


Figure 2.1. Schematic diagrams of the three estuary classifications namely; drowned river valley, barrier estuary, and saline coastal lake used by Roy (1984) for the Australian New South Wales coast. The diagram shows a plan view of the estuaries with regards to the tidal range, and sedimentary facies shown in a longitudinal profile (after Roy, 1984).

2.2.2. Classification by tidal range

Davies (1964) divided coasts into three major categories on the basis of tidal range: microtidal (range <2 m), mesotidal (2 to 4 m) and macrotidal (>4 m), from which Hayes (1975) classified estuaries according to the associated distinctive morphologies. Microtidal coasts are characterized by long, narrow and rather straight barriers with widely spread inlets. Washover features are prominent as are well developed flood tidal deltas, but ebb tidal deltas are small or nonexistent. Waves are the dominant physical process along this type of coast (Hayes, 1975; Hayes, 1979). Mesotidal coasts generally have short and wide barriers with closely spaced inlets. Inlets have well developed ebb tidal deltas, due to the relatively pronounced influence of tidal currents (Hayes, 1975; Hayes, 1979). Macrotidal coasts do not develop barriers, due to the dominance of pronounced tidal currents in the direction perpendicular to the shoreline. Funnel shaped embayments on macrotidal coastlines contain linear sand bodies oriented parallel to the tidal current direction (Hayes, 1975; Hayes, 1979).

Hayes (1979) later subdivided these three categories into five. In this later classification, the microtidal coast has a tidal range of <1 m with the same characteristics as the Davies (1964) microtidal characteristics. Mesotidal estuaries were subdivided into two categories, namely lower mesotidal with a tidal range of 1 to 2 m, and a higher mesotidal with a tidal range of 2 to 3.5 m. Lower mesotidal estuaries are characterized by an increasing number of inlets with decreasing amounts of washover features; these are generally found along mixed tidal and wave-dominated coasts. The high mesotidal coasts are characterized by abundant tidal inlets (Hayes, 1979). Macrotidal estuaries had a similar classification as previously described by Hayes (1975, 1979) with the tidal range being greater than 3.5 m.

2.2.3. Evolutionary classification

Dalrymple *et al.* (1992) proposed an evolutionary classification by combining wave, river and tidal processes with temporal aspects (Figure 2.2). The evolutionary aspect (relative time) can also be expressed in terms of transgression and progradation, with transgression being represented by a movement towards the front of the diagram (Figure 2.2) and progradation being represented by a movement towards the back (Figure 2.2). A vertical section through this prism can be used to classify the coastal deposition

system as either wave or tide dominated. Dalrymple *et al.* (1992) divided both tidal and wave dominated estuaries into three zones: 1) an outer zone dominated by marine processes; 2) a relatively low-energy central zone, where marine energy is in the long term balanced by fluvial energy; and 3) an inner, river dominated zone. This zonation pattern is superficially similar to the three-fold salinity subdivisions proposed by Fairbridge (1980). A variation in energy, morphology and sediment facies distribution can be identified in the tripartite zonation.

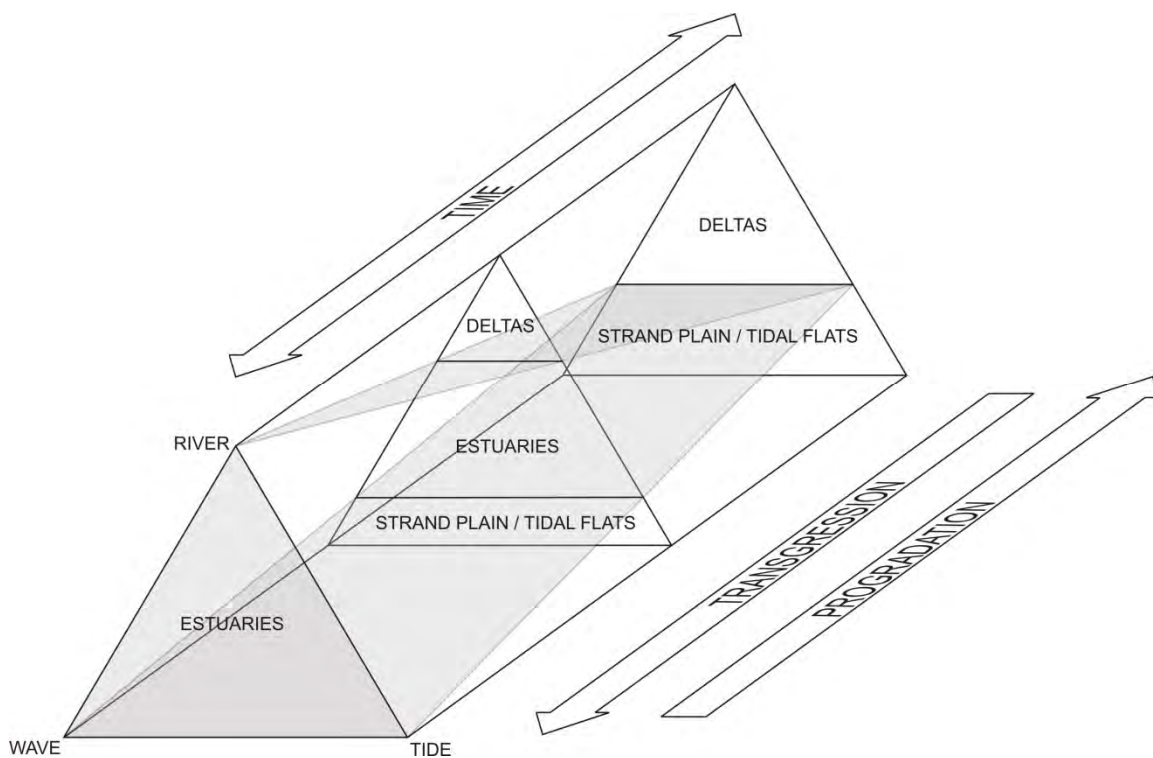


Figure 2.2. Diagram of the evolutionary classification of coastal environments as proposed by Dalrymple *et al.* (1992). The longitudinal axis represents time with regards to transgression and progradation. The edges of the prism relate to the dominant processes namely, fluvial, wave and tidal. The upper section represents delta environments, the wedge represents estuarine systems, and the lower section represents non-deltaic, prograding coasts (after Dalrymple *et al.*, 1992).

Wave-dominated estuaries

The tidal influence is small within wave-dominated estuaries (Dalrymple *et al.*, 1992), with the mouth of the system (outer zone) dominated by wave action. The dominant wave action in combination with any tidal current, produces littoral transport (longshore drift) of sediment, developing a subaerial barrier or submerged bar. This barrier prevents most of the wave energy entering the estuary. If the tidal prism of the estuary is insufficient to maintain breaching generated by storm surges or river floods, the estuary will close during fair weather, producing a “blind” estuary. Tidal energy becomes dissipated by friction in the inlet of many estuaries, resulting in the back barrier region having a smaller tidal range than the open ocean, where these estuaries are termed “hyposynchronous” (Salomon and Allen, 1983 in Dalrymple *et al.*, 1992; Nichols and Biggs, 1985). Fluvial energy decreases seawards due to the decreasing hydraulic gradient, which results in two areas of maximum total energy, one at the mouth caused by wave energy towards the tidal inlet and the other at the head of the estuary produced by fluvial currents. These high energy zones are separated by a pronounced zone of minimum energy in the central region of the estuary (Figure 2.3). This distribution of energy produces a tripartite distribution of sediments, from coarse sediments near the head and mouth of the estuary and fine sediments concentrated towards the centre (Dalrymple *et al.*, 1992).

Tide-dominated estuaries

Dalrymple *et al.* (1992) stated that “tide-dominated estuaries are less well known than their wave-dominated counterparts”, with the best known examples being in macrotidal environments. Tide-dominated estuaries can, however, develop in areas with smaller (micro to meso) tidal ranges, if wave action is limited and/or the tidal prism is large (Hayes, 1979; Davis and Hayes, 1984). If tidal energy exceeds wave energy at the estuary mouth, typically elongated sandbars develop, which dissipate with the existing wave energy (Figure 2.4). The incoming flood tide is progressively compressed by the characteristic funnel shaped geometry of these estuaries. This results in an increase in the speed of the flood tidal current into the estuary governed by Bernoulli’s principle. The tidal current decreases away from the tidal inlet due to the affects of frictional dissipation, exceeding the affects of the convergence. This results in the tidal energy decreasing to zero at the tidal limit. As with wave-dominated estuaries, the fluvial current decreases

seawards. An energy minimum is located in the region where the fluvial and tidal energy is balanced. The minimum energy point is somewhat less pronounced than that of wave-dominated systems due to tidal energy penetrating further headward than wave energy. This results in a less defined tripartite distribution, with sands occurring in the tidal channels, which traverse the length of the estuary (Dalrymple *et al.*, 1992).

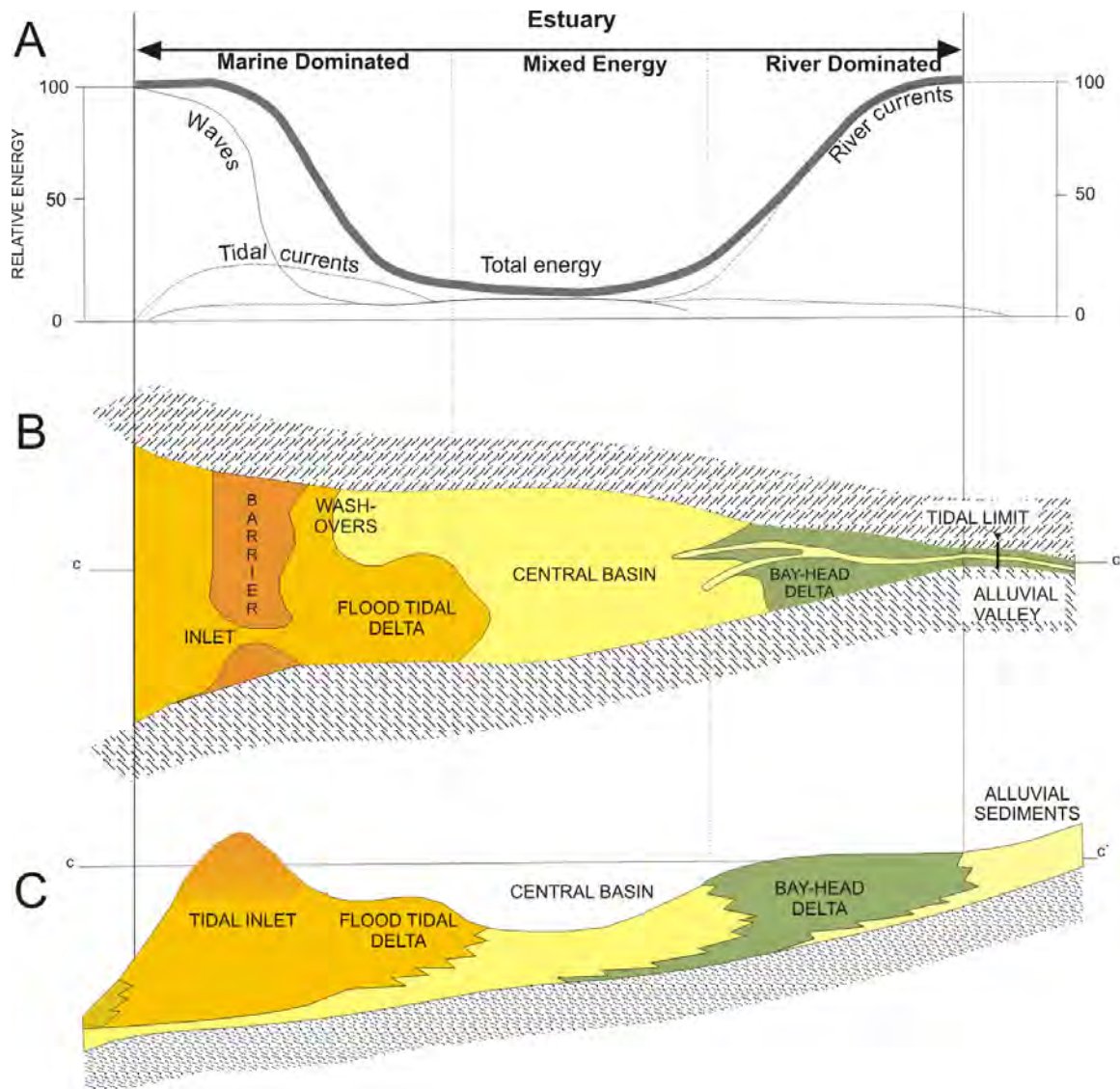


Figure 2.3. Schematic diagram of an idealized wave-dominated estuary showing the distribution of A) energy types, B) morphological features in plan view, and C) sedimentary facies in longitudinal section. Note the general decrease in total energy towards the central basin (after Dalrymple *et al.*, 1992).

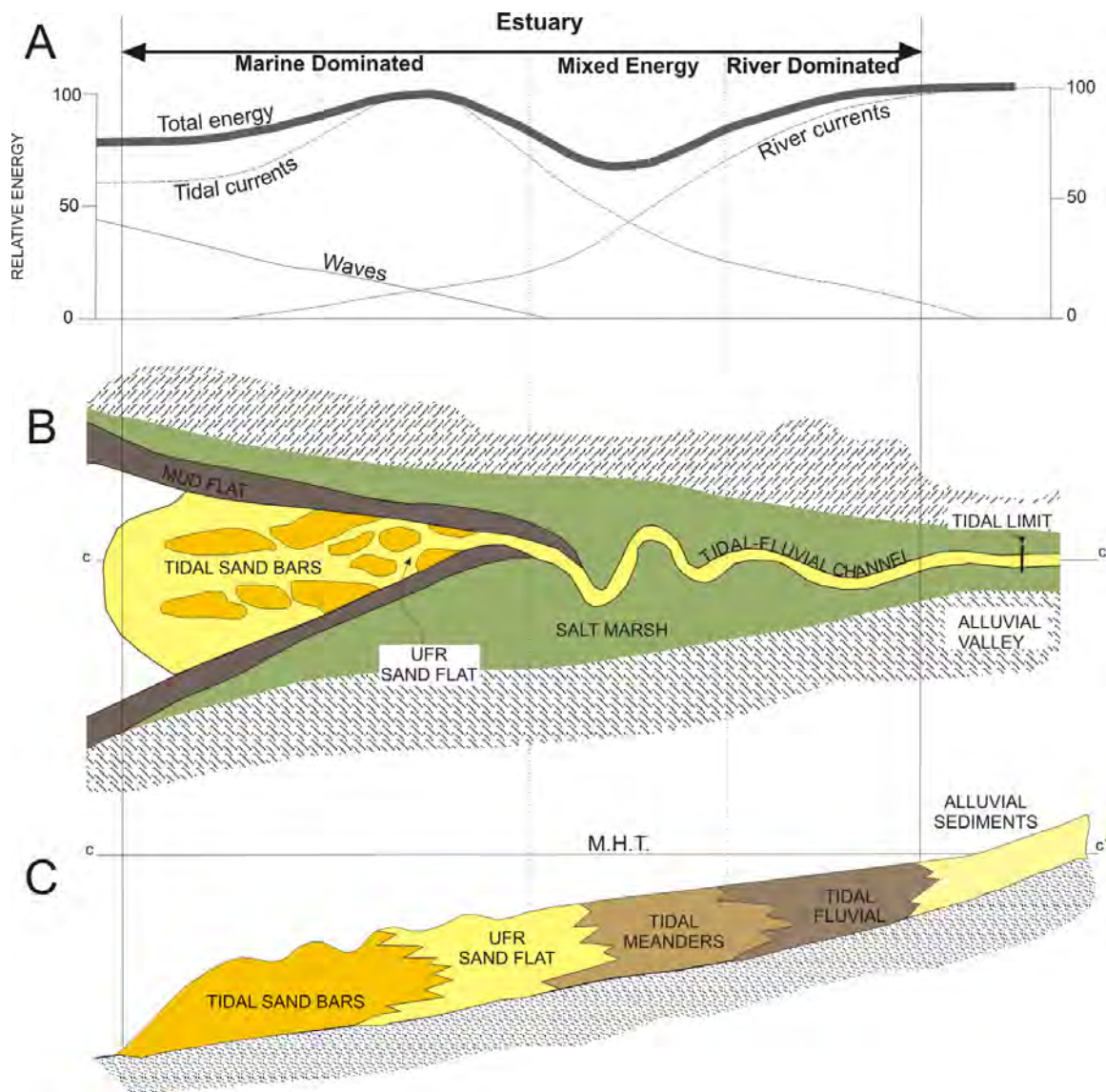


Figure 2.4. Schematic diagram of an idealized tide-dominated estuary showing the distribution of A) energy types, B) morphological features in plan view, and C) sedimentary facies in longitudinal section. URF = upper flow regime; M.H.T. = mean high tide. The longitudinal cross-section does not show any either the mud flat facies or salt marsh facies (after Dalrymple *et al.*, 1992).

2.2.4. Classification by salinity and stratification structure

Pritchard (1955) and Cameron and Pritchard (1963) classified estuaries based on their stratification and salinity distribution, so as to better understand the unique salinity and flow characteristics of coastal plain estuaries (Sharples *et al.*, 2001). They classified estuaries into three main categories, namely: highly stratified, partially mixed and well-mixed estuaries.

Highly stratified

Highly stratified, salt wedge estuaries show a relatively sharp transition between the outgoing fresh water and incoming saline water, with differences in densities causing the fresh water to flow seawards above the more dense saline water (Figure 2.5). This occurs throughout the estuary until the force of the fresh water is too great for the saline water to overcome. It must be noted, however, that the halocline is typically not a precisely defined surface between the underlying saline water and the overriding fresh water, as some mixing does occur. The partial mixed zone occurs due to “entrainment” caused by the shear forces between the two moving layers. This results in the salinity of the surface fresh water layer being greater than zero (Wright *et al.*, 1999; Sharples *et al.*, 2001).

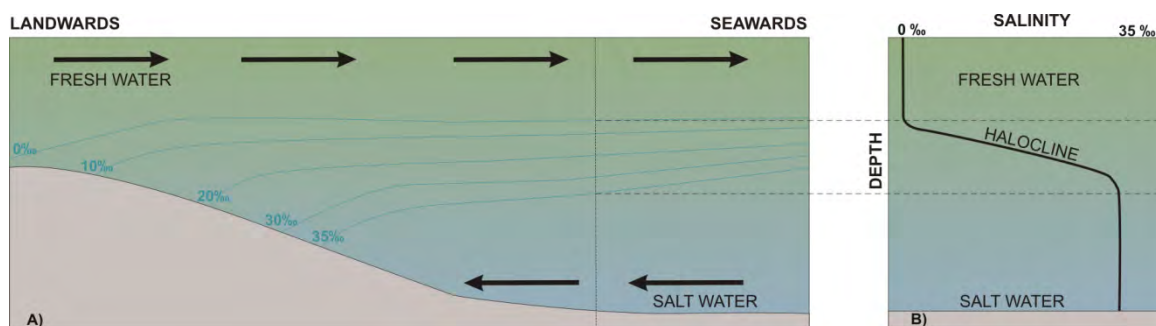


Figure 2.5. Schematic diagram of A) longitudinal section of highly stratified salt water wedge estuary and its salinity, and B) its halocline (salinity – depth profile) along the vertical dashed line, with salinity in parts per thousand (‰). The diagram shows the denser saline water flowing under the less dense fresh water. Entrainment caused by shear forces between the two moving layers results in partial mixing (after Wright *et al.*, 1999).

Partially mixed

River flow is relatively low compared to the tidal prism in a partially mixed estuary, resulting in a typical well-defined two layer flow. Mixing of fresh water and salt water in a partially mixed estuary is due to turbulence from frictional forces, producing dissipation of the incoming tidal energy (Figure 2.6). The resulting eddies mix the saltwater upward and the fresh water downward (Dyer, 1997). As the salinity of the surface water increases, the outgoing surface flow increases to maintain river flow, this causes the incoming flow along the bottom, resulting in the typical well-defined two-layer flow (Dyer, 1997; Wright *et al.*, 1999; Sharples *et al.*, 2001).

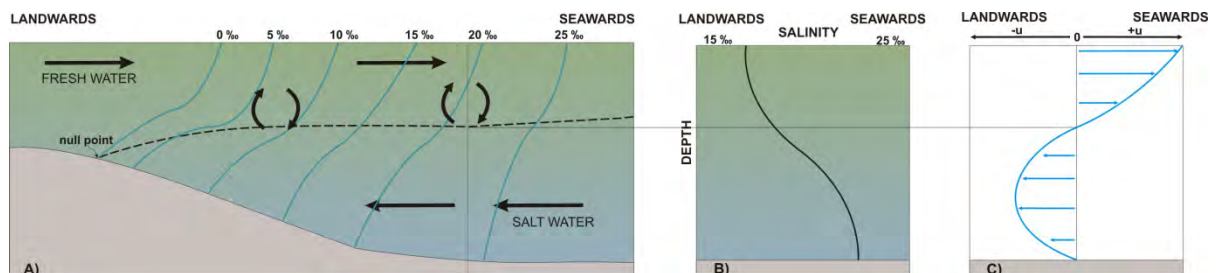


Figure 2.6. Schematic diagram of partially mixed estuary. A) shows the longitudinal section with water circulation and salinity gradient, B) is the salinity-depth profile along the dashed vertical line, with salinity in parts per thousand (‰), and C) relative velocity – depth profile through dashed vertical line showing upstream flow along bed (after Wright *et al.*, 1999).

Well-mixed or vertically homogeneous

In a well-mixed estuary the salinity remains approximately constant throughout the water column, with a decrease in salinity towards the head (Figure 2.7). Well-mixed estuaries occur when the river flow is significantly less than the tidal range resulting in turbulence produced by the velocity shear on the bottom. This turbulence may be large enough to mix the entire water column resulting in a vertically homogeneous estuary. Wide estuaries may become laterally inhomogeneous with the river flow occurring on the left side and the incoming flow on the right side in the southern hemisphere (facing down stream) due to Coriolis and centrifugal forces (Dyer, 1997; Wright *et al.*, 1999; Sharples *et al.*, 2001).

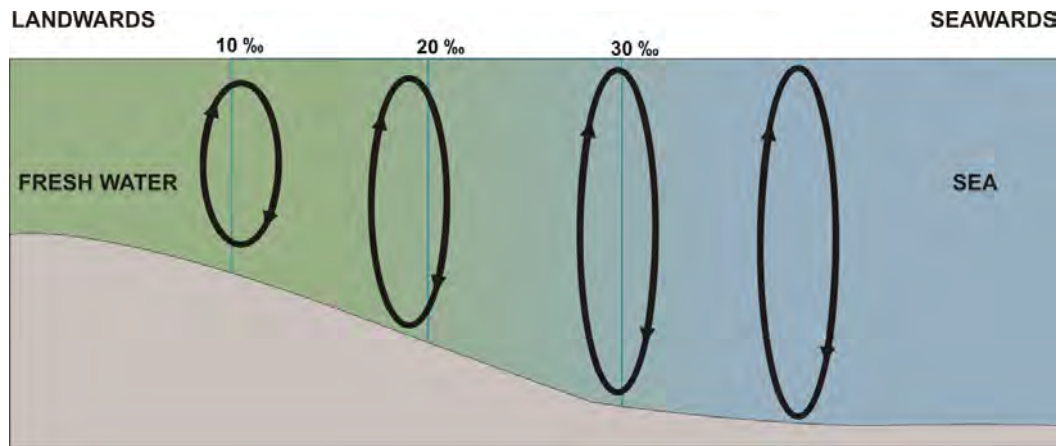


Figure 2.7. Schematic diagram of a longitudinal section of a well mixed estuary showing the strong tidal turbulence (ellipses) and the vertically uniform salinity, in parts per thousand (‰), from top to bottom with decreasing salinity towards the head of the estuary.

2.5. Morphological classification of South African estuaries

The South African coastline is typically a lower mesotidal to microtidal coast (Davies, 1964) with a tidal range averaging 2 m (Schumann and Orren, 1980). The swell regime defines the coast as wave-dominated, with the KwaZulu-Natal coast receiving persistent high-energy waves and prevailing large amplitude swells from the south-east for ~35% of the year and from the north-east to east for ~40% of the year.

Cooper (2001) used the main forms of morphological variability to create a hierarchical classification of South African estuaries. Due to the relatively constant nature of the tide, wave energy and sea level history, Cooper (2001) decided to base his estuarine classification on the highest level of discrimination, those that are “normally open”, and those that are “normally closed”. Open estuaries are further subdivided into systems that are essentially unbarred, and those that have a supratidal barrier with a surface drainage channel (Cooper, 2001). Barred estuaries range from those with small catchments and small discharges to much larger systems. The smaller systems are generally incapable of maintaining large tidal prisms and are therefore maintained in an open state by fluvial discharge. Open barred estuaries can therefore be subdivided into two categories, based on their mechanism for maintaining an open state: either tide-dominated or river discharge dominated, channel (Cooper, 2001).

Tide-dominated estuaries

Tide-dominated estuaries have sufficient tidal prism to permit the inlet to be maintained in an open state by tidal current despite the low tidal range (Cooper, 2001). Sediment deposition in such estuaries is typical of that described by Hayes (1979) for microtidal barrier island environment. Tide-dominated estuaries tend to have well developed flood-tidal deltas, with the ebb-tidal delta small or non-existent. They act as sinks for marine sediment through flood-tidal dominance at the estuary inlet. At the tidal limit of the estuary, sedimentation is replaced by the deposition of fluvial deltas. Tide-dominated microtidal estuaries exhibit a distinctive tripartite distribution, with marine influence near the inlet, fluvial inputs at the tidal head, and quiet suspension-settling dominated zone in the middle reaches (Cooper, 2001).

River-dominated estuaries

River-dominated estuaries have an insufficient tidal prism to maintain an open inlet against coastal processes such as wave, current and tidal action (Cooper, 2001). Flood-tidal deltas in these estuaries are much reduced in size or absent. The fluvial sediment generally extends to the barrier, with tidal influence being minimized by elevated bed levels. River flow in such a system is important to maintain an open outlet channel, with insufficient flow resulting in the prolonged closure of the mouth during droughts (Cooper, 2001).

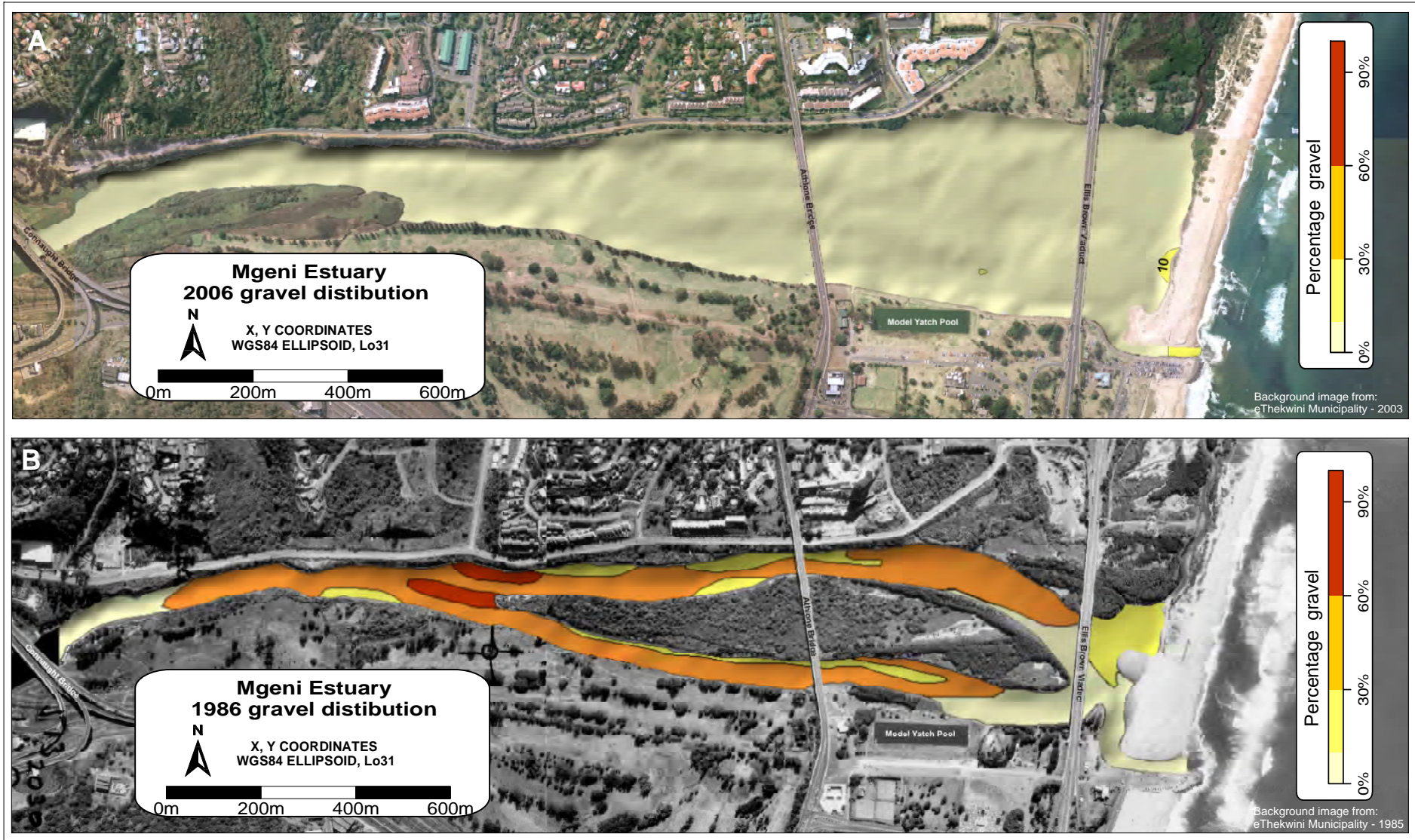


Figure 5.2. A) The 2006 gravel distribution, with only a few isolated pocket of gravel, located within the main channel off of the model yacht pool, in the tidal inlet, and in washover fans on the supratidal barrier. B) The 1986 distribution of gravel. Gravel is found throughout the estuary and generally comprises a large portion of the sediment.

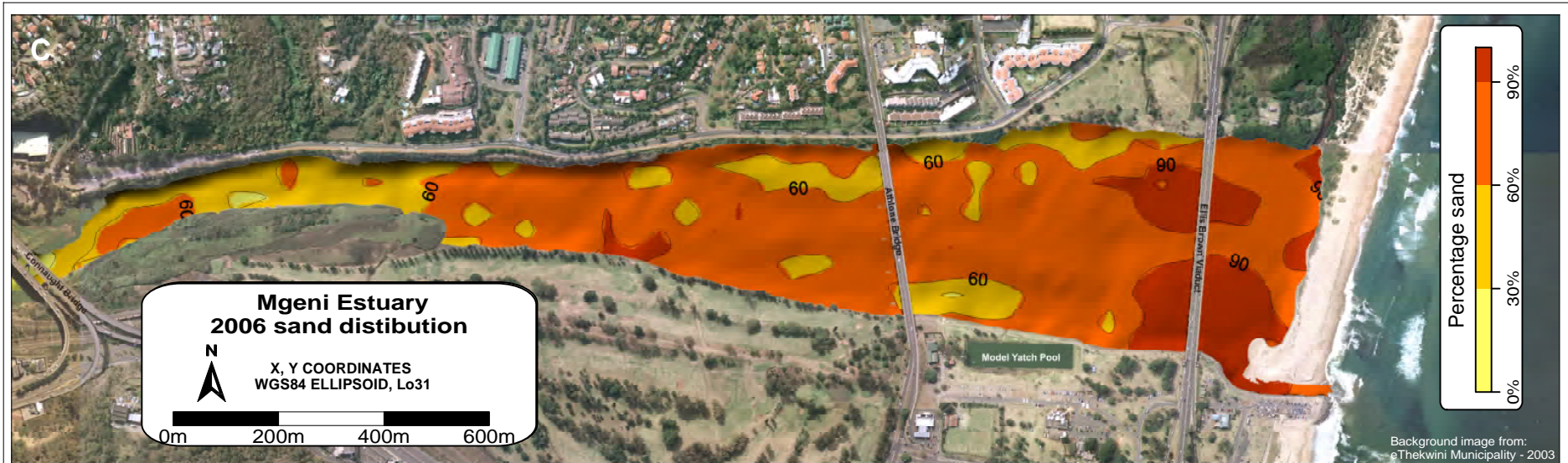


Figure 5.2. C) The 2006 distribution of the sand fraction (63 μ m and 2mm) within the Mgeni Estuary. There is a general increase in the amount of sand towards the tidal inlet, away from the head of the estuary. D) The 1986 distribution of sand within the estuary. There has been an increase in the overall sand percentage throughout the estuary, except for the area towards the head of the estuary.

CHAPTER 3

Regional setting

3.1. Catchment

The Mgeni Estuary as a catchment has a total area of 4500 km² (Badenhorst *et al.*, 1989) making it the fourth largest catchment of the 67 rivers, which discharge into the Indian Ocean along the coast of KwaZulu-Natal (Orme, 1976; Begg, 1978). The Mgeni River originates in the foothills of the Drakensberg in the uMgeni Vlei area at an altitude of 1889 m. The river discharges approximately 250 km east in the northern suburbs of the City of Durban at approximately 29°48`S and 31°02`E (Figure 3.1.A). The overall gradient of the Mgeni River is approximately 1:132 (0.0075 degrees), reducing to 1:550 (0.0018 degrees) in the lower 10 km (National Research Institute for Oceanology, 1986; Cooper, 1991; Cooper, 1993) (Figure 3.1.B). In the final 2.5 km where the Mgeni River discharges into the sea, it is subject to tidal salinity and water level fluctuations (Cooper, 1986; Cooper and Mason 1987).

The mean discharge from the catchment area varies according to the season, ranging from approximately 18.4 m³/s in the wet summer months to 6.5 m³/s in winter (Orme, 1974). However, the discharge reaching the estuary has been greatly reduced by the construction of four major dams upstream, namely: Midmar, Albert Falls, Nagle and Inanda Dams (Figure 1.1). These dams have a combined capacity of 753 million cubic metres of water, more than the mean annual runoff for the entire Mgeni Catchment. The most recently built Inanda Dam, completed in 1989, is situated in the Valley of a Thousand Hills (Figure 1.1). The construction of the dam has reduced the effective catchment area to 395 km², which is just 9% of the entire catchment area. This is, however, still a relatively large regional catchment area, for example, in comparison to the Mhlanga (80 km²) and Mloti (484 km²) Rivers, both of which are situated north of the Mgeni Estuary.

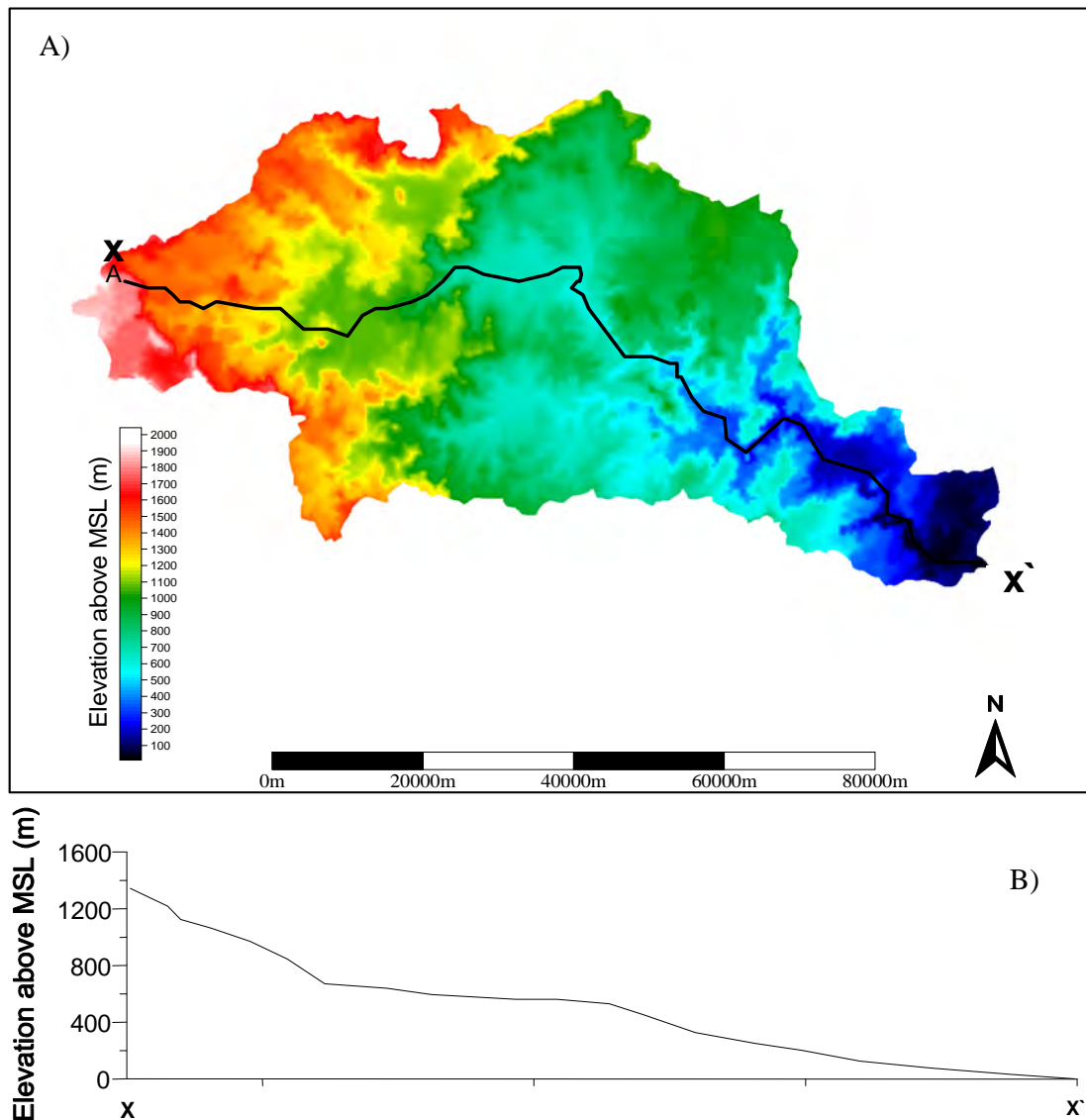


Figure 3.1. A) Topographical relief map of the Mgeni River catchment, showing the elevation with cross-section line from source (X) to the Mgeni Estuary (X'), approximately along the riverbed. B) Downstream profile of the Mgeni River from X to X', illustrating the decrease in a gradient towards the coast and the steep overall gradients typical of KwaZulu-Natal escarpment (data source: the eThekweni Municipality).

3.2. Mgeni Estuary characteristics

The Mgeni Estuary forms the lowermost 2.5 km of the Mgeni River as it discharges into the Indian Ocean. It is funnel shaped, with the mouth (tidal inlet) position diverted to the south by the presence of a southward extending sandbar. This position is stabilized by an artificial groyne on the southern bank designed to prevent tidal scour and the northward migration of sediment due to longshore drift (Cooper, 1986; Cooper and Mason 1987; Moleko, 1998; Njoya, 2002) (Figure 1.2). Although classified as a river-dominated estuary by Cooper (1993), the mouth periodically closes in response to low discharge, and is hence better classified as a temporary open/closed estuary (TOCE) (Cooper, 1986; Stretch and Parkinson, 2006).

The mean depth of the Mgeni Estuary is approximately 0.7 m reaching a maximum of 2.15 m near the head of the estuary (Begg, 1978; Begg, 1984). The effect of the tide in the estuary decreases away from the mouth as shown by the records of the Council for Scientific and Industrial Research (CSIR, 1976) which show a tidal range of 1.52 m at the Ellis Brown Viaduct to 1.2 m at Connaught Bridge over a spring tide (Figure 1.2).

The salinity in the estuary varies with the tide and the volume of the fresh water discharge. At high tide, the estuary can be entirely influenced by the sea water (Simpson *et al.*, 1972, in Cooper, 1986), whilst a salt wedge forms between the head of the estuary and Athlone Bridge during low tide (Cooper, 1986).

The only significant tributary within the estuary is the Beachwood Creek, which enters the estuary after flowing southwards parallel to the coastline for approximately 2 km through a mangrove forest, before connecting to the estuary through the northern bank near the mouth (Figure 1.2).

3.3. Coastal characteristics

The KwaZulu-Natal coastline is relatively straight with a uniform underwater topography (Harris, 1961). The coastline is wave-dominated with semi-diurnal tides. Mean spring tidal range at Durban is 2 m. This classifies the coastline as intermediate between lower mesotidal (Hayes, 1979) and microtidal (Davies, 1964). Water circulation along the coast is dominated by the south-ward flowing Agulhas Current. This current produces a large eddy system known as the Natal Gyre, which causes a

predominantly north to north-eastward flowing nearshore current or longshore drift (Harris, 1961; Pearce and Schuman, 1977). Longshore drift results in a net northeasterly movement of beach material (Kinmont, 1961) with a sediment flux calculated at 70 000 m³ annually by the CSIR (Garland and Kruger, 1986). Wave propagation along the coast is predominantly from the south/south-east.

3.4. Climate and hydrology

The KwaZulu-Natal climate can be described as subtropical with warm wet summers and cool dry winters. The mean annual rainfall is between 800 mm to 1000 mm, of which 80% occurs in the summer months (Tyson, 1987) (Figure 3.2). The seasonality of the rainfall leads to regular flooding during the summer months with severe flooding conditions associated with abnormal weather conditions (Tyson, 1987; Badenhorst *et al.*, 1989). In the steep hinterland, flow velocities during floods are particularly high leading to scouring of the estuary (Badenhorst *et al.*, 1989; Tyson and Preston-Whyte, 2000).

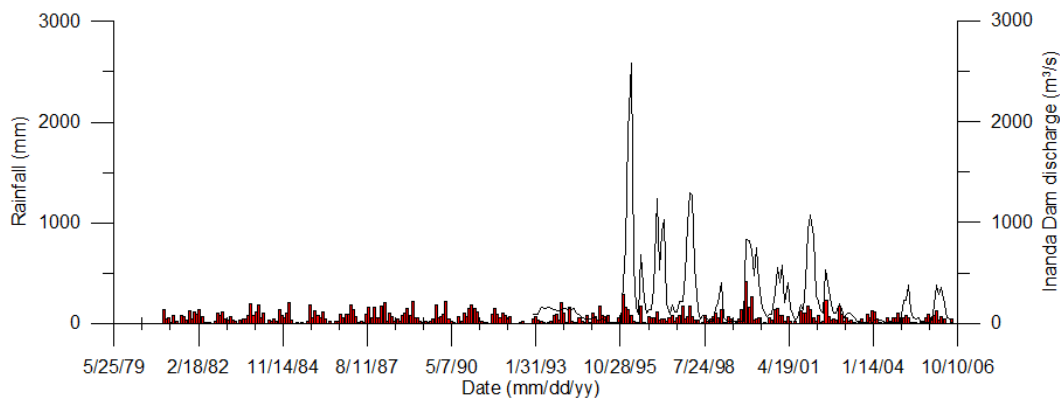


Figure 3.2 Graph showing the discharge (m³/s) from Inanda Dam and rainfall data (mm) for various months from 1981 till 2006. Discharge data available from 1993 onwards. Note the decrease in peak discharge from 1995 to 2006.

3.5. Catchment geology

The soils of the upper catchment in the foothills of the Drakensberg are formed from the weathering of the underlying lithologies (Figure 3.3). These are generally fine grained sedimentary rocks of the Karoo Supergroup, intruded by mid Jurassic Karoo Supergroup dolerite (Johnson *et al.*, 2006). The upper regions consist of Beaufort and Eccca Group lithologies. The Beaufort Group consists of light-coloured mudrocks, sandstones and occasional conglomerates (Brink, 1983; Johnson *et al.*, 1996). The lithologies of the Eccca Group are dominated by fine grained sandstones and shales (Brink, 1983).

The Valley of a Thousand Hills forms the middle and lower regions of the catchment and is dominated by granites and gneisses of the Natal Metamorphic Province. These are overlain by the Natal Group sandstones and tillite of the Permo-Carboniferous Dwyka Group (Johnson *et al.*, 2006). The pre-Karoo Supergroup lithologies are considered the main source of sediment input into the Mgeni River (Keinzle *et al.*, 1997) (Figure 3.4).

The area underlain by pre-Karoo lithologies dominates the sediment source as it has a rugged relief, increased water yield and harbours a high human population density with associated land that increases erosion. The pre-Karoo lithologies provide the expected mineral composition of the mean grains, quartz and feldspar noted by Cooper (1986) within the estuary.

In the lower region of the catchment, the Mgeni River incises through unconsolidated Recent alluvium and older partially consolidated Tertiary and Pleistocene coastal deposits that overlie the Dwyka Group tillite and shale bedrock (Figure 3.3).

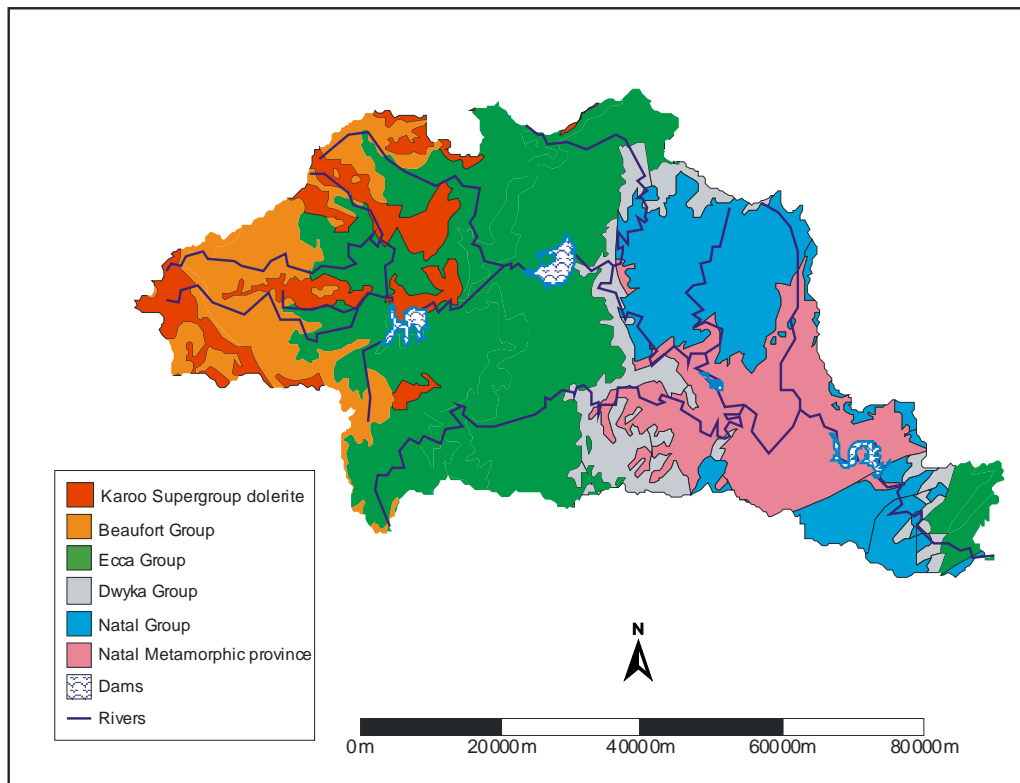


Figure 3.3 The geology of the Mgeni River catchment, showing the Dwyka and Ecca Groups in both the upper reaches and lower reaches of the catchment. Note that the middle to lower reaches of the catchment is dominated by Natal Group and Natal Metamorphic province granites and gneisses in the Valley of a Thousand Hills, which form the dominant sediment source for the estuary.

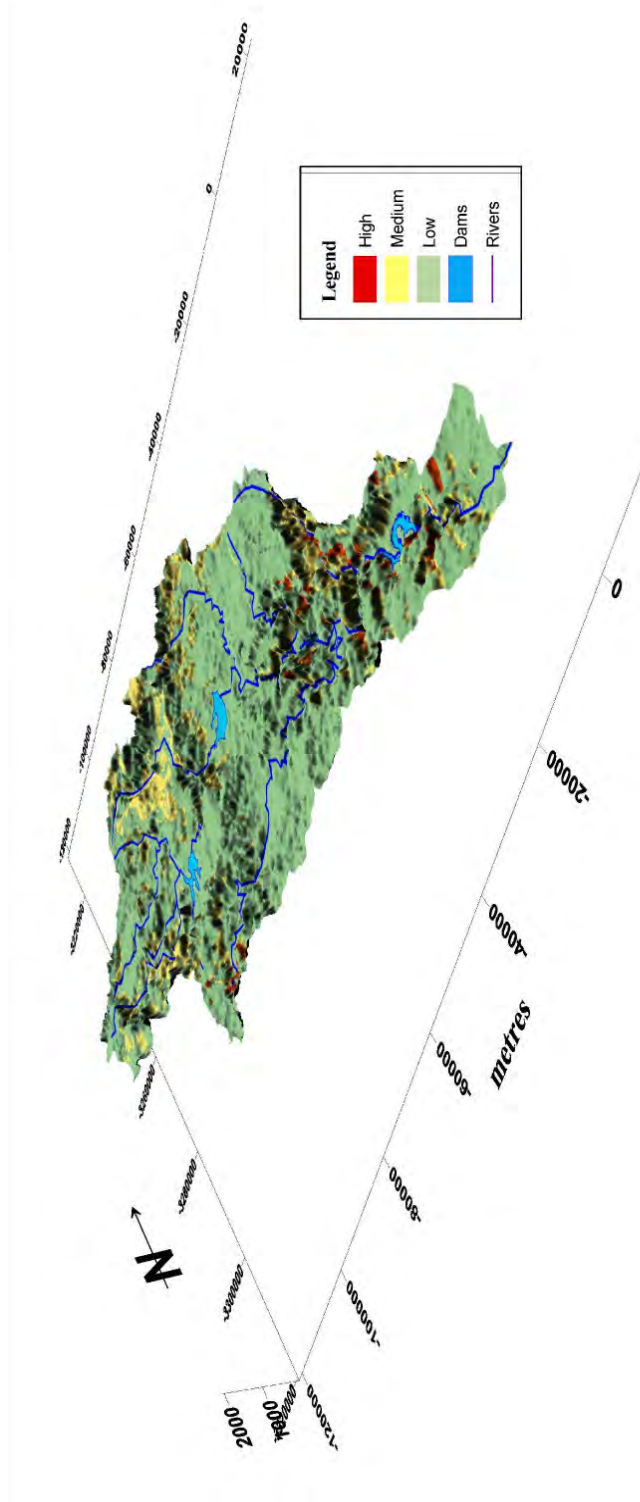


Figure 3.4. Relative sediment availability within the Mgeni catchment showing the highest sediment availability in the Valley of a Thousand Hills area around Inanda Dam. The map was created based on land use, sediment type, slope and rainfall data (after Ettchells *et al.*, 2005)

3.6. Local geology

Recent alluvial deposits form small isolated pockets in river valleys such as that of the Mgeni Estuary (Krige, 1932). These deposits can be broken down into three classes: a basal boulder bed, cohesionless deposits, and cohesive deposits (Francis, 1983).

The Mgeni River basal boulder bed overlies the bedrock lithologies, with a decrease in thickness of this unit towards the estuary mouth. Thicknesses vary from over 11 m under the Springfield Services Bridge to 6 m in thickness under the Connaught Bridge. The boulder bed is composed mainly of hard quartzitic sandstones and siliceous quartz arenites of the Kranzkloof Member of the Durban Formation of the Natal Group, with minor Dwyka Group tillite and Karoo Supergroup dolerite clasts (Francis, 1983; Johnson *et al.*, 2006). The resistance of the boulder bed would have aided in the protection of the underlying bedrock from further erosion (Schumm, 1977).

The composition of the overlying cohesionless deposits varies from fine sand to gravel, in an apparent upward fining cycle, typical of fluvial depositional environments (Orme, 1976, in Cooper, 1986). These deposits occur as widespread lenses and sheets intercalated with clay and silts. They vary in thickness from 2 m to 4 m and reach up to 15 m under the Connaught Bridge. The source of the sediment is believed to have been derived from pre-Karoo lithologies from the Valley of a Thousand Hills (Roberts, 1981).

The cohesive clay and silt deposits appear to be mainly confined to the lower reaches of the Mgeni River valley, increasing in thickness from 2 m under the Springfield Electricity Department to 15 m thick under the Springfield Service Bridge and Connaught Bridge (Figure 1.2).

Faulting is mainly confined to the middle and lower catchment, affecting all formations except those younger than the Karoo Supergroup. Major joint set structural readings within and adjacent to the Mgeni Estuary dip at between 040° and 050° and strike approximately north/south. The coast parallel normal faults, caused by extension and brittle deformation from active tectonic processes along the Falkland-Agulhas fracture zone during the break up of Gondwana, have led to the development of fault blocks dipping in an easterly to southeasterly direction (Krige, 1932; Brayshaw, 2001;

Watkeys and Sokoutis, 1998). This has also led to the repetition of certain lithologies, such as those of the Dwyka and Ecca Groups which are found in both the upper and lower catchment, separated by the underlying Natal Group sandstones and Basement Complex (Figure 3.3).

3.7. Geological development of the estuary

During the last Pleistocene marine regression of the last glacial maximum (LGM), the Mgeni River incised through earlier deposited Pliocene deposits into the underlying Dwyka and Ecca Groups bedrock. The maximum depth to which the sea-level dropped was approximately -130 m below present (Cooper, 1993) before rising to a maximum elevation of 5 m above present day sea level during the Holocene High of the Flandrian marine transgression (Deacon and Lancaster, 1998, in Cooper, 1993). This rise in sea level flooded the upper reaches of the present Mgeni Estuary, extending across the entire Springfield Flats (Cooper, 1986). Sea level fell to its present level about 5000 years B.P., resulting in the river course being diverged southward in front of the Berea Ridge behind a transgressive coastal barrier (Cooper, 1986; Cooper, 1993) before discharging into the Durban Bay. This is indicated by coarse-grained fluvial sediments in the low lying areas between the present estuary and Durban Bay, mainly deposited in a delta environment (King, 1962; Cooper, 1993). This river course was last recorded during the 1856 flood, and is still recognizable in satellite images of the KwaZulu-Natal coast (Barnes, 1984, in Cooper, 1993; Cooper, 1986; Ayers, 2004). The depth to bedrock of the underlying geology of the Mgeni Estuary varies from about -45 m under Connaught Bridge to -9 m (north bank) and -33 m (south bank) near the mouth. This suggests that the Mgeni River must have maintained its course to a point downstream of Connaught Bridge before being directed southwards some 4.8 km south to Durban Bay (King, 1962).

3.8. Human influences

The close proximity of the Mgeni Estuary to the Durban city centre has meant that it has been subjected to more direct anthropogenic influence than other estuaries in KwaZulu-Natal (Cooper, 1986). Construction within the estuary itself began in the 1930s in the form of an artificial groyne (Figure 1.2). The groyne was designed to stabilize the position of the mouth and was constructed in late 1920s to prevent the river from flowing along its previous path towards the city (Cooper, 1986). Three main bridges have been constructed within the estuary: Ellis Brown Viaduct, Athlone Bridge

and Connaught Bridge. In addition, the river upstream of Connaught Bridge was canalised in the early 1980s after a major flood that resulted in a number of deaths. This attempt to straighten the estuary by removing a large meander, reduced the effects of flooding of the Springfield Flats.

The largest human influence on the estuarine dynamics was arguably the construction of four major dams within the catchment area, namely: Nagle (1950), Midmar (1963), Albert Falls (1975) and Inanda (1989) Dams (Badenhorst *et al.*, 1989) (Figure 1.1). The most recent addition, Inanda Dam, resulted in the separation of the lower Mgeni catchment from the rest of the catchment, restricting the hydrological input into the estuary from the upper catchment and its constituents (Singh, 2001). This also reduced the flood intensity and bedload sediment supply (Cooper, 1986; Moleko, 1998; Garland and Moleko, 2000; Njoya, 2002). Inanda Dam is situated some 32 km upstream of the river mouth and has led to a slight reduction in the mean annual discharge to the lower reaches of the Mgeni from its pre-dam 323 million m³ to 309 million m³ (Garland and Moleko, 2000).

Other influences on the Mgeni River and Estuary have been sand winning operations above the estuary within the Springfield Flats, and the affects of industrialization of the Springfield Flats. During the 1970s and early 1980s production of sand from the river was calculated to be approximately 81 000 metric tonnes per year, this however decreased to about 21 000 metric tonnes in 1997 (Garland and Moleko, 2000).

3.9. Previous research on the Mgeni Estuary

Prior to the construction of the Inanda Dam in 1989, studies were focused mainly on the biology, such as micro- and macro-fauna and various flora (Brown, 1971; Simpson *et al.*, 1972; Begg, 1984; Steinke and Charles, 1986; Cooper, 1986; Cooper and McMillan, 1987), hydrology (National Research Institute for Oceanology, 1982), sedimentology and flooding of the estuary (Begg, 1978; Begg, 1984; Cooper and Mason, 1985; Cooper, 1986; Badenhorst *et al.*, 1989; Orme, 1974; Cooper *et al.*, 1990). Immediately prior to construction, several studies were also conducted on the potential effects of the dam on the Mgeni Estuary (Council for Scientific and Industrial Research, 1984; Diab and Scott, 1989; Scott and Diab, 1989).

Since completion, studies have focused on assessing the influence that the dam has had on the estuary (Moleko, 1998; Garland and Moleko, 2000; Njoya, 2002). Diab and Scott (1989), and the Council for Scientific and Industrial Research (CSIR, 1984) predicted that the reduction in river velocity below the dam would lead to an increase in deposition of sediment into the estuary and increased periodic mouth closure. Moleko (1998) however, showed that this would not be the case, if the dam's management policies were followed and peak flow rates were increased. This policy implementation is shown by an increase in flow rate from 1960 to 1981 compared to the more recent 1990 to 1997 period. Njoya's (2002) study, however, showed that due to changes in the dam's management release policies, there had been an overall reduction in the maximum daily average flow rate contrary to the results stated in Moleko's (1998) study. He concluded that there would be a gradual fining of sediment in the estuary, due to the dam and removal of coarse sand by sand winning activities and the continued erosion of the southern channel bank.

The September 1987 flood became the focus of numerous studies with Cooper (1993) calling it a "fortuitous occurrence" allowing for an assessment of such an event on the sedimentology of the estuary. Within the study, he focused on the historical development and changes in the morphology of the estuary from 1931 to 1991, the effects of the floods, the post flood recovery as well as creating a conceptual model for river-dominated estuaries. The Badenhorst *et al.* (1989) survey of the September 1987 flood dealt in depth with the effect of the flood on various rivers along the KwaZulu-Natal coast, with regards to sedimentation, flood duration, flood levels and damage. Their study highlighted the effects of catastrophic flooding on small estuaries with regards to the removal of accumulated sands, as well as determining the main geomorphological controls of erosion and the dynamics of the post-flood recovery.

Keinzle *et al.* (1997) based their studies on the hydrology and water quality of the Mgeni Catchment using a modeling approach. They identified the Valley of a Thousand Hills as the main source of sediment input into the Mgeni River and showed that this is due to factors such as topography, soil type, geology as well as increased water runoff due to a high population density. Keinzle *et al.* (1997) were able to determine that during flooding conditions, such as the 1987 flood, the transported sediment load can increase by up to 267 times its normal transport load and

discharge can reach 7200 m³/s as during the April 15, 1856 flood (Smith, 1992) (Table 3.1).

Table 3.1. Table of historical floods, flood level above mean sea level (AMSL), maximum depth of scour, and discharge. The September 1987 flood was only the 3 largest flood recorded since 1854 (Smith, 1992).

Date	Flood Level AMSL (m)	Maximum Depth (m)	Discharge (m ³ /s)
14 November 1854	7.64	5.12	2050
16 December 1854	7.48	4.97	1950
30 September 1855	7.95	5.4	2260
13 December 1855	7.48	4.97	1950
15 April 1856	9.44	10.45	7200
30 August 1868	7.48	8.02	4450
31 May 1905	6.68	4.22	1460
27 October 1917	9.08	9.43	5920
14 June 1935	6.83	4.36	1550
29 September 1987	8.36	8.8	5200

Singh (2001) used the application of the ACRU Agrohydrological Model, to model the stream flow and sediment yield of the lower Mgeni Catchment. The stream flow results indicated a season of “low” flow; with a mean monthly flow rate ranging from approximately 150 m³/s to 500 m³/s from April to September, and “high” flow rate ranging from approximately 580 m³/s to 1800 m³/s for the rest of the year. This is compared to flood conditions which have flow rates from 1460 m³/s, as in May 1905, to 7200 m³/s, as in April 1856 (Smith, 1992) (Table 3.1).

CHAPTER 4

Historical evolution

4.1. Introduction

The impact of urbanization along the banks of the Mgeni Estuary, as well as within the catchment area, results in a departure of the estuary from its former natural state towards a new state of equilibrium. To better understand the most recent of these changes it is necessary to understand the estuary's longer term dynamics so as to compare and contrast the short term changes and quality. This will enable a better understanding of the anthropogenic effects on the estuary as it deviates from its previous state. This study follows closely on that of Cooper (1986, 1991) continuing and updating it until 2007.

4.2. Methodology

Aerial photography, oblique images, and an 1860 Port Natal chart were used in conjunction with a literature study of the area to document the historical changes to the estuary. This allowed for the assessment of the long-term sedimentological and geomorphological changes within the estuary, before anthropogenic influences became a dominating factor in the development of the estuary. The use of aerial photography in establishing long term sedimentological and geomorphological trends of South African estuaries has been previously demonstrated by Van Heerden (1984), Esterhuysen and Reddering (1985), and Cooper (1986, 1991). Morphological changes in the Mgeni Estuary have previously been quantified until 1982 by the National Research Institute for Oceanology (1982) and Cooper (1986).

A series of aerial photographs dated between 1931 and 2003 were obtained from the eThekweni Municipality. These photographs were geo-referenced and mosaic'ed to obtain a single geo-referenced image from which the sub-aerial sandbars, mangrove populations and general outline of the estuary were digitized. The digitized images allowed for easier comparison of the geomorphology of the estuary through the time series. However, due to aerial photographs having been taken at different times within the tidal cycle undetermined variations in the amount of sub-aerial sediment exposure were incurred.

In addition to aerial photographs and the literature review, digital terrain models (DTMs) were created for the periods of 1986, 1987, 1989 and 2006. The historical models (1986, 1987 and 1989) were created using cross-sectional data originally surveyed by Cooper (1986, 1991). Data were transformed into digital form and used in combination with aerial-photograph interpretations to create contour maps. The digital contour data were then gridded to form DTMs. For the 2006 DTM, a Leica GS20 system was used to survey the estuary to sub-centimetre accuracy, achieved by the use of a base station and rover receiver. Coverage of the area was conducted using this system with a line spacing of between 50 m and 100 m.

4.3. Results

4.3.1. Holocene evolution of the Mgeni Estuary

Cooper (1991) discussed the Holocene evolution of the Mgeni Estuary from a combination of: borehole cores; fossil sea cliffs and beach ridges north of the present day river mouth; a change in dune and barrier orientation near the present day tidal inlet; the surrounding geomorphology and the incised river-mouth channel. Evidence of the migration of the position of the Mgeni Estuary is shown by paleo-channels flowing south and exiting through what is now Durban Harbour during the last glacial maximum (18 000 B.P). The anastomosing nature of the Mgeni River is further evident from pinger seismics data, which shows numerous incised paleo-channels within the Durban Bight (Garlic, 2008).

Cores obtained during the construction of bridges over the Mgeni River (Kantey and Templar Civil Engineers, 1964; Francis, 1983) revealed the bedrock channel to be at approximately -56 m below the present Mgeni River mouth. The valley fill sequence is dominated by medium to coarse sediment (Figure 4.1). This is believed to have occurred in the middle stages of the Holocene (Ramsay and Cooper, 2002) (Figure 4.2). The upper part of the sequence is characterised by coarse grained sediments, probably related to barrier retreat during a possible marine transgression. These deposits of sediment containing marine molluscs are overlain by fluvial gravels sands and mud layers at depths of -12 m to -8 m below mean sea level (MSL).

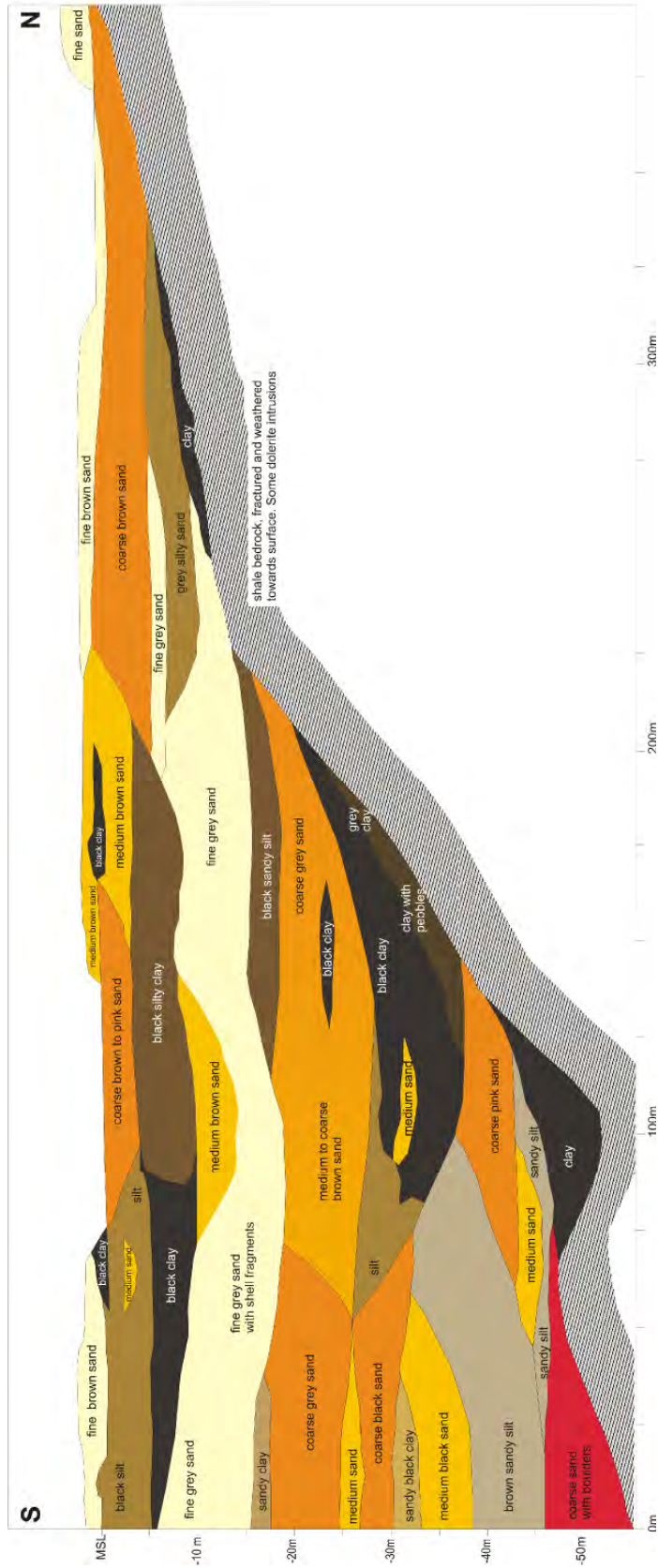


Figure 4.1. Cross sectional profile through the Mgeni Estuary at Athlone Bridge (after Orme, 1976). The cross section shows an infill dominated by medium to coarse sand with isolated pockets of mud and clay, and a continuous unit of fine sand at approximately 10 m below MSL.

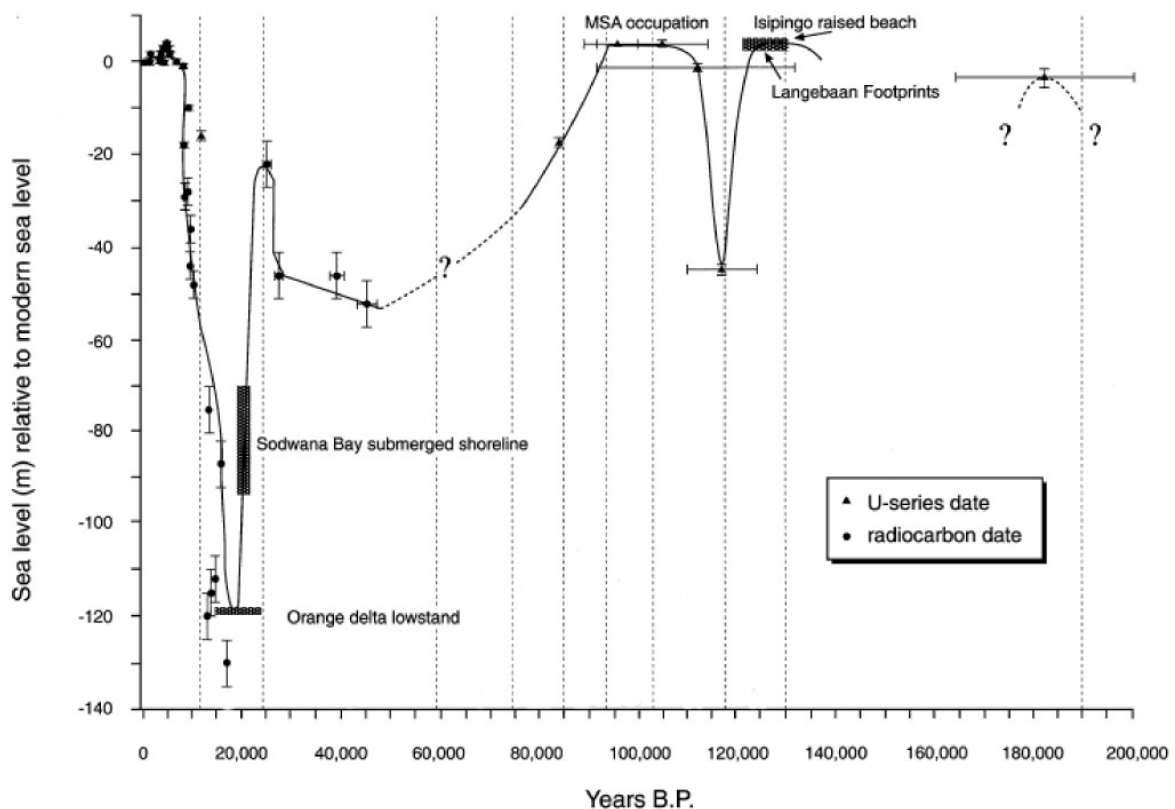


Figure 4.2. Late Quaternary sea-level curve for South Africa based on sea-level indicators from the South African coast and shelf (after Ramsay and Cooper, 2002). Note the sea-level of the last glacial maximum (LGM) at the Orange delta lowstand with the subsequent Flandrian Transgression to the present day Holocene sea-level.

This overlying fluvial sediment reflects an influx of sediment from the catchment as the paleo-valley was finally infilled (Cooper, 1991; Cooper, 1993).

During the late mid-Holocene, the Mgeni River flowed southward behind a transgressive coastal barrier into Durban Bay. This is supported by the topography of the area and the presence of coarse grained river sands in the shallow subsurface of the low lying area between the present day river mouth and Durban Bay (King, 1962).

Mid 1800s to 1899 geomorphology

The 1860 Port Natal Chart (Figure 4.3) shows that the estuary exited into the sea north of its present day position, between two sand barriers approximately mid way along the

spit. A lagoon extended northward where Beachwood Creek now flows. According to Cooper (1986), Russell (1899) noted that this lagoon was predominately closed and contained fresh water.

Two central island bars are also present on the 1860 chart, which appear to be un-vegetated, probably due to the removal of sandbars during the preceding April 1856 flood. This flood event had a discharge of approximately 7200 m³/s, which is the highest recorded flood discharge from the Mgeni Estuary to date. The southern Mgeni Estuary bank contains evidence of a flood channel that flowed into Durban Bay, as in the Holocene, marked by an elongated area of marshland. Maps of the mid-eighteenth century suggest that this was once the main channel with the river flowing into the Durban Bay (Cooper, 1986). This flood channel was last utilised during the floods in 1846 (Goetzche, 1966, in Cooper, 1986) and 1856 (Russell, 1899, in Cooper, 1986).

1900 to 1930

During the early part of the 20th century, there is evidence of a prominent central island bar extending to the upper reaches of the Mgeni Estuary from postcards of the time. The central island bar was probably removed during the October 1917 flood, which had an estimated discharge of 5920 m³/s (Smith, 1992). This is the second highest discharge noted in the estuary in the past 160 years. Other periods of higher than normal runoff or discharge were recorded in May of 1905 (Smith, 1992), and July of 1924 (Cooper, 1991). Construction in the Mgeni Estuary began during this period with the building of an artificial groyne on the southern bank in 1927, in attempt to stabilise the tidal inlet and prevent it from migrating northwards. This resulted in the deposition of fine grained sediment on the inside bend of the channel as the channel was diverted from its northwards course, leading to a reduction in size of the lagoon forming what is now known as Beachwood Creek (Cooper, 1986).

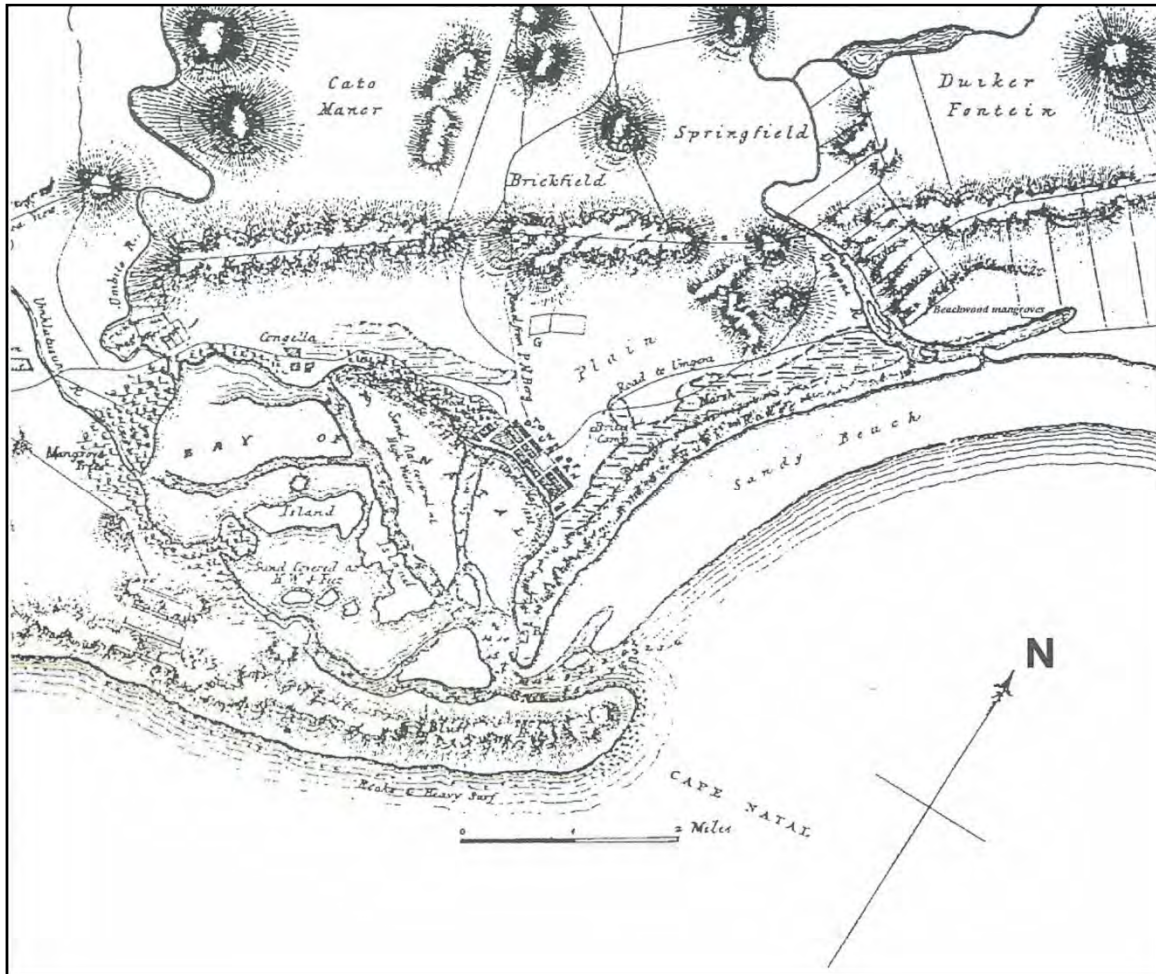


Figure 4.3. 1860 Port Natal chart showing the mouth of the Mgeni River diverted northwards forming an elongated lagoon which is now forming the Beachwood Mangrove area. The marshland extends southwards from the Mgeni River towards the Bay of Natal marking the former course of the river. Note the presence of the central island bar even in 1860.

1931 to 1950

Aerial photographs show that in December 1931, the Mgeni Estuary was predominantly a shallow braided river channel system, dominated by unvegetated, subaerial sandbars (Figure 4.4.A). These bars probably formed from the re-accumulation of sediment washed out to sea during the 1917 and 1924 floods, which removed the large central island bar present pre-1917. The reduction of the lagoon that occupied the Beachwood Creek area is evidenced by the presence of salt marshes on the northern bank. The morphology of the bars suggest that the dominant transport direction was seawards, with sediment addition onto the upstream side of the sandbars. Further construction during this time was that of the railroad bridge near the head of the estuary as well as the old Athlone Bridge. Ebb tidal deposits are also described at this time (Cooper, 1986; Cooper 1991; Cooper, 1993).

A large volume of sediment was deposited in the estuary following the flooding in 1935, further reducing the size of Beachwood Creek. Additional sediment was welded onto the northern bank, where Beachwood Creek enters the main channel. Sediment was also deposited onto the southern bank near the Connaught Bridge and subsequently anchored by vegetation, forming a major side-attached bar. A central island bar within the main channel, located around the old Athlone Bridge, was stabilised by vegetation. During this period, a flood tidal delta was also present instead of the ebb delta evident in the earlier 1931 aerial photos (Figure 4.4.A). There was a northward shift in the mouth position away from the artificial groyne, similar to what is seen prior to periods of present day mouth closures. There is a large hiatus in aerial photographs between 1937 and 1951.

1951 to 1960

The side-attached bar in the upper reaches of the Mgeni Estuary became part of the flood plain by 1951. This caused a narrowing of the channel, leading to a more defined funnel shaped estuary (Figure 4.4.B). The coalescence of the mid-channel bars, forming a larger more dominant central island bar, resulted in the bifurcation of the estuary channel. The raised nature of this central island bar allowed for scattered trees and shrubs to take root. The development of additional intertidal sandbars on both the north

and south banks of the central island bar further constricted both channels (Cooper, 1986; Cooper, 1991; Cooper, 1993) (Figure 4.4.B).

By 1959, the narrowing of the coast-parallel Beachwood Creek lagoon allowed for the development of sparsely vegetated mud flats with isolated mangrove colonies. Further construction of the Elis Brown Viaduct, which had been completed 200 m upstream from the tidal inlet, resulted in the deposition of sediment around the pilings, thereby anchoring part of the flood tidal delta to the adjacent areas (Cooper, 1986; Cooper, 1991; Cooper, 1993).

1961-1970

The most noticeable feature from the 1963 series of aerial photographs is the shift in the tidal inlet to the north, running northwest across the barrier. This is similar to the migration of the estuary mouth directly prior to periods of mouth closure. This time period is also characterised by the re-appearance of an ebb tidal delta.

Additional smaller island bars had become welded onto the main central bar by 1967, due to the steady shallowing of the channels between the braided bars. The now vegetated central island bar was furthermore increased in size by downstream accretion and upward growth. Various side-attached bars had also become vegetated and incorporated into part of the flood plain thus further constricting the estuary mouth (Figure 4.4.C). Mangroves had started to colonise the central island bar on the upstream side, in addition to the areas in and adjacent to Beachwood Creek. During the construction of the new Athlone Bridge, the southern channel was blocked upstream of the construction site (Figure 4.4.C). This resulted in the reduction of fluvial flow, promoting the settling of fine sediment in the southern channel. Further coastal retreat north of the artificial groyne had also occurred (Cooper, 1986; Cooper, 1991; Cooper, 1993).

1971 to 1980

The central island bar had become entirely vegetated by 1973, with mangrove colonies on the lower reaches of the bar. Additional braided bars had become attached and incorporated on the main central bar. The redevelopment of the flood tidal delta had

occurred as the tidal inlet had reformed against the artificial groyne. Washover fans forming over the spit had led to the landward widening of the barrier. Additional constriction of the estuary occurred due to sedimentation anchored by vegetation on the northern bank. A small intertidal bar had developed at the intersection between the estuary and Beachwood Creek due to the increase in washover fans into the creek. Construction of sand-trapping baffles and artificial dunes in 1975, aimed at preventing the deposition of additional sediment into the creek (Cooper, 1993) (Figure 4.4.D).

All intertidal sandbars had become incorporated into the main central island bar by 1976. The central island bar itself had become more prominent, although erosion of the sides had taken place, resulting in the narrowing of the bar and deepening of both north and south channels (Figure 4.4.D). Additional sedimentation had occurred on the northern bank adjacent to Beachwood Creek, anchored by mangrove colonies. Further washover fans had developed over the barrier leading to an inland widening of the spit. The mouth had maintained its position against the artificial groyne on the south bank (Cooper, 1986; Cooper, 1991; Cooper, 1993).



Figure 4.4. A to D shows a series of historical diagrams of the Mgeni Estuary from 1931 to 1976, showing the establishment of the central island bar and the constriction of the head of the estuary. Note the position of the tidal inlet in the 1963 aerial photograph northwards of its usual position. This northwards shift generally occurs directly prior to mouth closure. The 1963 aerial photograph also shows the presence of a poorly developed flood tidal delta, which is again present in the 1976 photograph.

1981-1990

In early 1980, intertidal sandbars on the landward margin of the spit had been extensively eroded, and the sandbar at the mouth of Beachwood Creek had been extended. A large flood tidal delta had developed in the estuary, which became submerged during high tides. By 1981, the flood tidal delta had become detached from the flood ramp and was migrating north-westwards. Furthermore, washover fans had formed towards the mouth of Beachwood Creek, causing the spit to extend even further inland. The remaining braided bars had become either incorporated onto the side banks or the central island. This resulted in the central island bar becoming well established and vegetated, slowly extending landward with the accumulation of sediment towards the head (Cooper, 1986; Cooper, 1991; Cooper, 1993).

The flood tidal delta had extended past the Ellis Brown Viaduct in both the north and south channels and an ebb tidal delta was also visible by 1984. The intertidal sandbar at the mouth of Beachwood Creek had also increased in area due to mud deposition. In February 1985, a wide estuary mouth had formed due to flooding, also resulting in a plume of sediment deposition extending out to sea. The spit had reformed prior to Cooper's 1986 study, with a configuration similar to that of November 1979 (Cooper, 1986).

Cooper's initial study of the area was conducted in 1986. The area had been relatively stable in the previous 10 years with little change. The upper 700 m of the estuary consisted of a constricted, narrow channel, with an average width of 60 m. This channel was confined between a prominent bedrock outcrop on the northern bank and a well-developed, vegetated side-attached bar on the southern bank. The estuary widened into a typical funnel shape in the lower 1.8 km (Figure 4.4.E), with a vegetated central island bar, which had a mean elevation of 2 m above MSL. This central island bar caused the channel to bifurcate, and recombine in the back barrier, before reaching the tidal inlet. The tidal inlet was generally located against the artificial groyne on the southern bank (Cooper, 1991; Cooper, 1993).

The tidal range in the estuary was limited to less than 1.4 m due to the constricted nature of the tidal inlet. This classifies the estuary as microtidal (Davies, 1964; Hayes,

1979). The salt wedge extended 2.5 km upstream during high tides, with limited upward mixing, by wind and wave action, due to the protected nature of the estuary behind the barrier (Cooper, 1991; Cooper, 1993).

An approximate volume of sediment was calculated to a base level of -5 m below MSL using DTMs created from Cooper's (1986) cross-sections (Figure 4.5.A). This -5 m baseline was chosen as this was the average depth of scour, which occurred during the September 1987 flood. The calculated volume of sediment within the estuary prior to the 1987 flooding event, was calculated to be 3 053 459 m³, to the -5 m below MSL baseline.

Flooding occurred in KwaZulu-Natal from the 26th of September to the 1st of October, 1987, with 800 mm of rain falling within a 5 day period. Water levels in the lower Mgeni Estuary rose to 5 m above the normal high tide level during this flood, resulting in flooding of the southern bank and the Mangrove swamp in the Beachwood Creek to the north. The floods resulted in a decrease in salinity to zero throughout the estuary as well as an increase in the suspended sediment concentrations from 165 mg/l (Brand *et al.*, 1967, in Badenhorst *et al.*, 1989) to 5698 mg/l (Badenhorst *et al.*, 1989) an increase of 3453%. Surface current velocities of 6 to 7 m/s were recorded in the estuary, with the estimated flood discharge around 1030 m³/s. These currents resulted in the scouring of the river bed to depths of over 5 m, and the complete removal of the intertidal barrier, and the central vegetated island (Figure 4.5.B). The flood also widened the estuary with most lateral erosion occurring on the southern bank (Badenhorst *et al.*, 1989) (Figure 4.4.F). Survey lines were conducted 20 days post flooding by Badenhorst *et al.* (1989) documenting the extent to which the erosion that had occurred in the estuary. A 3D model of the scouring was created utilising these survey lines, allowing for an estimate of the volume of sediment removed from the estuary by the flood event. Using a baseline for the calculation of -5 m below MSL, the estimated average depth of scouring, approximately 3 685 138 m³ of sediment was removed, greater than the calculated 3 053 459 m³ of sediment present in 1986 based on Badenhorst *et al.* (1989) cross sectional data (Figure 4.5.A and Figure 4.5.B). The additional sediment was derived from the complete removal of the southern side-attached bar and part of the mangrove colony on the northern bank, which was not taken into consideration during the 1986

calculation. The majority of the scouring occurred in the northern channel, which was eroded down to a depth of over 4 m near the head of the estuary. This was due to constriction, increasing the flow velocity, which was further exacerbated by the canalisation of the Mgeni River upstream of Connaught Bridge and the presence of hard bedrock on the northern bank. In contrast, the southern channel tended to be eroded laterally rather than vertically. The centre of the estuary was subjected to the least amount of downward erosion controlled by the pre-flood geology and geomorphology. Scouring increased towards the tidal inlet of the unconsolidated marine sediments resulting in the complete removal of the barrier.

Cooper (1991, 1993) gave a detailed description of the flood recovery, from the 10th of October 1987 to 17th of April 1990. The completion of Inanda Dam in 1989, some 32 km upstream from the estuary, led to a change in fluvial dynamics within the Mgeni Estuary. This resulted in the need for detailed studies to be conducted in the estuary in order to identify the long term affects the dam might have on the estuarine system.

A calculated redeposition of 2 793 439 m³ sediment back into the estuary (75% of the estimated loss) had occurred by 1989 (Figure 4.4.G). The side-attached bar on the southern bank, at the head of the estuary, had already started to redevelop, but remained unvegetated. A submerged sandbar could be identified between Athlone Bridge and the Ellis Brown Viaduct toward the northern bank from the DTM and aerial photographs (Figure 4.4.G and Figure 4.5.C). This allowed the main channel to develop towards the southern bank in the lower reaches of the estuary, and against the northern bank in the upper reaches where the river mouth was constricted. The barrier had begun to redevelop by this time, however, it was substantially narrower and approximately 1 to 2 m above MSL, compared to approximately 3 m above MSL recorded in 1986 (Figure 4.5.A and Figure 4.5.C). This allowed for the development of the large washover fans to form directly behind the barrier. The tidal inlet remained predominantly open against the artificial groyne on the southern bank (Figure 4.4.G).

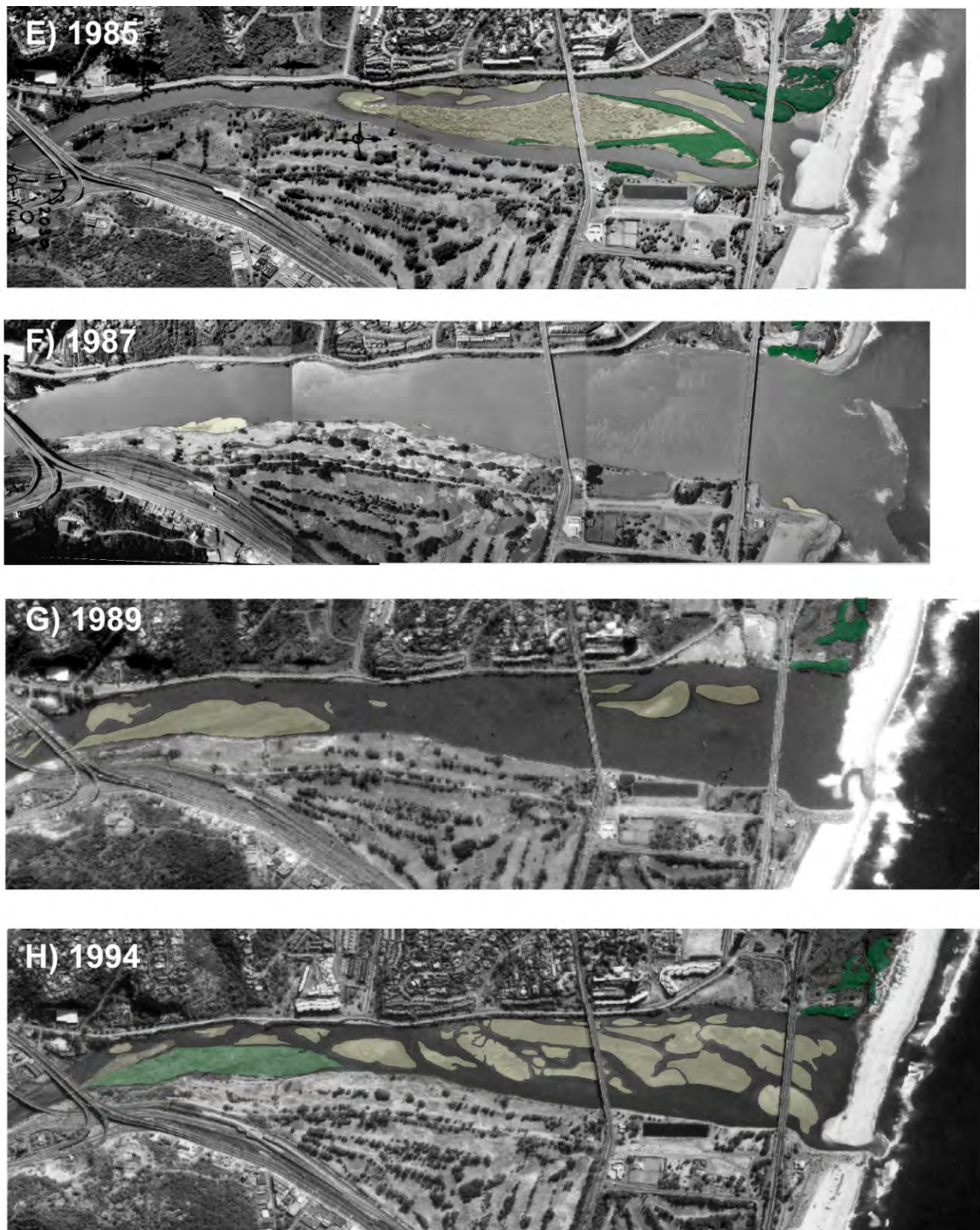


Figure 4.4. E to H represent a series of historical diagrams of the Mgeni Estuary from 1985 to 1994, showing the removal of the central island bar during the September 1987 flood, and the initial stages of re-establishment of sandbars within the estuary. The September 1987 flood removed all sandbars within the estuary in addition to widening it. The initial re-establishment started with an isolated bar near the northern bank, present in the 1989 aerial photograph. By 1994 a large amount of sediment had been re-deposited in the estuary with sandbars concentrated along the northern portion of the estuary.

1991 to 2000

Large sub-aerial bars had begun to re-establish themselves within the estuary by 1994 (Figure 4.4.H). The bar towards the head of the estuary had become attached and revegetated, thus constricting the head of the estuary. A decrease in flow rate with the widening of the estuary resulted in the deposition of a small sandbar. Subaerial, braided sandbars started to develop from the middle of the estuary towards the barrier predominantly against the northern bank prograding southwards, probably due to the tidal effects that now dominated. The flood tidal delta continued to increase in size, acting as a sediment supply mechanism, for the majority of the sandbars (Figure 4.4.H).

The 1997 aerial photographs show that the sub-aerial bars had become well established against the northern bank, with isolated patches of pioneer vegetation taking root (Figure 4.4.I). The aerial photograph, unfortunately, appears to have been taken during high tide, thus the less prominent sandbars are not apparent. A faint remnant of the submerged flood tidal delta can however be observed. The flood tidal delta appears elongated, migrating up-stream beneath the Ellis Brown Viaduct (Figure 4.4.I).

A further increase in vegetation density had stabilized the sub-aerial bars against the northern bank by 1999 (Figure 4.4.J). The estuary had begun to infill, shallowing throughout. Additional sandbars had developed in the middle of the estuary, becoming welded onto the side-attached bar. The sandbar located at the widening of the estuary had become well developed, diverting the main channel further towards the northern bank. The formation of bedforms on the sandbars became apparent, allowing for rudimentary sediment transport directions to be determined, showing the predominant upstream migration of sediment. Sediment is piled up on the northern bank due to refraction, with minor downstream transport occurring only at the head of the estuary (Figure 4.4.J).

2001 to 2007

The estuary appeared to have reached equilibrium by 2003, with little to no change being observed between 2003 and 2007 (Figure 4.4.K). The DTM model shows that at this stage there is a volume of 3 222 317 m³ sediment within the estuary above the -5 m baseline chosen for the study (Figure 4.5.D). This is an increase of 168 855 m³ sediment

relative to the volume estimated from Cooper's (1984) cross-sections (Cooper, 1986; Badenhorst *et al.*, 1989) (Figure 4.5.A). The majority of the sedimentation had occurred in the upper regions of the estuary, where it has accreted up to a height of 4 m in some areas. However, due to the underlying topography scoured by flooding, a rise in the sub-bottom topography had formed towards the centre of the estuary where the central island bar was previously situated (Figure 4.5.D).

Bedform analysis during the pilot study identified asymmetric sand waves, with wavelengths up to 100 m and amplitudes of 30 to 40 cm, with crests trending approximately 294°. These asymmetric sand waves indicate that the main direction of flow and sediment transport in the lower reaches of the estuary was from the inlet upstream towards the head. Superimposed on the sand waves, are minor ripples that varied in wave length from 2 to 75 cm with amplitudes of up to 5 cm. The ripples are predominantly lingoid and flat topped with varying orientation indicating varying flow directions. Ripples on the northern edge of the flood tidal delta show the direction of the ebb tide in the ebb channel being approximately 260° towards the tidal inlet and increasing to approximately 320° towards the centre of the estuary due to refraction. The side-attached bar ripples were orientated in a southerly direction, which correlates to water draining off the sandbars into the main channel, leaving behind mud drapes. The lack of defined ripples on the lower side-attached bars indicates reduced flow in the area and therefore lower energy. It must be noted that these bedform measurements were taken during periods of low tide as these bars are predominantly submerged during high tides, resulting in the minor bedform directions representing only the ebb flow direction (Tinmouth, 2005).



Figure 4.4. I to K represents a series of historical interpreted air photographs of the Mgeni Estuary from 1997 to 2003, showing the dynamics of sandbars within the estuary. Sediment is progressively concentrated against the northern bank forming a series of side-attached bars. In 1997 isolated pockets of the first post flood vegetation colonised supratidal bars, increasing rapid covering a large portion of the sand bars by 1999. By 2003 the flood tidal delta had become a dominant feature in the mouth.

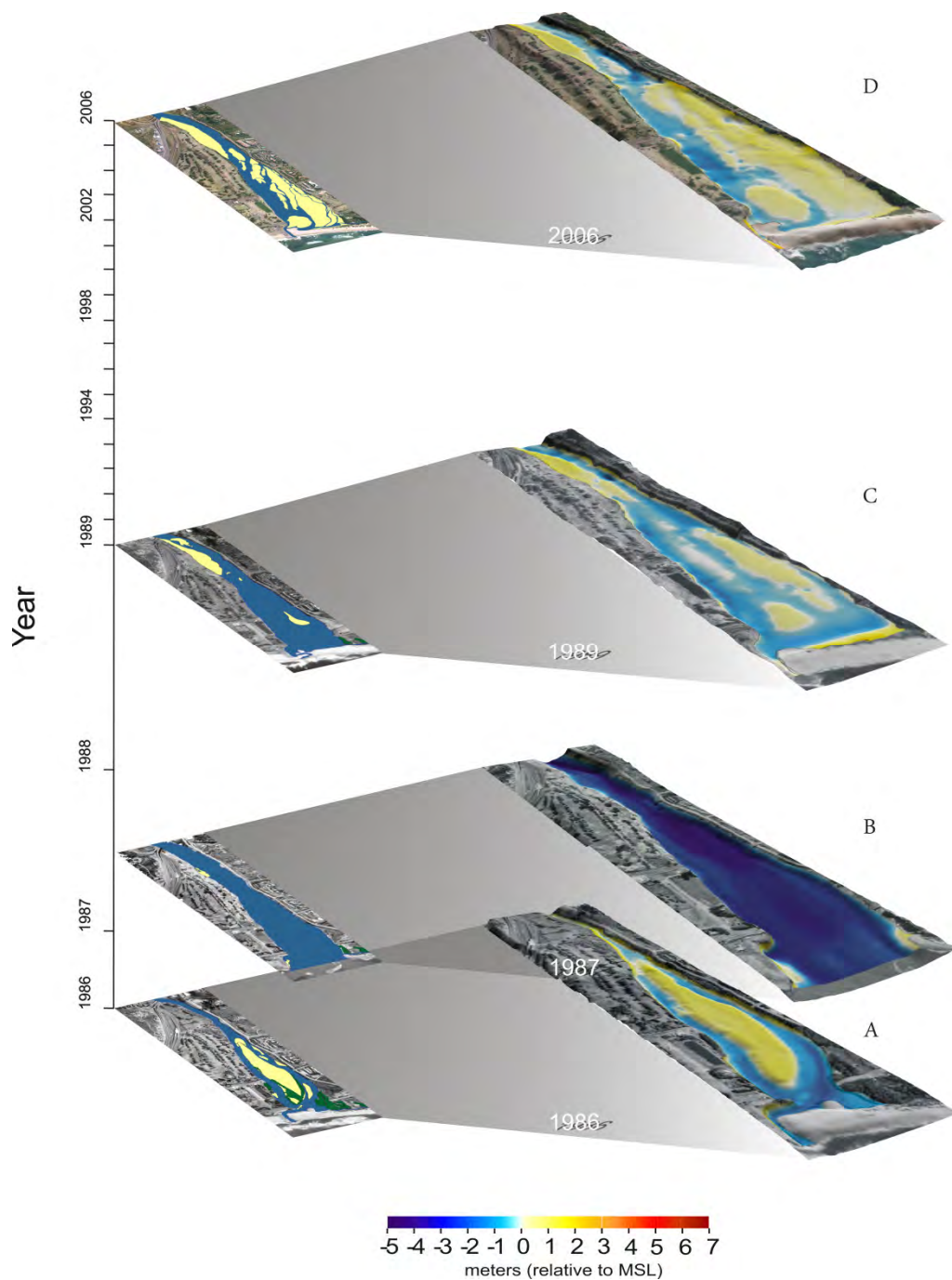


Figure 4.5. A to D represents a series of DTMs of the Mgeni Estuary from 1986 to 2006. B) shows the depth of the estuary directly after the 1987 flood. These depths are shallower than the scour depths due to the rapid deposition of gravels and muds once the flood waters had subsided. By 1989 (C) most of the sediment had been redeposited back into the estuary with the average depth being shallower than 1986 (A). The rate of deposition rapidly decreased between 1989 (C) and 2006 (D) with only 428878 m³ of sediment being deposited in the 17 year period.

4.4. Discussion

The dynamics of the estuary were controlled by ebb-flow sediment transport prior to the 1987 flood, forming a large central island bar and a bifurcated main channel. This bar was repeatedly removed during major flooding events and subsequently reformed post-flooding. A change in this pattern occurred after the 1987 flood whereby the development of the sand bars within the estuary was concentrated against the northern bank. This phenomenon may be related to the completion of Inanda Dam at this time. The dam resulted in a prolonged period of low flow velocities during the flood recovery period, an important period that appears to predetermine the geomorphology of the estuary until the next flooding event.

The post Inanda Dam modern morphology of the estuary is dominated by a well developed sub-aerial sandbar attached to the northern bank, which has slowly widened southwards. This sandbar appears to be fed by the development of a flood tidal delta into the estuary. The flood tidal delta periodically becomes detached allowing for the upstream migration of the marine sediment where it is then deposited and subsequently stabilized by intertidal mud drapes. This process has led to an increase in the volume of sediment contained within the estuary from a calculated 3 053 459 m³ during the ebb-dominated system of pre-1987 to 3 222 317 m³ at present.

The presence of the flood tidal delta is most likely related to the decrease in fluvial discharge allowing for an increase in marine incursion. The mouth of the estuary has become stabilised against the artificial groyne on the southern bank, although a slight northward migration prior to mouth closure was observed during the study period. This is again probably due to the decreased fluvial discharge resulting in the estuary being unable to maintain an open mouth. Marine sediments are therefore deposited on the leeward side of the artificial groyne as sediment is transported northwards by littoral drift.

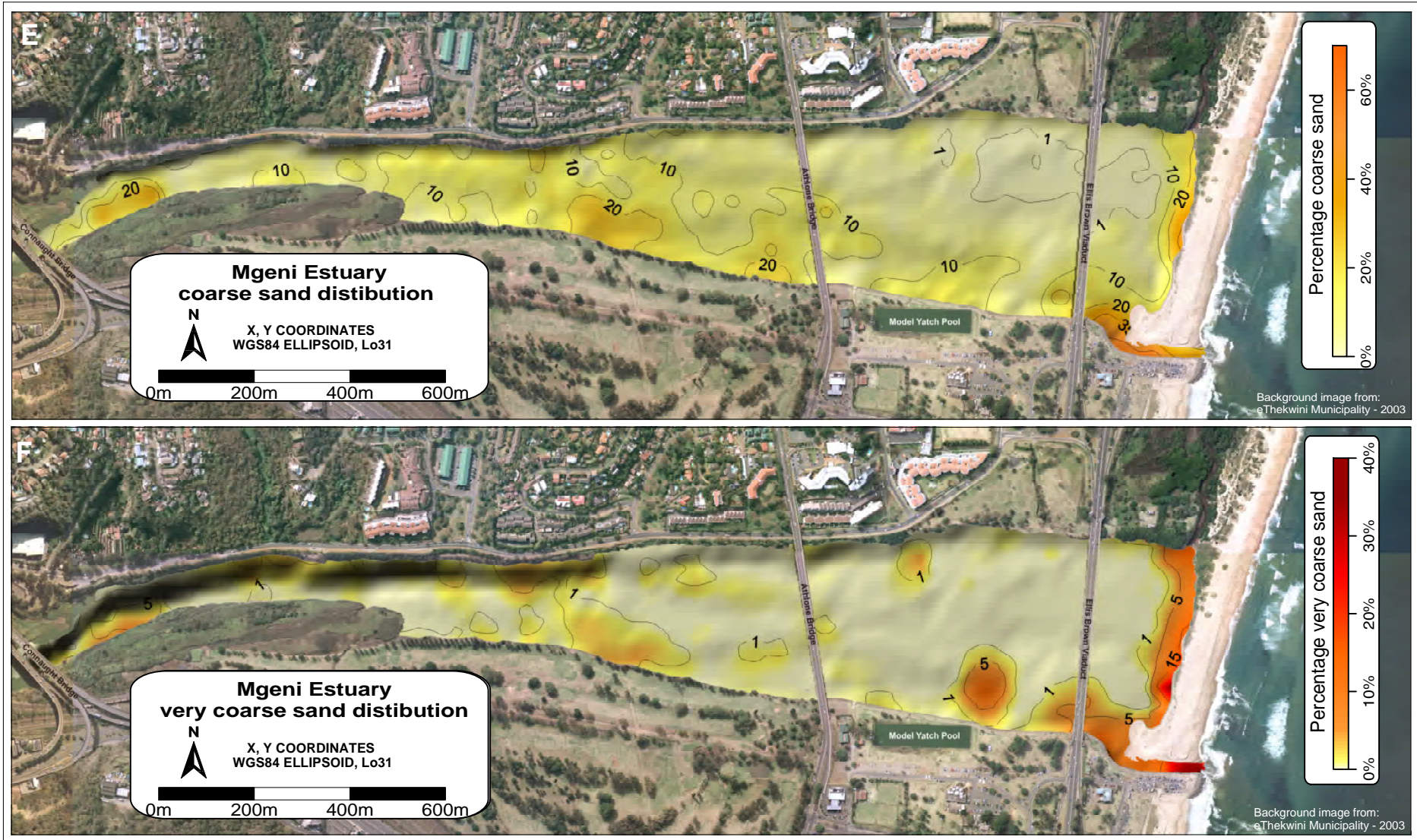


Figure 5.2. E) The 2006 distribution of coarse sand within the Mgeni Estuary. F) The 2006 distribution of very coarse sand within the estuary. The high current velocities required to transport coarse to very coarse sediment restrict the sediment to the areas of the main channel and tidal inlet. Very coarse sand is also located in the form of washover fans on the estuary side of the supratidal barrier.

CHAPTER 5

Sedimentology

5.1. Introduction

Estuaries are widely regarded as net accumulation zones for sediment, receiving sediment from a variety of sources and transport mechanisms including marine, fluvial, and aeolian. (Cooper, 2001). The transportation and deposition of these sediments is predominantly governed by the dynamic processes that circulate and mix estuarine waters (Meade, 1972). The present-day surface sediment distribution can therefore be used to better understand the modern dynamics acting within estuary. These results can then be compared to previous studies to gain a better understanding of any changes that may have occurred in the estuary. The subsequent section aims to describe various present-day sediment patterns and dynamics occurring in the estuary in order to identify changes and to aid in the possible reclassification of the estuary.

5.2. Methodology

A total of 500 surface sediment samples with an approximate sample density of one sample every 50 m to 100 m were collected and stored in 250 ml plastic bottles to avoid loss of the fine fraction and to reduce the possibility of contamination. Sample locations were established with a handheld *Garmin eTrex Venture* GPS system. 369 samples were collected between May and September 2005 (Tinmouth, 2005) and additional 131 samples collected between January and February 2006 (Figure 5.1) (Appendix A.1). Due to the extended period of sampling and the dynamic nature of estuaries, random samples were retaken on various sampling trips to determine possible changes. Results from these samples showed that changes in the estuary during these two periods were negligible; therefore, the description and interpretation presented by Tinmouth (2005) have remained largely unchanged (Appendix A.2).

Sample site selection used here differed from that of previous studies (Cooper, 1986; Moleko, 1998; Njoya, 2002), which sampled along transect lines.

Figure 5.1 A) Shows the 500 sediment sample sites distributed throughout the estuary. This high sample density allowed for the creation of more precise sediment distribution maps. Sediments were analyzed for various grain sizes, statistical parameters, carbonate content and organic content. Certain samples were also analyzed under microscope. B) The localities of the cores taken. A total of 25 cores were taken throughout the estuary. These sites were limited to shallow regions due to logistics. The cores were logged and sampled at each horizon and analyzed for grain size.

Samples in this study were initially taken from areas determined by the observed changes in the grain size during the field investigations. Further sample sites were identified by combining the initial results with the 2003 aerial photograph of the study area. The decision to use this method rather than sampling transects was influenced by the present day complexity of the sandbars and channels in the estuary compared to that of a single central island in Cooper's 1986 study. This method was also used to increase the gridding resolution.

Particle size analysis was undertaken for all collected samples and selected samples were also used to determine the organics and carbonate content. The grain size analysis or particle size distribution (PSD) of these samples were defined by both standard sieving technique and Malvern laser grain size analysis, depending on whether the sample contained particles greater than 1.4 mm. Samples with particles greater than 1.4 mm were oven dried and prepared for sieving as the coarser grains (> 1.4 mm) resulted in blockages in the Malvern Mastersizer pump. The correlation of the two techniques may vary by up to 10%, in certain size classes as estimated by Shillabeer *et al.* (1992). The variation between the two sets of results is due to laser diffraction using the mean grain diameter to calculate the percentage of the grain size class as a volume percent, whilst the sieving techniques evaluates the intermediate size of 3-axis to calculate the percentage in weight percent.

Numerous techniques have been published on this subject in an attempt to correlate the results (Singer *et al.*, 1988; Shillabeer *et al.*, 1992; Loizeau *et al.*, 1994; Murray and Holtum, 1996; Konert and Vandenberghe, 1997), however, the variation in densities of the constituents within the sediments can drastically influence the re-calculated results (Loizeau *et al.*, 1994). This variation, however, was deemed acceptable as it falls within the possible error of random sampling and the testing techniques used.

5.2.1. Malvern Mastersizer 2000 analyzer

The analyzer operates by pumping the suspended sediment through a thin slow-cell, forcing the particles to interact with a laser beam (Ayers, 2004). The grain size is determined by the diffraction of the laser beam by the moving grains passing through the cell. The deviation due to the interaction of the laser beam is detected by sensors, which

can then be used to calculate the particle sizes and distribution. The Malvern Mastersizer 2000 can analyze up to 1000 particles per second, but should not be overloaded due to inaccuracies that might be incurred from multiple diffractions and interference (Ayers, 2004).

Before a sample was analyzed, the system was flushed with water to avoid contamination. It was then calibrated for the background particle level of the water into which the sample was placed. Due to the high cohesive nature of the majority of sediments (mainly clays) 4 drops of a 2% sodium hexametaphosphate solution was added to the water as a deflocculant. The sample was then added, and sonically dispersed at a frequency of 300 Hz for 15 seconds, to further disperse cohesive particles. It must be noted that in Cooper's (1986) study, study samples were not dispersed to reflect the natural depositional grain size distributions. The particle size distribution (PSD) was then calculated from a set of three repetitions and the PSD curves plotted after each sample. The average of the results was then used as the final PSD result. Data were then exported into an Excel format and used to yield the clay, silt, mud; fine, medium, and coarse sand percentages, as well as the mean, median, sorting and skewness of each individual sample.

5.2.2. Sieving

The samples selected for sieving were dried under a light, before being split through a riffler to obtain smaller representative samples. These were then sieved through a stack of 2000 μm , 1400 μm , 1000 μm , 750 μm , 500 μm , 300 μm , 250 μm , 125 μm , 90 μm , and 63 μm sieves. These results were used to determine the same statistical parameters as described for the Malvern results.

5.2.3. Statistical parameters

The grain size analyses were used to determine specific statistical parameters. These parameters are useful indicators of the provenance, movement and depositional processes occurring within the estuary and include the median, mean, sorting, and skewness.

The **mean** grain size in phi (Φ) is the best measure of the average grain size, where $\Phi = \log_2 d$ and d = the grain size diameter size (Tucker, 1988). It is calculated from the 16th, 50th, and 84th percentiles using the Folk and Ward (1957) equation:

$$M = \frac{\Phi_{16} + \Phi_{50} + \Phi_{84}}{3}$$

From the mean grain size, the general flow velocities of the transport medium can be determined with, for example, coarser grains transported in higher energy environments.

The **sorting** or standard deviation of the individual samples was calculated from Folk and Ward (1957) equation:

$$\sigma\Phi = \frac{\Phi_{84} - \Phi_{16}}{4} + \frac{\Phi_{95} - \Phi_5}{6.6}$$

The sorting measures the distribution of the grain size, and this determines the efficiency of the transportation medium to separate the varying grain size classes (Tucker, 1991). Sorting can be related to the maturity of the sediment whereby mature sediments tend to be more well sorted than immature sediments. Sorting, however, also depends on numerous other factors such as the composition of the grains, the source, and the transporting agent.

The **skewness** is the measure of the symmetry or asymmetry of the distribution of grain size classes. It is determined by the following Folk and Ward (1957) equation:

$$Sk = \frac{\Phi_{16} + \Phi_{84} - 2\Phi_{50}}{2(\Phi_{84} - \Phi_{16})} + \frac{\Phi_5 + \Phi_{95} - \Phi_{50}}{2(\Phi_{95} - \Phi_5)}$$

The **median** grain size is calculated directly from the 50th percentile and is the point at which half the particles in the sample are coarser and half are finer. It is by far the most commonly used measure and the easiest to determine, however, it is not affected by the

extremes of the curve and therefore does not reflect the overall size of sediments especially for skewed and bimodal sediment (Folk and Ward, 1957).

5.2.4. Carbonate content

The carbonate content (%) was calculated using a carbonate bomb. This device measures the amount of carbonate by the reaction of the carbonates with hydrochloric acid (HCl). Before testing the sample, the device was calibrated by reacting known specific weights of analytical calcium carbonate (CaCO_3) with HCl and reading the pressure. Once calibrated, a dried sample of known mass is crushed and placed into the device with 10 ml of HCl, before being sealed. The device is then shaken to mix the HCl and sample and the evolved CO_2 from the reaction is measured on a pressure gauge. The carbonate percentage of the sample is then derived by comparison to the calibrated readings.

5.2.5. Organic content

The hydrogen peroxide method was used to determine the organic content due to the reproducibility and efficiency of this method. Approximately 50 g of sample was oven dried at 60 °C before being crushed and placed into a 500 ml flat bottom flask of a known mass. 150 ml of hydrogen peroxide was added and the samples left to dissolve. The samples were then boiled at 70 °C and constantly stirred to avoid bubbling over. After complete reaction with the hydrogen peroxide, the samples were placed back in the oven to evaporate the remaining hydrogen peroxide. The samples were then reweighed, with the difference in mass representing the loss of organics, calculated as a weight percent.

All the above results were then tabulated with the GPS positions and gridded by the Kriging method using the *Surfer 8* software package, from which the various sediment maps were generated.

5.3. Results

5.3.1. Particle size distribution

Gravel fraction

The gravel fraction comprises grains coarser than 2000 μm in diameter. These grains travel as part of the bed load and are deposited in relatively high energy environments within the estuary (Figure 5.2.A). The results from the samples containing gravel cannot be directly correlated to other fine-grained samples used for Malvern analysis, due to the variations between laser diffraction and sieving techniques used for various grain size analyses, as mentioned above. The gravel fraction within the Mgeni Estuary consists of approximately equal proportions of quartz and feldspars, with subordinate lithic fragments (Cooper, 1986). This composition is representative of the mineralogy of the catchment geology, with quartz and feldspar being derived from the granites exposed in the Valley of a Thousand Hills and the lithics from the overlying supracrustal formations.

The main concentration of gravel was previously located on the western-most edge of the central island bar as recorded in the Cooper (1986) study (Figure 5.2.B). This distribution is indicative of the gravel being fluvially deposited. Further pockets of gravel were located in washover fans on the landward side of the barrier, and on the northern banks of both channels.

In contrast, this study has shown that the gravel fraction was concentrated on the landward side of the barrier and in isolated pockets within the main channel towards the mouth (Figure 5.2.A). Gravel deposits on the barrier were deposited as subaerial washover fans during storm events washing over the barrier (Tinmouth, 2005). The washover fans are concentrated in areas where the barrier is low, and in some cases, individual washover fans coalesce to form washover aprons as noted by Cooper (1988). Badenhorst *et al.* (1989) also identified similar washover fans after the 1987 flood, formed from the reworking of sediment washed out to sea during the 1987 flood. These washover fans are generally surface deposits up to a few centimeters thick and therefore do not represent the complete infilling of the barrier (Tinmouth, 2005).

Figure 5.2. A) The 2006 gravel distribution, with only a few isolated pocket of gravel, located within the main channel off of the model yacht pool, in the tidal inlet, and in washover fans on the supratidal barrier. B) The distribution of gravel from Cooper's 1986 study. Gravel is found throughout the estuary and generally comprises a large portion of the sediment.

Deposition of gravel within the main channel probably occurred during storm events with gravel sourced from both fluvial and marine environments due to the increased energy regime (Tinmouth, 2005). Strong current velocities through the channel remove finer sediments, except for cohesive clays and muds, leaving behind gravel lag deposits. Periods of marine incursions rework the marine gravel deposits back into the estuary. Evidence for this reworking is the lack of gravel adjacent to the head of the estuary, where deposition during fluvial flooding would occur (Tinmouth, 2005). The isolated pocket of gravel located towards the northern bank may be the result of gravel sourced from nearby roadworks (Tinmouth, 2005).

Sand fraction

The sand fraction constitutes a wide range of grain sizes, from 63 μm to 2000 μm , and is therefore deposited by a range of current velocities. The means of transport depends on the individual grain size, and is controlled by the current velocity and boundary layer conditions (Cooper, 1986). There is a widespread distribution of sand throughout the estuary, with the percentage of the sand fraction values ranging between 20% (within the channels) to 100% (on the flood tidal delta) (Figure 5.2.C and Figure 5.2.D) (Tinmouth, 2005). Previous studies have grouped the sand-size fraction together. To obtain a better understanding of the dynamics at work in the estuary, the sand fraction is broken into three subclasses; very fine to fine, medium, and coarse to very coarse sands, which are described in detail in the subsequent sections (Tinmouth, 2005).

Coarse to very coarse sand

Sediments with a grain diameter between 500 μm and 2000 μm are classified as coarse to very coarse sand (Folk and Ward, 1957). Coarse sand, is generally transported as part of the bed load by relatively high energy currents, with velocities greater than 0.25 m/s (Hjulström, 1935, in Kennish, 2001). The highest concentrations of coarse sand are located within and around the tidal inlet and adjacent areas (Tinmouth, 2005). In addition, coarse to very coarse sand is deposited on the barrier where it constitutes part of the washover fans. The percentage of the coarse sand fraction in the sediments of the tidal inlet decreases away from the mouth of the estuary, so that only minor amounts of coarse sand are recovered from the head region, although coarse sands are present throughout the main channel (Figure 5.2.E and Figure 5.2.F) (Tinmouth, 2005).

Figure 5.2. C) The 2006 distribution of the sand fraction (63 μm and 2mm) within the Mgeni Estuary. There is a general increase in the amount of sand towards the tidal inlet, away from the head of the estuary. D) The 1986 distribution of sand within the estuary. There has been an increase in the overall sand percentage throughout the estuary, except for the area towards the head of the estuary.

Figure 5.2. E) The 2006 distribution of coarse sand within the Mgeni Estuary. F) The 2006 distribution of very coarse sand within the estuary. The high current velocities required to transport coarse to very coarse sediment restrict the sediment to the areas of the main channel and tidal inlet. Very coarse sand is also located in the form of washover fans on the estuary side of the supratidal barrier.

This decreasing concentration of coarse sands away from the estuary mouth indicates a decrease in the flood tide velocity towards the head of the upper reaches of the estuary (Tinmouth, 2005). The minor amounts of coarse sand in the sediments from the head of the estuary reflect the influence of the high energy ebb currents in this area. The reduced amount of coarse sediment near the head of the estuary in comparison to that of the tidal inlet can be argued to reflect 1) a decrease in the amount of coarse sediment entering the system via fluvial input, possibly being retained behind Inanda Dam, as suggested by Moleko (1998). The increased coarse fraction near the inlet would then result from the reworking of sediments back into the estuary; 2) that the ebb current velocity at the head is less than that of the flood current at the tidal inlet; or 3) silting up of the estuary results in the reduction in coarse sediment as part of a natural fining-up sequence, with the tidal inlet again including reworked coarse sand fractions (Tinmouth, 2005).

Medium sand

The medium sand fraction constitutes grains with a diameter of 250 μm to 500 μm and is generally transported by current velocities greater than 0.2 m/s (Hjulström, 1935, in Kennish, 2001). Medium sands are recovered throughout the estuary, with concentrated pockets located towards the head of the estuary and on the flood-tidal delta, where it comprises over 55% by weight of the sediment. In the upper region of the intertidal back channel, the sediment is comprised up to 50% of the medium sand fraction, with the presence of medium sands decreasing away from the head. In general, the overall distribution pattern of the medium sand size fraction is similar to that observed for the coarse sand size fraction (Figure 5.2.G).

The dominance of medium sands in the sediments of the Mgeni Estuary is indicative of a relatively high energy regime, where currents of >0.2 m/s must be present. The upper reaches of the channel between Connaught Bridge and the estuarine head comprises only 10 to 25% medium sand fraction, where this distribution may be skewed due to the settling of fine organic mud over the medium sand (Figure 5.2.G) (Tinmouth, 2005).

Figure 5.2. G) The 2006 distribution of medium grained sand (250 μm to 500 μm) in the Mgeni Estuary. The distribution pattern is similar to that of coarse sand transported by current velocities greater than 0.2 m/s. The medium sand sized fraction is the dominant grain size throughout the estuary. This suggests that there has been a general decrease in grain size from that of Cooper's 1986 study, which in turn indicates decreased current velocities in the estuary.

Very fine to fine sand

The very fine to fine sand fraction varies in size between 63 µm and 250 µm. Very fine to fine sand shows a similar distribution to mud (<63 µm) in that both these fractions are transported as part of the suspended sediment. Settlement velocities generally vary from 3×10^{-3} m/s for very fine sand to 1.28×10^{-2} m/s for fine sands (King, 1975, in Kennish, 2001).

The concentration of the combined fine and very fine sand is highest on the intertidal sandbar directly behind the supratidal barrier adjacent to Beachwood Creek (Figure 5.2.H and Figure 5.2.I). The very fine sand fraction (63-125 µm) is a minor constituent of the sand fraction and comprises a maximum of 25% of the total sediment in a given area within the estuary. The highest concentration was recovered from within the flood channel. Fine sand (125-250 µm), however, can be more prominent comprising up to 55% of the sediment on the northern side-attached bar (Figure 5.2.H and Figure 5.2.I) (Tinmouth, 2005).

The intertidal sandbar directly behind the supratidal barrier adjacent to Beachwood Creek represents a naturally low energy environment. It is protected from flood currents by the supratidal barrier and flood tidal delta, whilst the fluvial ebb current decreases seawards. This protected environment allows for deposition of the very fine to fine sand fraction. Additional input of fine and very fine sand may be derived from the aeolian erosion of the supratidal barrier and from the man-made dunes in Beachwood Mangrove Nature Reserve (Swart, 1987). Sediments eroded from these dunes are deposited into Beachwood Creek and transported into the estuary where they are re-deposited (Tinmouth, 2005).

The flood channel acts as a depression for deposition of very fine sand. Sediment is initially transported into the channel by fluvial currents as the system moves towards low tide. During the transition from low tide to high tide, the ebb channel becomes a low energy environment as it is protected from the incoming tide by the supratidal barrier and flood tidal delta. The low current velocities during this tidal stage allows settlement of the very fine sand fraction from suspension (Tinmouth, 2005).

Figure 5.2. H) The 2006 distribution of the very fine sand fraction within the Mgeni Estuary. The very fine sand fraction is generally transported as part of the suspended sediment. Its distribution is therefore concentrated in quite areas where it is allowed to settle out, such as the back channel and the leeward side of the flood tidal delta towards Beachwood Creek. I) shows the distribution of fine sand, which is concentrated throughout the lower reaches of the estuary on the northern side-attached bar.

Mud fraction

The mud fraction can be defined as the sediment fraction less than 63 μm , including the silt (3.9-63 μm) and clay fractions (<3.9 μm). These particles are easily transported through the water column as part of the suspended load, even in relatively low energy environments. The settling velocity of the mud fraction is, therefore, generally low with velocities ranging from 8.4×10^{-4} m/s for the silt-sized fraction of 31.2 μm to 1.15×10^{-8} m/s for a clay fraction of 0.12 μm (King, 1975, in Kennish, 2001). The settling velocity is, however, also dependent on grain density.

Cooper's (1986) pre-flood survey of the surface sediment indicated that the mud percentage was found to be substantially higher than in samples taken at a depth of 50 cm. Mud concentrations were located on both the northern and southern banks in the areas adjacent to Connaught Bridge, the southern bank between Athlone Bridge and the Ellis Brown Viaduct, the southern bank of the northern channel landwards of the Athlone Bridge and at the rejoining of the bifurcated channel. High mud concentrations were also recovered in all channels of the estuary, except for areas around the tidal inlet (Figure 5.2.K).

This current study recovered surface sediments with mud fraction concentrations that vary from 0% (in the tidal inlet), to over 80% (in the main channel) (Figure 5.2.J). These results are based upon surface sediment sampling only, and the observed mud recovery could be biased as mud is often deposited as a drape over coarser sediment, as noted by Fenies *et al.* (1999) in the Gironde Estuary, France. The main concentration of mud was recovered from near the head of the estuary adjacent to Connaught Bridge. In addition, mud concentrations were recovered from the side-attached bar and within the intertidal back channel. High mud concentrations (>80%) were also recovered from the centre of the main channel (Figure 5.2.J) (Tinmouth, 2005).

The mud beds adjacent to Connaught Bridge tend to be relatively thick in nature, with thicknesses generally greater than 0.1 m. The muds are organic-rich, often including visible decaying organic matter. This area also represents the highest point of the salt water penetration into the estuary during periods of high tides. This suggests that the salt activity promotes flocculation, resulting in settling of clays and muds.

The mud-rich units located within the intertidal back channel region were brown in colour and formed relatively thin surface drapes, with a maximum thickness of 0.1 m (Figure 5.2.J). The back channel and side-attached bar form part of the intertidal area, which becomes submerged during high tide and periods of mouth closure. During the transition to low tide, this area becomes emergent with muddy water being retained in the troughs between sand dunes. These troughs become isolated from currents throughout the low tide period, allowing settling from the suspended load. In certain regions on the side-attached bar, this has resulted in an interfingering of areas of high and low mud concentration. Mud concentrations in these intertidal areas increases in two directions: 1) away from the channel, and 2) away from the head of the estuary related to the decrease in velocity in both directions. Mud drapes were also identified on a smaller scale forming in ripple troughs. This mode of deposition is similar to that of the intertidal clay-drape couplets identified by Fenies *et al.* (1999) in the Gironde Estuary which also has a semi-diurnal tide. In the Mgeni Estuary, mud deposits may also have developed by the addition of mud from three storm water drains and sewerage outlets. The mud transported from these outlets flocculates due to the change from fresh to saline water (Tinmouth, 2005).

The concentration of the mud fraction on the vegetated region of the side-attached bar is increased due to the binding properties of plant roots, coupled with the reduction in velocity induced by the vegetation. Individual mud pockets recovered from near the head of the estuary are located in troughs between intertidal sandbars, in some instances separating the individual bars by up to 5 m. These pockets contain thick black mud units, approximately 0.8 m thick. Coring of sites on the surrounding sandbars showed no noticeable mud rich layers underlying the coarser sediment. This ruled out the possibility that the mud was deposited post-flooding and exposed by scouring of the lee face of sand waves. These pockets of thick mud are therefore argued to be due to flocculation of sediment in a turbidity maxima zone, which are associated with high amounts of suspended sediments. These suspended sediments are allowed to accumulate due to the protected nature of the inter-dune depressions (Tinmouth, 2005).

Mud concentration in the centre of the main channel increases towards the centre of the estuary, before decreasing again seawards (Figure 5.2.J). This is similar to the pattern

described for the concentrations of suspended sediment in the Miramichi Estuary in New Brunswick by Kranck (1981) (Tinmouth, 2005). She attributed this pattern to the development of the turbidity maxima in the area of high mud concentration. Flocculation of the increased sediment load leads to the high mud concentration. Clay-sized particles in suspension carry a negative electrostatic charge. In water with low electrolyte content, such as fresh water, particles repel each other and remain in suspension. With an increase in the electrolyte content of water, the electrolyte potential of the suspended particles decreases, varying in an amount dependent on the mineralogy. The resulting differences in the electrolyte potential causes some particles to become mutually attractive, forming chains and open clusters called flocs. These flocs have a larger mass than the particles that form them. They are usually unaffected by Brownian movement and settle quickly under gravity or centrifugal forces. These flocculated particles are easily transported and generally form a layer of relatively high concentration close to the deepest parts of the riverbed (McDowell and O'Connor, 1977). Dalrymple *et al.* (1992) identified the central region of estuaries (Figure 5.2.J) as the low energy area where fine grained organic mud accumulates. The amount of flocculated constituents increases as salinity increases from 0 to 15-20‰ (Sholkovitz, 1976).

The various isolated areas of high mud concentration throughout the channels of the Mgeni Estuary are suggestive of numerous areas of turbidity maxima, or a migrating turbidity maxima constantly shifting with the changing tides and the associated salt water wedge as noted during this study. This shifting turbidity maxima would allow for flocculation to occur at the head of the estuary during high tide and towards the tidal inlet during low tides. Additional input of suspended sediments, such as from storm water and sewerage outlets located throughout the estuary, also contribute to the distribution of fine sediment. Frequent prolonged periods of mouth closure could also result in a wider distribution of flocculated sediments (Tinmouth, 2005).

There is a noticeable increase in the volume of surface mud from that depicted by Cooper (1986) (Figure 5.2.J and Figure 5.2.K). It must, however, be noted that in Cooper's (1986) study samples were not dispersed by the use of deflocculants and/or sonic dispersion. This would have led to a decrease in the determined percentage of mud, as flocculated particles would bias grain size analysis to a coarser grain size as

these flocs becoming part of the bottom sediment deposits (Kranck, 1975). The use of dispersion agents allows grain size analysis of samples to be undertaken, which should theoretically determine particle size distribution prior to flocculation and settlement.

Figure 5.2. J) The 2006 distribution of mud within the Mgeni Estuary. Mud is located throughout the estuary except in the tidal inlet and on the flood tidal delta. High concentrations of mud are found at the head of the estuary, the back channel of the northern side-attached bar, and in an isolated pocket in the main channel immediately upstream of the model yacht pool. This is in contrast to K), which shows the 1986 distribution of mud. Cooper's study showed relatively smaller mud concentrations throughout the estuary with isolated pockets of mud against both the northern and southern bank and on the northern bank of the central island bar.

5.3.2. Statistical parameters

Statistical parameters are useful for the discrimination of environments in which the sediments are deposited. The most useful of these parameters are the mean, standard deviation and sorting (El-Ella and Coleman, 1985).

Mean

The mean grain size is the best measure of the average grain size (Tucker, 1988) and can therefore be used to determine the average relative current velocity that occurs within the various estuarine environments. Low energy environments are, therefore, dominated by finer mean grain sizes, and high energy environments by coarser mean grain sizes.

The distribution pattern of mean grain size (Figure 5.3.A) shows a similar distribution pattern to that of percentage mud fraction, with the lowest mean grain size being in the area towards the head of the estuary, and the largest mean grain size being located in the area around the tidal inlet and in washover fans. The side-attached bar environment contains the lowest mean grain size within the estuary, which varies from 200 μm (fine sand) to 100 μm (very fine sand). The coarsest mean grain size is recovered from both the tidal inlet (900 μm to 500 μm), and the estuary head (350 μm to 400 μm) (Tinmouth, 2005).

The side-attached bar area is intertidal, with very fine to fine sand deposition occurring during periods of submergence, when the estuary is tide-dominated. Within the side-attached bar region, the mean grain size decreases towards the head of the estuary. The coarse mean grain size at the tidal inlet and head of the estuary suggests higher current velocities in these areas, due to the flood and ebb tides respectively. The mean grain size decreases towards the center of the estuary, between Athlone Bridge and the Ellis Brown Viaduct (Figure 5.3.A). The tripartite distribution is similar to that of wave-dominated estuaries described by Dalrymple *et al.* (1992), and tide-dominated estuaries described by (Cooper, 2001). This varies from Cooper's (2001) classification of the Mgeni Estuary as being a river-dominated system (Tinmouth, 2005).

Sorting (ϕ)

The sorting of the sediments can be used to interpret the efficiency of the transportation medium, the maturity of the sediment, and the variation of the current velocities of an area over time. Sediments from areas that maintain a constant flow velocity are typically, relatively well sorted in comparison to sediments from a system having variable velocities (Tucker, 1991).

The majority of sediment in the Mgeni Estuary are poorly to very poorly sorted, with exceptions of the moderately sorted sediments in the upper reaches of the estuary and well-sorted sediments in the tidal inlet and flood tidal delta (Figure 5.3.B). The improved sorting in the tidal inlet and flood tidal delta area reflects the continual flow that occurs here due to both the ebb and flood current (Tinmouth, 2005).

The very poorly sorted sediments in the main channel appear to show a bimodal grain size distribution (Figure 5.3.B) having a relatively high concentrations of mud, fine and coarse sand fractions, with a low percentage of medium sand. This is suggestive of either 1) the mud and fine sand fraction settling over the coarser sediments transported along the channel, or 2) the result of winnowing of the medium sand fraction, with the cohesive mud and coarser sand fractions left behind due to the higher flow velocities required to erode and transport these particles (Tinmouth, 2005).

The poor sorting on the side-attached bar (Figure 5.3.B) is attributed to the mud drape over the sand fraction. However, results could possibly have been skewed by mud aggregates, which did not disperse during analysis even with the use of a dispersing agent and the ultrasonic disperser.

Figure 5.3. A) The 2006 mean grain size of sediment within the Mgeni Estuary. The mean grain size offers an estimate the relative current velocities. The mean grain size decreases away from the tidal inlet. B) The 2006 sorting of sediment within the estuary. Sorting can indicate the efficiency of the transportation medium. Sorting within the estuary varies from very well sorted near the tidal inlet, to very poorly sorted in the central region of the estuary, between Ellis Brown Viaduct and Athlone Bridge.

Skewness

The skewness is a measure of the symmetry or asymmetry of the distribution in size classes and helps to determine whether the sediment is dominated by fine, medium or coarse fractions. The majority of sediment recovered from the estuary are near symmetrically skewed (-0.01 to 0.2) to fine skewed (0.2 to 1) (Figure 5.3.C), coarsening seawards due to the removal of the fine fraction by tidal and wave action during high tides and by wind action during low tide periods. Areas on the landward side of the coastal barrier (Figure 5.3.C) tend to be the strongly coarse skewed, which is interpreted to be due to the addition of coarse particles from the washover fans and aprons (Tinmouth, 2005).

Median

The median (Φ) is directly calculated from the 50th percentile, whereby half the sediments are coarser and half finer than the median. The median shows a similar distribution pattern to that of the mean grain size (Figures 5.3.A and Figure 5.3.D) (Tinmouth, 2005).

5.3.3. Carbonate

Calcium carbonate is predominantly derived from marine shell fragments, although in the upper regions of the estuary increased carbonate is interpreted to reflect the presence of certain benthic fauna, such as the fresh water molluscs that are resident to the area. The carbonate content can, therefore, be used to indicate the extent of marine influence into the estuarine system. As expected carbonates tend to be concentrated within the tidal inlet and the flood ramp, reaching the highest percentage towards the upper limit of the flood tidal delta (Tinmouth, 2005).

The distribution of carbonate is promoted by the low density and irregular shape of the bioclastic material, which favours transport of these grain over rounded and more dense quartz and feldspar sediments. Shell fragments are consequently transported further under lower velocities than either quartz or feldspar grains of the same size. In addition the low density and shape of the bioclastics is also more conducive to aeolian transport, leading to an enrichment of carbonate in intertidal and supratidal areas (Tinmouth, 2005).

Figure 5.3. C) Skewness of the sediment within the Mgeni Estuary in 2006. Sediments are strongly skewed towards the coarse sediments in the area around the tidal inlet and flood tidal delta. At the head of the estuary there are mixed pockets of strongly coarse skewed and strongly finely skewed sediment. The middle of the estuary tends to be close to symmetrical. D) The 2006 median phi distribution. This distribution is similar to that of the mean grain size but does not account for the skewness. The median grain size tends to decrease away from the tidal inlet.

Cooper's (1986) study identified that the carbonate was restricted to the area directly around the tidal inlet, decreasing to zero throughout the rest of the estuary except for localized area near the head of the estuary (Figure 5.4.B). This study however, shows that there is a significant increase in the carbonate content for the majority of the sediments recovered from throughout the estuary relative to the earlier results of Cooper (1986), although carbonate levels are still relatively low (<2%) (Figure 5.4.A and Figure 5.4.B). This increase in carbonate content and distribution is interpreted to reflect the gradual change from a previously river-dominated estuary to one that is currently more tidally influenced. These changes in the dynamics of the estuary are proposed to result from a decrease in the amount of discharge reaching the estuary as a result of the construction of Inanda Dam in 1989.

5.3.4. Organic content

Organic content within an estuarine system plays an important role as an influencing factor in heavy metal accumulations within the sediments, and therefore on the amount of pollution within the estuarine system (Horowitz, 1985, in Callow, 1994; Leuci, 1998). Organic matter may accumulate metals by ion-exchange, complexing and chelation (Roy and Crawford, 1984). Organic material is typically introduced into an estuary by sewerage, industrial effluent, fluvial input, planktonic and benthic processes, as well as by mixing processes in the ocean (Williams, 1985).

As expected organic content within the Mgeni Estuary is concentrated on the vegetated area of the side-attached bar, in the ebb channel, and in the mud troughs, reaching a maximum of 12% near the head of the estuary (Figure 5.5.A). In contrast, the organic content tends towards zero near the inlet and in the lower reaches of the side-attached bar (Tinmouth, 2005). This distribution pattern is similar to that described for the mud fraction of the sediments. This distribution pattern is also similar to that described by Cooper (1986), who recovered sediments with high organic concentrations (>7%) towards the head of the estuary (Figure 5.5.B). Cooper (1986) similarly noted that the surface organic concentration mirrored the mud fraction distribution. The decrease in the present day organics towards the tidal inlet contrasts with Cooper's (1986) results which had a more widespread distribution (Figure 5.5.A and Figure 5.5.B).

Figure 5.4. A) The 2006 distribution of carbonate in the Mgeni Estuary. Carbonate is concentrated in the area of the tidal inlet and flood tidal delta, as well as in the main channel towards the head of the estuary. This is in contrast to B) which shows the distribution in 1986 limited to the areas directly adjacent to the flood tidal delta, tidal inlet and supra tidal barrier. This increase in carbonate concentration from 1986 to 2006 represents an increase in marine incursion into the Mgeni Estuary.

Figure 5.5. A) The 2006 organic content distribution within the Mgeni Estuary. Since 1986 (B) there has been a definite increase in organic content towards the head of the estuary and a decrease in organic content towards the tidal inlet. This increase in organic content could be related to the increase in mud concentration within the estuary, whilst the decrease at the tidal inlet is an effect of the increased marine incursion.

5.4. Discussion and conclusion

The estuary was previously classified as a river-dominated system in the pre-flood study (Cooper, 1986) with the estuarine sediments dominated by fluviially-derived gravels and sands. Sediment distribution, post-September 1987 flooding, suggests that there has been a change from the predominantly fluvial influence sedimentation with low carbonate concentration to river dominated sediments with high carbonate content indicating an increase in marine incursion.

In addition to the increase in sediment volume in the estuary, there appears to have been an increase in the percentage of the mud fraction in the recovered sediments. This is interpreted to reflect mud drapes, which are deposited on the surface during intertidal periods. Mud drapes also result in the surface sediment sample being biased towards very fine sand to mud. Cooper (1986) suggested the deposition of fine sediment was due to low current velocities, with the process being accelerated by the spread of sediment-trapping mangroves. However, the increased rate of fine sand fraction deposition as recovered in the post-flooding deposit can be directly related to the decrease in fluvial flow velocity reflecting the low discharge rates of Inanda Dam. This change in sediment dynamics was argued by Diab and Scott (1989) and the Council for Scientific and Industrial Research (1984) as a likely consequence of the dam construction. This construction has also led to an increase in the sediment volume of the estuary, through infilling, and hence an overall shallowing of the estuary. The shallowing of the estuary has resulted in the formation of large subaerial and supratidal bars, in contrast to the single central island bar described in the estuary in 1986 prior to completion of Inanda Dam.

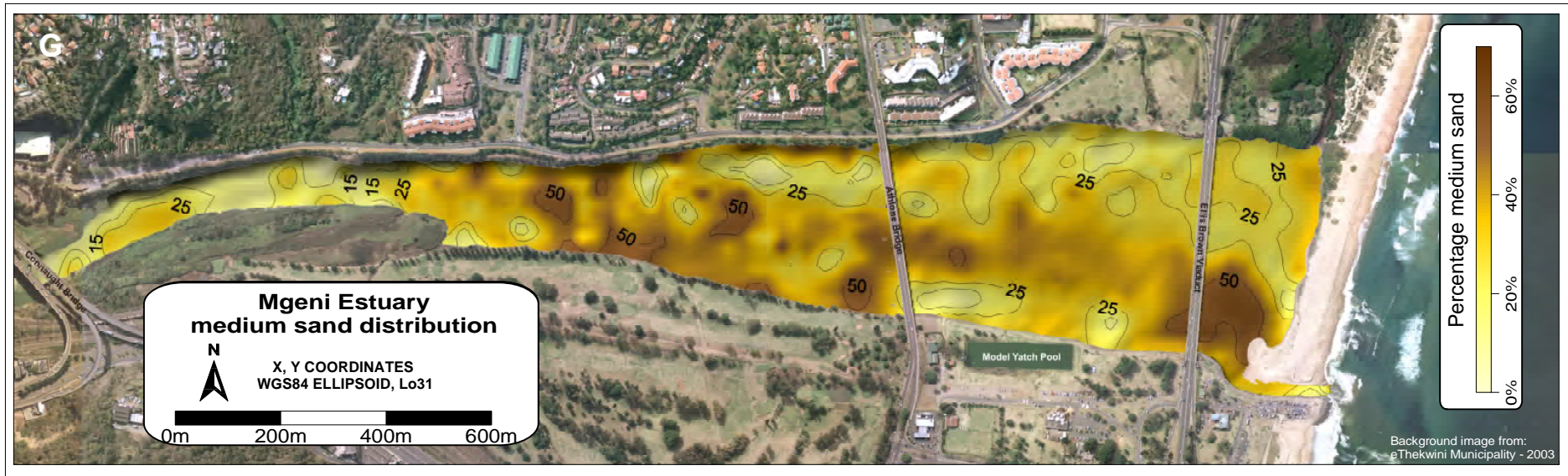


Figure 5.2. G) The 2006 distribution of medium grained sand (250 μm to 500 μm) in the Mgeni Estuary. The distribution pattern is similar to that of coarse sand transported by current velocities greater than 0.2 m/s. The medium sand sized fraction is the dominant grain size throughout the estuary. This suggests that there has been a general decrease in grain size from that of Cooper's 1986 study, which in turn indicates decreased current velocities in the estuary.

CHAPTER 6

Cores

6.1. Introduction

The complex and dynamic nature of an estuary is represented by the surface sediment distribution patterns (Wright et al., 1999), with both time and local geomorphology playing a significant role in this complexity (Chapter 5). Ideally, this two dimensional surface sediment distribution pattern approach should be modeled in the third dimension; providing the shape and volume of each sedimentary facies within the estuary through time, which would then allow construction of a four dimensional model of the estuary dynamics. In order to achieve this objective, subsurface samples would be required whilst maintaining, as best as possible, their relative *in situ* relationships. This was achieved in this study by collecting numerous sediment cores through the various sedimentary environments identified.

6.2. Methodology

Sediment cores were collected throughout the estuary with 15 vibro-cores and 10 hammer-cores recovered using 2 m long PVC tubes, with an internal diameter of 6 cm, and plastic core catchers to help prevent the loss of material during extraction of the tubing from the ground. These cores were collected within a couple of weeks of each other in order to avoid seasonal variability and the possibility of mass erosion or deposition storm-related events. The recovery location for each of the cores was recorded with a handheld *Garmin eTrex Venture* GPS system (Figure 6.1.) (Appendix B).

The recovered penetration depths of the cores collected in this study varied considerably throughout the estuary, with only a few of the cores obtaining a full penetration length. The amount of penetration was predominantly controlled by the sediment type, likely reflecting grain size variation, porosities and expelled pore water (e.g. Crusius and Anderson, 1991, Wright, 1993) and the relative vibration frequency for the vibro-core samples. Due to the nature of both vibro- and hammer-coring methods used, some settlement and compaction of the samples occurred, which was then calculated and corrected for using a compression ratio calculated by:

Figure 6.1. 2003 Aerial photograph of the Mgeni Estuary overlain with the location of the 15 vibro-cores and 10 hammer-cores taken during this study. Core locations were chosen based on the various sedimentary environments as well as along approximate transect lines

$$\text{Compression ratio} = \frac{\text{The length of the retained sample}}{\text{The amount of penetration}}$$

This ratio, however, is calculated using the settlement of the entire core recovered, and does not take into account any internal variations in settlement within the various sedimentary layers present within the core.

The sediment cores were split open using an electric saw. After being split open, the cores were photographed and logged. Significant sedimentary units were identified on basis of obvious grain size variations, texture, colour and other features such as mottling and bioturbation. Representative sediment samples (221 samples) collected from the identified significant sedimentary units were analysed using both the standard sieving technique and Malvern laser grain size analysis, depending on the grain size. The sample descriptions and logs are included in Appendix B.

In order to determine whether a potential marker layer could be recognised within the Mgeni Estuary cores, the maximum depth of penetration for each core was compared to the estimated 1989 surface model depth. This, however, proved unsuccessful as the vast majority of cores failed to penetrate to a significant enough depth and therefore did not intersect this proposed surface (Chapter 4). The variable penetrations, and lack of identifiable marker horizons in the recovered cores, in combination with the complex and dynamic nature of the Mgeni Estuary, posed numerous problems for the modelling of the sediment dynamics in this estuarine system.

To simplify the overall complexity in the recovered cores, the general rate of increase or decrease in sediment grain-size up the cores, was calculated by:

$$\text{Grain size variation (GSV)} = (x_1 - x_2)/(y_1 - y_2)$$

Where x_1 is the mean sediment grain size of the top layer excluding the mud draping, x_2 is the mean grain size from the bottom most layer of the core excluding the flood recovery sequence. y_1 is the corrected depth for x_1 and similarly y_2 is the corrected depth

of layer x_2 . Positive values show a coarsening up sequence, whilst negative values show a fining upwards up sequence (Figure 6.2.A).

6.3. Results

The majority of sediment cores collected during this study of the Mgeni Estuary (core logs are included in Appendix B) show a dominant coarsening upwards sequence. This trend shows superimposed fluctuations, within the sand bars showing an overall average increasing sediment grain size up core, which is contrasted by a dominant fining upwards sequence within the cores recovered from the main channel. The rate (change in grain size versus change in depth), at which the sediments coarsen upwards, typically increases away from the estuarine mouth (Figure 6.2.A).

Exceptions to the trends described above include cores 18 and 19, recovered from the head of the estuary, which show a rapid rate of increase in grain size up the cores. In addition, cores 5 and 7, collected towards the centre of the present day sand bars, show a slow rate in the overall increase in sediment grain size (Figure 6.2.A).

Cores 18 and 19 show an initial high rate of coarsening upwards, probably related to the change in bathymetry at this location, whereby the estuary simultaneously shallows and widens (Figure 4.5). This results in a rapid decrease in fluvial flow and therefore an increase in deposition and formation of sandbars. As these resulting sandbars shallowed further, the rate of flow continually decreased, thereby resulting in the overall fining upwards sequence visible at the top of both cores (Appendix B).

Deposition of sediments recovered in cores 5 and 7, is interpreted to have occurred soon after 1987 floods, forming the main sandbar nucleus present in the 1989 aerial photographs (Figure 6.3). The relatively short time period during which the sediment in these incipient sandbar areas was deposited resulted in the sediment being relatively vertically homogenous, and well sorted in the coarser sediment layers. The overall grain size, within these cores, fall within the very fine to fine sand category suggesting deposition during periods of relatively reduced flow from 3×10^{-3} m/s for very fine sand to 1.28×10^{-2} m/s (King, 1975, in Kennish, 2001). These layers are interbedded with 3 finer grained layers. The mean grain size within these cores, such that core 7 contains predominantly coarser sand than that recovered from core 5, i.e. a decrease in grain size

Figure 6.2. A) Increase/decrease in grain size up the core along set transect lines. Note contrast between sediments deposited in the sand bars (showing coarsening upwards sequences) versus the main channel (showing a fining upwards sequence). Cores 5 and 7 show the slowest rate of upwards increase. B) Average mean grain size of the individual cores. Grain size tends to be coarser in the main channel as expected and decreases towards the north.

Figure 6.3) Increase/decrease in grain size up the core overlain by the sand bars out lines for 1989, 1994 and 2006. Note the decrease in the rate of increase in grain size in cores 5 and 7, which fall on the edge of the sand bar nucleolus. Core 9 shows a slight decrease in grain size up the core, this appears to be related to its position within the main channel until after 1994. Cores 10 and 11 show numerous coarsening fining upwards sequences, related to the shifting the flood tidal delta.

away from the head of the Mgeni Estuary (Figure 6.2.B). This grain size variation suggests deposition during a period dominated by fluvial flow with core 5 being in the lee side of the developing sand bar, which corresponds to the shape of the sand bar present during this period (see Chapter 4).

Cores 10 and 11 show alternating coarsening and fining upwards sequences within the fine to very fine grain size range (Appendix B). These alternating sequences appear to be related to the shifting of the flood tidal delta, which is a dominant factor effecting the sediment dynamics in the area (Figure 6.3).

Cores 18, 13, and 12, directly adjacent to the northern bank, show an interbedded sand and mud sequence towards the base of the cores, at approximately 0 m relative to Mean Sea Level (MSL). The thickness of these interbedded sequences increase away from the centre of the estuary and could possibly be related to the shifting of sand bars, channels and resulting mud flats during the initial stage of the Mgeni Estuary redevelopment following the catastrophic erosion of the 1987 flood event

Within the main channel of the Mgeni Estuary, there is an overall fining upward sequence present, with cores 23 and 24 (located towards the middle of the main channel) showing an initial coarsening up sequence overlain by a fining up sequence (Figure 6.2.A). It is possible that the coarser sand layers represent pulses of coarse sediments that are periodically brought into the estuary during storms. As the tidal and wave energy decrease, the finer sediment fractions gradually settle out. The high percentage of mud, which caps most of the cores in the channel, as well as the sand-bars, suggests that the estuary is subjected to prolonged periods of reduced tidal and fluvial flow. This is most likely related to the more frequent closure of the estuary mouth (Leuci, *pers. comm.*, 2005), which again shows the dominant source of flow in the Mgeni Estuary has shifted from being a river-dominated system as described by Cooper (1986), to a tidal-dominated estuary in recent times as shown by this study.

6.4. Discussion and conclusion

The sediments of the Mgeni Estuary, both surficial sediment samples and the stratigraphic record, show considerable variation in grain size and composition as is typical of estuarine environments (Caeiro, 2002) (Figure 6.4). The overall grain-size variation patterns identified in the 25 cores, however, suggest an overall increase in the dominance of marine incursions on the depositions of sediments. The decrease in fluvial input into the estuary, related to the decrease in discharge from Inanda Dam (Figure 3.2), implies that the decreasing energy and hence decreasing grain sizes should be recovered in sediment cores from the Mgeni Estuary. However, the cores recovered from the various environments within the modern Mgeni Estuary show a coarsening upwards sequence. This upward coarsening is therefore interpreted to indicate that the coarser material is most likely to be of marine origin. The apparent increase in influence of marine incursions over time has resulted in an “apparent” transgression as a result of the decrease in opposing fluvial discharge. However, the core samples were too few and of insufficient depth to be able to extract a definite rate of change or when the change first started.

The significant landwards migration/transport of marine sediments suggests that the Mgeni Estuary is a partially mixed (moderately stratified) system, with a significant landwards movement of the bottom salt water and seawards movement of surface fresh water (Wright et al., 1999). Increased accommodation space following erosion associated with the 1987 flood favoured rapid deposition of the predominantly sand units recovered (Slagle, 2006).

In order to better understand the cores and the infill of the estuary, a more detailed study would need to be conducted. Core depths would need to be increased to reach, at least, the flood recovery sequence to obtain a starting point for the deposition, marker layers would need to be ascertained to help correlated the individual cores, and detailed carbonate content for all of sediment layered should be conducted in correspondence with a provenance study to determine the true source of the sediment.

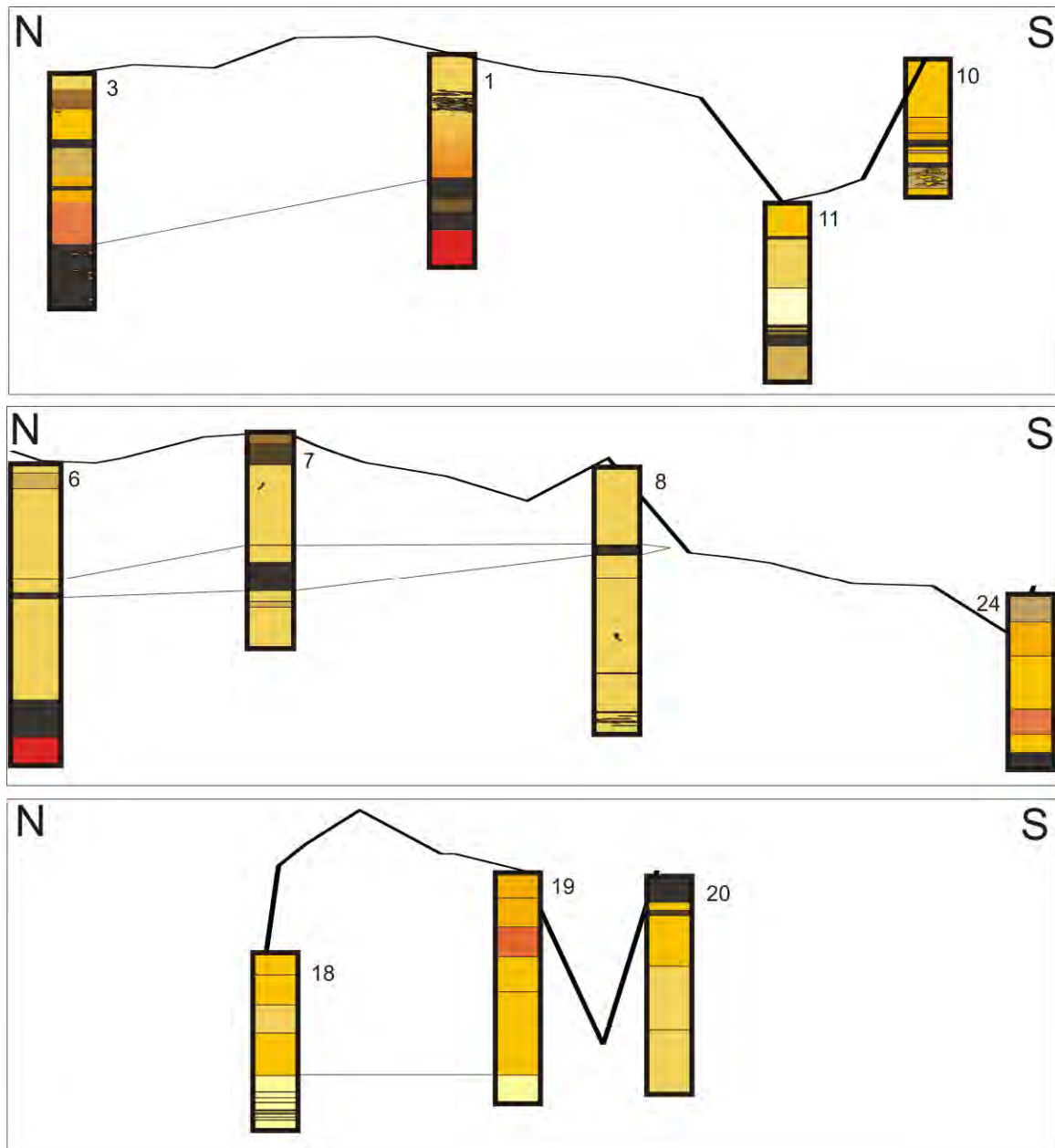


Figure 6.4. Schematic representation of 3 sets of cores along transects near the mouth (3, 1, 11, 10), centre (6, 7, 8, 24), and head of the estuary (18, 19, 20). These cores show the varying depth of penetration, as well as the dynamic nature of the estuary with inter connecting layers few and far between (see appendix B for more detailed core logs).

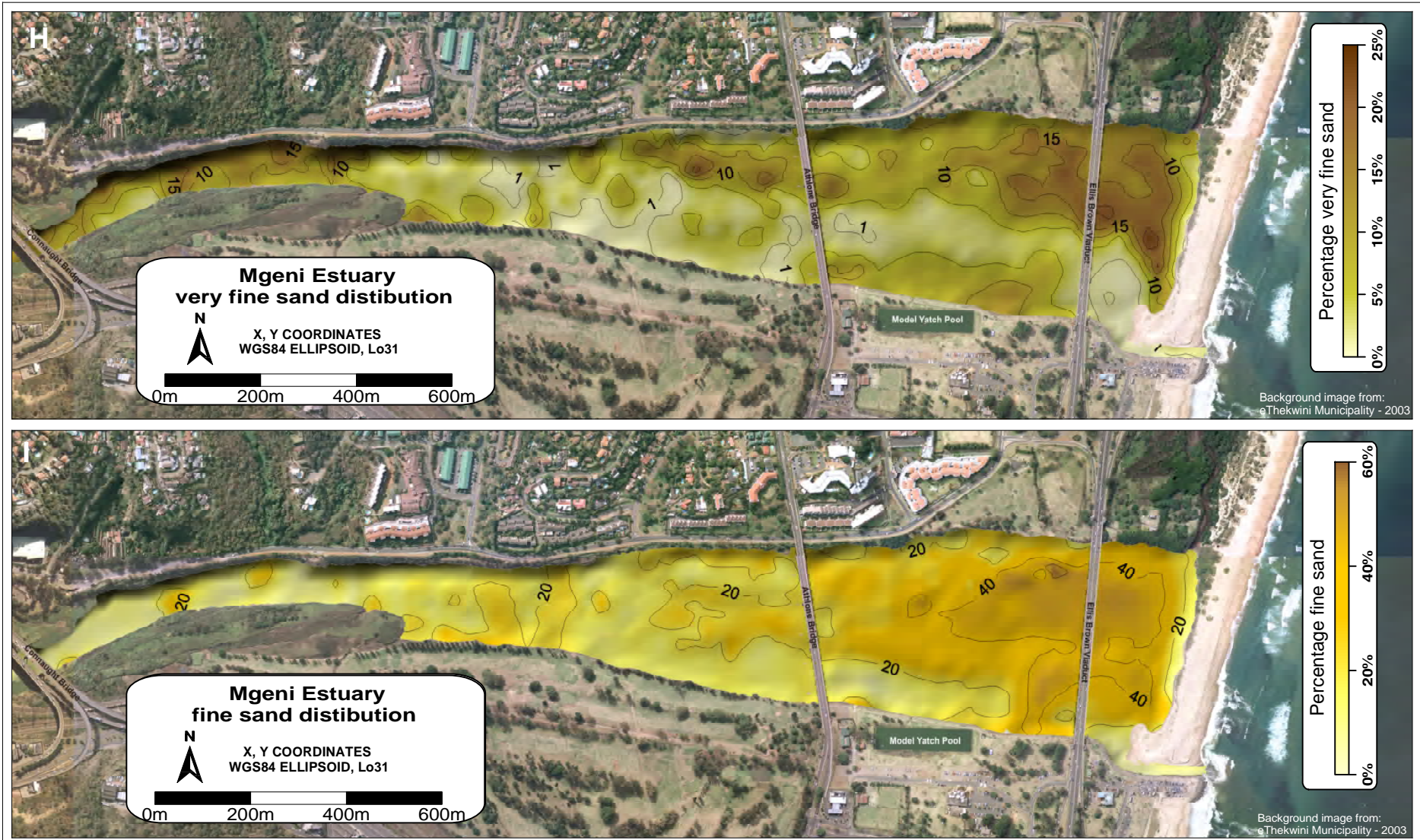


Figure 5.2. H) The 2006 distribution of the very fine sand fraction within the Mgeni Estuary. The very fine sand fraction is generally transported as part of the suspended sediment. Its distribution is therefore concentrated in quite areas where it is allowed to settle out, such as the back channel and the leeward side of the flood tidal delta towards Beachwood Creek. I) shows the distribution of fine sand, which is concentrated throughout the lower reaches of the estuary on the northern side-attached bar.

CHAPTER 7

Geochemistry

7.1. Introduction

Estuaries are commonly regarded as sediment sinks, trapping suspended sediment and their associated trace metals (Kennedy, 1984). The sheltered nature of estuaries allows for both chemical and physical processes to occur, before sediment is swept out to sea. These processes, therefore, also allow for the accumulation and retention of contaminants such as heavy metals. The amount of recorded sediment accumulation can vary from estuary to estuary with, for example, approximately 13% of the Lead (Pb) input being retained in the Grinode Estuary, whereas in the Scheldt Estuary 93% of the Lead and 90% of the Cadmium (Cd) input are retained (Fergusson, 1990).

Metals may be mobilised as a result of natural processes or anthropogenic activity. Mobilised metals can be taken up by marine organisms and vegetation, increasing the potential for entry into the food chain (Liaghati *et al.*, 2003). The anthropogenic effect on estuarine sediment contamination is now recognised as a major source of ecosystem health stress. This anthropogenic influence, therefore, needs to be taken into consideration in coastal zone management, as well as the management of the industrial and urban areas surrounding and upstream of the estuary (Feng *et al.*, 2004; Caeiro *et al.*, 2005).

Surface sediment geochemistry can be used to monitor the chemical, biological, and physical conditions of rivers, lakes, estuaries and coastal environments (Förstner, 1989; Leoni and Satori, 1997). Geochemical analysis of the sediment, therefore, plays a fundamental role in environmental forensic investigations. Such investigations can help in determining the source of pollution, and can provide some understanding of anthropogenic effects on natural systems (Goldberg *et al.*, 1977).

Organic content and grain size are commonly accepted as the most important factors affecting metal accumulation in sediments. Horowitz (1985, in Callow, 1994) argues that an increase in metal concentration in estuarine sediments is strongly correlated to “decreasing grain size and increasing surface area, surface charge, cation exchange capacity and organic content”. Metal concentrations are consequently generally higher in

finer sediments, due to sorption (both absorption and adsorption), co-precipitation and complexing of metals on particle surfaces and coatings (Moore *et al.*, 1989, in Callow, 1994). It is therefore generally accepted that coarser material acts as a dilutant, altering the severity of metal concentrations. It is therefore important to granulometric or geochemically normalize the data.

Once the effects of grain size, mineralogy and provenance, on natural variability in the system are normalised, then the extent of anthropogenic contaminants in the estuary can be established. As contaminants tend to be concentrated in the fine fraction of sediment, a correlation between the total concentration of trace metals and weight percent of the fine fraction can often be used as an effective method of normalization, subsequently referred to as the granulometric method (Forstner, 1989; Loring and Rantala, 1992, in Leuci, 1998). Geochemical normalization of trace metals to inert/conservative elements, such as Iron (Fe) and Aluminium (Al), can be used to compensate for both grain size and mineralogy, and is, therefore, a more useful method to determine background trace metal levels compared to the granulometric method (Leuci, 1998).

Heavy metals are not necessarily permanently fixed to the sediment, but may be remobilised via various chemical, biological and physical processes (Dickinson *et al.*, 1996). These potentially toxic metals can be monitored by water analysis, however it is generally accepted that these measurement are not conclusive due to discharge fluctuations and short residence times.

7.2. Methodology

A total of 53 samples were selected from the surface sediment sample for geochemical analysis by X-ray fluorescence spectrometry (XRF) to determine the major and trace element chemistry in each bulk sediment sample (Appendix C.1). This method was chosen, as the natural background levels for the Mgeni Estuary had been predetermined using this method by Leuci (1998).

A Phillips PW 105 and Phillips X'Unique II X-Ray photometer were used for the analysis. X-Ray fluorescence (XRF) spectrometry involves the excitation of a sample by a primary X-ray beam, which excites secondary X-rays. These secondary X-rays have

wavelengths characteristic of the elements present in the sample. The intensity of the secondary X-rays is used to determine the concentrations of the elements, by reference to calibration standards, with appropriate corrections being made for instrumental errors and the effect the composition of the individual samples have on the X-ray emission intensities (Rollinson, 1993, in Leuci, 1998).

The preparation of the samples involved oven drying, at 100° C, approximately 100 to 200 g of representative samples. These representative samples were then milled using an agate pestles and mortar. The milled samples were the split into 6 to 10 g samples for XRF, and 1 g samples for loss of ignition (LOI) organic content analysis. The samples used for organic content were heated to 550° C and the loss of organic matter, due to ignition, being calculated as a weight percentage. The ability of organic matter to concentrate trace metals in and on soils has been well documented (Horowitz, 1985, in Callow, 1994). Although the organic content is removed prior to XRF analysis via loss of ignition, metal cations remain a part of the fraction of the total dried sediment (Callow, 1994). The portion of sample used for XRF was treated and prepared in two different ways, a pressed powder disc form for trace elements, and a glass bead made from powdered sample fused with lithium metaborate or tetraborate for major element analysis (Rollinson, 1993, in Leuci, 1998).

The major advantages of using XRF are the ability to rapidly detect concentrations down to parts per million, including the analysis for Tin (Sn), which most other geochemical techniques cannot do. XRF is also a non destructive technique, allowing the samples to be re-used and re-analysed.

For each analysed sample an enrichment factor (EF) was calculated (Appendix C.2). This enrichment factor is determined using Metal (ME) to Aluminium (Al) content in the sample divided by the background ratio. It is expressed mathematically:

$$EF = \frac{\left(\frac{ME}{Al}\right)_{Sample}}{\left(\frac{ME}{Al}\right)_{Background}}$$

The $(ME/Al)_{Sample}$ is the Metal to Aluminium ratio in the sample; and $(ME/Al)_{Background}$ is the natural local background ratio of Aluminium to trace Metal (Salomons and Förstner, 1984, in Santos *et al.*, 2005; Zhang, 1995, in Santos *et al.*, 2005; Feng *et al.*, 2004). The natural local background level ratios were adopted from Leuci (1998).

The enrichment factor is a useful indicator for the state of environmental contamination. If the enrichment factor is between 0.5 and 1.5, it is interpreted that the sample has negligible contamination, whereas samples with an enrichment factor >1.5 are thought to have a significant portion of the trace metal content derived from another source. Leuci (1998) proposed that nine specific trace metals can be used to assess sediment contamination in the Mgeni Estuary; namely Arsenic (As), Chromium (Cr), Cobalt (Co), Copper (Cu), Lead (Pb), Nickel (Ni), Tin (Sn), Vanadium (V) and Zinc (Zn). The same trace metals were tested during this study with the enrichment factor of the individual samples being gridded to create enrichment factor contaminant maps (Figure 7.A to I).

7.3. Results

Arsenic (As)

Arsenic is mainly used in pesticides, weed killers, herbicides and rodenticides (Athar and Vohora, 1995). It is also used as a wood preservative and for hardening Copper, Lead and other alloys. Burning of treated wood is of particular concern, as the smoke released may contain dangerous amounts of Arsenic compounds and other chemicals used to treat the wood (such as Chromium (VI) and Copper compounds) (National Pollutant Inventory, 2007).

Arsenic compounds enter the atmosphere as gases or small particles settling into the soil or water. Arsenic itself is not water soluble, but many of its compounds are, allowing them enter the ground water and fluvial systems (National Pollutant Inventory, 2007).

Arsenic does not break down, but does change forms. It is highly toxic to aquatic life, birds and land animals. Fish and shellfish build up organic Arsenic compounds, which are not as toxic as the inorganic (non-carbon based) forms. Arsenic and its compounds were ranked as 10 out of 400 on the NPI database, with an environmental rating of 1.7 (National Pollutant Inventory, 2007).

Arsenic tends to be enriched throughout the estuary with an enrichment factor of between 0.7 and 6.7, with the majority of samples being greater than 1.5, which is the suggested limit for the natural background levels determined by Leuci (1998). The highest concentrations of Arsenic are located towards the head of the estuary on both the northern and southern banks, although there is also a relatively high area of enrichment on the southern bank near the model yacht pool. Concentrations of Arsenic contaminants tend to be higher in areas adjacent to storm water outlets on both the northern and southern banks (Figure 7.A).

Chromium (Cr)

Chromium is used for the chemical manufacturing of dyes for paints (soluble chromate compounds), rubber and plastic products, matches and pyrotechnics, as well as for chrome plating of wood, stone, clay and glass products, bricks and linings for furnaces (Athar and Vohora, 1995; National Pollutant Inventory, 2007). Cement also contains chromium and can be released into the environment from cement producing plants and from the incineration of council refuse and sewage sludge. Chromium can be emitted into the air from brake linings that contain chromium and from motor vehicle exhaust (crude oil contains traces of Chromium (III) compounds, which may oxidise to the chromium (VI) state during fuel combustion in vehicle engines (National Pollutant Inventory, 2007).

Chromium (VI) released into the atmosphere can be carried by dust particles until it settles and contaminates soil and water. Airborne Chromium (VI) particles will settle in less than 10 days, depending on particle size, and will stick strongly to soil particles with small amounts penetrating into the groundwater. Chromium (VI) in water will stick to fine particles, which sink to the bottom. Little to no Chromium is typically lost by dissolution (National Pollutant Inventory, 2007) (Figure 7.B).

Figure 7. A) The distribution of arsenic enrichment in the Mgeni Estuary. The enrichment distribution of arsenic closely follows that of finer grained sediments, with high enrichment towards the northern side-attached bar, main channel and in the organic rich muds close to Connaught Bridge. B) The distribution of Chromium enrichment. With high enrichment around the storm water drain on the northern bank, and the organic rich muds towards Connaught Bridge.

There are two main compounds of Chromium on the National Pollutant Inventory (NPI) reporting list, namely Chromium (VI) and Chromium (III). The environmental effects of Chromium (VI) compounds vary from those of Chromium (III) compounds. In particular, Chromium (VI) can have a high to moderate, acute toxic effect on plants, birds or land animals. Chromium (VI) does not breakdown or degrade easily, resulting in a high potential for accumulation in fish. On an environmental rating of 0 to 3 Chromium (VI) compounds register 3. This placed it 2 out of approximately 400 substance considered for inclusion on the NPI reporting list (National Pollutant Inventory, 2007).

The Chromium enrichment factor in the Mgeni Estuary varies from 0.3 to 5.3, with the majority of contamination being located towards the head of the estuary and on the northern bank. The highest Chromium concentration is recovered directly adjacent to a storm water drain on the northern bank between Athlone Bridge and Ellis Brown Viaduct (Figure 7.B).

Cobalt (Co)

The largest use of Cobalt is in the manufacture of alloys, which retain strength even when very hot. Cobalt compounds are also used as humidity and water indicators, in electroplating, as a fertilizer and feed additive, in trace amounts in pigments for ceramics and glass, in fast drying paints and varnishes, in semiconductors, and in enamel coatings on steel (Athar and Vohora, 1995). It is also naturally found in trace amounts in seawater (National Pollutant Inventory, 2007).

Cobalt is mainly emitted into the air, land or water from the production of steel and other alloys. Automotive repair shops may also be significant emitters (to air) of Cobalt. Trace amounts of Cobalt are present in motor vehicle exhausts and, therefore, will be contained in roadside dust. Industrial emissions of Cobalt and its compounds can produce elevated, but still low level concentrations in the atmosphere. Because of its short life expectancy in the atmosphere (5 to 15 days) Cobalt and Cobalt compounds are expected to be confined to the local area within which they are emitted (National Pollutant Inventory, 2007).

Cobalt and its salts have high acute (short-term) toxicity on aquatic life. They also have high chronic (long-term) toxicity on aquatic life and bioaccumulate in fish tissues. Cobalt

and its compounds were ranked 27 on the NPI reporting list with an environmental rating of 2.0 (National Pollutant Inventory, 2007).

Cobalt shows a different distribution pattern to other contaminants in the Mgeni Estuary, with the majority of the enrichment occurring seawards of the head with the highest concentrations adjacent to Beachwood Creek (Figure 7.C). This distribution is suggestive of a marine source of Cobalt into the estuary. Cobalt is concentrated in areas where seawater becomes entrained, allowing it to accumulate due to its high persistence in water. The enrichment factor ranges from 0.1 to 7.6, with a maximum of 107 parts per million (ppm). The enrichment of cobalt shows no correlations when plotted against other elements, grain size, muds, or organics (Appendix C.3 and C.4). These enrichment factors are higher than expected in comparison to results from an earlier background levels study (Leuci, 1998) (Figure 7.C).

Copper (Cu)

Copper, and its compounds, have a widespread use in a range of applications, such as in electrical products and electronics in building construction. It is used in pigments and dyes, insulation for liquid fuels, cement, insecticides, herbicides and fungicides (Athar and Vohora, 1995). It is also used in pollution control devices, wood preservatives, timber treatments, anti-fouling paints, electrolysis and electroplating processes, as well as in fabrics and textiles, flame proofing materials, glass and ceramics. Water supply, sewerage and drainage surfaces as well as timber dressing activities can also emit Copper. Copper is also involved in chemical manufacture, electricity supply, coal mining, cement, lime, plaster and concrete product manufacture, transport equipment manufacturing, iron and steel manufacturing, petroleum and coal product manufacturing. It is also present, generally in low concentrations in fresh and sea water (National Pollutant Inventory, 2007).

Copper can be released as particles into the atmosphere or as dissolved compounds in water. It usually attaches strongly through complex bonds to particles of organic matter,

Figure 7. C) The cobalt enrichment within the Mgeni Estuary. The enrichment distribution differs to other elements round the supratidal barrier and the storm water drain on the southern bank. D) Distribution of copper enrichment. Enrichment is limited to the head of the estuary especially in the organic rich mud around Connaught Bridge.

clay, soil or sand, which strongly reduces its toxicity. Copper, as an element, does not breakdown in the environment (National Pollutant Inventory, 2007). However, the free Copper (II) ion is potentially very toxic to aquatic life and is expected to bioaccumulate in fish tissues, both acutely and chronically (National Pollutant Inventory, 2007). Coppers bio availability is a factor of the form taken by the metal, which is in turn dependent on environmental factors such as the pH or alkalinity, redox potential, soil and sediment type, organic content and water hardness (Flemming and Trevors, 1998; National Pollutant Inventory, 2007).

Copper enrichment is limited to the upper reaches of the estuary in the areas adjacent to Connaught Bridge, with the enrichment factor being limited to between 0 and 5 throughout the estuary (Figure 7.D). The enrichment factor of Copper is reduced to below 1.5 at the head of the estuary, where the estuary widens. The only major exception, is on the most vegetated north-western bank, where a plume of Copper enrichment in the sediments is observed extending westwards from a storm water drain (Figure 7.D). The plume of enrichment shows a trend of pollution being transported upstream from this storm-water drain. Concentration of Copper is at its highest again on the northern bank and on the southern side-attached bar (Figure 7.D).

Lead (Pb)

Metallic Lead is commonly used in the production of batteries, in leaded fuels (petrol) as an antiknock agent (Athar and Vohora, 1995). Lead compounds are used in the manufacturing process of plastics, rubbers, and metals and are also used in pigments, dyes, paints rodenticides and insecticides (National Pollutant Inventory, 2007).

Lead and its compounds are often released into the atmosphere by the burning of fossil fuels and from smelting plants. It binds to dust particles and may remain airborne for about 10 days, depending on weather conditions. Lead will stay in soil, dust and sediments for many years. It is also released into land and water via the manufacturing industries and waste sites (National Pollutant Inventory, 2007). Because Lead has been found in top soils, which were contaminated in the 4th century (Davies, 1988, in Fergusson, 1990), Lead is probably one of the least mobile heavy elements (Kabata-Pendias and Pendias, 1984, in Fergusson, 1990).

The immediate effects of exposure to Lead can mean death of animals, birds or fish and death or low growth rate in plants, with bioaccumulation expected to occur in fish tissue as Lead does not break down and is highly persistent in water. In soft water, Lead is highly poisonous to plants, birds or land animals with the long-term effects on animal life being a shortened lifespan, reproductive problems, lower fertility rates and changes in appearance or behaviour. Lead and compounds were ranked as 11 on the NPI reporting list with an environmental rating of 1.5 (National Pollutant Inventory, 2007).

The Lead enrichment factor of the Mgeni Estuary ranges from 1.2 to 9, with Lead contamination being widespread throughout the estuary. The highest concentration of contaminant enrichment is around Connaught Bridge, along the northern bank, the easternmost point of the southern side-attached bar at the confluence of the back channel and the estuary, and adjacent to the storm-water outlet upstream of the model yacht pool (Figure 7.E).

The concentration on the northern bank is probably related to the contamination of roadside dust, even though the use of such fuels has decreased in the past years with the introduction of unleaded and lead replacement fuels. Lead's high persistence levels reflect the fact that it does not break down naturally in the environment, which may also result in the widespread distribution of contamination throughout the estuary.

Nickel (Ni)

Nickel is used in many industrial applications, including battery manufacturing and the construction, transport, automotive, aerospace, electronics and consumer product sectors (National Pollutant Inventory, 2007). It is commonly used for alloys in corrosion-resistant equipment, such as in cooking utensils, coins, heating elements, gas turbines, electroplating, paints and pigments (Athar and Vohora, 1995). It is also released into the environment from diesel fuel and gasoline, lubricating oil and brake emissions. The major anthropogenic sources of Nickel pollution include the combustion of coal and heavy fuel oil and from the incineration of municipal waste. Emissions from refineries and from refinery products (including road tar) are particularly important because of the large amount of Nickel they contain (National Pollutant Inventory, 2007).

Figure 7. E) The distribution of lead enrichment in the Mgeni Estuary. Lead enrichment is found throughout the estuary, with the highest concentrations being found towards the head of the estuary and in the areas adjacent to storm water drains. F) The Nickel distribution. Nickel enrichment occurs only at the head of the estuary where enrichment factors are as high as 18.

Nickel and its compounds have high acute (short-term) and chronic (long-term) toxicity to aquatic life, with Nickel and other Nickel-compounds being highly persistent in the environment and tend to bioaccumulate and become concentrated in faunal tissues. Nickel is registered as 1.7 on the environmental spectrum (National Pollutant Inventory, 2007).

The Nickel enrichment factor has a high variation within the estuary ranging from 0 to 27.6, which is indicative of areas with high Nickel contamination. The enrichment pattern is limited to the upper estuary and follows a similar distribution pattern as that shown by Copper (Figure 7.F).

There is a possibility of error in the results of the calculated Nickel enrichment. One set of samples (those seaward of the head) where run for Nickel and those landward were tested for NiO, and converted to Nickel using the given conversion factor of 800 ppm Nickel, to every 0.001% NiO. The samples collected at the head of the estuary show highly elevated Nickel levels compared to those samples taken in lower reaches of the estuary.

Very low to no Nickel contamination is expected in the estuary, as other studies of the Durban Harbour showed no contamination (Leuci, 1998; Ayers, 2004). The Durban Harbour Basin drains the same geology as that of the estuary, but due to the nature of activities and industries, which are conducted in and around the Durban Harbour, higher levels of Nickel contamination would be expected in the harbour than in the estuary.

Tin (Sn)

Tin is mainly used for corrosion-resistant coatings for metals, as an alloying agent, painting of steel, soldering, packaging, fungicide, industrial biocide and PVC heat stabilizers (Athar and Vohora, 1995). Tin compounds are commonly released from industrial manufacture facilities in the form of industrial effluent and are generally transported in solution.

The major environmental concern of Tin compounds are the organotins which are based on Tin with hydrocarbon substituents. Organotins can be used for powerful fungicides, bactericides, biocides, antifouling paints and wood preservatives (National Pollutant

Inventory, 2007). Biocidal applications are the major contributors to organotin compounds in the environment. Organotins have low water solubility and a strong tendency to adhere to suspended materials and sediments. These suspended particles eventually settle, making widespread surface-water contamination. Organotin compounds are moderately persistent, with reported half-lives ranging from several days in freshwater to several weeks in saline conditions, depending on the initial concentration. Although leaching from soil and transport in soil may be possible, it is unlikely to occur due to the ability of organotins to adsorb strongly to the soil particles (National Pollutant Inventory, 2007). Organotins registers a 1.8 on the environmental spectrum.

The enrichment factor of Tin compounds in the estuary range from 1.2 to 12.6, suggesting wide spread contamination. The highest area of contamination is towards the head of the estuary (Figure 7.G). This area has been identified using sediment distribution patterns as a possible turbidity maxima zone. Settling of suspended particles, to which the Tin compounds have been attached, results from flocculation as the fresh and saline waters mix in this area. The raised vegetated bar on the northern bank is the only area that shows little to no Tin contamination. This most likely reflects the raised nature of the bar, which is seldom submerged, hence preventing the settling of suspended particles that contain Tin compounds. This lack of contamination on the vegetated bar is further evidence for Tin contamination resulting from water-born rather than via the atmospheric sources (Figure 7.G).

Vanadium (V)

The enrichment factors of Vanadium within the entire estuary fall within the 0.2 to 1.1 range, which is within the range given to represent the uncontaminated natural background levels by Feng *et al.*, (2004) (Figure 7.H).

Zinc (Zn)

Zinc is mainly used for galvanizing of iron and steel as well in the production of zinc alloys, it is also used in rubber (vulcanising, pigment), photocopy paper, chemicals, in glasses, paints, fabrics, plastics, lubricants, and in rayon manufacture (Athar and Vohora, 1995; National Pollutant Inventory, 2007). Emissions of zinc into the air, water and soil can occur at all stages of production and processing of zinc, particularly from

mining and refining of zinc ores, and from galvanising plants. Sewage treatment plants and waste sites for industrial and household wastes can also be a major source of zinc contaminants. Zinc is also released into the environment via the corrosion of galvanised structures as well as due to the wear and tear of car tyres and fuel combustion. These processes lead to elevated levels of zinc in roadside dust, which are then released into the soil and ground and run-off water (National Pollutant Inventory, 2007). Zinc attaches to the dust particles in the air and adheres to sediment particles, where most of the zinc will remain bound and can be transported and deposited in estuaries or in the marine environment. Zinc may, however, also be transported as dissolved compounds in natural water with some moving into streams and rivers, where it combines with other organic or inorganic matter (National Pollutant Inventory, 2007).

Zinc tends to bioaccumulate in fish and other organisms, but is unlikely to build up in plants. On an environmental spectrum of 0 to 3, Zinc and Zinc compounds register 2. A score of 3 represents a very high hazard to the environment and 0 a negligible hazard (National Pollutant Inventory, 2007). The majority of sample sites taken within the Mgeni Estuary showed a varying degree of Zinc contamination, with enrichment factors ranging from 0.2 to 19.4 (Figure 7.1). The highest level of contamination was recovered from samples located in the organic-rich muds on the northern bank near Connaught Bridge, with the enrichment levels decreasing seawards.

Enrichment on the northern banks is generally higher than that of the southern bank, especially in the areas directly adjacent to storm water and sewerage drains, which transport trace metals directly into the estuary. The location of sewage outlets, combined with the organic-rich mud deposits, which have collected in the back-channel environment, allow for contaminants to rapidly accumulate in this area. The enrichment of Zinc on the northern bank in comparison to that of the southern bank could also possibly be due to the close proximity of Riverside Road and its associated roadside dust. The decreasing Zinc enrichment towards the tidal inlet is probably due to the coarse nature of these associated sediments acting as a diluent. This area is also kept flushed by the incoming and outgoing tides, which would aid the prevention of trace metal accumulation (Figure 7.1).

Figure 7. G) The enrichment distribution of tin throughout the estuary. The highest concentration of tin is found towards the head of the estuary. There is an isolated pocket of no concentration against the northern bank. H) The vanadium enrichment within the estuary. There is little to no vanadium enrichment within the Mgeni Estuary.

Figure 7. 1) Zinc enrichment distribution in the Mgeni Estuary. The highest concentrations of zinc are found in the organic rich muds towards Connaught Bridge depleting east-wards towards the tidal inlet, where the enrichment is diluted with cleaner and coarser marine sediments. Zinc pollution is derived predominantly from the galvanizing of iron and steel.

7.4. Discussion and Conclusion

The overall heavy metal distribution pattern matches closely to that of mud fraction and organic concentration distribution patterns described from the sediment sampling program. The majority of contamination are interpreted to originate upstream of the estuary as the Mgeni River meanders its way through industrial areas. The contaminant distribution pattern shows a concentration of all contaminants, except Cobalt, towards the head of the estuary. In addition to the concentrations of these heavy metals towards the head, there are isolated pockets of Arsenic, Lead and Chromium concentration adjacent to storm-water drains. Both Chromium and Lead probably originate from the burning of fuels by motor vehicles, whilst Arsenic is commonly found in pesticides and herbicides. These trace metals, attached to dust particles, eventually settling along the roadside and adjacent areas before being washed out by heavy rainfalls. The runoff from rainfall gets channelled into the estuary via the storm-water drains, where contaminated particles are deposited and allowed to accumulate in isolated pools. Towards the tidal inlet the effects of the contamination are diluted by the increased amount of uncontaminated coarser marine sediment.

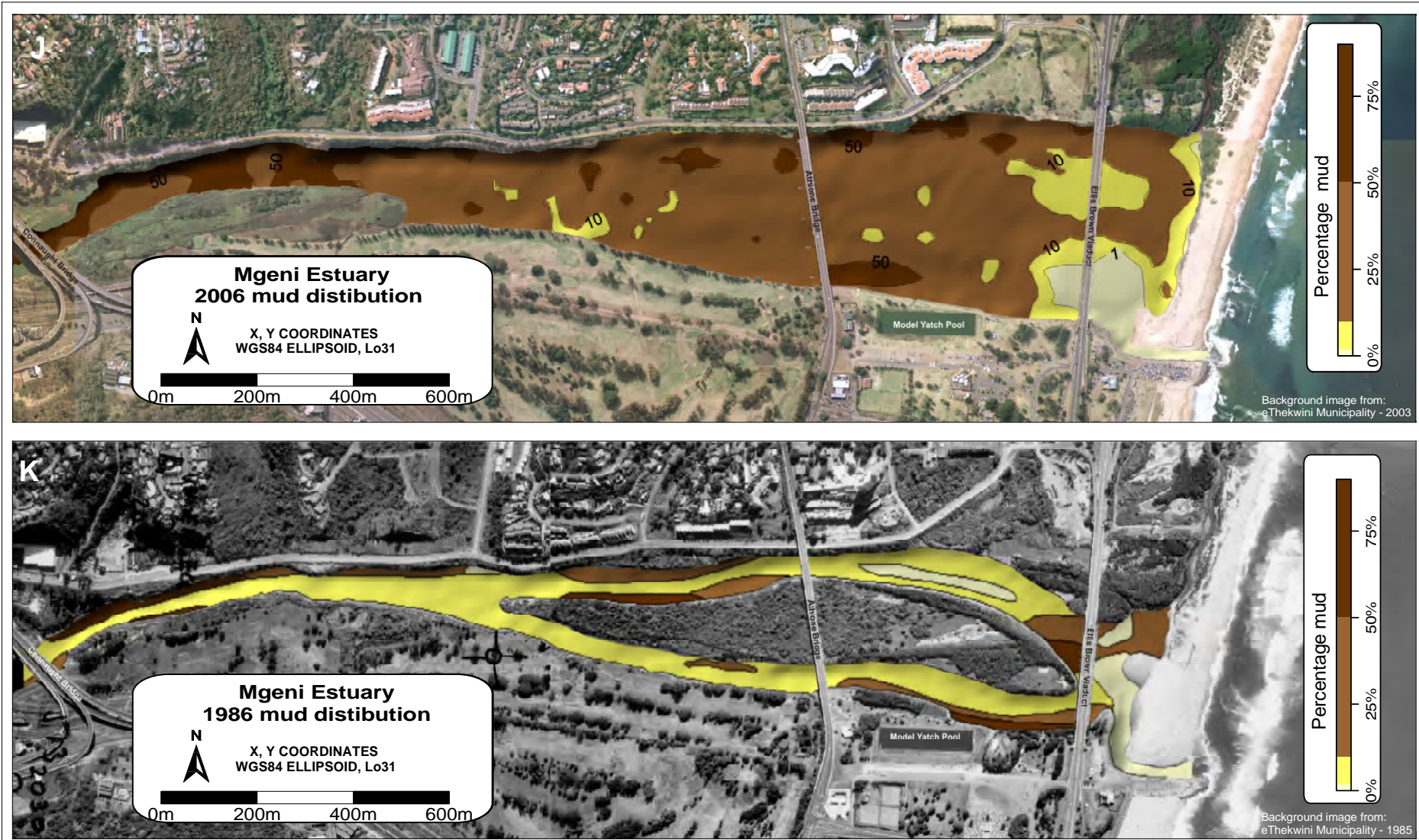


Figure 5.2. J) The 2006 distribution of mud within the Mgeni Estuary. Mud is located throughout the estuary except in the tidal inlet and on the flood tidal delta. High concentrations of mud are found at the head of the estuary, the back channel of the northern side-attached bar, and in an isolated pocket in the main channel immediately upstream of the model yacht pool. This is in contrast to K), which shows the 1986 distribution of mud. Cooper's study showed relatively smaller mud concentrations throughout the estuary with isolated pockets of mud against both the northern and southern bank and on the northern bank of the central island bar.

CHAPTER 8

Conclusion

The Mgeni Estuary has been anthropogenically influenced by the considerable construction of infrastructure, such as dams, roads and bridges, stream canalization, and storm-water outlets, throughout the 20th century. The completion of Inanda Dam in 1989, the most recently major completed construction influencing the estuary, is considered to have had major a impact on the dynamics of the Mgeni Estuary system. This study was undertaken in order to better understand the changes that have occurred since 1989, and to add a time line to the changing dynamics of this important estuarine system. The results of the current study were compared to those of Cooper (1986) pre-Inanda Dam study and Cooper's (1991) study in order to assess and describe any changes that had occurred over the last 20 years.

Previous studies by Cooper (1986, 1991) had classified the Mgeni Estuary as a river-dominated estuarine system. Diab and Scott (1989) argued that the construction of Inanda Dam on the Mgeni River would result in reduced fluvial flow rates, increased marine incursions into the estuary and more frequent mouth closures. Moleko and Garland (2000) disputed these conclusions and argued that the intended water release policy had led to an increase in the frequency and magnitude of peak flows, which resulted in an increase in scouring events. The analysis of historical aerial photographs undertaken during this study, as well as the sediment distribution patterns and bedform orientation, described in the previous chapters, has provided evidence that supports the earlier predictions of Diab and Scott (1989).

It is argued here that the anthropogenic influences, and the construction of Inanda Dam in particular, has changed the status of the Mgeni Estuary from a river-dominated to tide-dominated estuarine system. Historically, the morphology of the Mgeni Estuary was dominated by the presence of a central island bar. This central bar was typically eroded and removed during flooding events and then reestablished during post-flood recovery. Interpretation of historical aerial photographs showed that the post 1987 flood recovery deviated from this trend, with the development of the main bar now occurring against the northern bank. This northern side-attached bar is argued to form due to the aggregation of marine sediments transported by the detachment and inland migration of the flood tidal delta. The inability of the system to

transport sediment out to sea has resulted in an increase in the quantity of sediment trapped within the estuary. This additional sediment load has resulted in the formation of large subaerial and supratidal bars, in contrast to the single central island bar present in the estuary prior to the completion of Inanda Dam. More frequent periods of mouth closure, as predicted by Diab and Scott (1989) have also been noted during the period of this study. This study has shown that the flood tidal delta has become a dominant feature within the estuary following the post 1987 flood recovery, suggesting that the tidal flood flow dominates, reflecting a decrease in the fluvial discharge as a result of the dam construction and the resultant decreased catchment area. The analysis of the dominant bedform orientations based on structural readings taken in the field in 2005 and 2006 showed a net landwards trend, indicating the inland migration of sediment. The transported sediment is then refracted northwards as it enters further up the estuary due to the bathymetry, aggrading on to the northern side-attached bar.

The sediment distribution patterns within the Mgeni Estuary have changed considerably from those described in the study of Cooper (1986), with a definite trend towards a fining of sediment over this time interval. The results of the current study may be slightly skewed towards a finer sediment fraction, due to the presence of an ubiquitous mud drape on the surface sediment throughout most of the low-tide flats where samples were collected. However, this fining trend is supported by core data, which indicates a fining upward sequence during the redevelopment of the estuary since the 1989 floods. A decrease in sediment grain size is suggestive of a decrease in the flow velocity in the estuary. Further evidence in support of decreased fluvial flow rates and increased marine flow and associated marine incursion into the estuary is an increase in the amount of carbonate recovered from sediments of the estuary. Cooper (1986) indicated that carbonate concentrations were only located in the area directly adjacent to the tidal inlet. In contrast, carbonate analysis from this study show that carbonate is transported as far inland as the head of the estuary.

The highest concentration of heavy metal contamination is found towards the head of the Mgeni Estuary and in isolated pockets adjacent to storm water drains. The concentration of heavy metals in the sediments decrease towards the tidal inlet, interpreted to be due, in part, to the dilution by coarser uncontaminated sediments of marine origin. The overall heavy metal contaminant distribution pattern closely follows that of the mud fraction and organic matter concentrations in the estuarine sediments. This reflects the increase in surface area, surface

charge and cation-exchange capacity of the fine organic-rich sediments. The high levels of contaminants in the estuary and the correlation with fine sediment and organic matter within the estuary is interpreted to indicate that modern contamination is exacerbated by the presence of Inanda Dam and its direct effects on the Mgeni River fluvial discharge rates. In addition, the contamination of estuarine sediments is increased by trapping of effluents as a result of the associated increased mouth closures, where previously contaminants would have been flushed out to sea. It must be noted that the increased in marine incursions into the estuary could be masking the severity of contamination, by dilution of the sediments with uncontaminated marine components, making the results of this study only a best case scenario for the state of the Mgeni Estuary ecosystem.

In order to better understand the changes in the Mgeni estuarine dynamics, it is important that continued studies be conducted. These studies need to build on the framework that has already been established. In addition, new research is required to establish what effects any changes in the estuarine system dynamics will have on the ecology of the system as well as to understand any associated long-term effects. Better understanding of the estuarine system will allow for more informed decisions to be made regarding the future management of the system in order to protect the already environmentally-vulnerable diverse and productive ecosystem of the Mgeni Estuary.

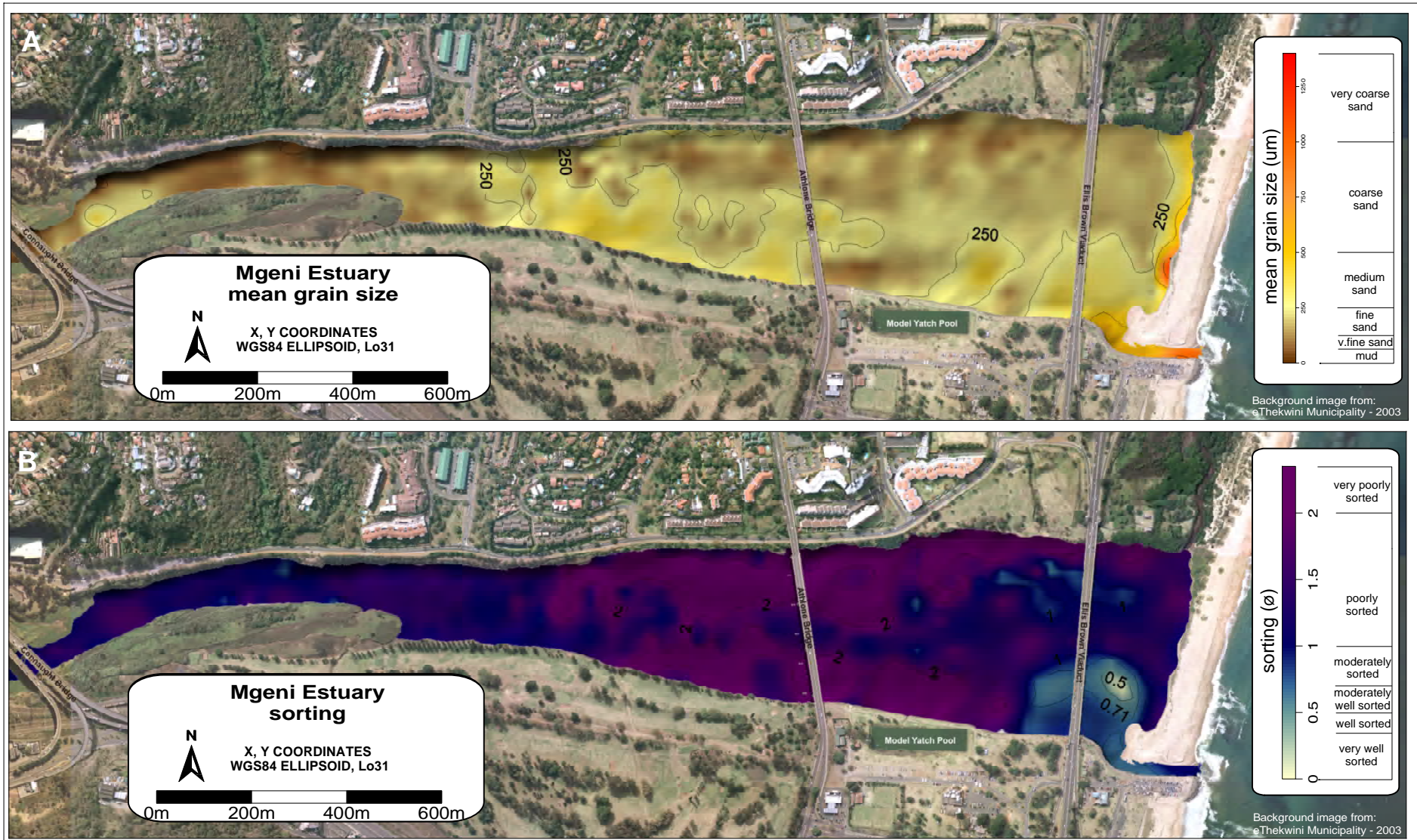


Figure 5.3. A) The 2006 mean grain size of sediment within the Mgeni Estuary. The mean grain size offers an estimate the relative current velocities. The mean grain size decreases away from the tidal inlet. B) The 2006 sorting of sediment within the estuary. Sorting can indicate the efficiency of the transportation medium. Sorting within the estuary varies from very well sorted near the tidal inlet, to very poorly sorted in the central region of the estuary, between Ellis Brown Viaduct and Athlone Bridge.

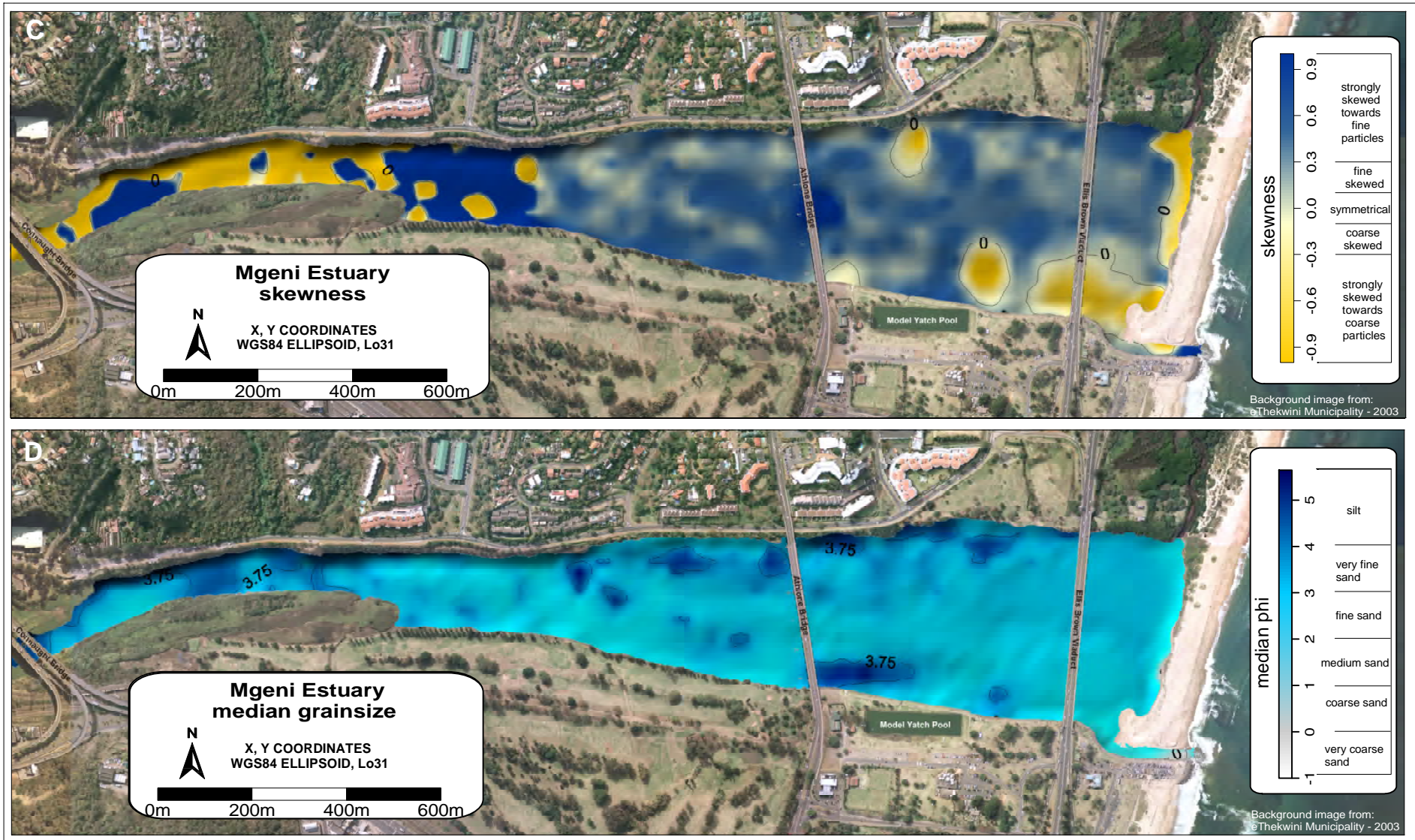


Figure 5.3. C) Skewness of the sediment within the Mgeni Estuary in 2006. Sediments are strongly skewed towards the coarse sediments in the area around the tidal inlet and flood tidal delta. At the head of the estuary there are mixed pockets of strongly coarse skewed and strongly finely skewed sediment. The middle of the estuary tends to be close to symmetrical. D) The 2006 median phi distribution. This distribution is similar to that of the mean grain size but does not account for the skewness. The median grain size tends to decrease away from the tidal inlet.

References

Allanson, B.R. (2001). Some factors governing the water quality of microtidal estuaries in South Africa. *Water SA*, **27**, 373-386.

Athar, M. and Vohora, S.B. (1995). *Heavy metals and environment*. Wiley Eastern Limited, 216pp.

Ayers, B. (2004). *The Durban Harbour Yacht Basin: A geophysical and sedimentological study*. B.Sc Hons. (unpubl), School of Geological Sciences, University of KwaZulu-Natal, 72pp.

Badenhorst, B., Cooper, J.A.G., Crowther, J., Gonslaves, J., Grobler, N.A., Illinberger, W.K., Laubscher, W.I., Mason, T.R., Moller, J.P., Perry, J.E., Reddering, J.S.V. and van der Merwe, L. (1989). Survey of the September 1987 Natal floods. *South African National Scientific Programmes Report*, **164**, 13-43.

Begg, G.W. (1978). The estuaries of Natal. *Natal Town and Regional Planning Report*, **41**, 657pp.

Begg, G.W. (1984). The estuaries of Natal. Part 2. *Natal Town and Regional Planning Report*, **55**, 631pp.

Brand, P.A.J., Kemp, P.H., Pretorius, S.J. and Schoonbee, H.J. (1967). Water quality and the abatement of pollution in Natal rivers. Part II, *Natal Town and Regional Planning Report*, **13**, 224.

Brayshaw, M. (2001). *Brittle deformation in southern coastal KwaZulu-Natal in relation to Gondwana break-up*. B.Sc Hons. (unpubl), University of Natal, Durban.

Brink, A.B.A. (1983). Engineering geology of Southern Africa. *Building Publishers*, 320pp.

Brown, D.S. (1971). Ecology of gastropoda in a South African mangrove swamp. *Proceedings of the Malacological Society of London*, **39**, 263-279.

Caeiro, S., Costa, M.H., Ramos, T.B., Fernandes, F., Silveira, N., Coimbra, A., Medeiros, G. and Pianho, M. (2005). Assessing heavy metal contamination in Sado estuary sediment: An index analysis approach. *Ecological Indicators*, **5**, 151-169.

Caeiro, S., Goovaerts, P., Painho, M., Costa, H. and Sousa, S. (2002). Optimal spatial sampling design for mapping estuarine sediment management areas. 5th AGILE Conference on Geographic Information Science, Palma (Balearic Islands, Spain).

Callow, S. (1994). *Aspects of heavy metal concentrations in Natal estuarine sediments*. (unpubl), M.Sc Thesis, Department of Applied Geology, University of Natal, 130pp.

Cameron, W.M. and Pritchard, D.W. (1963). Estuaries. In: Hill, M.N., ed., *The Sea*. Wiley-Interscience, New-York, **2**, 306-324.

Cooper, J.A.G. (1986). *Sedimentation in the Mgeni Estuary, Natal, South Africa*. MSc thesis (unpubl), University of Natal, Durban, 219pp.

Cooper, J.A.G. (1988). Sedimentary environments and facies of the subtropical Mgeni estuary, south-east Africa. *Geological Journal*, **23**, 59-73.

Cooper, J.A.G. (1991). *Sedimentary models and geomorphological classification of river mouths on a subtropical, wave-dominated coast, Natal, South Africa*. PhD thesis (unpubl), University of Natal, Durban, 401pp.

Cooper, J.A.G. (1993). Sedimentation in a river-dominated estuary. *Sedimentology*, **40**, 979-1017.

Cooper, J.A.G. (2001). Geomorphological variability among microtidal estuaries from the wave-dominated South African coast. *Geomorphology*, **40**, 99-122.

Cooper, J.A.G. and Mason, T.R. (1985). Barrier washover fans in the Beachwood mangrove area, Durban, South Africa: cause, morphology and environmental effect. *Journal of Shoreline Management*, **2**, 23-67.

Cooper, J.A.G. and Mason, T.R. (1987). Sedimentation in the Mgeni estuary. *Department of Geology & Applied Geology, University of Natal, Durban, S.E.A.L. Report*, **2**, 1-97.

Cooper, J.A.G. and McMillan, I.K. (1987). Foraminifera of the Mgeni estuary, Durban and their sedimentological significance. *South African Journal of Geology*, **90**, 489-498.

Cooper, J.A.G., Mason, T.R., Redding, J.S.V. and Illenberger. (1990). Geomorphological effects of catastrophic flooding on a small subtropical estuary. *Earth Surface Processes and Landforms*, **15**, 24-41.

Council for Scientific and Industrial Research. (1984). Effect of the Inanda Dam on the Mgeni estuary and adjacent coastline. *CSIR Report C/SEA 8426*.

Cox, M., Scheltinga, D., Rissik, D., Moss, A., Counihan, R. and Rose, D. (2004). Assessing condition and management priorities for coastal waters in Australia. *Cooperative Research Centre for Coastal Zone, Estuary and Waterway Management*, 551-557.

Crusius, J., and Anderson, R.F. (1991). Core compression and surficial sediment loss of lake. *Limnology and Oceanography*, **36** (5), 021-1031.

Dalrymple, R.W., Zaitlin, R.A., and Boyd, R. (1992). A conceptual model of estuarine sedimentation. *J. of Sed. Pet.*, **62**, 1130-1146.

Davies, B.E. (1988). Trace metals in soils. *Chem. Brit*, **24**, 149-154.

Davies, J.L. (1964). A morphogenic approach to world shorelines. *Zeitschr. Fur Geomorph.*, **8**, 27-42.

Davis, R.A. and Hayes, M.O. (1984). What is a wave-dominated coast? *Marine Geology*, **60**, 313-329.

Day, J.H. (1980). What is an estuary? *S. Afr. J. Sci.*, **76**, 198pp.

Deacon, J. and Lancaster, N. (1988). *Late Quaternary Palaeoenvironments of southern Africa*. Clarendon Press, Oxford, 236pp.

Diab, R.D and Scott, D. (1989). Inanda Dam: A case study of estuarine Impacts. *Internation Journal of Environmental Studies*, **34**, 271-278.

Dickinson, W.W., Dunbar, G.B. and McLeod, H. (1996). Heavy metal history from cores in Wellington Harbour, New Zealand. *Environmental Geology*, **27**, 59-69.

Ducrotoy, J.P. and Elliott, M. (2006). Recent developments in estuarine ecology and management. Editorial, *Marine Pollution Bulletin*, **53**, 1-4.

Dyer, K.R. (1997). *Estuaries: a physical introduction*. (2nd ed), John Wiley and Sons, Chichester, 195.

El Ella, R.A. and Coleman, J.M. (1985). Discrimination between depositional environments using grain-size analyses. *Sedimentology*, **32**, 743-748.

Esterhuysen, K. and Reddering, J.S.V. (1985). Sedimentation in the Nahoon estuary. *R.O.S.I.E. report no. 10*. Dept. of Geology, University of Port Elizabeth, 98.

Estuaries Management and Planning. (2005). Government of South Australia, Department for Environment and Heritage, Coasts and marine conservation program, last accessed: 3rd December 2008, <http://www.environment.sa.gov.au/coasts/estuaries.html>

Etchells, S.J., Russell, T.M. and Tinmouth, N. (2005). A conceptual model of soil erodibility in the uMgeni Catchment, KwaZulu-Natal. Poster Presentation.

Fairbridge, R.W. (1980). The estuary: Its definition and geodynamic cycle. In: Olausson, E. and Cato, I., eds., *Chemistry and Biochemistry of Estuaries*. Wiley, New-York, 1-35.

Feng, H., Han, X., Zhang, W. and Yu, L. (2004). A preliminary study of heavy metal contamination in Yangtze river intertidal zone due to urbanization. *Marine Pollution Bulletin*, **49**, 910-915.

Fenies, H., De Resseguier, A. and Tastet, J-P. (1999). International clay-drape couplets (Grinod estuary, France), *Sedimentology*, **46**, 1-15.

Fergusson, E.J. (1990). The heavy elements: Chemistry, environmental impact and health effects. *Pergamon Press*, Oxford, 614pp.

Flemming, C.A. and Trevors, J.T. (1989). Copper toxicity and chemistry in the environment: A review. *Journal Water, Air and Soil Pollution*, Springer Netherlands, **44**, 143-158.

Folk, R.L. and Ward, W.C. (1957). Brazos River bar: a study in the significance of grain-size parameters. *J. of Sed. Pet.*, **27**, 3-26.

Förstner, U. (1989). *Contaminated sediments*. Bhattacharji, S., Friedman, G.M., Neugebauer H.J. and Seilacher, A., eds., Springer-Verlag, London, 157.

Francis, T.E. (1983). *The engineering geology of the lower Umgeni Valley*. M.Sc Thesis (unpubl), University of Natal, Durban.

Garland, G.G. and Kruger, D. (1986). Durban's beaches reclaimed. *Geogr. Mag.*, **42**, 608-612.

Garland, G.G. and Moleko, L.P. (2000). Geomorphological impacts of Inanda Dam on the Mgeni Estuary, North of Durban, South Africa. *Bull. Eng. Geol. Env.*, **59**, 119-126.

Garlic, L. (2008). *A high-resolution seismic study of the Durban Bight, central KwaZulu-Natal, South Africa*. B.Sc Hons. (unpubl), School of Geological Sciences, University of KwaZulu-Natal, 71pp.

Goetzsche, E. (1966). *Father of a city*. Shuter and Shooter, Pietermaritzburg, 216.

Goldberg, E.D., Gamble, E., Griffin, J.J. and Koide, M. (1977). Pollution history of Narrangansett Bay as recorded in its sediments. *Estuarine and Coastal Marine Science*, **5**, 549-561.

Harris, T.F.W. (1961). The nearshore circulation of water. *Marine Studies off the Natal Coast C.S.I.R. Sympos.*, **No. S2.**, 18-30.

Hayes, M.O. (1975). Morphology of sand accumulation in estuaries. In: Cronin, L.E., ed., *Estuarine Research*. Academic Press, New York, 3-22.

Hayes, M.O. (1979). Barrier island morphology as a function of a tidal and wave regime. In: Leatherman, S.P., ed., *Barrier Islands*. Academic Press, New York, 1-27.

Hjulström, F. (1935). Studies of the Morphological activity of rivers as illustrated by the river Fyris. *Bull. Geol. Inst. Uppsala*, **25**, 221.

Horowitz, A.J. (1985). A primer on trace metal – sediment chemistry. *U.S. Geological Survey Water Supply Paper*, **2277**, 67.

International Maritime Organisation (1994). Review and evaluation of the “guidelines for the application of the annexes to the disposal of dredged material”, 27.

Johnson, M.R., Anhaeusser, C.R. and Thomas, R.J. (Eds.) (2006). *The geology of South Africa*. Geol. Soc. S. Afri. Jhb / Council for Geoscience. Pretoria, 69pp.

Johnson, M.R., Van Vuuren, C.J., Hegenberger, W.F., Key, R., & Shoko, U. (1996). Stratigraphy of the Karoo Supergroup in South Africa: An overview. *J. of Afr. Earth Sci.* **23**, 3-15.

Kabata-Pendias, A. and Pendias, H. (1984). *Trace elements in soils and plants*. CRC Press, 432pp.

Kantey and Templar Civil Engineers (1964). Report to the City Engineer, Durban on foundation investigations for proposed new bridge over the Umgeni river. Durban, 35.

Keinzle, S.W. Lorents, S.A. and Schulze, R.E. (1997). Hydrology and water quality of the Mgeni Catchment. *Water Research Commission, Pretoria, Report TT87/97*.

Kennedy, V.S. (1984). *The estuary as a filter*. Academic Press, 511pp.

Kennish, M.J. (2001). *Practical handbook of marine science*. Third Edition. CRC Press, New York, 896pp.

King, C.A.M. (1975). *Introduction to marine geology and geomorphology*. Edward Arnold, London, 309pp.

King, L.A. (1962). The Post-Karoo stratigraphy of Durban. *Trans. Geol. Soc. S. Afr.*, **65**, 85-93.

Kinmont, A. (1961). The nearshore movement of sand at Durban. *Marine Studies off the Natal Coast C.S.I.R. Sympos.*, **No. S2.**, 46-58.

Konert, M. and Vandenberghe, J. (1997). Comparison of laser grain size analysis with pipette and sieve analysis: a solution for the underestimation of the clay fraction. *Sedimentology*, **44**, 523-535.

Kranck, K. (1975). Sediment deposition from flocculated suspensions. *Sedimentology*, **22**, 111-123.

Kranck, K. (1981). Particulate matter grain-size characteristics and flocculation in a partially mixed estuary. *Sedimentology*, **28**, 107-114.

Krige, L.J. (1932). The geology of Durban. *Trans. Geol. Soc. South Africa*, **35**, 37-67.

Leoni, L. and Satori, F. (1997). Heavy metal and arsenic distributions in sediments of the Elba-Argentario basin, southern Tuscany, Italy. *Environmental Geology*, **32**, 83-91.

Leuci, R. (1998). *An assessment of trace metal contamination in sediments of Durban Harbour and Beachwood Mangroves*. B.Sc. Hons. (unpubl), Department of Geology and Applied Geology, University of Durban, Natal, 79pp.

Liaghati, T., Preda, M. and Cox M. (2003). Heavy metal distribution and controlling factors within coastal plain sediments, Bells Creek Catchment, southeast Queensland, Australia. *Environmental International*, **29**, 935-948.

Loring, D.H. and Rantala, R.T.T. (1992). Manual for the geochemical analyses of marine sediments and suspended particulate matter. *Earth-Science Reviews*, **32**, 235-283.

McDowell, D.M. and O'Connor, B.A. (1977). *Hydraulic behavior of estuaries*. The McMillan Press LTD, 17-21.

Meade, R.H. (1972). Transport and deposition of sediments in estuaries. *In: Nelson, B.W., ed., Environmental framework of coastal plain estuaries*. The Geological Society of America, Inc., U.S.A., 91-120.

Miller, G.T. (2000). *Living in the environment; Principles, connections, and solutions*, Brooks/Cole Publishing Company, 189pp.

Moleko, L.P. (1998). *Pre-and post-dam sediment characteristics below Inanda Dam at the Mgeni River, Natal, South Africa*. M.Sc thesis (unpubl) Department of Geographical and Environmental Sciences, University of Natal, Durban.

Moore, J.N., Brook, E.J. and Johns, C. (1989). Grain size partitioning of metals in contaminated, coarse grained river floodplain sediment: Clark Fork River, Montana, U.S.A. *Environ. Geol. Water Sci.*, **14**, No. 2, 107-115.

Murray, D.M. and Holtum, D.A. (1996). Technical Note: Inter-Conversions of Malvern and Sieve Size Distributions. *Mineral Engineering*, **9**, 1263-1268.

National Pollutant Inventory. (2007). Australian Government, Department of the Environment, Water, Heritage and the Arts, last accessed: 2nd December 2008, <http://www.npi.gov.au/database/substance-info/profiles/index.html>

National Research Institute for Oceanology. (1982). Hydrological/hydraulic study of Natal estuaries: Data Report No. 7. Mgeni NN1. *CSIR/NRIO Confidential Report*, 1-13.

National Research Institute for Oceanology. (1986). Basic physical geography - hydro data for Natal estuaries. *CSIR/NRIO Data Report D8607*, 6pp.

Neal, C., Leeks, G.J.L., Millward, G.E., Harris, J.R.W., Huthnance, J.M. and Rees, J.G. (2003). Land-ocean interaction: Processes, functioning and environmental management from a U.K. perspective: An introduction. *The Science of the Total Environment*, **314-316**, 3-11.

Nichols, M.M. and Biggs, R.B. (1985). Estuaries. In: Davis, R.A. (Ed.), *Coastal Sedimentary Environments*, Springer-verlag, New York, 77-186.

Njoya, S.G. (2002). Post-dam sediment dynamics below the Inanda Dam at the Mgeni Estuary, KwaZulu Natal, South Africa. M.Sc thesis (unpubl) Department of Geographical and Environmental Sciences, University of Natal, Durban.

Orme, A.R. (1974). Estuarine sedimentation along the Natal coast, South Africa. *Technical Report 5, Office of Naval Research, U.S.A.*, 53pp.

Orme, A.R. (1976). Late Pleistocene channels and Flandrian sediments beneath Natal estuaries: A synthesis. *Annals of the South African Museum*, **71**, 77-85.

Pacheco, A., Carrasco, A.R., Vila-Conceja, A., Ferreira, O. and Dias J.A. (2007). A coastal management program for channels located in backbarrier systems. *Ocean & Coastal Management*, **50**, 119-143.

Pearce, A.F. and Schumann, E.H. (1977). A review of present concepts of Natal coast circulation. *Progressing Report, CSIR/NIWR, 34th Steering Committee meeting*, **33**, 1-15.

Perillo, G.M.E. (1995). Definitions and geomorphologic classifications of estuaries. In, Perillo, G.M.E. (ed), *Geomorphology and Sedimentology of Estuaries*, Elsevier Science, Amsterdam, 17-47.

Pritchard, D.W. (1952). Salinity distribution and circulation in the Chesapeake Bay estuarine system. *J. Mar. Res.*, **11**, 106-123.

Pritchard, D.W. (1955). Estuarine circulation patterns. *Proc. Am. Soc. Civ. Eng.*, **81**, 1-11.

Pritchard, D.W. (1960). *Lectures on estuarine oceanography*. B. Kinsman (editor), J. Hopkins University, 154.

Ramsay, P.J. and Cooper, J.A.G. (2002). Late Quaternary sea-level change in South Africa. *Quaternary Research*, **57**, 82-90.

Roberts, D.L. (1981). *The stratigraphy and sedimentology of the Natal Group in the Durban area*. M.Sc. thesis (unpubl), University of Natal, Durban.

Rollinson, H. (1993). *Using geochemical data: Evaluation, presentation, interpretation*. Longman Publishers, Singapore, 352.

Roy, P.S. (1984). New South Wales estuaries: The origin and evolution. In: Thom, B.G., ed, *Coastal Geomorphology in Australia*, Academic Press, Australia, 99-121.

Roy, P.S. and Crawford, E.A. (1984). Heavy metals in a contaminated Australian estuary- dispersion and accumulation trend. *Estuarine, Coastal and Shelf Science*, **13**, 341-358.

Russell, G. (1899). *The history of old Durban and reminiscences of an immigrant of 1860*. P. Davis and Sons, Durban, 512.

Salomon, J.C. and Allen, G.P. (1983). Role sēdimetologique de la marée dans les estuaries a fort mornage compagnie Française des Pétroles. *Notes et Mēmoires*, **18**, 35-44.

Salomons, W. and Förstner, U. (1984). *Metals in the hydrocycle*. Springer-Verlag, Berlin, 349pp.

Santos, I.R., Silva-Filho, E.V., Schaefer, C.E.G.R., Albuquerque-Filho, M.R. and Campos, L.S. (2005). Heavy metal contamination in coastal sediments and soils near the Brazilian Antarctic Station, King George Island. *Marine Pollution Bulletin*, **50**, 185-194.

Schumann, E.H. and Orren, M.J. (1980). The physico-chemical characteristics of the south-west Indian Ocean in relation to Maputoland. In, Bruton, M.N. and Cooper, K.H. (eds), *Studies on the Ecology of Maputoland*, Wildlife Society of South Africa, Durban, 8-11.

Schumm, S.A. (1977). *The fluvial system*. John Wiley, New York, 338pp.

Scott, D. and Diab, R.D. (1989). Inanda Dam: a case study of the social impacts of infrastructural development in the South African context. *International journal of environmental studies*, **34**, 43-55.

Sharples, J., Waniek, J. and Ribeiro, C. (2001). Quantifying the variability of vertical turbulent mixing and its role in controlling stability and mass transport in a partially-mixed estuary. University of Southampton, Southampton Oceanography Centre, last accessed: 4th of December 2008, http://www.soes.soton.ac.uk/research/groups/soton_water/index.html

Shillabeer, N., Hart, B. and Riddle, A.M. (1992). The use of a mathematical model to compare particle size data derived by dry-sieving and laser analysis. *Estuarine, Coastal and Shelf Science*, **35**, 105-111.

Sholkovitz, E.R. (1976). Flocculation of dissolved organic and inorganic matter during the mixing of river water and sea water. *Geochim. Cosmochim. Acta.*, **40**, 831-845.

Simpson, D.E., Metz, H., Livingstone, D.J. and Calder, M. (1972). *Natal Coast estuaries: Environmental surveys*. Survey no. 5. The estuary and lower reaches of the Umgeni River, 12pp.

Singer, J.K., Anderson, J.B., Ledbetter, M.T., McCave, I.N., Jones, K.P.N. and Wright, R. (1988). *J. of Sed. Pet.*, **58**, 534-543.

Singh, M.L. (2001). *Modelling stream flow and sediment yield in the lower Mgeni Catchment*. M.Sc. (unpubl). Department of Geographical and Environmental Sciences, University of Natal, Durban.

Slagle, A.L., Ryan, W.B.F., S.M. Carbotte, S.M., Bell, R., Nitsche, F.O., and Kenna, T. (2002). Late-stage estuary infilling controlled by limited accommodation space in the Hudson River. *Marine Geology*, **232** (3-4), 181-202.

Smith, A.M. (1992). Palaeoflood hydrology of the lower Umgeni River from a reach south of Inanda Dam, Natal. *South African Geographical Journal*, **74**, 63-68.

Steinke, T.D. and Charles, L.M. (1986). Litter production by mangroves. In: Mgeni Estuary. *South African Journal of Botany*, **52**, 552-558.

Stretch, D. and Parkinson, M. (2006). The breaching of sand barriers at perched, temporary open/closed estuaries: A model study. *Coastal Engineering Journal*, **48**, 13-30.

Swart, D.H. (1987). Erosion of manmade dune in Beachwood Mangrove Nature Reserve. *CSIR Rep. T/SEA 8713*, 28.

Tinmouth, N. (2005). *A sedimentary study of the Mgeni Estuary*. B.Sc Hons. (unpubl), School of Geological Sciences, University of KwaZulu-Natal, 120pp.

Tucker, M.E. (1988). *Techniques in sedimentology*. Blackwell Scientific Publications Oxford, 408pp.

- Tucker, M.E. (1991). *Sedimentary petrology*. Second edition. Blackwell Scientific Publications Oxford, 259pp.
- Tyson, P.D. (1987). *Climatic change and variability in southern Africa*. Oxford University Press, Cape Town, 232pp.
- Tyson, P.D. and Preston-Whyte, R.A. (2000). *The weather and climate of southern Africa*. Oxford University Press, Cape Town, 187pp.
- Van Heerden, I.L. (1984). Barrier/estuary processes, Bot river estuary – an interpretation of aerial photographs. *Trans. Roy. Soc. South Africa*, **45**, 239-251.
- Watkeys, M.K. and Sokoutis, D. (1998). Transtension in south-eastern Africa with Gondwana break-up, In: Holdsworth, R.E., Strachan, R.A. and Dewey, J.F. (Eds.). (1998). *Continental Transpressional and Transtensional Tectonics*, Geological Society, London, Special Publications, **135**, 203-214.
- Williams, P.J. leB. (1985). Analysis: Organic matter. In: Head, P.C., ed., *Practical Estuarine Chemistry*. Cambridge University Press, 160-200.
- Wright, H. E. Jr. (1993). Core compression. *Limnology and Oceanography*, **38** (3), 699-701.
- Wright, J., Colling, A. and Park, D. (1999). *Waves, tides and shallow-water processes* (2nd Edition). The Open University, Milton Keynes and Butterworth Heinemann, Singapore, 227pp.
- Zhang, J. (1995). Geochemistry of trace metals from Chinese river/estuary systems: An overview. *Estuarine, Coastal and Shelf Science*, **41**, 631-658.

Appendix A

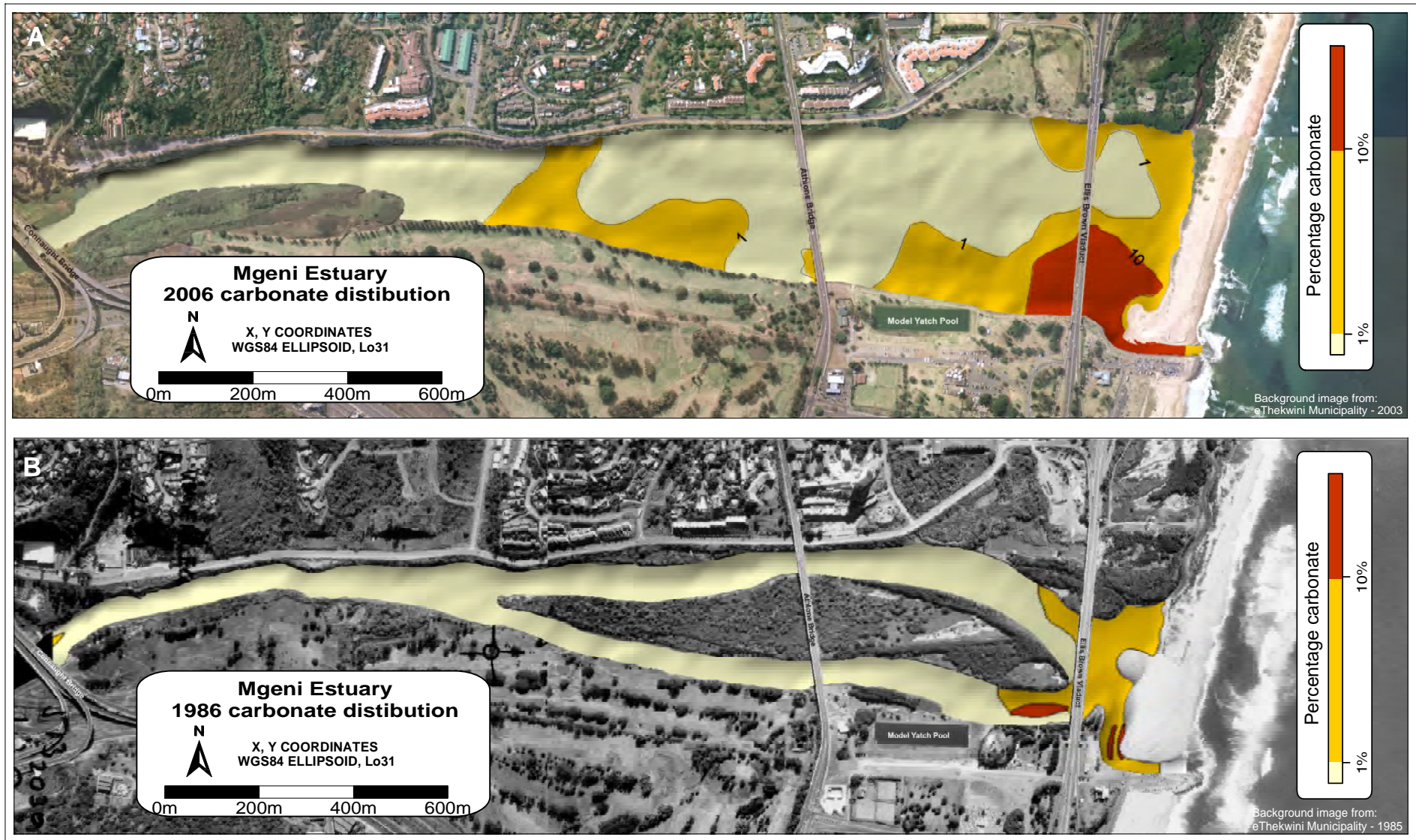


Figure 5.4. A) The 2006 distribution of carbonate in the Mgeni Estuary. Carbonate is concentrate in the area of the tidal inlet and flood tidal delta, as well as in the main channel towards the head of the estuary. This is in contrast to B) which shows the distribution in 1986 limited to the areas directly adjacent to the flood tidal delta, tidal inlet and supra tidal barrier. This increase in carbonate concentration from 1986 to 2006 represents an increase in marine incursion into the Mgeni Estuary.

Sample	y	x	Carbonate	Organics	Mud	Very fine sand	Fine sand	Medium sand	Coarse sand	Very coarse sand	Gravel	Mean (um)	Median (phi)	Mean (phi)	Sorting (phi)	Skewness	all Sand
A13	-3298978	2908	0.0		34.9	3.7	17.0	33.7	10.6	0.0	0.0	222.9	2.2	2.2	2.4	0.6	65.1
A27	-3298967	2755	0.0		60.4	6.6	10.9	16.2	5.8	0.0	0.0	120.4	4.9	3.1	2.6	-0.1	39.6
A28	-3298970	2751	0.0		14.6	3.5	27.5	42.5	12.0	0.0	0.0	276.6	1.9	1.9	1.5	0.4	85.4
A31	-3298946	2724	0.0		51.4	5.2	11.1	22.1	9.8	0.5	0.0	159.5	4.2	2.6	2.6	0.0	48.6
A32	-3298933	2714	0.0		0.0	0.0	25.4	62.5	11.8	0.3	0.0	336.6	1.6	1.6	0.5	0.0	100.0
A32	-3298933	2714	0.0		0.0	0.5	27.6	58.4	10.8	2.1	0.4	296.6	1.7	1.8	0.7	-0.3	99.6
A33	-3298919	2721	0.0		18.5	2.5	18.7	41.7	18.4	0.2	0.0	288.6	1.7	1.8	2.0	0.6	81.5
A51	-3298931	2466	0.0		15.4	1.8	24.1	44.3	14.1	0.2	0.0	286.0	1.8	1.8	1.5	0.5	84.6
A52	-3298941	2539	0.0		5.1	0.0	11.5	57.4	24.9	1.0	0.0	401.7	1.4	1.3	0.9	0.2	94.9
A57	-3299108	3006	0.0	0.4	24.4	1.3	14.2	40.9	18.9	0.3	0.0	282.4	1.7	1.8	2.5	0.7	75.6
A58	-3299120	3058	0.0		11.4	0.2	13.0	57.0	18.4	0.0	0.0	356.5	1.5	1.5	1.3	0.4	88.6
A59	-3299123	3122	0.0		22.4	6.1	20.9	38.7	11.9	0.0	0.0	245.0	2.0	2.0	2.1	0.6	77.6
A62	-3299123	3219	0.0	1.1	62.7	8.6	9.6	14.6	4.4	0.0	0.0	107.1	5.2	3.2	2.7	-0.1	37.3
A64	-3299132	3275	0.0	0.1	94.7	4.7	0.6	0.0	0.0	0.0	0.0	17.9	6.2	5.8	1.6	0.2	5.3
A72	-3298987	3702	0.0		9.7	18.6	46.5	24.0	1.2	0.0	0.0	187.3	2.5	2.4	1.2	0.3	90.3
B32	-3299018	3870	0.0	0.0	14.2	15.0	42.9	26.2	1.6	0.0	0.0	188.4	2.5	2.4	1.3	0.4	85.8
B45	-3299017	3760	0.0	0.0	13.4	21.0	45.0	20.1	0.5	0.0	0.0	169.6	2.6	2.6	1.3	0.4	86.6
B46	-3299021	3816	0.0		9.7	19.0	46.9	23.6	0.8	0.0	0.0	185.3	2.5	2.4	1.2	0.3	90.3
B48	-3298962	3833	0.0		7.9	9.0	49.6	32.5	1.0	0.0	0.0	215.4	2.3	2.2	1.0	0.3	92.1
B50	-3298879	3809	0.0	0.3	35.1	13.8	31.0	18.9	1.3	0.0	0.0	138.1	3.0	2.9	2.3	0.5	64.9
B53	-3298959	3779	0.0	0.1	5.7	16.0	53.9	24.1	0.4	0.0	0.0	193.1	2.5	2.4	0.9	0.3	94.3
B57	-3299027	3612	0.0	0.1	23.0	6.4	36.9	31.6	2.1	0.0	0.0	182.6	2.4	2.5	2.0	0.6	77.0
B58	-3299075	3606	0.0		17.0	3.5	39.0	38.1	2.4	0.0	0.0	203.8	2.2	2.3	1.8	0.6	83.0
B61	-3299067	3456	0.0	0.2	27.2	3.4	29.2	35.9	4.3	0.0	0.0	198.9	2.2	2.3	2.3	0.7	72.8
B66	-3299054	3317	0.0	0.0	12.8	2.1	43.1	40.6	1.5	0.0	0.0	234.5	2.1	2.1	1.1	0.4	87.2
B72	-3298995	3311	0.0		47.3	6.7	22.3	21.5	2.3	0.0	0.0	133.2	3.5	2.9	2.5	0.4	52.7
M02	-3298871	3111	0.0		17.9	0.4	27.9	48.8	5.1	0.0	0.0	230.8	1.9	2.1	1.9	0.7	82.2
M03	-3298884	3107	0.0		47.4	9.3	18.3	20.3	4.5	0.0	0.0	136.8	3.7	2.9	2.4	0.2	52.6
M04	-3298905	3097	0.0		53.1	9.4	15.7	18.1	3.8	0.0	0.0	120.4	4.3	3.1	2.6	0.1	46.9
M10	-3299025	3079	0.0		7.8	0.7	29.1	53.3	9.2	0.0	0.0	302.0	1.8	1.7	1.0	0.3	92.2
M25	-3298916	2981	0.0	3.8	42.5	9.9	15.9	21.8	8.6	1.4	0.0	171.7	3.2	2.5	2.6	0.3	57.5
M43	-3298860	2861	0.0		5.2	1.0	32.4	53.1	8.3	0.0	0.0	298.4	1.8	1.7	0.8	0.3	94.8
M47	-3298898	2836	0.0	5.0	66.4	13.9	9.6	5.7	2.9	1.6	0.0	64.1	5.0	4.0	2.4	0.0	33.6
N02	-3298916	3398	0.0	0.8	47.7	8.8	21.4	19.4	2.6	0.0	0.0	127.0	3.7	3.0	2.5	0.3	52.3
N09	-3298877	3294	0.0		28.3	3.7	29.5	34.6	4.0	0.0	0.0	196.2	2.3	2.3	2.0	0.6	71.7
N13	-3298956	3182	0.0		49.1	18.5	21.2	9.9	1.1	0.2	0.0	93.7	3.9	3.4	2.4	0.3	50.9
N16	-3298896	3200	0.0		32.3	4.2	27.4	32.3	3.8	0.0	0.0	188.9	2.4	2.4	2.1	0.6	67.7
P8	-3298957	3373	0.0		0.0	5.5	52.2	40.5	1.9	0.0	0.0	230.9	2.1	2.0	0.6	0.0	100.0
R59	-3298839	3507	0.0		24.1	6.2	34.1	32.3	3.2	0.0	0.0	188.0	2.3	2.4	2.1	0.6	75.9
A45	-3298990	2606	1.3		4.1	0.2	18.4	53.9	22.6	0.8	0.0	381.0	1.5	1.4	0.7	0.1	95.9
A81	-3299064	3368	1.7		1.8	3.2	43.2	46.9	5.0	0.0	0.0	269.9	2.0	1.9	0.6	0.0	98.2
A60	-3299120	3135	1.9		43.3	7.1	17.1	24.0	8.4	0.1	0.0	174.3	3.0	2.5	2.4	0.4	56.7
A48	-3298963	2553	2.0		77.8	9.6	5.7	4.7	2.1	0.2	0.0	40.1	5.5	4.6	2.1	0.0	22.2
A74	-3299129	3575	2.0		13.7	4.1	25.7	43.8	12.6	0.0	0.0	281.6	1.9	1.8	1.5	0.5	86.3
A37	-3298892	2677	2.0		54.9	13.6	11.1	10.7	7.1	2.7	0.0	129.8	4.3	2.9	2.6	0.0	45.1
B31	-3299036	3764	2.4	0.3	16.2	18.4	43.5	21.3	0.6	0.0	0.0	167.7	2.6	2.6	1.4	0.4	83.8
A12	-3299026	2887	2.4		74.2	8.6	7.5	7.0	2.5	0.2	0.0	54.6	5.7	4.2	2.4	-0.1	25.8
B62	-3299098	3453	2.4		10.1	1.2	39.1	47.0	2.6	0.0	0.0	256.5	2.0	2.0	1.1	0.4	89.9
A02	-3299051	2974	2.5		6.3	1.7	37.1	49.0	5.9	0.0	0.0	277.5	1.9	1.8	0.9	0.3	93.7
B55	-3299044	3705	2.7		19.8	15.6	40.7	23.1	0.8	0.0	0.0	161.6	2.6	2.6	1.7	0.5	80.2
B43	-3298890	3886	2.9		0.8	5.1	28.9	35.8	17.4	6.9	5.1	348.2	1.6	1.5	1.2	-2.8	94.1
R5	-3298893	3701	2.9		5.0	19.7	54.7	20.5	0.1	0.0	0.0	183.1	2.5	2.4	0.7	0.1	95.0
P17	-3299136	3894	3.0		0.0	0.9	1.3	2.1	9.0	53.7	29.5	1644.0	-0.7	-0.7	0.7	0.4	67.1
B36	-3298951	3904	3.2	0.4	23.6	10.3	27.1	26.6	9.6	2.8	0.0	218.2	2.4	2.2	2.3	0.5	76.4
B35	-3298921	3939	3.9		0.8	2.3	16.5	43.3	20.4	10.7	6.0	448.7	1.3	1.2	1.2	-2.5	93.2
B38	-3298908	3908	4.8		15.2	3.0	22.8	40.2	16.5	2.2	0.0	302.9	1.8	1.7	1.7	0.5	84.8
B22	-3299055	3782	4.9	14.5	24.6	5.5	24.2	36.0	9.8	0.0	0.0	227.3	2.1	2.1	2.1	0.6	75.4
A70	-3299078	3894	4.9	0.2	6.5	7.2	22.4	32.1	21.7	10.1	0.0	422.0	1.6	1.2	1.4	0.1	93.5
B37	-3298864	3919	5.6	0.1	0.1	12.3	22.7	26.5	14.5	14.7	8.3	418.7	1.6	1.3	1.6	-4.1	90.7
B34	-3299029	3920	5.8		0.2	0.8	7.6	36.8	33.2	15.9	5.5	575.4	0.9	0.8	1.1	-0.8	94.2
Mouth1	-3299301	3958	6.3		0.0	2.3	6.3	10.5	20.0	39.7	19.3	1037.9	-0.3	-0.1	1.2	4.3	78.8
B65	-3299176	3555	6.7	0.5	58.4	15.6	15.2	7.8	2.6	0.3	0.0	78.1	4.7	3.7	2.3	0.1	41.6
A71	-3299223	3876	7.5		0.0	0.3	11.8	42.2	28.6	14.7	2.3	507.5	1.1	1.0	1.0	-1.1	97.7
P18	-3299209	3874	7.9		0.1	11.2	20.8	24.0	11.4	19.7	11.2	474.7	1.3	1.1	1.7	-5.1	87.2
B03	-3299225	3828	8.4		0.0	0.1	9.8	52.1	22.7	12.8	2.5	480.8	1.3	1.1	1.0	-1.9	97.5
Mouth2	-3299308	3958	8.9		0.0	0.5	2.7	18.9	24.6	32.3	17.3	1010.5	-0.1	0.0	1.2	1.3	79.1
B07	-3299193	3836	9.5		0.0	2.7	36.4	50.5	10.4	0.0	0.0	304.1	1.8	1.7	0.6	0.0	100.0
Mouth3	-3299318	3958	9.7		0.0	0.3	0.9	14.8	41.9	36.4	5.6	883.5	0.2	0.2	0.8	0.4	94.4
B02	-3299280	3838	9.9		0.0	0.0	4.8	37.2	37.9	20.1	0.0	664.7	0.8	0.6	0.8	-0.1	100.0
B1	-3299294	3966	11.0		0.0	0.0	17.5	66.2	16.3	0.0	0.0	365.5	1.5	1.5	0.5	0.0	100.0
B26	-3299167	3727	11.5		0.0	0.7	21.5	49.9	21.4	6.0	0.5	363.3	1.5	1.5	0.9	-0.9	99.5
B09	-3299193	3764	11.9		0.2	1.9	34.5	44.4	15.5	3.0	0.5	299.2	1.8	1.7	0.9	-0.8	99.3
B08	-3299207	3746	12.2		0.0	0.2	19.0	55.1	19.5	5.5	0.7	368.6	1.5	1.4	0.8	-1.0	99.3
B21	-3299072	3780	12.3		0.0	1.6	38.8	52.4	7.0	0.2	0.0	292.6	1.9	1.8	0.6	0.0	100.0
B25	-3299202	3723	12.5		0.1	1.0	23.8	55.7	14.8	4.3	0.3	327.0	1.7	1.6	0.8	-0.8	99.6
B06	-3299155	3838	12.6		0.0	1.2	38.8	54.0	6.0	0.0	0.0	291.1	1.9	1.8	0.6	0.0	100.0
B20	-3299159	3771	12.9		0.0	0.2	29.7	59.0	11.1	0.0	0.0	325.3	1.7	1.6	0.6	0.0	100.0
B4	-3299280	3896	13.0		0.0	3.7	15.0										

Sample	y	x	Carbonate	Organics	Mud	Very fine sand	Fine sand	Medium sand	Coarse sand	Very coarse sand	Gravel	Mean (um)	Median (phi)	Mean (phi)	Sorting (phi)	Skewness	all Sand
9.00	-3299088	1562			53.1	7.4	5.0	16.3	13.9	4.2	0.0	108.1	4.1	3.2	1.7	-12.5	46.9
10.00	-3299091	1578			10.6	9.1	34.6	38.0	7.7	0.0	0.0	244.3	2.1	2.0	0.9	1.8	89.4
11.00	-3299081	1600			17.7	15.5	35.9	27.0	3.9	0.0	0.0	150.8	2.5	2.7	1.2	2.0	82.3
12.00	-3299060	1595			30.1	2.7	5.4	28.3	25.4	8.2	0.0	231.0	1.5	2.1	1.8	7.8	69.9
13.00	-3299027	1596			80.1	11.2	5.4	3.0	0.4	0.0	0.0	58.5	4.4	4.1	0.8	-2.7	19.9
14.00	-3299015	1598			75.6	13.7	6.4	3.1	1.1	0.1	0.0	67.4	4.3	3.9	1.0	-3.8	24.4
15.00	-3299036	1618			69.1	11.8	7.2	8.0	3.6	0.3	0.0	68.4	4.3	3.9	1.1	-6.0	30.9
16.00	-3299061	1645			45.2	6.4	10.2	23.4	13.8	1.0	0.0	143.3	2.7	2.8	1.6	0.3	54.8
17.00	-3299028	1650			10.6	1.3	3.8	38.3	37.4	8.6	0.0	463.4	1.1	1.1	1.2	5.1	89.4
20.00	-3298989	1615			74.2	11.0	8.3	5.5	1.1	0.0	0.0	62.6	4.3	4.0	1.0	-4.0	25.8
21.00	-3298976	1639			63.6	12.6	9.7	7.2	4.4	2.5	0.0	75.9	4.2	3.7	1.3	-8.1	36.4
23.00	-3298977	1662			63.5	15.3	9.1	8.0	3.8	0.3	0.0	72.0	4.2	3.8	1.2	-6.0	36.5
27.00	-3298936	1723			71.5	13.3	10.4	4.2	0.6	0.0	0.0	62.3	4.3	4.0	0.9	-3.2	28.5
31.00	-3299177	3232			0.5	5.6	50.6	40.7	2.6	0.0	0.0	225.8	2.1	2.1	0.6	-0.2	99.5
32.00	-3298948	1765			43.0	6.3	11.5	21.3	13.7	4.2	0.0	141.8	2.9	2.8	1.7	-2.9	57.0
33.00	-3298949	1765			51.0	17.3	17.8	9.3	2.9	1.7	0.0	82.0	4.0	3.6	1.2	-5.6	49.0
34.00	-3298925	1786			62.0	9.4	13.0	13.7	1.9	0.0	0.0	79.4	4.2	3.7	1.2	-6.2	38.0
35.00	-3298914	1825			76.1	13.8	6.3	3.1	0.6	0.0	0.0	67.3	4.3	3.9	1.0	-3.6	23.9
36.00	-3298895	1897			63.5	15.3	12.9	6.3	1.4	0.6	0.0	69.2	4.2	3.9	1.0	-4.3	36.5
37.00	-3298895	1897			77.4	14.4	5.4	2.1	0.5	0.1	0.0	62.6	4.4	4.0	0.9	-2.7	22.6
38.00	-3298889	1938			69.1	12.9	10.5	6.6	0.8	0.0	0.0	64.5	4.3	4.0	1.0	-4.1	30.9
39.00	-3298880	1971			57.0	13.2	13.9	7.9	4.1	4.0	0.0	81.5	4.1	3.6	1.4	-9.3	43.0
40.00	-3298874	2003			47.3	15.2	22.0	12.9	2.2	0.4	0.0	97.8	3.4	3.4	1.2	-1.2	52.7
41.00	-3298872	2035			50.4	17.5	13.8	9.6	5.7	2.9	0.0	88.8	4.0	3.5	1.4	-8.3	49.6
42.00	-3298894	2108			65.4	14.0	9.0	5.8	3.9	1.9	0.0	70.4	4.2	3.8	1.2	-7.0	34.6
43.00	-3298891	2156			55.4	12.4	13.6	13.3	5.0	0.3	0.0	85.8	4.1	3.5	1.3	-7.0	44.6
44.00	-3298887	2205			47.3	17.8	18.2	10.8	4.1	1.8	0.0	96.3	3.5	3.4	1.3	-3.3	52.7
45.00	-3298881	2274			74.7	13.5	7.4	3.1	1.1	0.3	0.0	65.8	4.3	3.9	1.0	-3.7	25.3
46.00	-3298879	2312			68.7	14.0	9.0	4.8	2.2	1.3	0.0	64.1	4.3	4.0	1.0	-4.9	31.3
48.00	-3298883	2355			18.3	0.5	11.8	52.6	16.7	0.0	0.0	211.8	1.6	2.2	1.4	7.3	81.7
49.00	-3298918	2350			16.0	0.6	14.4	50.1	18.7	0.1	0.0	223.8	1.6	2.2	1.4	6.7	84.0
51.00	-3298885	2410			82.3	9.5	4.9	2.9	0.3	0.0	0.0	52.8	4.4	4.2	0.7	-2.2	17.7
53.00	-3298889	2461			20.4	1.8	18.7	41.9	16.7	0.4	0.0	200.5	1.8	2.3	1.5	6.2	79.6
101.00	-3298969	1790			15.5	10.5	37.3	33.1	3.5	0.0	0.0	172.7	2.4	2.5	1.1	2.4	84.5
102.00	-3299000	1782			27.9	3.4	11.0	30.6	22.2	4.9	0.0	210.2	1.7	2.2	1.7	6.3	72.1
103.00	-3298964	1760			18.3	2.5	10.5	37.6	26.6	4.4	0.0	241.9	1.5	2.0	1.6	7.5	81.7
104.00	-3298951	1761			63.7	10.9	7.8	11.6	5.8	0.1	0.0	82.1	4.2	3.6	1.3	-7.9	36.3
105.00	-3298937	1822			31.5	19.3	31.2	16.3	1.3	0.5	0.0	114.8	3.0	3.1	1.2	1.0	68.5
106.00	-3298976	1836			78.3	13.0	4.5	2.7	1.3	0.2	0.0	61.3	4.4	4.0	0.9	-3.1	21.7
107.00	-3298932	1858			48.7	13.6	20.4	15.7	1.5	0.0	0.0	92.4	3.7	3.4	1.2	-3.3	51.3
108.00	-3298976	1867			67.5	9.5	10.1	10.5	2.4	0.0	0.0	72.9	4.3	3.8	1.2	-6.0	32.5
109.00	-3298926	1902			65.5	7.7	5.4	14.0	7.3	0.1	0.0	86.9	4.2	3.5	1.4	-9.1	34.5
111.00	-3298964	1954			18.2	15.7	38.0	25.9	2.2	0.0	0.0	145.5	2.6	2.8	1.2	2.1	81.8
112.00	-3298959	1953			82.8	10.3	3.3	2.7	0.8	0.0	0.0	50.4	4.4	4.3	0.6	-1.9	17.2
113.00	-3298919	1946			59.4	17.2	7.2	9.8	5.9	0.5	0.0	81.2	4.2	3.6	1.3	-7.5	40.6
114.00	-3298912	1970			29.6	11.4	28.7	26.5	3.8	0.0	0.0	134.0	2.7	2.9	1.3	1.9	70.4
115.00	-3298963	2023			29.6	6.9	20.1	33.3	10.1	0.0	0.0	158.5	2.3	2.7	1.4	3.4	70.4
116.00	-3298963	2024			75.0	8.8	4.1	8.0	4.0	0.1	0.0	61.3	4.3	4.0	1.0	-5.9	25.0
117.00	-3298897	1993			10.0	8.4	34.8	38.7	8.1	0.0	0.0	242.0	2.1	2.0	1.0	1.9	90.0
118.00	-3298957	2047			45.1	4.4	6.6	27.5	16.2	0.3	0.0	139.2	2.9	2.8	1.6	-1.3	54.9
119.00	-3298907	2033			67.6	18.5	8.5	4.2	1.2	0.0	0.0	64.1	4.3	4.0	0.9	-3.4	32.4
120.00	-3298919	2090			69.6	15.9	8.0	4.6	1.6	0.3	0.0	63.4	4.3	4.0	1.0	-3.9	30.4
121.00	-3298904	2098			29.2	3.0	14.6	39.2	13.9	0.0	0.0	179.9	1.9	2.5	1.5	6.2	70.8
122.00	-3298958	2093			38.3	5.9	15.0	31.2	9.6	0.0	0.0	143.4	2.6	2.8	1.5	1.7	61.7
123.00	-3298961	2118			74.1	4.7	4.0	10.7	6.2	0.3	0.0	79.0	4.3	3.7	1.3	-8.8	25.9
124.00	-3298923	2114			82.3	8.0	2.5	5.0	2.2	0.0	0.0	52.9	4.4	4.2	0.8	-4.2	17.7
125.00	-3298919	2144			29.8	20.9	28.7	18.2	2.5	0.0	0.0	118.5	3.0	3.1	1.2	0.6	70.2
126.00	-3298964	2143			58.9	10.2	14.1	14.6	2.1	0.0	0.0	81.7	4.2	3.6	1.2	-6.2	41.1
127.00	-3298963	2181			86.9	7.8	1.9	2.6	0.8	0.0	0.0	46.6	4.4	4.4	0.5	-1.2	13.1
128.00	-3298923	2170			37.9	2.1	5.7	33.2	19.6	1.4	0.0	187.2	1.9	2.4	1.6	6.5	62.1
129.00	-3298913	2209			51.4	7.2	15.6	21.6	4.2	0.0	0.0	92.3	4.0	3.4	1.4	-6.8	48.6
130.00	-3298967	2199			50.9	7.2	18.1	20.6	3.2	0.0	0.0	90.8	4.0	3.5	1.3	-6.3	49.1
131.00	-3298981	2268			43.6	3.5	8.6	29.3	14.6	0.3	0.0	146.0	2.7	2.8	1.6	0.8	56.4
132.00	-3298927	2274			21.0	0.8	8.5	50.3	19.3	0.1	0.0	212.9	1.6	2.2	1.5	7.9	79.0
133.00	-3298923	2311			20.8	4.0	25.8	39.9	9.5	0.0	0.0	179.4	2.0	2.5	1.4	5.0	79.2
134.00	-3298993	2303			21.0	3.1	25.3	41.1	9.6	0.0	0.0	180.9	2.0	2.5	1.4	5.3	79.0
135.00	-3299004	2358			38.5	4.8	10.6	33.0	13.1	0.0	0.0	156.4	2.4	2.7	1.5	3.3	61.5
136.00	-3298945	2347			31.6	4.5	14.2	36.2	13.5	0.0	0.0	173.5	2.0	2.5	1.5	5.6	68.4
137.00	-3298963	2391			17.2	2.3	27.0	44.3	9.3	0.0	0.0	190.9	1.9	2.4	1.3	5.2	82.8
138.00	-3299010	2387			33.0	3.9	23.1	33.6	6.5	0.0	0.0	147.9	2.4	2.8	1.4	3.3	67.0
139.00	-3299014	2415			18.5	0.8	12.1	44.0	22.5	2.1	0.0	227.4	1.5	2.1	1.5	7.2	81.5
140.00	-3298955	2429			24.4	3.3	14.7	37.7	18.9	1.0	0.0	199.0	1.8	2.3	1.5	6.3	75.6
141.00	-3298952	2450			17.3	0.4	22.1	49.2	11.0	0.0	0.0	198.7	1.8	2.3	1.3	5.9	82.7
142.00	-3299008	2423			76.9	10.1	6.3	5.1	1.6	0.1	0.0	65.7	4.3	3.9	1.0	-4.7	23.1
143.00	-3298895	2080			86.3	10.2	2.1	1.1	0.2	0.0	0.0	46.7	4.4	4.4	0.5	-1.2	13.7
144.00	-3298899	2111			75.2	10.5	8.4	5.3	0.5	0.0	0.0	63.4	4.3	4.0	1.0	-3.9	24.8
145.00	-3298895	2160			69.4	11.9	8.1	8.2	2.3	0.1	0.0	66.8	4.3	3.9	1.1	-5.2	30.6
146.00	-3298887	2208			44.5	2.2	12.5	30.6	10.2	0.0	0.0	138.1	2.7	2.9	1.5	0.9	55.5
147.00	-3298891	2268			41.7	3.2	13.5	30.7	10.8								

Sample	y	x	Carbonate	Organics	Mud	Very fine sand	Fine sand	Medium sand	Coarse sand	Very coarse sand	Gravel	Mean (um)	Median (phi)	Mean (phi)	Sorting (phi)	Skewness	all Sand
119 (03/02/06)	-3298996	2477			15.0	3.8	30.7	40.7	9.7	0.1	0.0	266.8	2.0	1.9	0.9	2.6	85.0
120 (03/02/06)	-3299010	2465			53.1	8.7	9.4	15.5	9.5	3.8	0.0	100.7	4.1	3.3	1.6	-11.2	46.9
121 (03/02/06)	-3298975	2390			35.2	2.9	13.7	35.5	12.7	0.0	0.0	165.9	2.1	2.6	1.5	4.9	64.8
122 (03/02/06)	-3298969	2342			65.8	5.9	5.8	15.5	7.0	0.1	0.0	87.3	4.2	3.5	1.4	-9.1	34.2
123 (03/02/06)	-3298943	2260			55.6	4.6	9.9	22.4	7.4	0.0	0.0	94.7	4.1	3.4	1.5	-8.6	44.4
124 (03/02/06)	-3298943	2194			35.4	3.4	9.1	32.8	18.6	0.7	0.0	182.9	1.9	2.5	1.6	6.0	64.6
125 (03/02/06)	-3298938	2069			45.9	5.0	7.5	24.9	15.6	1.1	0.0	144.6	2.8	2.8	1.6	-0.3	54.1
126 (03/02/06)	-3298953	1997			46.5	6.5	6.7	21.7	15.8	2.8	0.0	149.1	2.7	2.7	1.7	-0.6	53.5
127 (03/02/06)	-3298954	1901			75.1	5.3	4.3	9.8	5.3	0.1	0.0	73.4	4.3	3.8	1.3	-7.8	24.9
128 (03/02/06)	-3298959	1855			74.0	7.2	4.8	8.8	4.9	0.3	0.0	69.7	4.3	3.8	1.2	-7.2	26.0
129 (03/02/06)	-3298965	1852			43.7	6.1	14.1	22.4	12.3	1.5	0.0	133.5	3.0	2.9	1.6	-1.9	56.3
130 (03/02/06)	-3298981	1774			19.9	1.8	2.8	31.6	35.8	8.1	0.0	272.7	1.1	1.9	1.7	9.8	80.1
131 (03/02/06)	-3299013	1730			26.5	2.6	7.9	32.1	24.8	6.1	0.0	225.6	1.5	2.1	1.7	7.6	73.5
132 (03/02/06)	-3299067	1603			54.0	16.6	11.6	7.0	6.5	4.2	0.0	87.4	4.1	3.5	1.5	-9.9	46.0
133 (03/02/06)	-3299083	1614			29.1	19.9	24.6	19.9	6.4	0.1	0.0	126.4	3.0	3.0	1.3	-0.4	70.9
134 (03/02/06)	-3299094	1612			61.4	18.6	10.7	4.5	2.7	2.0	0.0	69.3	4.2	3.9	1.1	-5.6	38.6
135 (03/02/06)	-3299077	1701			85.4	9.1	3.2	1.5	0.7	0.0	0.0	46.9	4.4	4.4	0.5	-1.1	14.6
136 (03/02/06)	-3299068	1707			84.3	9.3	3.7	2.0	0.7	0.0	0.0	47.1	4.4	4.4	0.6	-1.5	15.7
137 (03/02/06)	-3298986	1821			28.1	16.3	29.5	23.3	2.8	0.0	0.0	128.2	2.8	3.0	1.3	1.3	71.9
138 (03/02/06)	-3298993	1823			64.8	15.8	9.6	4.6	3.2	2.0	0.0	68.0	4.2	3.9	1.1	-6.2	35.2
139 (03/02/06)	-3298989	1824			67.3	14.6	9.5	5.0	2.4	1.2	0.0	65.5	4.3	3.9	1.0	-5.0	32.7
141 (03/02/06)	-3298996	2014			75.5	11.3	3.8	3.5	3.6	2.4	0.0	65.8	4.3	3.9	1.2	-7.6	24.5
142 (03/02/06)	-3299026	2038			63.9	12.4	11.5	6.9	3.3	2.0	0.0	73.4	4.2	3.8	1.2	-6.8	36.1
143 (03/02/06)	-3298968	2226			19.8	4.3	32.4	38.4	5.1	0.0	0.0	167.0	2.2	2.6	1.3	4.1	80.2
144 (03/02/06)	-3298999	2223			53.1	17.7	16.1	9.6	2.3	1.2	0.0	79.9	4.1	3.6	1.2	-5.2	46.9
145 (03/02/06)	-3299046	2229			62.1	16.0	11.9	6.6	2.1	1.3	0.0	71.2	4.2	3.8	1.1	-5.2	37.9
146 (03/02/06)	-3299039	2229			29.2	6.1	25.3	31.1	7.9	0.5	0.0	151.9	2.4	2.7	1.4	2.9	70.8
147 (03/02/06)	-3299064	2228			43.5	7.4	18.5	21.8	7.0	1.8	0.0	127.8	2.9	3.0	1.5	-0.2	56.5
148 (03/02/06)	-3299040	2358			45.6	13.8	20.4	14.5	3.8	1.9	0.0	115.4	2.9	3.1	1.3	0.6	54.4
149 (03/02/06)	-3299009	2327			55.6	17.4	16.5	8.7	1.1	0.8	0.0	76.2	4.1	3.7	1.1	-4.4	44.4
150 (03/02/06)	-3299002	2334			19.7	4.1	28.3	39.5	8.4	0.0	0.0	177.5	2.1	2.5	1.3	4.6	80.3
151 (03/02/06)	-3299019	2380			11.4	4.6	35.7	41.8	6.6	0.0	0.0	232.0	2.0	2.1	1.0	2.6	88.6
152 (03/02/06)	-3299033	2433			20.6	6.7	35.6	33.6	3.5	0.0	0.0	154.3	2.4	2.7	1.2	3.4	79.4
153 (03/02/06)	-3299039	2434			37.7	7.3	23.2	25.6	5.3	0.8	0.0	129.9	2.8	2.9	1.4	1.1	62.3
154 (03/02/06)	-3299039	2463			16.8	3.2	33.8	40.6	5.6	0.0	0.0	177.4	2.1	2.5	1.3	4.2	83.2
1.00	-3299015	2547			8.8	0.1	16.6	50.3	21.9	2.2	0.0	378.4	1.5	1.4	1.2	0.3	91.2
2.00	-3299027	2594		0.6	8.3	0.2	24.0	53.3	14.2	0.0	0.0	327.1	1.7	1.6	1.1	0.3	91.7
3.00	-3299037	2638			11.0	0.1	18.1	52.4	18.2	0.3	0.0	346.6	1.6	1.5	1.3	0.4	89.0
4.00	-3299005	2647			17.3	2.1	15.4	40.5	22.3	2.4	0.0	324.8	1.6	1.6	1.9	0.6	82.7
5.00	-3298970	2673			21.2	0.8	18.4	39.4	17.5	2.6	0.0	290.8	1.8	1.8	2.2	0.6	78.8
6.00	-3298988	2698			14.9	0.6	15.2	44.2	22.2	2.8	0.0	359.9	1.5	1.5	1.5	0.4	85.1
7.00	-3299027	2706			3.8	0.1	11.1	52.7	29.9	2.4	0.0	432.4	1.3	1.2	0.7	0.0	96.2
8.00	-3299064	2714			14.8	0.5	12.3	41.8	26.2	4.4	0.0	394.2	1.4	1.3	1.6	0.4	85.2
9.00	-3299027	2759			17.6	1.7	16.6	42.3	20.4	1.4	0.0	308.5	1.6	1.7	1.9	0.6	82.4
10.00	-3299054	2784			5.4	0.3	17.7	45.1	25.6	5.8	0.0	424.3	1.4	1.2	1.1	0.2	94.6
11.00	-3299084	2791		1.3	24.0	0.7	12.8	44.2	17.9	0.3	0.0	283.7	1.7	1.8	2.3	0.7	76.0
12.00	-3299040	2826			27.6	2.7	10.8	34.7	21.7	2.5	0.0	306.8	1.7	1.7	2.5	0.6	72.4
13.00	-3299045	2866			10.0	1.8	24.8	47.8	15.5	0.0	0.0	319.6	1.7	1.6	1.2	0.4	90.0
14.00	-3299074	2879			36.5	4.8	14.8	28.8	13.2	1.9	0.0	235.4	2.3	2.1	2.6	0.5	63.5
15.00	-3299110	2891		0.6	12.6	0.2	12.8	57.2	17.1	0.0	0.0	348.9	1.5	1.5	1.2	0.4	87.4
16.00	-3299087	2919			47.8	4.1	12.9	26.1	9.2	0.0	0.0	168.9	3.5	2.6	2.8	0.3	52.2
17.00	-3299062	2926			37.5	4.4	17.4	31.3	9.4	0.0	0.0	208.5	2.4	2.3	2.5	0.6	62.5
18.00	-3299119	2959			35.7	3.4	18.0	31.1	11.4	0.4	0.0	221.6	2.3	2.2	2.5	0.6	64.3
19.00	-3299140	3020			20.9	1.8	14.4	40.9	20.9	1.1	0.0	302.2	1.7	1.7	2.2	0.6	79.1
20.00	-3299066	3011		1.5	69.4	8.4	7.9	8.6	3.7	2.0	0.0	83.9	5.3	3.6	2.5	-0.1	30.6
21.00	-3299086	3062			7.5	0.1	14.8	54.9	22.4	0.3	0.0	378.0	1.5	1.4	1.1	0.3	92.5
22.00	-3299060	3069			37.1	3.9	11.9	29.3	15.1	2.6	0.0	253.5	2.1	2.0	2.7	0.6	62.9
23.00	-3299070	3107			20.5	0.5	17.1	47.7	14.2	0.0	0.0	271.2	1.7	1.9	2.0	0.7	79.5
24.00	-3299147	3096		0.8	15.0	0.7	11.7	49.1	22.8	0.7	0.0	355.1	1.5	1.5	1.5	0.5	85.0
25.00	-3299154	3210		2.1	64.3	9.9	9.9	11.1	4.1	0.7	0.0	95.0	5.0	3.4	2.5	-0.1	35.7
26.00	-3299163	3285			41.4	6.6	10.0	25.2	14.8	2.1	0.0	226.6	2.7	2.1	2.7	0.4	58.6
27.00	-3299176	3343			38.2	6.4	11.9	28.5	14.2	0.8	0.0	230.1	2.4	2.1	2.6	0.5	61.8
28.00	-3299165	3410			24.0	6.2	16.2	36.0	16.8	0.7	0.0	268.2	1.9	1.9	2.4	0.6	76.0
29.00	-3299184	3465			15.8	9.9	21.7	36.2	15.8	0.6	0.0	277.4	1.9	1.9	1.7	0.5	84.2
30.00	-3299142	3510			1.8	7.4	17.3	26.7	15.6	17.9	13.4	507.9	1.2	1.0	1.6	-2.2	84.8
31.00	-3299210	3598			2.4	6.5	47.7	38.7	3.7	0.9	0.0	247.6	2.1	2.0	0.7	0.0	97.6
32.00	-3299160	3623		0.7	3.1	9.9	54.0	32.1	1.0	0.0	0.0	218.2	2.3	2.2	0.6	0.0	96.9
33.00	-3299219	3662		0.5	4.8	8.8	36.6	37.4	10.3	2.0	0.0	278.4	2.0	1.8	0.9	0.1	95.2
34.00	-3299240	3758			0.0	0.2	3.5	29.1	47.6	16.9	2.7	637.7	0.7	0.6	0.8	-0.4	97.3
35.00	-3299248	3788			0.0	0.0	6.0	52.5	37.3	4.2	0.0	488.7	1.1	1.0	0.6	-0.1	100.0
36.00	-3299299	3798			0.0	0.4	2.9	30.2	58.2	8.0	0.3	583.2	0.8	0.8	0.6	0.1	99.7
37.00	-3299311	3912			0.0	0.1	2.1	11.6	31.0	38.3	16.7	1062.4	-0.1	-0.1	0.9	1.0	83.0
38.00	-3299184	3894			10.7	11.3	25.8	30.4	16.6	5.3	0.0	318.4	1.9	1.7	1.6	0.2	89.3
39.00	-3299126	3896			0.1	0.7	3.7	16.2	20.0	22.0	31.5	1345.7	-0.5	-0.4	1.6	-0.5	62.6
40.00	-3299124	3864		1.1	14.2	22.0	41.3	18.2	2.1	2.1	0.0	172.5	2.7	2.5	1.3	0.3	85.8
41.00	-3299113	3822			0.0	3.7	48.7	45.0	2.6	0.0	0.0	256.8	2.0	2.0	0.6	0.0	100.0
42.00	-3299074	3843			20.3	25.9	37.6	12.4	1.4	2.4	0.0	139.7	2.9	2			

Sample	y	x	Carbonate	Organics	Mud	Very fine sand	Fine sand	Medium sand	Coarse sand	Very coarse sand	Gravel	Mean (um)	Median (phi)	Mean (phi)	Sorting (phi)	Skewness	all Sand
56.00	-3299044	2926			6.9	0.1	22.8	59.7	10.6	0.0	0.0	323.5	1.7	1.6	0.9	0.3	93.1
57.00	-3298992	2985			16.8	0.7	22.9	48.0	11.6	0.0	0.0	265.1	1.8	1.9	1.8	0.6	83.2
58.00	-3299010	3024			19.6	1.8	28.0	42.1	8.5	0.0	0.0	234.6	2.0	2.1	2.0	0.6	80.4
59.00	-3298877	3164			16.0	0.6	31.4	47.9	4.0	0.0	0.0	233.6	2.0	2.1	1.6	0.6	84.0
60.00	-3298867	3180		1.0	53.1	4.8	18.6	20.2	3.0	0.2	0.0	119.8	4.5	3.1	2.4	0.0	46.9
61.00	-3298874	3240			63.5	7.0	15.9	12.3	1.0	0.4	0.0	87.1	5.2	3.5	2.5	-0.1	36.5
62.00	-3298891	3239			20.5	1.7	33.0	41.1	3.7	0.0	0.0	211.3	2.1	2.2	1.9	0.7	79.5
63.00	-3299022	3205			11.1	0.6	28.7	50.8	8.8	0.0	0.0	291.9	1.8	1.8	1.2	0.4	88.9
64.00	-3299040	3183			12.7	0.9	30.3	48.8	7.3	0.0	0.0	278.0	1.9	1.8	1.3	0.4	87.3
65.00	-3299091	3265			18.9	1.0	12.2	46.5	20.8	0.6	0.0	306.8	1.6	1.7	2.0	0.7	81.1
66.00	-3299047	3264			0.0	0.9	38.5	54.6	6.0	0.0	0.0	292.5	1.8	1.8	0.5	0.0	100.0
67.00	-3299010	3266			33.5	2.7	23.2	34.4	6.2	0.0	0.0	202.8	2.3	2.3	2.4	0.6	66.5
68.00	-3298850	3445			68.5	10.6	12.7	7.6	0.5	0.0	0.0	66.4	5.2	3.9	2.2	0.0	31.5
69.00	-3298865	3451			27.2	6.6	33.4	30.0	2.7	0.0	0.0	179.9	2.4	2.5	2.1	0.6	72.8
70.00	-3298989	3649			5.0	13.9	52.2	28.1	0.9	0.0	0.0	205.0	2.4	2.3	0.7	0.1	95.0
71.00	-3298855	3779			17.4	12.5	39.5	27.4	2.7	0.4	0.0	185.3	2.4	2.4	1.6	0.5	82.6
72.00	-3298870	3810			24.2	14.8	35.8	22.4	2.0	0.8	0.0	161.5	2.7	2.6	1.9	0.5	75.8
73.00	-3298920	3860		1.1	13.2	16.7	44.5	23.9	1.3	0.5	0.0	184.8	2.5	2.4	1.3	0.4	86.8
74.00	-3298935	3812			3.8	9.5	52.8	32.8	1.1	0.0	0.0	219.9	2.3	2.2	0.6	0.1	96.2
75.00	-3298943	3847			12.5	20.1	43.4	22.0	1.4	0.6	0.0	179.4	2.6	2.5	1.3	0.3	87.5
76.00	-3298985	3872			18.6	20.9	39.5	18.4	1.4	1.1	0.0	158.6	2.7	2.7	1.6	0.4	81.4
77.00	-3299227	3854			15.4	7.5	22.9	35.3	15.4	3.5	0.0	293.2	1.9	1.8	1.7	0.4	84.6
78.00	-3299307	3864			0.0	0.4	3.6	32.6	57.0	6.1	0.4	567.0	0.8	0.8	0.6	0.2	99.6
A01	-3299045	2979			10.8	1.8	34.6	47.0	5.9	0.0	0.0	269.0	2.0	1.9	1.2	0.4	89.2
A03	-3299050	2960			54.4	6.3	14.0	19.1	5.9	0.3	0.0	130.0	4.5	2.9	2.7	0.0	45.6
A04	-3299011	2929			14.4	4.9	30.1	40.7	9.8	0.0	0.0	260.4	2.0	1.9	1.4	0.4	85.6
A05	-3298990	2953		0.7	39.2	3.9	16.9	30.5	9.4	0.0	0.0	205.9	2.4	2.3	2.5	0.6	60.8
A06	-3298958	2943			27.0	2.7	24.9	37.7	7.7	0.0	0.0	219.7	2.1	2.2	2.2	0.6	73.0
A07	-3298986	2915			30.5	2.7	17.0	37.3	12.6	0.0	0.0	242.5	2.0	2.0	2.4	0.6	69.5
A08	-3299002	2907			8.2	0.9	22.7	45.7	19.6	2.8	0.0	359.1	1.6	1.5	1.2	0.3	91.8
A09	-3298999	2901			32.6	3.9	19.5	33.8	10.2	0.0	0.0	221.1	2.2	2.2	2.5	0.6	67.4
A10	-3299034	2889			34.4	8.5	22.1	27.2	7.7	0.1	0.0	189.0	2.6	2.4	2.4	0.5	65.6
A11	-3299033	2892			56.4	8.7	16.1	15.6	3.1	0.0	0.0	107.0	4.7	3.2	2.6	0.0	43.6
A14	-3298949	2892			46.9	5.9	14.5	25.0	7.7	0.0	0.0	161.4	3.5	2.6	2.5	0.3	53.1
A15	-3298990	2868			3.3	0.4	32.4	57.4	6.5	0.0	0.0	299.6	1.8	1.7	0.6	0.1	96.7
A16	-3299010	2841			11.6	0.3	17.5	52.8	17.8	0.0	0.0	343.0	1.6	1.5	1.3	0.4	88.4
A17	-3299002	2828			8.3	0.1	23.1	57.4	11.0	0.0	0.0	320.4	1.7	1.6	1.1	0.4	91.7
A18	-3298969	2821			22.2	2.5	19.9	39.7	15.6	0.2	0.0	265.5	1.9	1.9	2.2	0.6	77.8
A19	-3298958	2822			8.6	0.1	15.0	59.7	16.6	0.0	0.0	354.2	1.5	1.5	1.1	0.4	91.4
A20	-3298955	2822			12.1	0.3	18.5	53.2	15.9	0.0	0.0	332.6	1.6	1.6	1.3	0.4	87.9
A21	-3298949	2819			17.4	1.4	15.1	44.7	20.9	0.5	0.0	308.7	1.6	1.7	1.9	0.6	82.6
A22	-3298908	2818			45.9	7.7	19.2	22.0	5.2	0.0	0.0	148.3	3.4	2.8	2.4	0.3	54.1
A23	-3298911	2793			9.4	0.2	16.8	53.2	20.3	0.2	0.0	360.2	1.5	1.5	1.2	0.4	90.6
A24	-3298927	2777			33.6	2.7	14.7	35.0	14.0	0.1	0.0	244.4	2.0	2.0	2.6	0.6	66.4
A25	-3298927	2780			67.4	5.8	8.5	13.6	4.6	0.0	0.0	102.4	5.5	3.3	2.7	-0.2	32.6
A26	-3298941	2772			4.1	0.0	16.0	61.4	18.4	0.1	0.0	368.3	1.5	1.4	0.6	0.1	95.9
A29	-3298974	2751			71.7	10.4	7.6	6.3	3.3	0.7	0.0	57.3	5.6	4.1	2.5	-0.1	28.3
A30	-3298956	2731			63.8	12.6	11.0	9.1	3.4	0.1	0.0	78.3	5.0	3.7	2.6	0.0	36.2
A34	-3298918	2715			39.4	4.1	12.7	29.8	13.6	0.4	0.0	229.7	2.3	2.1	2.5	0.6	60.6
A35	-3298893	2720			73.8	6.8	7.7	8.5	2.8	0.4	0.0	66.6	5.7	3.9	2.5	-0.2	26.2
A36	-3298877	2724			6.9	0.2	12.5	60.8	19.7	0.0	0.0	373.9	1.5	1.4	0.9	0.3	93.1
A38	-3298901	2682			11.4	0.4	15.0	41.9	25.9	5.4	0.0	411.2	1.4	1.3	1.4	0.3	88.6
A39	-3298909	2680			79.6	10.8	5.7	2.8	1.2	0.0	0.0	33.7	5.8	4.9	2.2	0.0	20.4
A40	-3298936	2687			73.9	7.7	7.7	7.5	2.7	0.5	0.0	61.1	5.7	4.0	2.5	-0.1	26.1
A41	-3298955	2678		17.4	79.6	9.1	5.3	3.7	2.2	0.1	0.0	34.5	6.0	4.9	2.3	-0.1	20.4
A42	-3298956	2648			20.8	1.0	23.8	42.7	11.5	0.1	0.0	249.6	1.9	2.0	2.1	0.7	79.2
A43	-3298966	2637			27.1	2.6	17.6	34.3	15.8	2.7	0.0	271.9	1.9	1.9	2.3	0.6	72.9
A44	-3298986	2622			25.4	5.4	24.2	33.8	11.0	0.2	0.0	228.4	2.1	2.1	2.2	0.6	74.6
A46	-3298976	2573			9.0	3.7	25.1	45.3	16.9	0.1	0.0	320.4	1.7	1.6	1.3	0.4	91.0
A47	-3298975	2559		7.3	72.6	10.0	6.7	5.7	3.5	1.5	0.0	56.7	5.5	4.1	2.4	-0.1	27.4
A49	-3298956	2549			18.5	1.2	29.3	44.8	6.3	0.0	0.0	232.0	2.0	2.1	1.8	0.6	81.5
A50	-3298945	2505			13.7	0.4	23.3	49.7	12.9	0.0	0.0	306.3	1.8	1.7	1.3	0.4	86.3
A53	-3298933	2566			4.8	0.1	10.2	57.9	26.3	0.7	0.0	408.6	1.4	1.3	0.6	0.1	95.2
A54	-3298938	2591			14.9	0.1	19.7	48.9	16.0	0.3	0.0	319.8	1.7	1.6	1.5	0.4	85.1
A55	-3298934	2613			12.7	2.3	26.2	41.7	15.5	1.6	0.0	311.3	1.8	1.7	1.4	0.3	87.3
A56	-3299036	3052			33.6	4.9	12.5	26.9	21.9	0.1	0.0	272.3	2.1	1.9	2.6	0.6	66.4
A61	-3299119	3185			58.1	11.1	11.2	15.0	4.7	0.0	0.0	114.0	4.6	3.1	2.6	0.0	41.9
A63	-3299126	3239			74.1	12.0	5.8	4.6	2.6	0.9	0.0	46.5	5.2	4.4	2.1	0.0	25.9
A65	-3299140	3317			57.5	8.0	9.4	17.3	7.5	0.3	0.0	134.7	4.7	2.9	2.7	0.0	42.5
A66	-3299139	3365			55.8	8.9	11.6	18.7	5.0	0.0	0.0	127.0	4.5	3.0	2.6	0.0	44.2
A68	-3299079	3916			0.0	0.1	3.6	31.5	43.7	18.3	2.9	630.3	0.7	0.7	0.8	-0.6	97.1
A69	-3299079	3905			0.3	1.3	11.7	44.3	26.0	12.8	3.6	491.6	1.2	1.0	1.0	-1.3	96.1
A73	-3299028	3675			12.8	9.1	40.9	34.7	2.6	0.0	0.0	217.8	2.3	2.2	1.4	0.4	87.2
A75	-3299065	3553			14.9	2.6	36.1	42.4	4.0	0.0	0.0	242.5	2.1	2.0	1.4	0.5	85.1
A76	-3299006	3562			12.6	12.3	44.3	29.3	1.5	0.0	0.0	200.5	2.4	2.3	1.3	0.4	87.4
A77	-3298958	3548		0.4	24.6	13.1	38.5	22.9	0.9	0.0	0.0	156.0	2.6	2.7	2.0	0.6	75.4
A78	-3298989	3349			12.8	4.6	41.8	38.3	2.5	0.0	0.0	230.7	2.2	2.1	1.2	0.4	87.2
A79	-3298985	3373			6.5	1.1	38.3	50.6	3.4	0.0	0.0	270.2	1.9	1.9	0.9	0.3	93.5
A80	-3299024	3368			18.7	1.4	31.3	44.0	4.5	0.0	0.0	222.9	2.0	2.2	1.8	0.7	81.3
B02	-3299280	3838			0.0	0.2	6.0	63.2									

Sample	y	x	Carbonate	Organics	Mud	Very fine sand	Fine sand	Medium sand	Coarse sand	Very coarse sand	Gravel	Mean (um)	Median (phi)	Mean (phi)	Sorting (phi)	Skewness	all Sand
B54	-3299020	3702			8.5	17.7	46.6	25.9	1.3	0.0	0.0	194.1	2.5	2.4	1.1	0.3	91.5
B56	-3299013	3606			13.9	12.7	43.8	28.3	1.3	0.0	0.0	194.6	2.4	2.4	1.4	0.4	86.1
B59	-3298961	3480			13.1	6.4	45.5	33.6	1.4	0.0	0.0	214.6	2.3	2.2	1.3	0.4	86.9
B60	-3299041	3461		0.0	12.0	2.2	37.8	44.3	3.6	0.0	0.0	251.9	2.0	2.0	1.2	0.4	88.0
B63	-3299116	3450		0.2	32.8	3.6	20.8	35.0	7.7	0.0	0.0	211.3	2.2	2.2	2.4	0.6	67.2
B64	-3299135	3436		0.2	33.4	9.0	14.9	28.7	13.4	0.5	0.0	226.1	2.4	2.1	2.5	0.5	66.6
B67	-3299084	3336			29.5	3.4	25.2	35.9	6.0	0.0	0.0	206.7	2.2	2.3	2.3	0.6	70.5
B68	-3299029	3211		0.0	19.4	1.1	28.5	44.7	6.3	0.0	0.0	230.4	2.0	2.1	1.9	0.6	80.6
B69	-3299098	3200		0.3	32.3	2.8	11.2	34.2	18.4	1.1	0.0	275.7	1.9	1.9	2.6	0.6	67.7
B70	-3299005	3203		0.4	17.8	0.8	27.6	47.3	6.5	0.0	0.0	239.5	1.9	2.1	1.7	0.6	82.2
B71CLA	-3298982	3205			42.6	9.9	21.6	21.4	4.4	0.0	0.0	147.9	3.2	2.8	2.4	0.4	57.4
B73	-3299021	3429			13.5	3.0	39.9	41.1	2.6	0.0	0.0	237.6	2.1	2.1	1.2	0.4	86.5
B74	-3299032	3493		0.1	11.3	3.0	41.1	42.0	2.6	0.0	0.0	243.0	2.1	2.0	1.1	0.4	88.7
M01	-3298854	3133			45.7	12.2	17.5	17.2	6.1	1.2	0.0	143.3	3.6	2.8	2.4	0.2	54.3
M05	-3298922	3093			54.9	10.0	15.0	15.3	4.2	0.6	0.0	115.0	4.4	3.1	2.6	0.1	45.1
M06	-3298953	3088			52.7	18.7	15.5	9.0	3.4	0.6	0.0	93.1	4.1	3.4	2.3	0.2	47.3
M07	-3298949	3089			21.7	4.4	25.9	39.5	8.6	0.0	0.0	231.3	2.0	2.1	2.0	0.6	78.3
M08	-3298972	3086			19.4	1.3	21.5	44.5	13.3	0.0	0.0	263.5	1.8	1.9	2.0	0.6	80.6
M09	-3298998	3085			13.2	1.7	27.6	47.4	10.1	0.0	0.0	285.9	1.9	1.8	1.2	0.4	86.8
M11	-3298999	3064			18.8	11.7	37.0	29.9	2.6	0.0	0.0	188.0	2.4	2.4	1.6	0.5	81.2
M12	-3298978	3060			12.0	0.9	25.7	50.3	11.2	0.0	0.0	300.8	1.8	1.7	1.3	0.4	88.0
M13	-3298966	3060			27.2	3.1	18.0	36.8	14.5	0.3	0.0	255.1	2.0	2.0	2.3	0.6	72.8
M14	-3298959	3057			54.5	6.3	13.5	20.7	5.0	0.0	0.0	129.0	4.5	3.0	2.6	0.0	45.5
M15	-3298953	3050			46.7	21.7	19.5	8.9	2.6	0.7	0.0	97.4	3.8	3.4	2.2	0.3	53.3
M16	-3298926	3056			42.6	13.7	17.3	18.8	6.6	0.9	0.0	151.8	3.5	2.7	2.4	0.3	57.4
M17	-3298903	3055			53.9	10.0	14.7	16.6	4.6	0.1	0.0	120.1	4.3	3.1	2.6	0.1	46.1
M18	-3298885	3062		0.8	59.1	11.8	14.6	12.0	2.4	0.0	0.0	91.6	4.8	3.4	2.6	0.1	40.9
M19	-3298885	3056			11.6	2.3	34.5	45.9	5.7	0.0	0.0	264.4	2.0	1.9	1.2	0.4	88.4
M20	-3298862	3043			10.1	0.7	28.7	52.1	8.4	0.0	0.0	293.8	1.8	1.8	1.1	0.4	89.9
M21	-3298861	3014		1.0	39.5	4.1	19.3	30.7	6.4	0.0	0.0	191.1	2.5	2.4	2.5	0.6	60.5
M22	-3298867	2993			11.9	0.2	25.4	55.1	7.5	0.0	0.0	294.9	1.8	1.8	1.2	0.4	88.1
M23	-3298882	2993			51.9	12.8	19.3	14.4	1.5	0.0	0.0	105.3	4.1	3.2	2.2	0.1	48.1
M24	-3298889	2990			47.7	10.8	18.6	18.3	4.4	0.1	0.0	130.8	3.8	2.9	2.4	0.2	52.3
M26	-3298944	2958			37.7	9.2	23.1	24.4	5.6	0.1	0.0	168.2	2.8	2.6	2.4	0.5	62.3
M27	-3298939	2933			21.3	9.3	28.3	33.9	7.2	0.0	0.0	215.3	2.2	2.2	1.8	0.5	78.7
M28	-3298920	2933			48.7	15.6	16.0	13.0	5.2	1.6	0.0	123.9	3.9	3.0	2.4	0.2	51.3
M29	-3298892	2936			56.7	11.9	13.4	13.6	4.4	0.1	0.0	108.7	4.5	3.2	2.5	0.1	43.3
M30	-3298877	2931			17.9	3.8	27.2	41.8	9.2	0.0	0.0	243.9	2.0	2.0	1.7	0.6	82.1
M31	-3298843	2882			13.2	0.5	25.2	51.0	10.0	0.0	0.0	295.4	1.8	1.8	1.3	0.4	86.8
M32	-3298883	2914			62.2	10.6	11.5	10.3	4.2	1.3	0.0	95.3	4.9	3.4	2.6	0.0	37.9
M33	-3298908	2901			61.2	17.9	10.4	4.9	3.4	2.2	0.0	69.7	4.6	3.8	2.4	0.1	38.8
M34	-3298927	2894			31.1	26.1	26.0	10.1	4.4	2.3	0.0	128.9	3.2	3.0	2.0	0.3	68.9
M35	-3298939	2894			20.5	12.1	31.1	30.5	5.9	0.0	0.0	200.9	2.4	2.3	1.8	0.5	79.5
M36	-3298930	2875			28.8	14.4	27.2	25.1	4.5	0.0	0.0	173.8	2.7	2.5	2.0	0.4	71.2
M37	-3298923	2876			58.4	14.7	13.5	8.2	3.3	1.9	0.0	87.8	4.6	3.5	2.5	0.1	41.6
M38	-3298898	2879		1.7	64.1	10.1	8.8	11.1	5.6	0.4	0.0	101.0	5.0	3.3	2.7	0.0	35.9
M39	-3298876	2877			55.1	16.7	12.9	8.7	4.7	1.9	0.0	98.7	4.3	3.3	2.5	0.1	44.9
M40	-3298870	2867			24.0	3.0	28.7	38.1	6.2	0.0	0.0	213.2	2.1	2.2	2.2	0.7	76.0
M41	-3298870	2867			19.8	0.7	24.3	46.6	8.6	0.0	0.0	243.8	1.9	2.0	1.9	0.7	80.2
M42	-3298853	2872			13.4	0.6	22.1	51.8	12.1	0.0	0.0	307.1	1.7	1.7	1.3	0.4	86.6
M44	-3298857	2852			7.4	0.2	19.8	56.4	16.3	0.0	0.0	345.6	1.6	1.5	1.0	0.3	92.6
M45	-3298861	2846			32.9	13.5	26.1	23.7	3.9	0.0	0.0	162.8	2.8	2.6	2.1	0.5	67.1
M46	-3298883	2840			45.9	14.8	18.9	14.9	4.2	1.3	0.0	126.5	3.7	3.0	2.4	0.3	54.1
M48	-3298907	2815			32.5	16.6	32.0	18.9	0.0	0.0	0.0	135.9	3.0	2.9	2.1	0.5	67.5
M49	-3298893	2788			34.9	13.0	29.5	21.0	1.6	0.0	0.0	144.6	2.9	2.8	2.3	0.5	65.1
M50	-3298880	2790			47.9	17.8	15.9	9.4	5.6	3.4	0.0	121.6	3.9	3.0	2.6	0.2	52.1
M51	-3298876	2788		2.4	56.3	13.5	15.4	11.9	2.8	0.0	0.0	95.8	4.5	3.4	2.5	0.1	43.7
M52	-3298873	2794			35.0	13.9	27.0	21.6	2.4	0.0	0.0	148.5	2.9	2.8	2.2	0.5	65.0
N01	-3298904	3449			24.2	14.1	39.8	21.3	0.6	0.0	0.0	152.8	2.7	2.7	1.9	0.6	75.8
N03	-3298881	3400			48.1	7.9	22.7	19.1	2.2	0.0	0.0	124.9	3.7	3.0	2.4	0.3	51.9
N04	-3298864	3398			27.3	5.7	32.7	31.3	3.0	0.0	0.0	183.8	2.4	2.4	2.1	0.6	72.7
N05	-3298866	3386			0.1	0.9	27.4	46.1	14.8	7.5	3.1	344.7	1.7	1.5	1.0	-2.1	96.8
N06	-3298837	3371			59.8	12.7	14.2	10.6	2.2	0.5	0.0	89.0	4.6	3.5	2.4	0.1	40.2
N07	-3298855	3323			49.9	8.1	19.5	19.2	3.3	0.0	0.0	123.8	4.0	3.0	2.5	0.2	50.1
N08	-3298857	3310			22.5	4.9	34.4	34.8	3.4	0.0	0.0	197.1	2.3	2.3	1.9	0.6	77.5
N10	-3298881	3293		1.4	57.0	13.9	17.2	10.9	1.0	0.0	0.0	87.0	4.5	3.5	2.4	0.1	43.0
N11	-3298925	3282			46.7	9.9	23.1	18.4	1.8	0.0	0.0	123.5	3.6	3.0	2.4	0.3	53.3
N12	-3298914	3269			15.6	5.1	36.1	38.7	4.5	0.0	0.0	228.4	2.1	2.1	1.4	0.5	84.4
N14	-3298921	3188			19.3	4.4	33.8	37.9	4.6	0.0	0.0	211.2	2.2	2.2	1.8	0.6	80.7
N15	-3298901	3190			53.0	8.6	20.2	15.3	1.9	0.9	0.0	106.5	4.4	3.2	2.6	0.1	47.0
N17	-3298891	3090			71.0	8.0	9.3	9.9	1.9	0.0	0.0	72.2	5.5	3.8	2.6	-0.1	29.0
R1	-3298848	3712			52.3	12.0	14.9	16.2	4.7	0.1	0.0	121.0	4.2	3.0	2.6	0.2	47.7
R10	-3298885	3688			27.3	14.9	33.3	22.4	2.0	0.0	0.0	156.1	2.7	2.7	2.0	0.5	72.7
R11	-3298870	3694			29.6	13.2	33.1	22.5	1.6	0.0	0.0	152.9	2.7	2.7	2.2	0.6	70.4
R12	-3298866	3695			19.8	9.1	37.7	30.7	2.7	0.0	0.0	186.4	2.4	2.4	1.8	0.6	80.2
R13	-3298854	3700			35.2	13.6	29.9	20.1	1.2	0.0	0.0	141.1	2.9	2.8	2.2	0.5	64.8
R14	-3298846	3698			62.9	14.4	10.8	8.5	3.3	0.1	0.0	75.9	4.8	3.7	2.4	0.1	37.1
R15	-3298839	3682			58.5	14.5	13.6	9.9	3.4	0.1	0.0	87.7	4.6	3.5	2.5	0.1	41.5
R16	-3298845	3683			36.2	11.9	29.1	20.9	2.0	0.0	0.0	145.3	2.9	2.8	2.3	0.5	63.8
R17	-3298861	3676			40.9	12.4	26.6	18.7	1.3	0.0	0.0						

Sample	y	x	Carbonate	Organics	Mud	Very fine sand	Fine sand	Medium sand	Coarse sand	Very coarse sand	Gravel	Mean (um)	Median (phi)	Mean (phi)	Sorting (phi)	Skewness	all Sand	
R27	-3298868	3650			46.1	22.2	23.8	7.7	0.2	0.0	0.0	90.2	3.8	3.5	2.2	0.4	53.9	
R28	-3298861	3653			40.9	12.8	24.3	17.7	2.5	1.9	0.0	137.3	3.2	2.9	2.4	0.4	59.1	
R29	-3298847	3657			34.1	11.3	28.6	23.1	2.9	0.0	0.0	156.3	2.8	2.7	2.3	0.5	65.9	
R3	-3298872	3710			19.2	10.5	38.5	29.7	2.2	0.0	0.0	183.0	2.4	2.4	1.8	0.6	80.8	
R30	-3298834	3660		0.2	29.4	10.8	32.3	25.2	2.2	0.0	0.0	163.4	2.6	2.6	2.2	0.6	70.6	
R31	-3298835	3638			59.7	13.4	13.3	9.2	3.1	1.2	0.0	87.8	4.7	3.5	2.5	0.1	40.3	
R32	-3298845	3635			39.6	7.5	25.1	24.2	3.6	0.0	0.0	158.9	2.8	2.7	2.4	0.5	60.4	
R33	-3298831	3633			24.5	4.6	30.7	35.2	5.0	0.0	0.0	202.4	2.2	2.3	2.1	0.6	75.5	
R35	-3298871	3631			14.3	17.7	45.3	22.1	0.6	0.0	0.0	175.0	2.6	2.5	1.4	0.4	85.7	
R36	-3298889	3626			4.5	10.4	54.0	30.5	0.7	0.0	0.0	212.6	2.3	2.2	0.7	0.1	95.5	
R37	-3298896	3624			47.4	17.1	22.9	11.6	1.0	0.0	0.0	100.7	3.8	3.3	2.4	0.4	52.6	
R38	-3298922	3618			4.2	8.4	51.4	34.8	1.3	0.0	0.0	225.1	2.2	2.2	0.7	0.1	95.8	
R39	-3298950	3593			9.1	17.7	47.9	24.8	0.5	0.0	0.0	189.1	2.5	2.4	1.1	0.3	90.9	
R4	-3298876	3701			30.6	16.2	31.2	20.2	1.8	0.0	0.0	145.7	2.9	2.8	2.1	0.5	69.4	
R40	-3298938	3589			29.7	16.8	36.2	16.9	0.4	0.0	0.0	134.5	2.9	2.9	2.2	0.6	70.3	
R41	-3298931	3591			4.9	11.8	53.4	29.3	0.6	0.0	0.0	208.5	2.3	2.3	0.7	0.1	95.1	
R42	-3298907	3588			6.7	12.1	52.9	27.8	0.5	0.0	0.0	203.3	2.4	2.3	1.0	0.3	93.3	
R43	-3298884	3591			24.4	18.7	37.9	18.4	0.7	0.0	0.0	143.7	2.8	2.8	1.9	0.5	75.6	
R44	-3298875	3590			5.4	16.2	55.3	22.9	0.2	0.0	0.0	190.4	2.5	2.4	0.9	0.3	94.6	
R45	-3298849	3598			45.6	19.3	25.7	9.3	0.0	0.0	0.0	96.4	3.7	3.4	2.2	0.4	54.4	
R46	-3298840	3600			48.4	12.1	23.0	15.3	1.2	0.0	0.0	110.7	1.2	3.8	3.2	2.4	0.3	51.6
R50	-3298953	3560			25.6	15.1	38.5	20.2	0.5	0.0	0.0	147.3	2.7	2.8	2.0	0.6	74.4	
R51	-3298938	3562			15.5	23.7	44.1	16.5	0.1	0.0	0.0	155.4	2.8	2.7	1.3	0.4	84.5	
R52	-3298935	3563			0.0	13.0	58.9	27.9	0.2	0.0	0.0	207.7	2.3	2.3	0.6	0.0	100.0	
R53	-3298893	3555			3.2	9.5	53.3	33.1	0.9	0.0	0.0	220.3	2.3	2.2	0.6	0.1	96.8	
R54	-3298884	3556			28.7	21.7	37.2	12.4	0.0	0.0	0.0	122.9	3.0	3.0	1.9	0.6	71.3	
R55	-3298876	3560			65.4	10.5	16.4	7.5	0.2	0.0	0.0	68.3	5.4	3.9	2.4	0.0	34.6	
R56	-3298852	3560			54.7	11.0	20.4	13.0	0.9	0.0	0.0	94.3	4.5	3.4	2.5	0.1	45.3	
R57	-3298844	3558			42.2	7.8	23.6	21.4	3.6	1.3	0.0	152.8	3.0	2.7	2.4	0.5	57.8	
R58	-3298831	3504			20.7	4.5	29.5	36.2	8.7	0.4	0.0	224.8	2.1	2.2	2.0	0.6	79.3	
R6	-3298916	3704			2.9	7.2	50.7	37.5	1.7	0.0	0.0	234.1	2.2	2.1	0.6	0.0	97.1	
R60	-3298842	3509			47.4	6.9	23.2	20.4	2.1	0.0	0.0	131.1	3.5	2.9	2.4	0.4	52.7	
R61	-3298873	3502			77.0	7.2	7.7	5.7	1.5	0.9	0.0	47.8	5.8	4.4	2.5	-0.1	23.0	
R62	-3298883	3499			11.9	7.7	47.4	31.9	1.0	0.0	0.0	210.8	2.3	2.2	1.2	0.4	88.1	
R63	-3298886	3502			69.5	9.8	13.3	7.2	0.2	0.0	0.0	63.4	5.4	4.0	2.4	0.0	30.5	
R64	-3298908	3490			18.4	20.9	43.9	16.8	0.0	0.0	0.0	148.0	2.7	2.8	1.5	0.5	81.6	
R65	-3298923	3488			1.8	5.5	56.8	35.4	0.5	0.0	0.0	227.4	2.2	2.1	0.5	0.0	98.2	
R66	-3298948	3493			12.8	2.1	43.1	40.6	1.5	0.0	0.0	234.5	2.1	2.1	1.1	0.4	87.2	
R67	-3298946	3480			29.5	3.4	25.2	35.9	6.0	0.0	0.0	206.7	2.2	2.3	2.3	0.6	70.5	
R68	-3298942	3477			19.4	1.1	28.5	44.7	6.3	0.0	0.0	230.4	2.0	2.1	1.9	0.6	80.6	
R69	-3298924	3477			32.3	2.8	11.2	34.2	18.4	1.1	0.0	275.7	1.9	1.9	2.6	0.6	67.7	
R7	-3298919	3690			10.1	18.8	51.1	19.9	0.2	0.0	0.0	176.4	2.6	2.5	1.1	0.3	89.9	
R70	-3298997	3425			20.0	2.6	33.7	39.4	4.3	0.0	0.0	209.5	2.1	2.3	2.0	0.7	80.0	
R71	-3298988	3430			7.4	6.2	53.9	32.2	0.4	0.0	0.0	216.2	2.3	2.2	0.9	0.3	92.6	
R72	-3298955	3433			40.1	10.7	28.3	19.4	1.5	0.0	0.0	136.9	3.0	2.9	2.3	0.5	59.9	
R73	-3298961	3427			47.2	11.9	25.6	14.4	0.9	0.0	0.0	111.5	3.6	3.2	2.3	0.4	52.8	
R74	-3298914	3442			12.9	11.2	48.5	26.8	0.6	0.0	0.0	193.9	2.4	2.4	1.3	0.4	87.1	
R8	-3298904	3691			6.1	22.3	53.9	17.7	0.1	0.0	0.0	174.1	2.6	2.5	0.9	0.3	93.9	
R9	-3298894	3676			5.2	14.9	53.9	25.5	0.4	0.0	0.0	197.4	2.4	2.3	0.9	0.2	94.8	

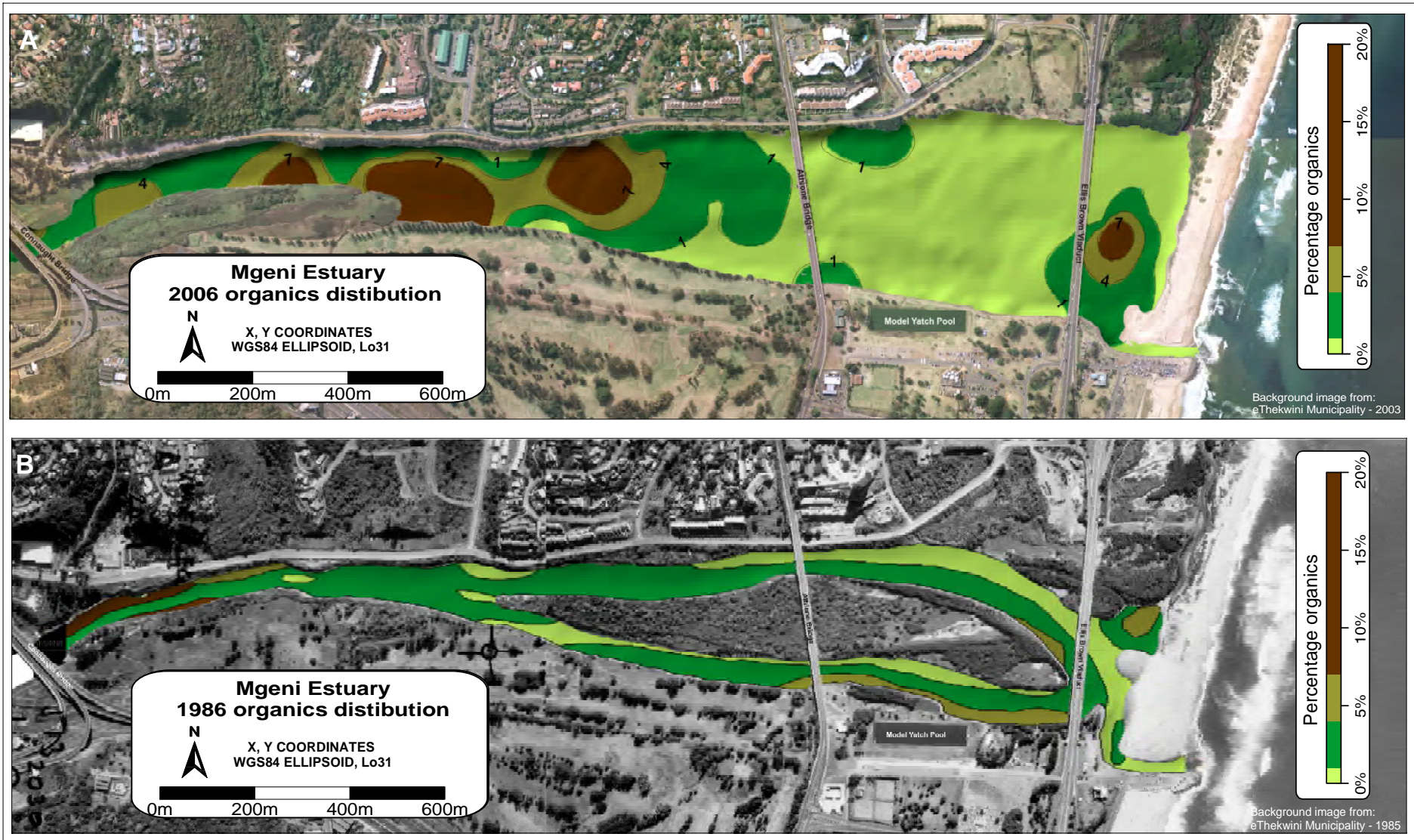
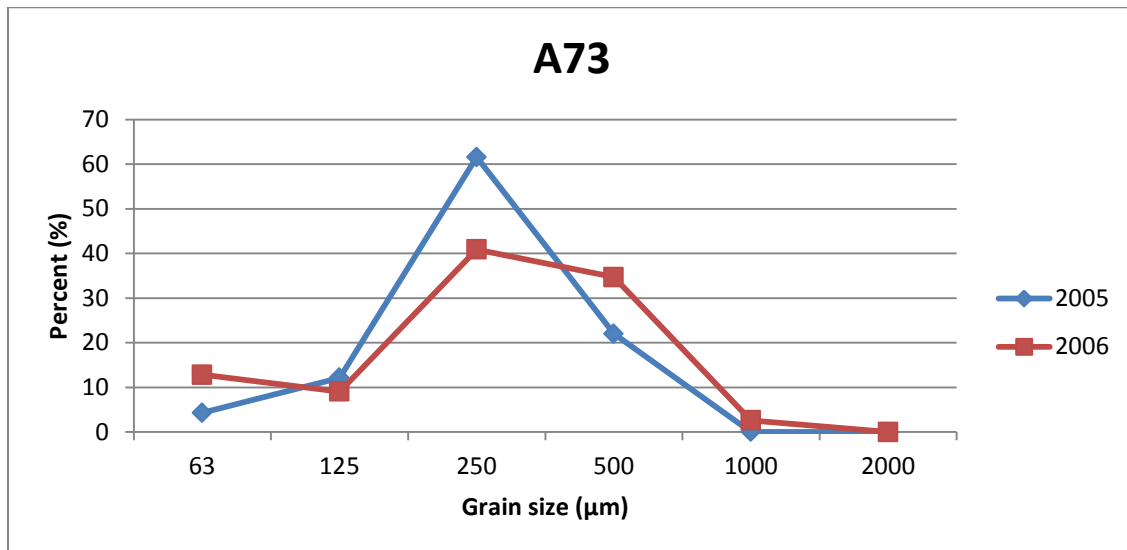
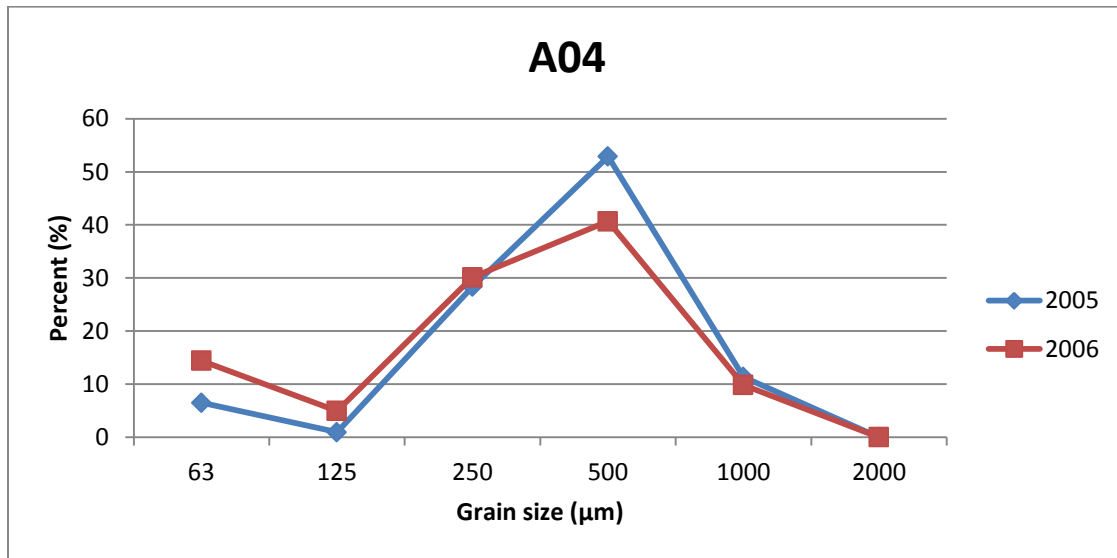
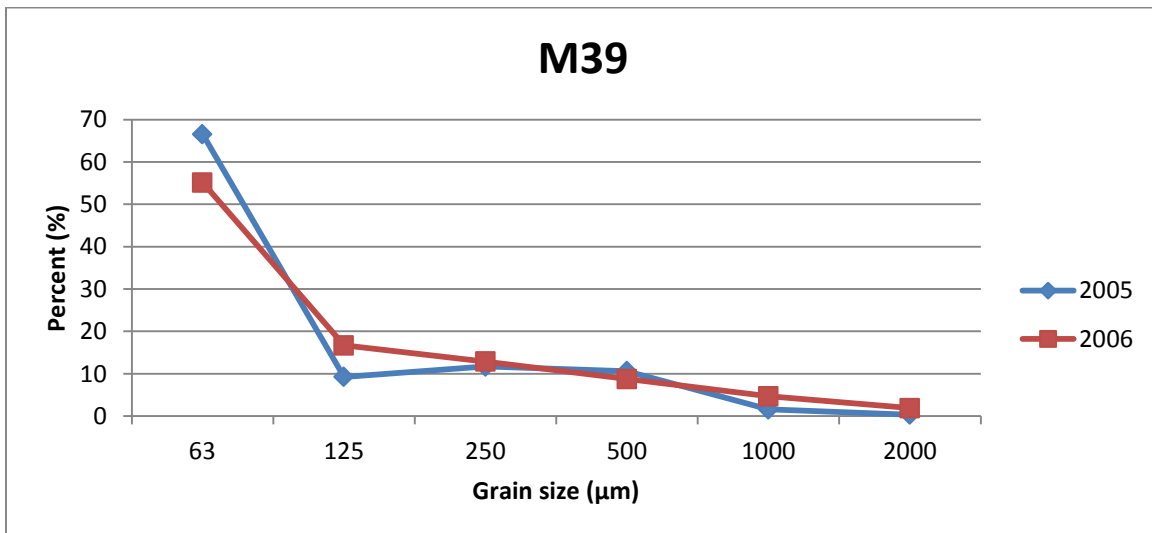
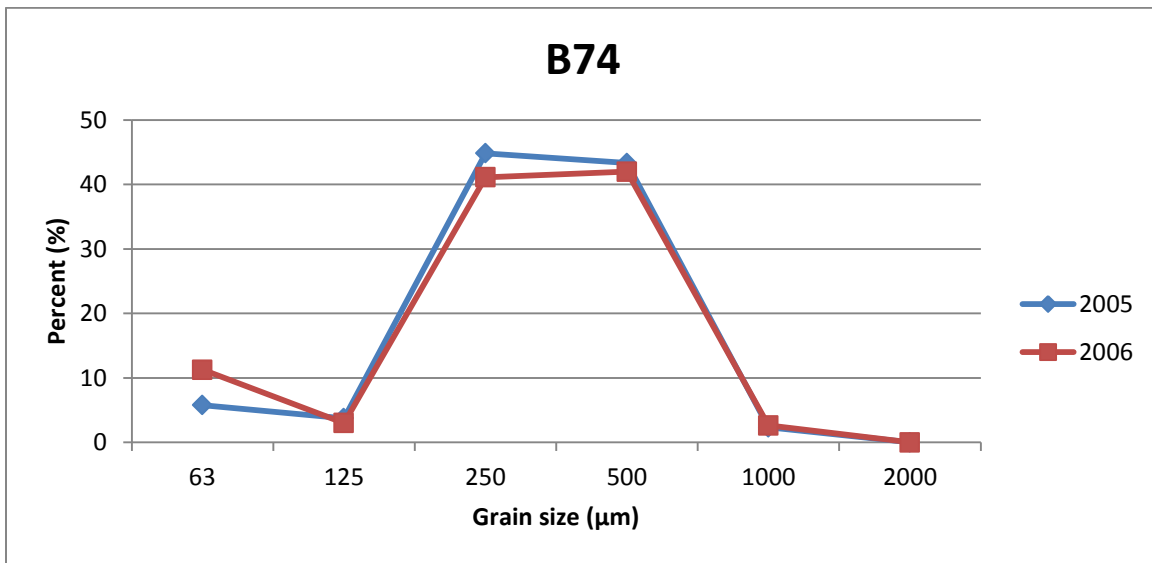
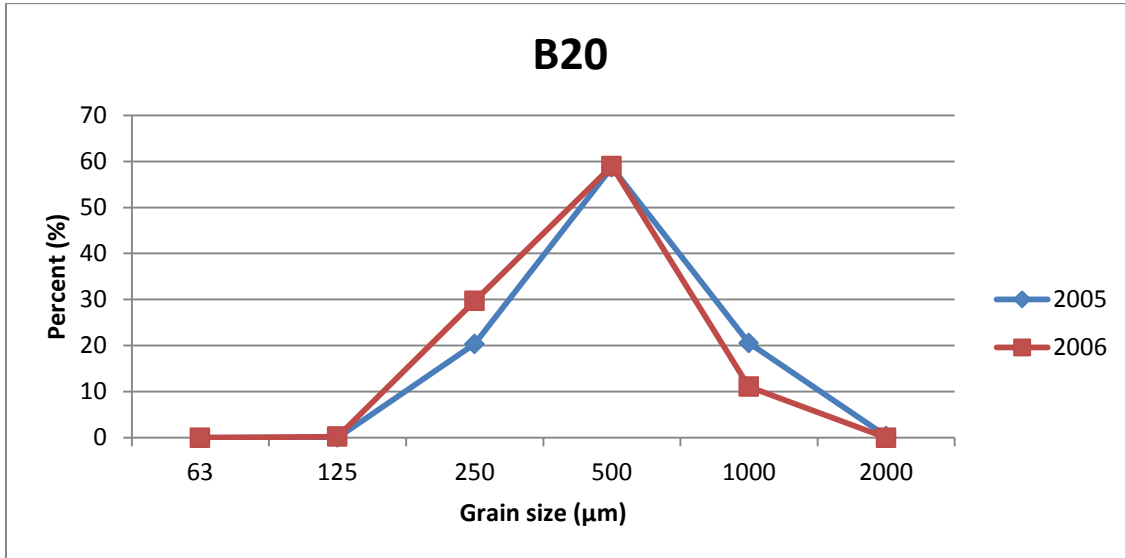
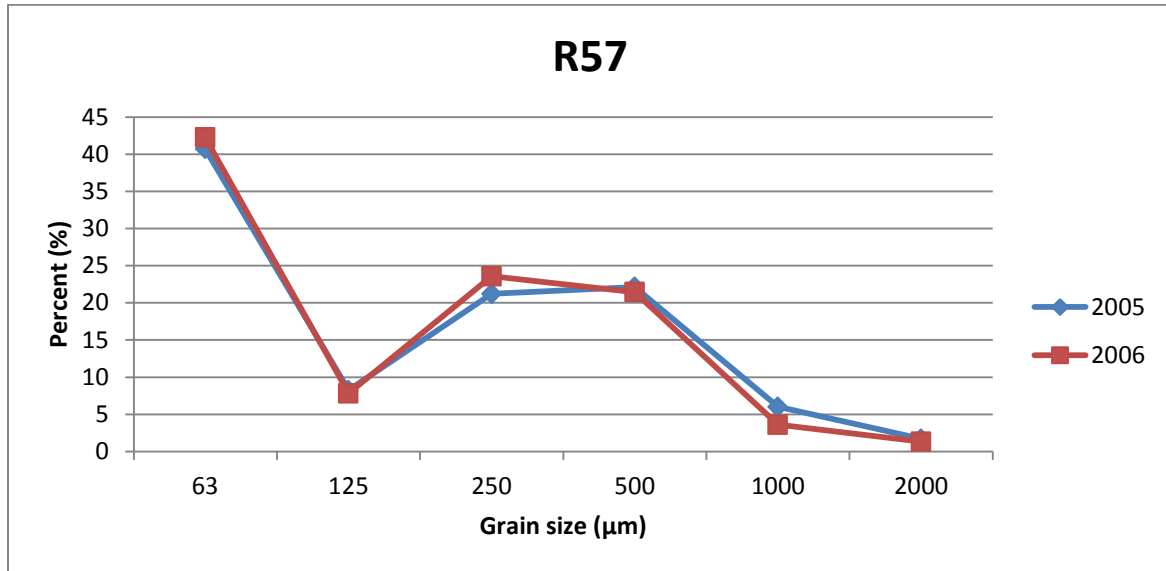
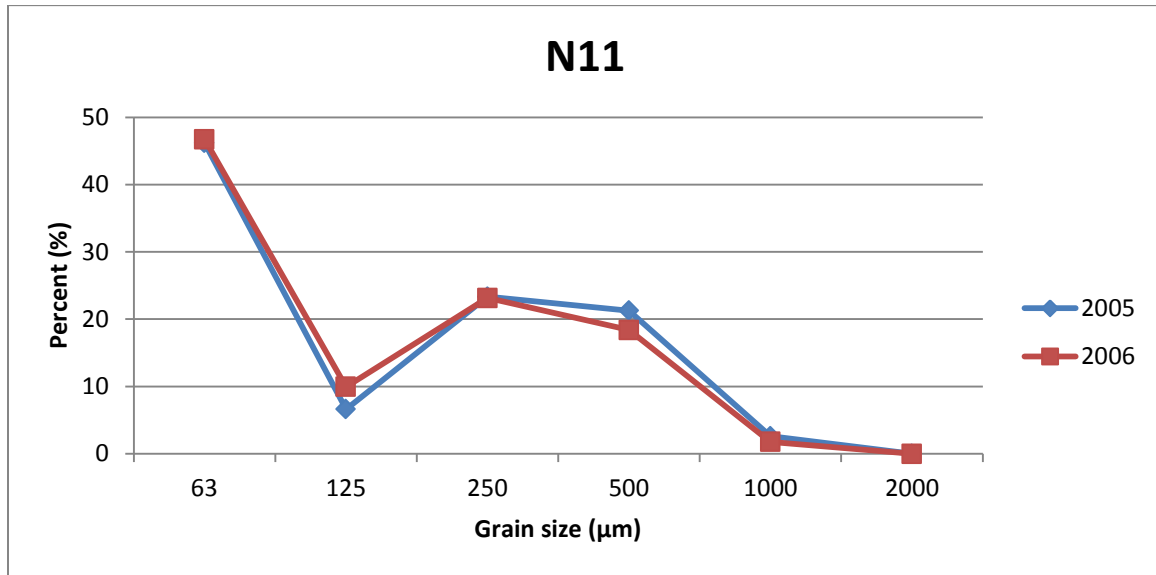


Figure 5.5. A) The 2006 organic content distribution within the Mgeni Estuary. Since 1986 (B) there has been a definite increase in organic content towards the head of the estuary and a decrease in organic content towards the tidal inlet. This increase in organic content could be related to the increase in mud concentration within the estuary, whilst the decrease at the tidal inlet is an effect of the increased marine incursion.







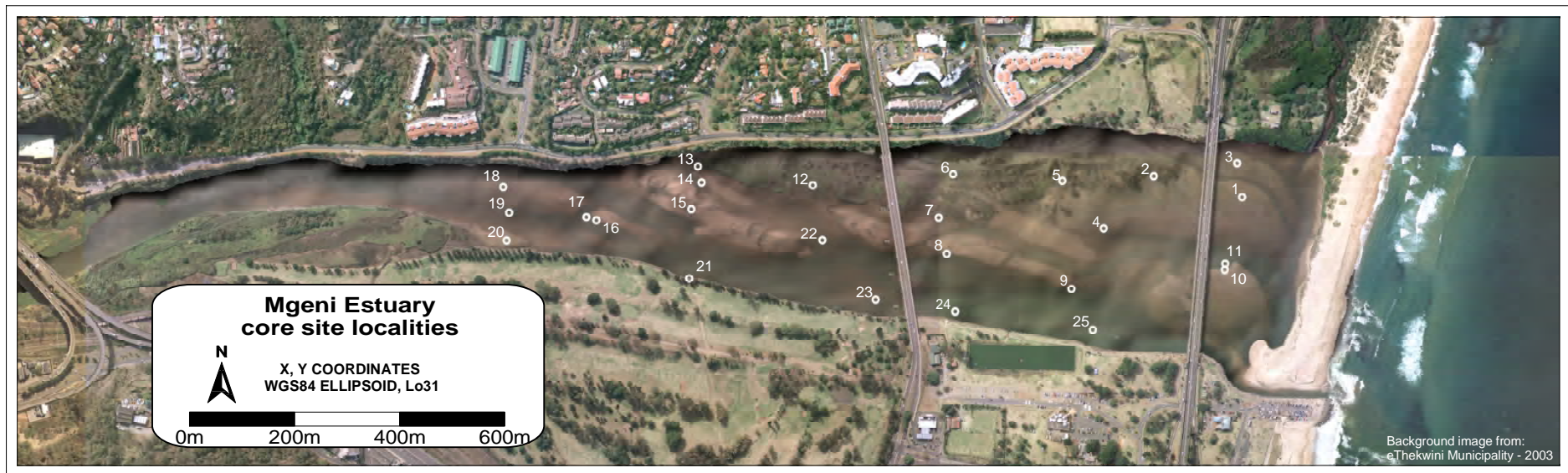


Figure 6.1. 2003 Aerial photograph of the Mgeni Estuary overlain with the location of the 15 vibro-cores and 10 hammer-cores taken during this study. Core locations were chosen based on the various sedimentary environments as well as along approximate transect lines

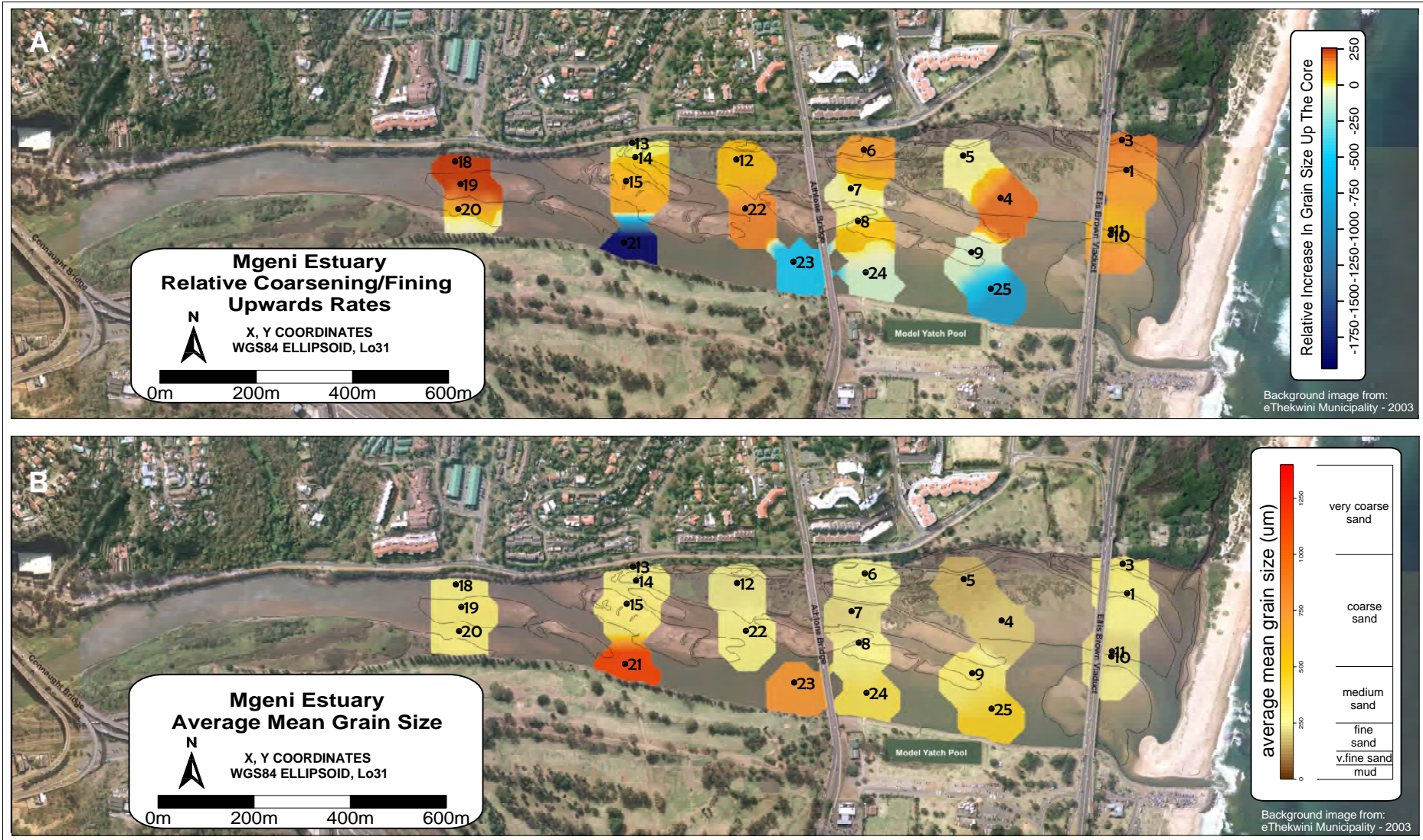


Figure 6.2. A) Increase/decrease in grain size up the core along set transect lines. Note contrast between sediments deposited in the sand bars (showing coarsening upwards sequences) versus the main channel (showing a fining upwards sequence). Cores 5 and 7 show the slowest rate of upwards increase. B) Average mean grain size of the individual cores. Grain size tends to be coarser in the main channel as expected and decreases towards the north.

Appendix B

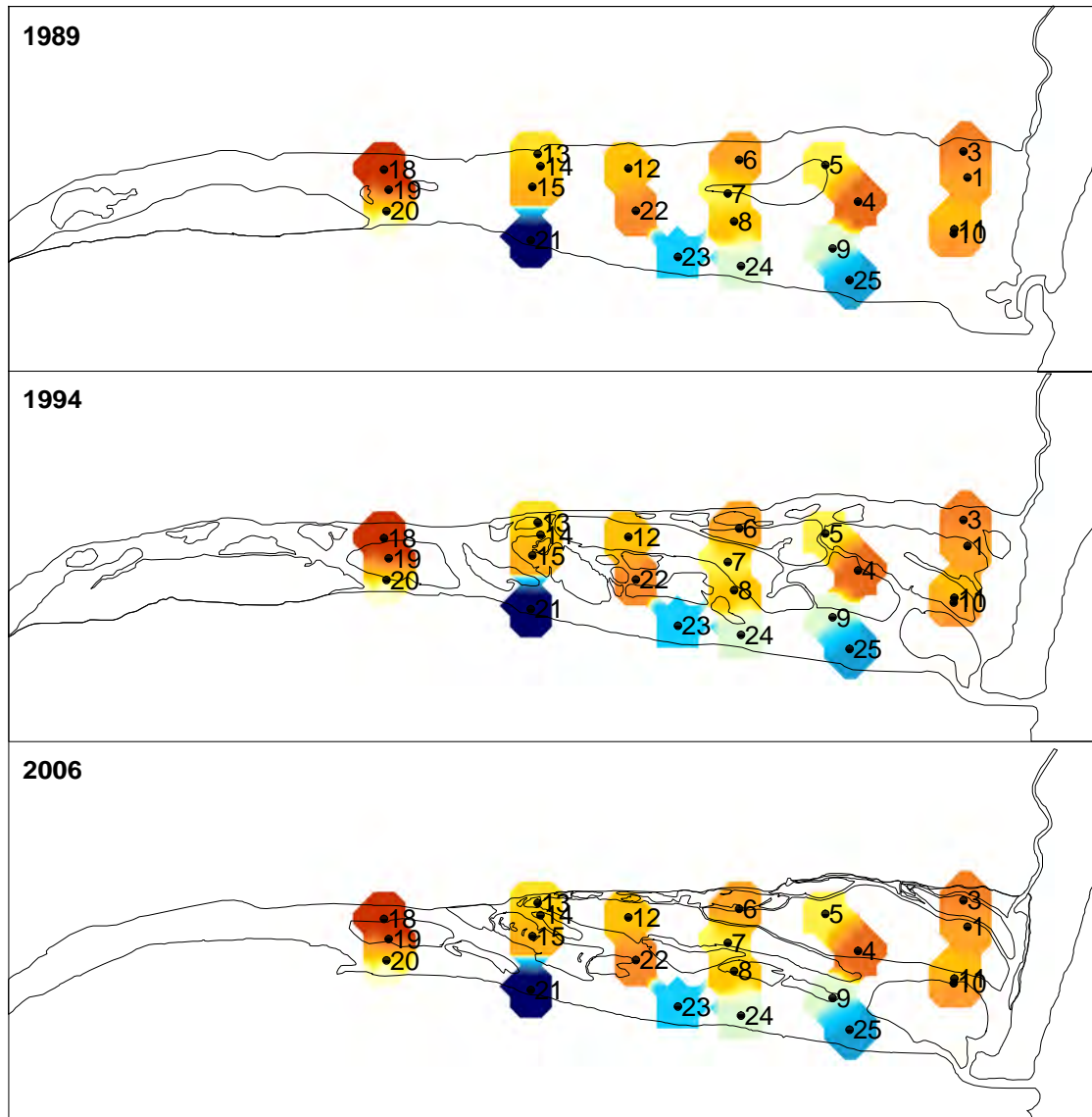
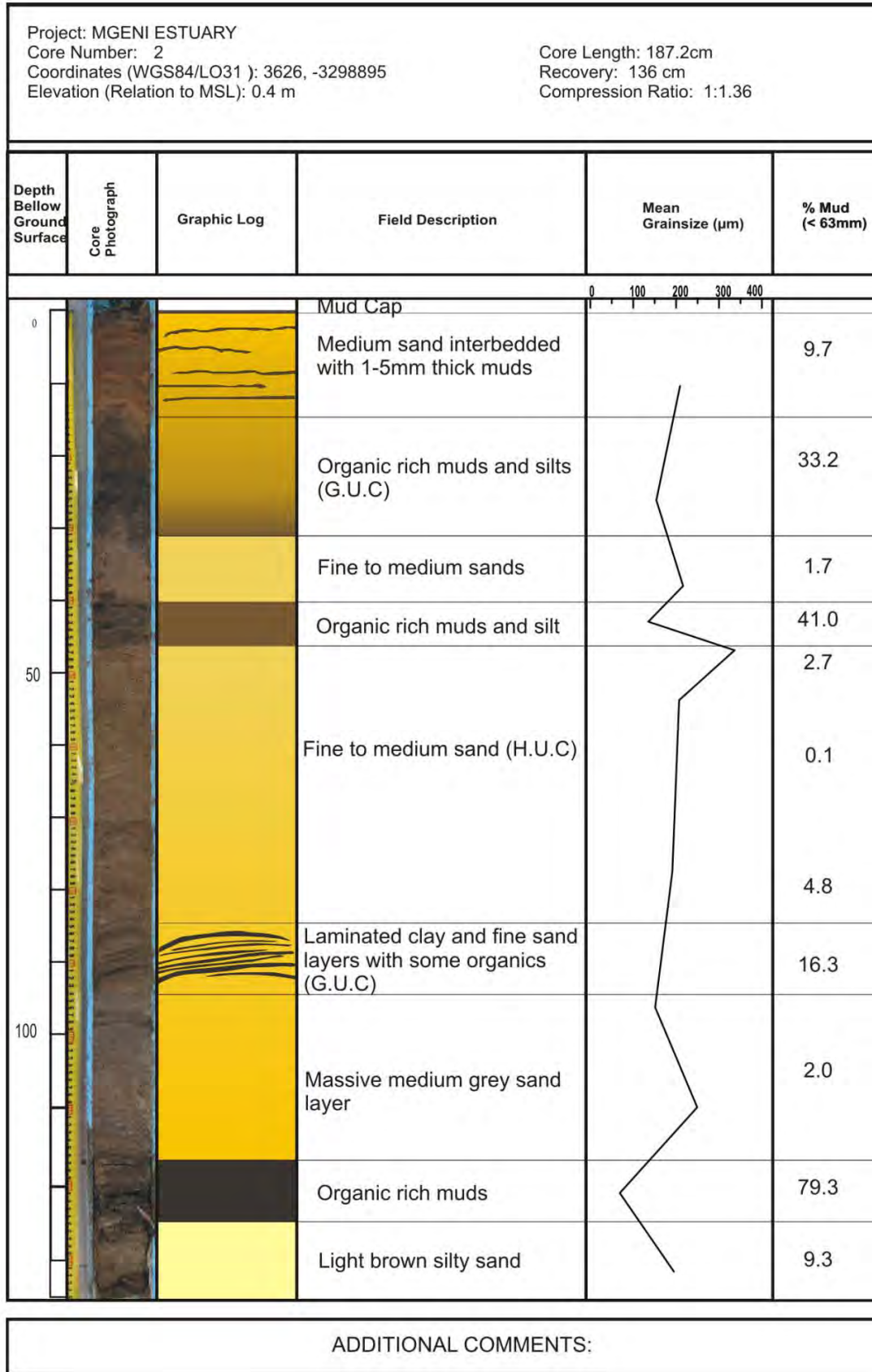


Figure 6.3) Increase/decrease in grain size up the core overlain by the sand bars out lines for 1989, 1994 and 2006. Note the decrease in the rate of increase in grain size in cores 5 and 7, which fall on the edge of the sand bar nucleolus. Core 9 shows a slight decrease in grain size up the core, this appears to be related to its position within the main channel until after 1994. Cores 10 and 11 show numerous coarsening fining upwards sequences, related to the shifting the flood tidal delta.

Project: MGENI ESTUARY Core Number: 1 Coordinates (WGS84/LO31): 3792, -3298934 Elevation (Relation to MSL): 0.5 m Core Length: 140 cm Recovery: 124 cm Compression Ratio: 1:1.29					
Depth Below Ground Surface	Core Photograph	Graphic Log	Field Description	Mean Grainsize (µm)	% Mud (< 63mm)
0			Mud Cap		
			Fine to medium sand with Mud filled J shaped Burrows and organic matter		3.6
			Organic rich sands interbedded with Organic rich clays (G.U.C)		16.7
50			Fining upwards sequence with coarse sand fining to fine to med sand. Some isolated shell fragments, gravels and organic rich clay laminations (H.U.C)		1.3
			Organic rich clays intebedded with fine sands and lighter coloured clays (H.U.C)		0.5
			Very fine sand and mud		85.0
100			Organic rich clays intebedded with fine sands and lighter coloured clays		51.9
			Fining upwards sequence with basal gravels with some pebbles fining upward to coarse sand (H.U.C)		84.2
				1.1	
				0.3	

ADDITIONAL COMMENTS: G.U.C = gradational upper contact; H.U.C = hard upper contact
 : Gap in core due to loss of sediment from base of core during removal from hole. This allowed the bottom section to separate and move downward while the top section remained in place.



Project: MGENI ESTUARY Core Number: 3 Coordinates (WGS84/Lo31): 3783, -3298871 Elevation (Relation to MSL) 0.4 m Core Length: 215 cm Recovery: 137 cm Compression Ratio: 1:1.56					
Depth Bellow Ground Surface	Core Photograph	Graphic Log	Field Description	Mean Grainsize (µm)	% Mud (< 63mm)
0			Mud Cap	0	
			Fine to medium sand	~100	5.7
			Fine to medium sand with mud	~150	8.8
			Mud with fine to med sand	~200	17.3
			Medium sand	~250	0.0
			Organic rich mud	~300	3.1
			Fine to medium sand with Mud	~350	78.8
			Medium to coarse sand (G.U.C)	~400	2.5
			Organic rich mud (H.U.C)	~450	1.4
			Medium to coarse grey sand (H.U.C)	~500	2.6
			Band of dark grey coarse	~550	0.1
			Light grey coarse to very coarse sand	~600	0.1
			Organic rich mud interbedded with light brown and dark grey bands of very fine sand (H.U.C)	~650	0.0
			Very fine sand to mud (H.U.C)	~700	62.6
				56.0	
ADDITIONAL COMMENTS:					

Project: MGENI ESTUARY Core Number: 4 Coordinates (WGS84/LO31): 3531, -3298992 Elevation (Relation to MSL) 0.3 m Core Length: 237 cm Recovery: 136 cm Compression Ratio: 1:1.74					
Depth Below Ground Surface	Core Photograph	Graphic Log	Field Description	Mean Grainsize (µm)	% Mud (< 63mm)
0			Dark coloured medium sand	~180	4.0
~28			Med sand with mud matrix and mud burrow at 28-33 cm	~120	29.5
~33			Medium sand. Orange brown towards the top grading to grey brown at base of layer. Pebble at 48 cm	~200	1.6
~48				~250	1.3
~55				~280	3.0
~65			Interbedded bioturbated mud and sand. Fine sand in middle of layer	~100	71.2
~85			Medium sand	~180	2.1
~136				~180	2.1
ADDITIONAL COMMENTS:					

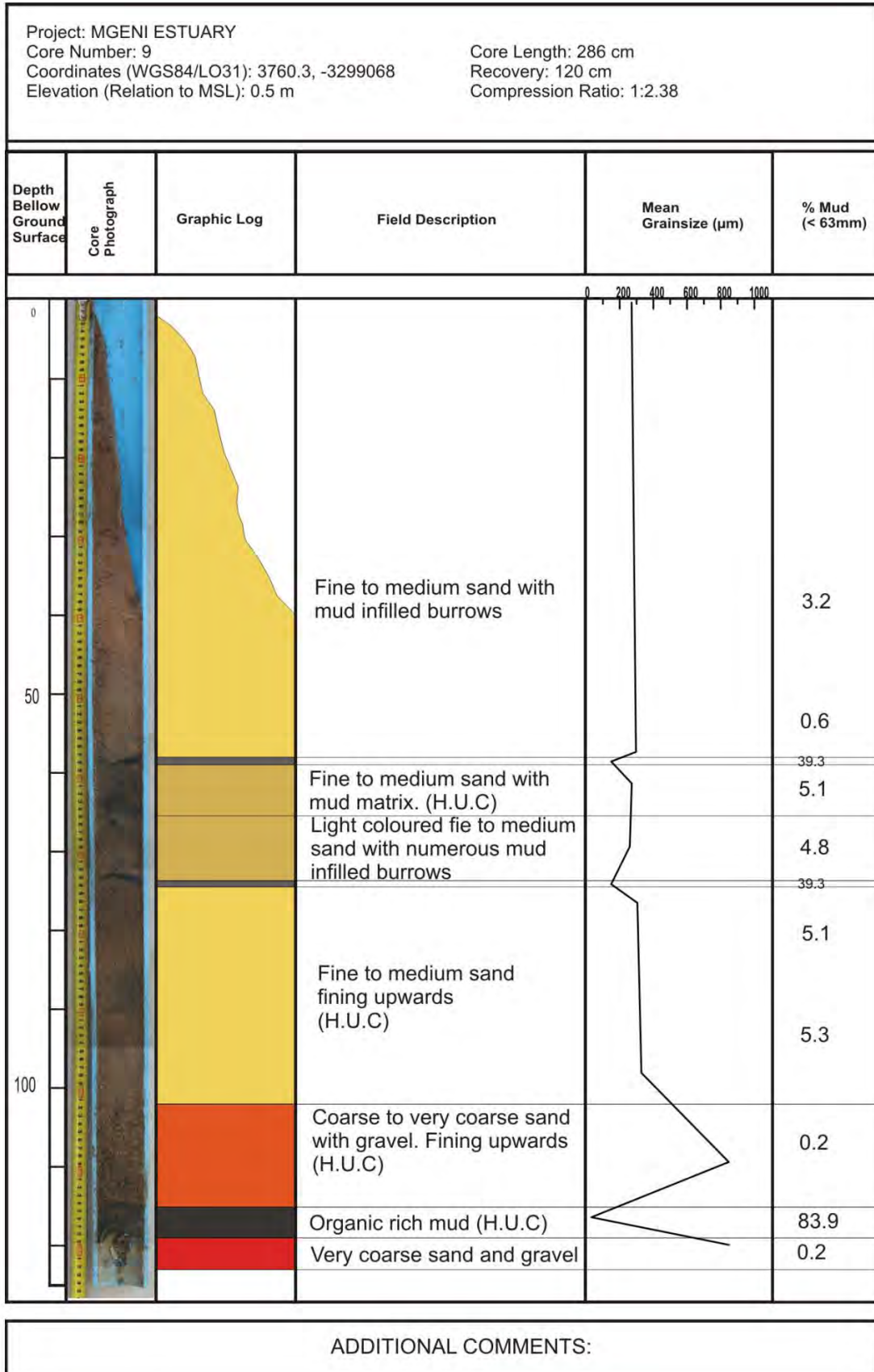
Project: MGENI ESTUARY Core Number: 5 Coordinates (WGS84/LO31): 3453, -3298904 Elevation (Relation to MSL): 0.9 m Core Length: 158 cm Recovery: 94 cm Compression Ratio: 1:1.68					
Depth Below Ground Surface	Core Photograph	Graphic Log	Field Description	Mean Grainsize (µm)	% Mud (< 63mm)
0			Mud cap	0	
			Fine to medium sand	12.0	
			Fine sand to mud (G.U.C)	29.1	
			Fine to medium sand (G.U.C)	18.5	
				8.8	
			fine to medium sand fining upwards "J" shaped burrow at 21-25 cm (H.U.C)	1.9	
50				0.0	
			Mud layer (H.U.C)	67.8	
			Medium sand darker towards top due to mud matrix	11.9	
			Mud layer	1.8	
		82.2			
		2.1			
		fine to med sand, orange in colour (G.U.C)	2.1		

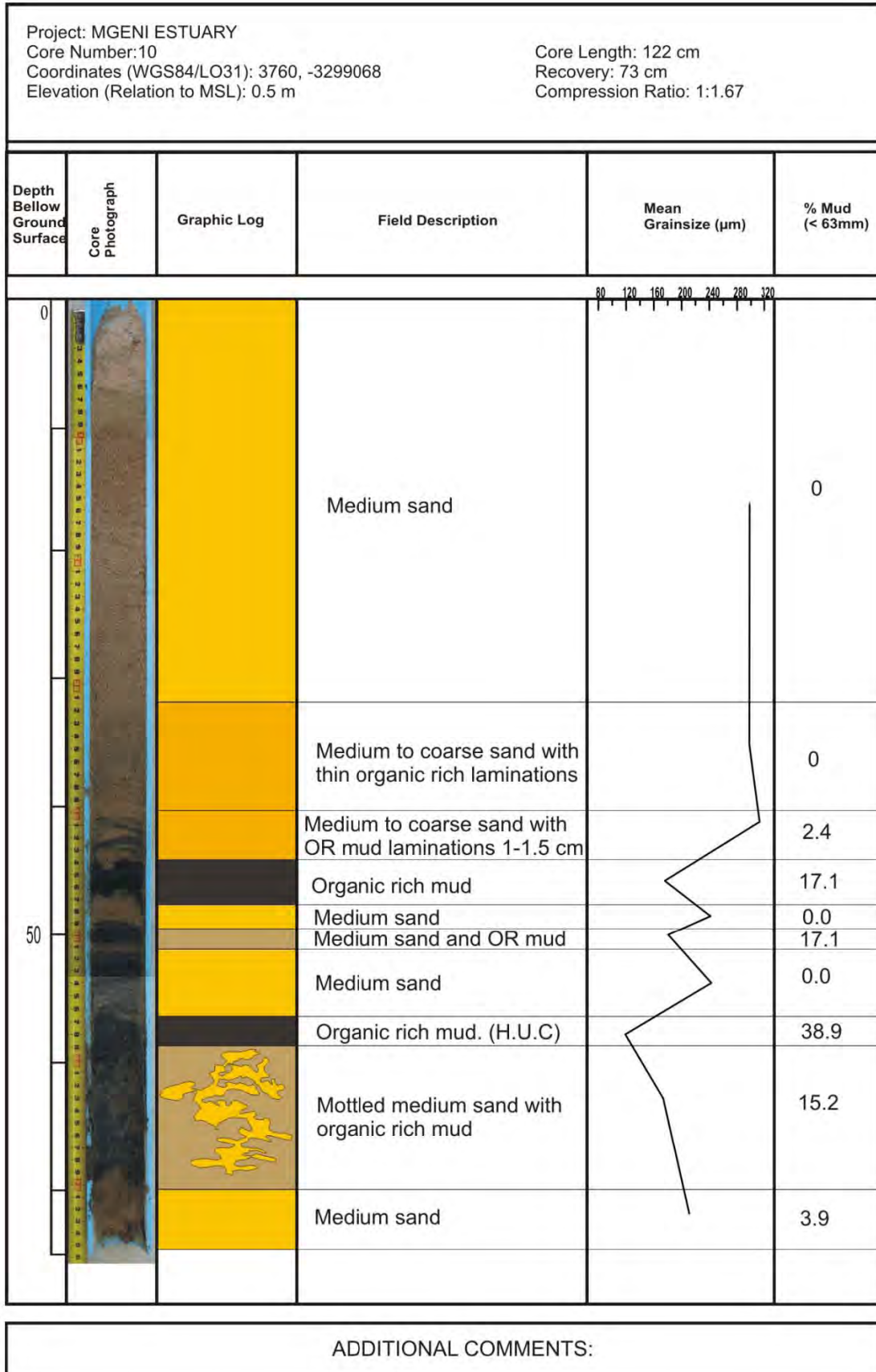
ADDITIONAL COMMENTS:

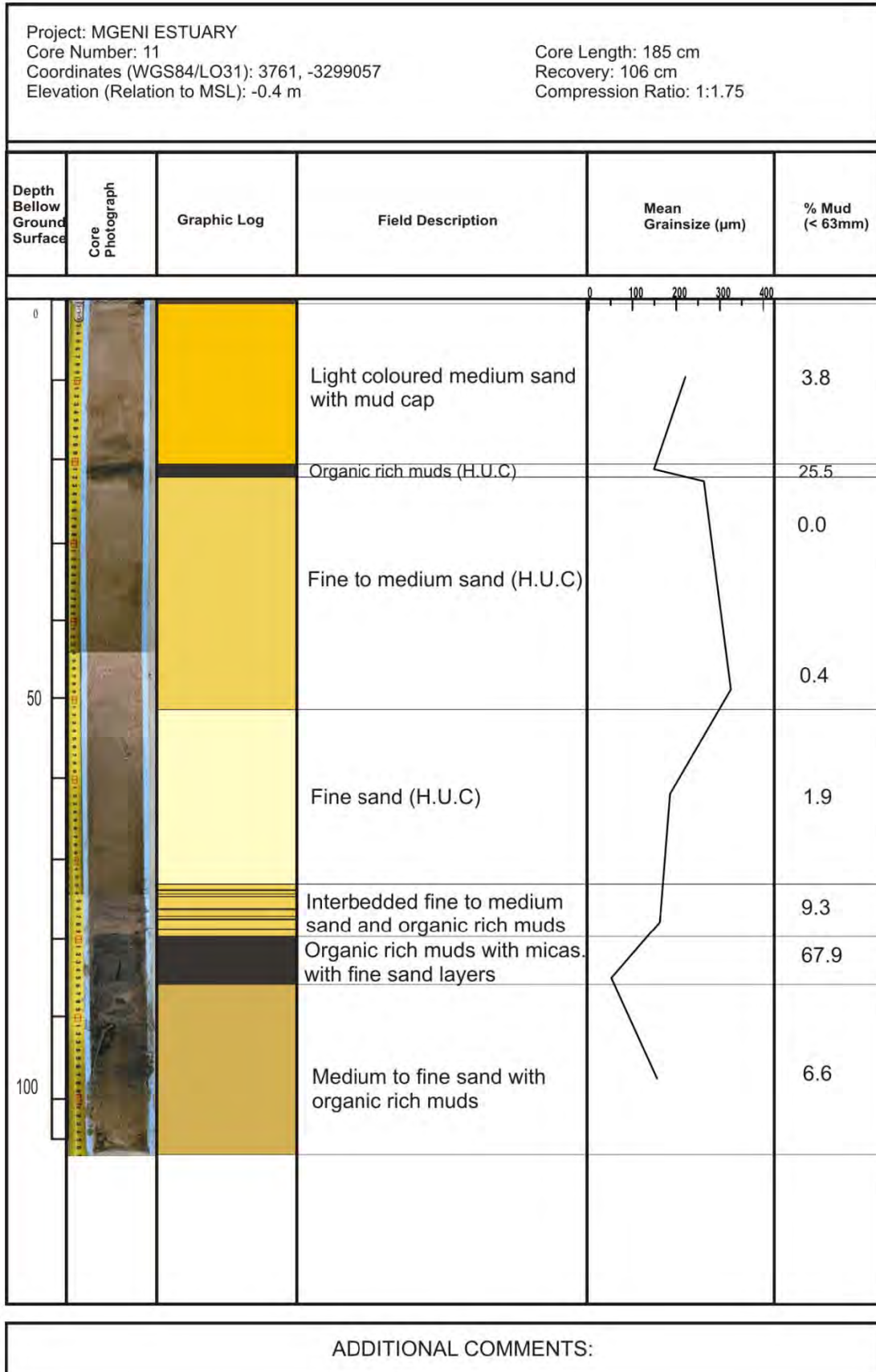
Project: MGENI ESTUARY Core Number: 6 Coordinates (WGS84/LO31): 3247, -3298892 Elevation (Relation to MSL): -0.1 m Core Length: 252 cm Recovery: 146 cm Compression Ratio: 1: 1.72					
Depth Below Ground Surface	Core Photograph	Graphic Log	Field Description	Mean Grainsize (µm)	% Mud (< 63mm)
0			Fine to medium sand		8.3
			Fine to medium sand with mud matrix		8.7
			Fine to medium sand with two mud filled burrows at 18-20 cm and 55-56 cm and mud layer at 57 cm. (G.U.C)		0.0
50					2.0
			Organic rich mud (H.U.C)		76.0
			Fine to medium sand with alternating band of light and dark sand and organic rich muds rythmites. Laminations vary in size from 1-2 cm(light layers) to 0.1 cm (dark layers) (G.U.C)		2.3
100					10.9
					8.6
			Organic rich mud with dark and light layering		80.4
	Gravels fining upwards to very coarse sand and gravel	1.7			
ADDITIONAL COMMENTS:					

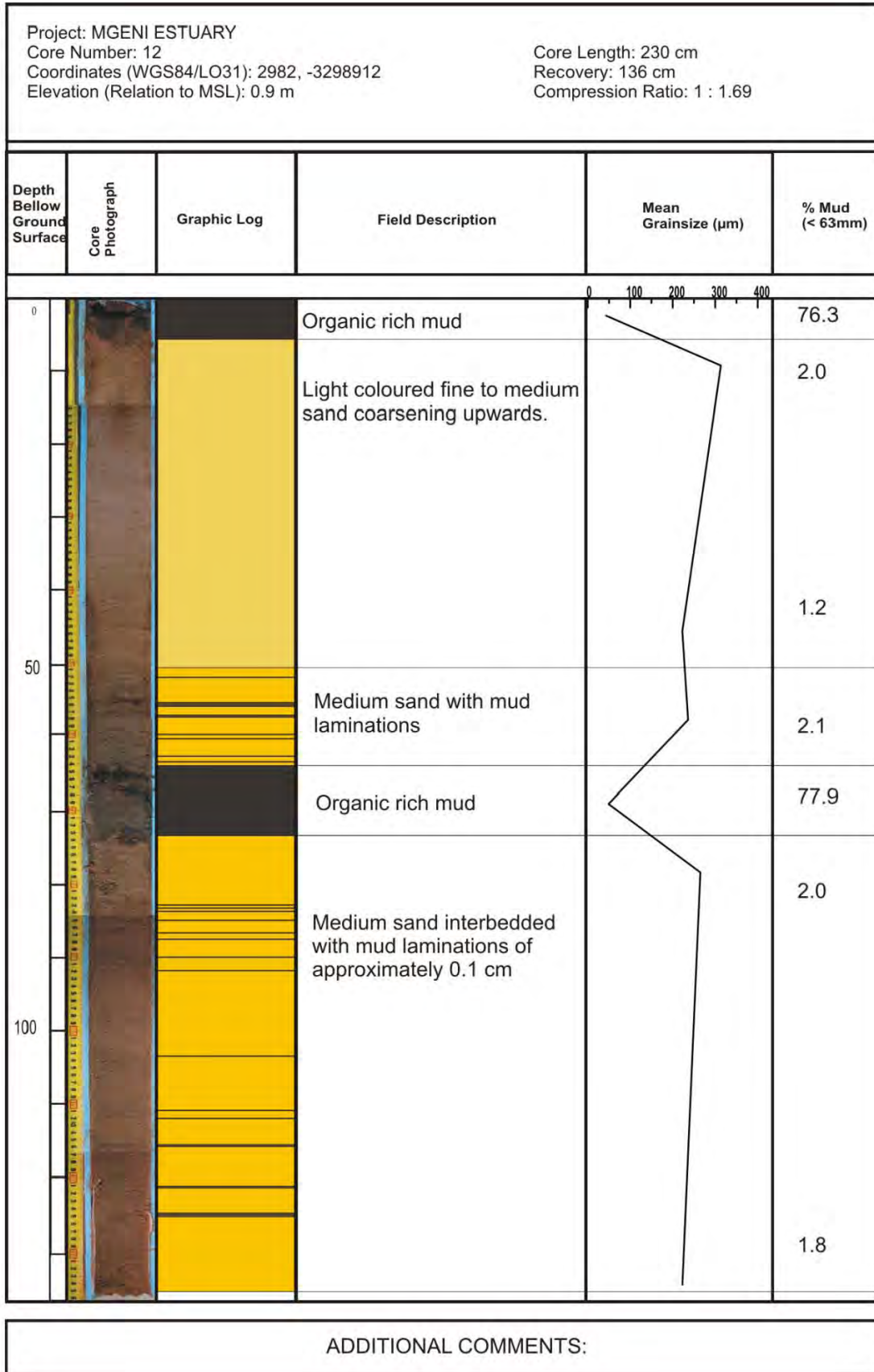
Project: MGENI ESTUARY Core Number: 7 Coordinates (WGS84/LO31): 3220, -3298972 Elevation (Relation to MSL): 0.8 m Core Length: 171 cm Recovery: 102 cm Compression Ratio: 1:1.67					
Depth Bellow Ground Surface	Core Photograph	Graphic Log	Field Description	Mean Grainsize (µm)	% Mud (< 63mm)
0			Fine sand with mud matrix		16.5
			Redish brown mud		56.9
			Fine to medium sand. Infilled burrow at 21-34 cm. Some isolated mud balls. (H.U.C)		5.0
50			Fine to medium sand with organic rich black sand		1.4
			Organic rich mud. Some laminations of fine sand (H.U.C)		1.3
			Fine to medium sand (H.U.C)		80.3
			Fine to med sand with OR mud		9.5
			Fine to med sand with OR mud		25.5
			Fine to medium sand (H.U.C)		2.9
100			Fine to medium sand (H.U.C)		1.5
ADDITIONAL COMMENTS:					

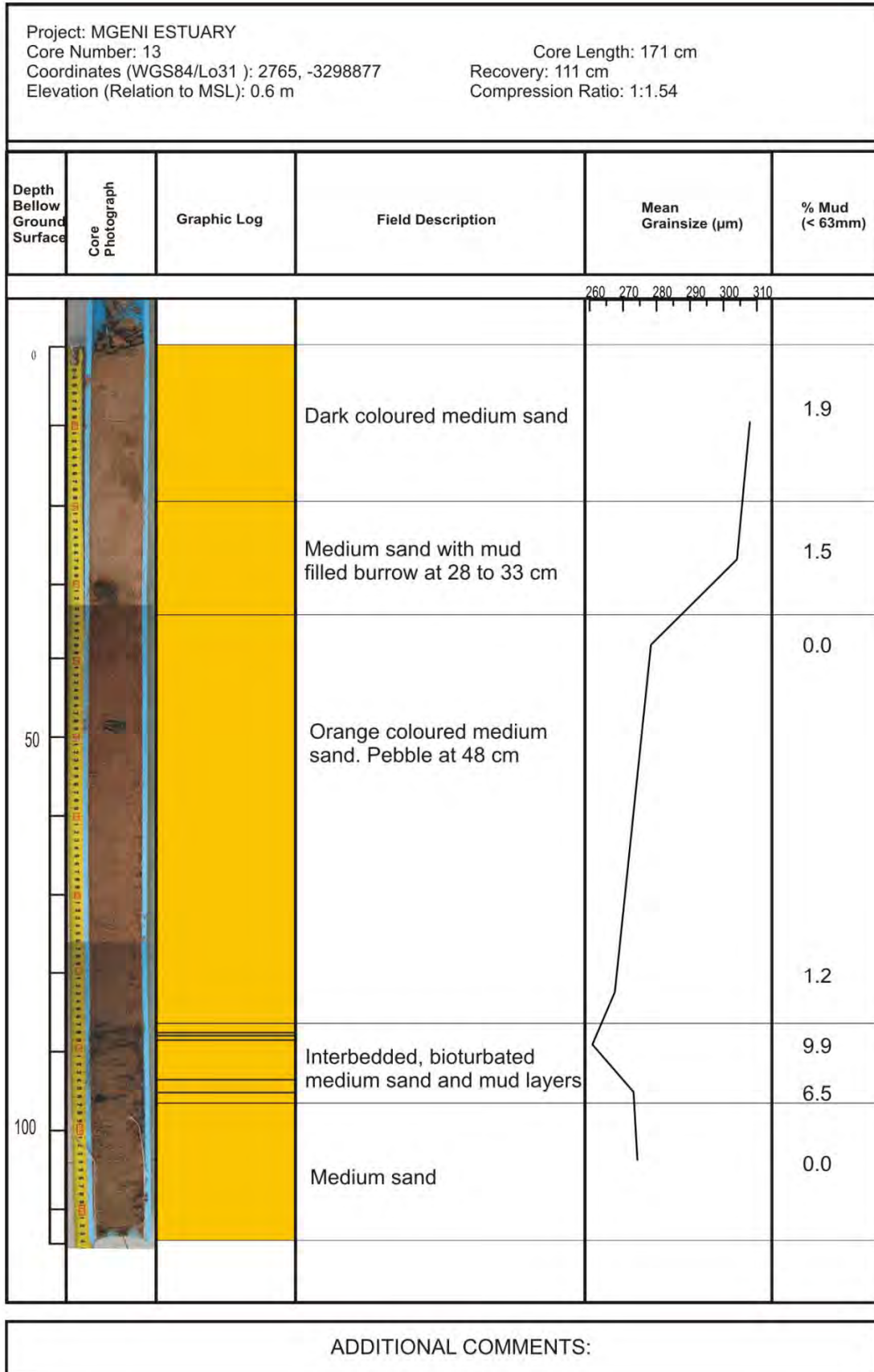
Project: MGENI ESTUARY Core Number: 8 Coordinates (WGS84/LO31): 3235, -3299039 Elevation (Relation to MSL): 0.5 m Core Length: 211 cm Recovery: 127 cm Compression Ratio: 1:1.66					
Depth Below Ground Surface	Core Photograph	Graphic Log	Field Description	Mean Grainsize (µm)	% Mud (< 63mm)
0			Fine to medium sand	160 200 240 280 320 360	3.0
			Organic rich mud (H.U.C)		1.6
50			Light coloured fine to medium sand (H.U.C)		30.8
			Fine to medium sand with mud infilled burrows. "J" shaped burrow at 80-84 cm		1.7
100					0.0
			Medium to fine sand slightly darker in colour (G.U.C)		1.5
				0.2	
			Fine to medium sand, with some mud laminations		2.0
ADDITIONAL COMMENTS:					

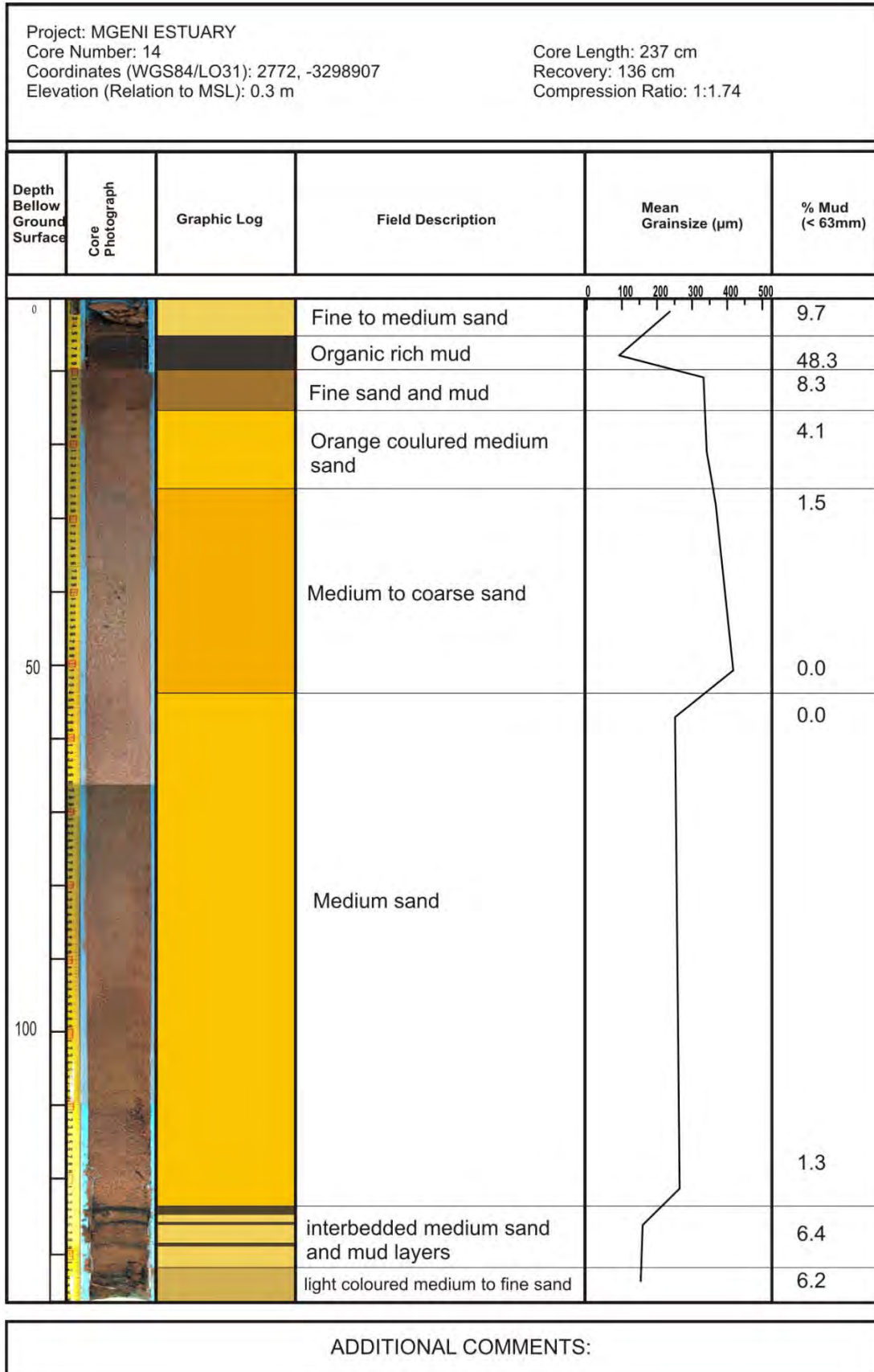


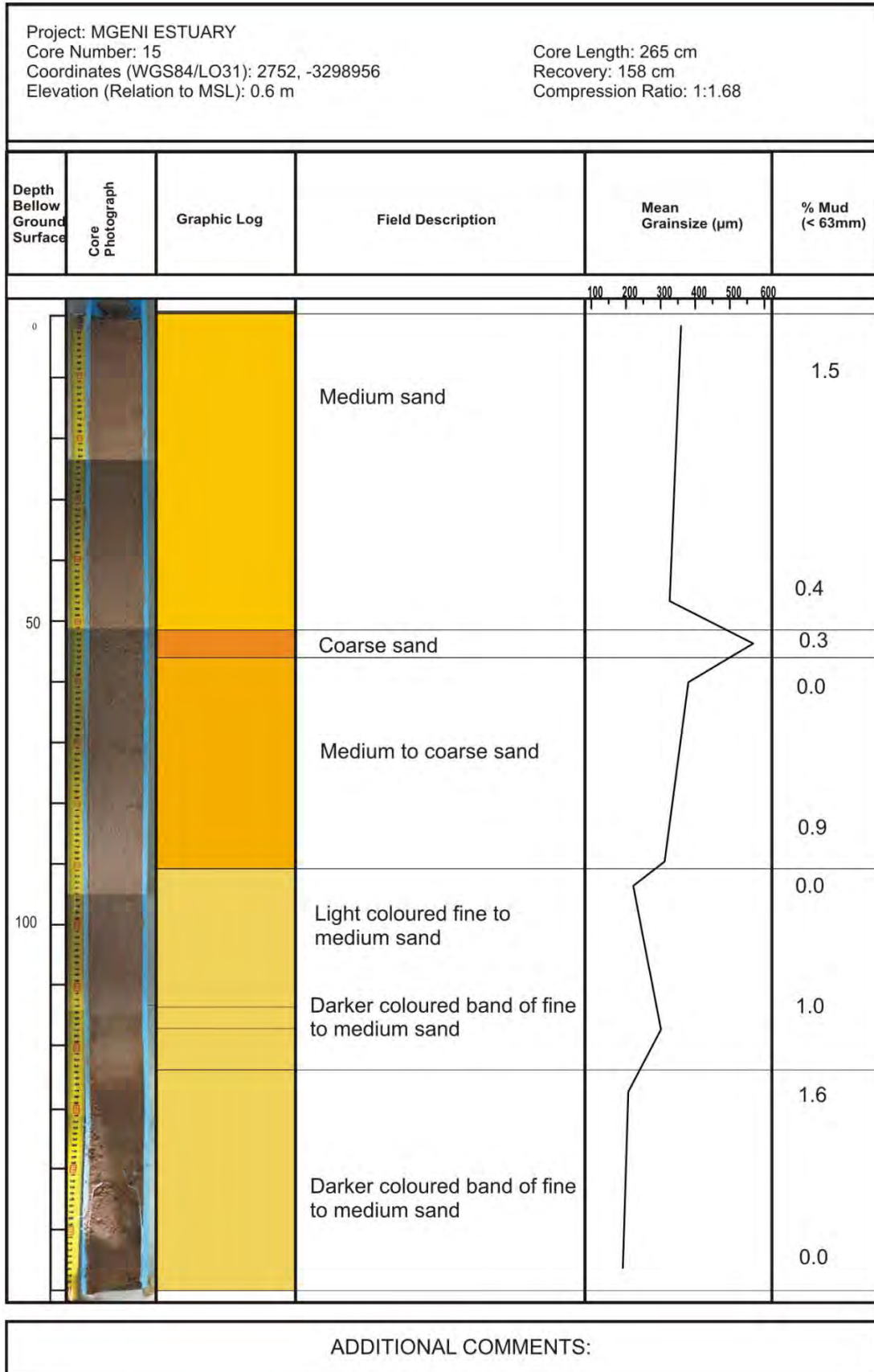


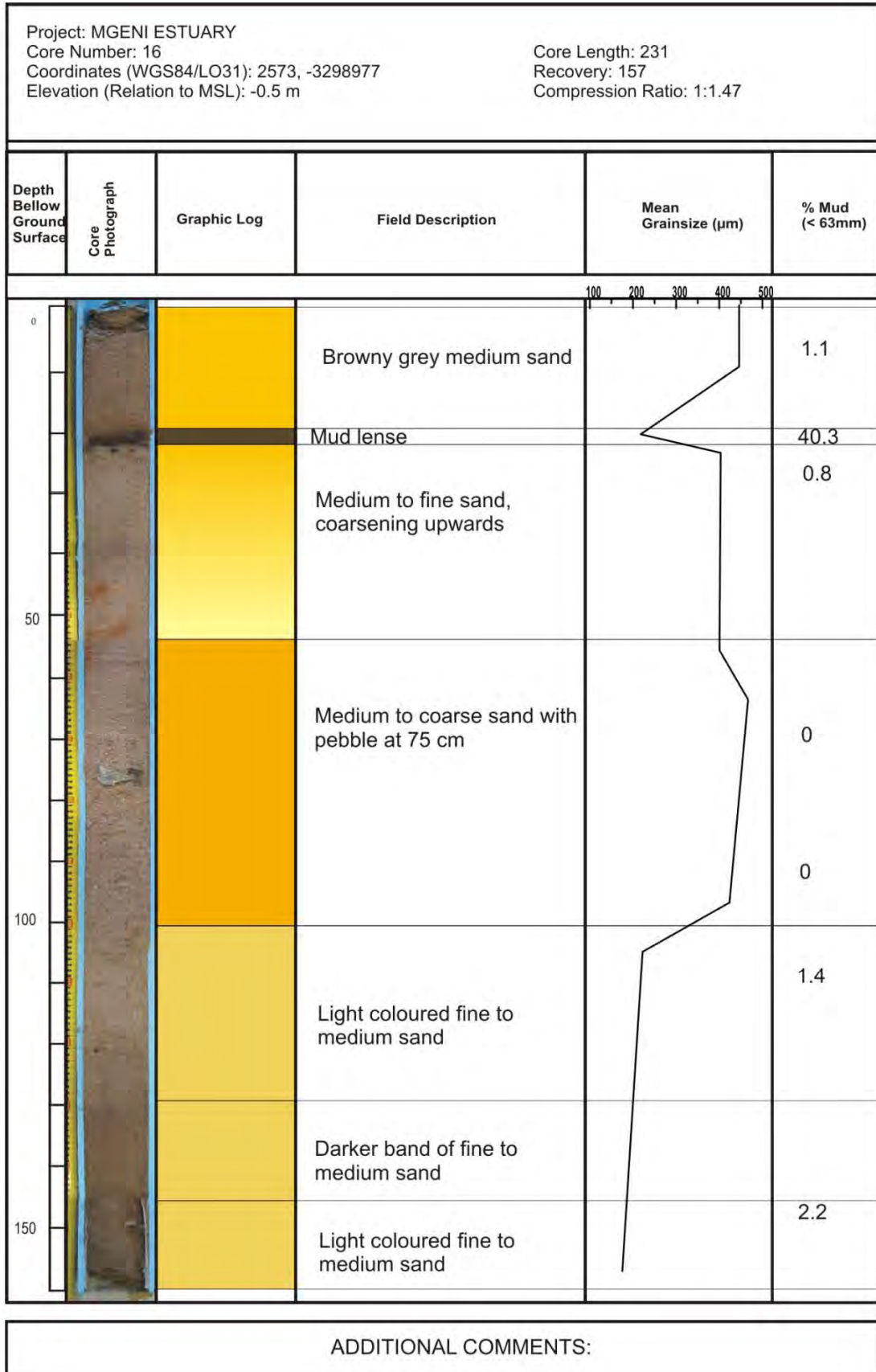


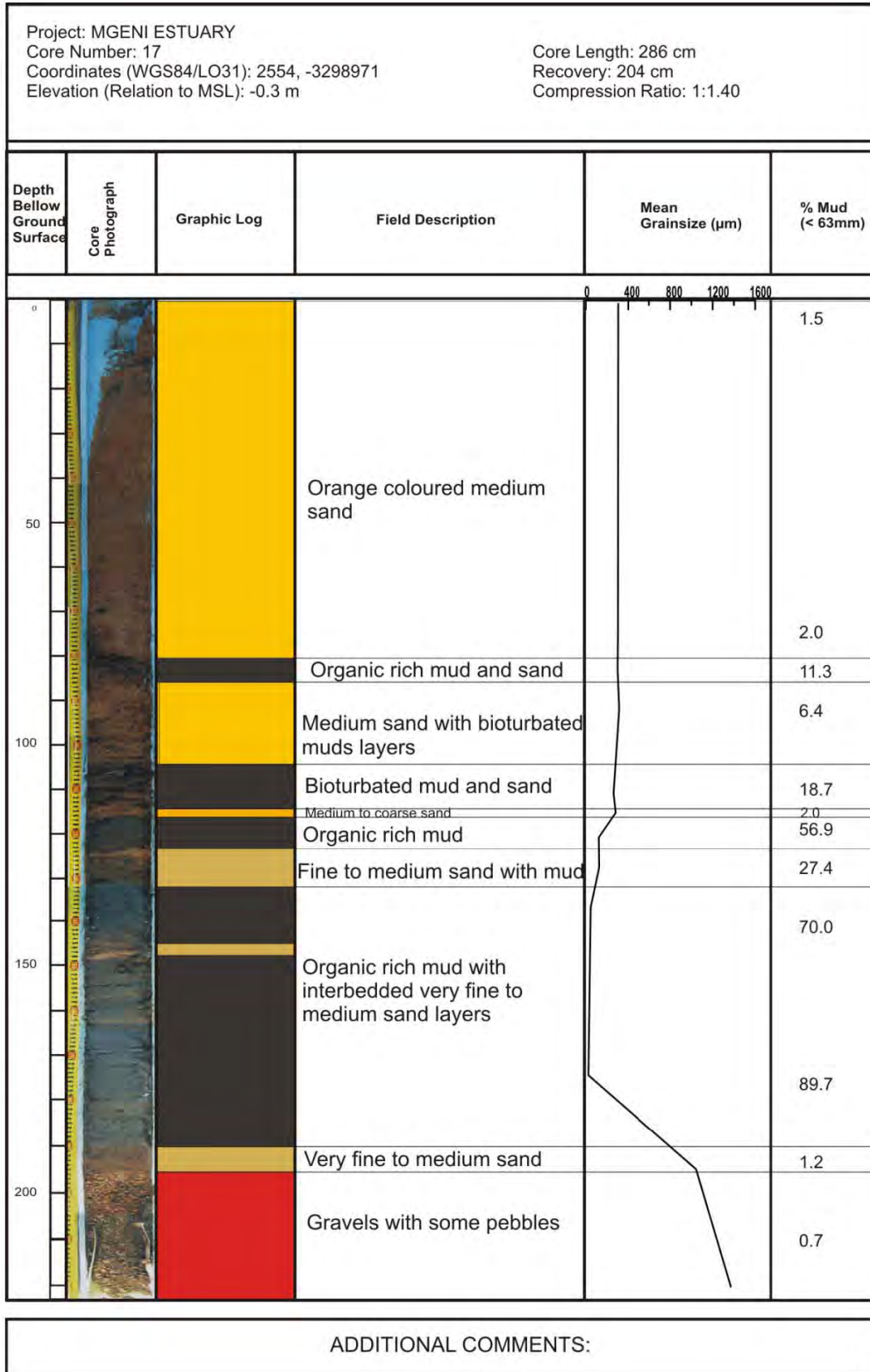


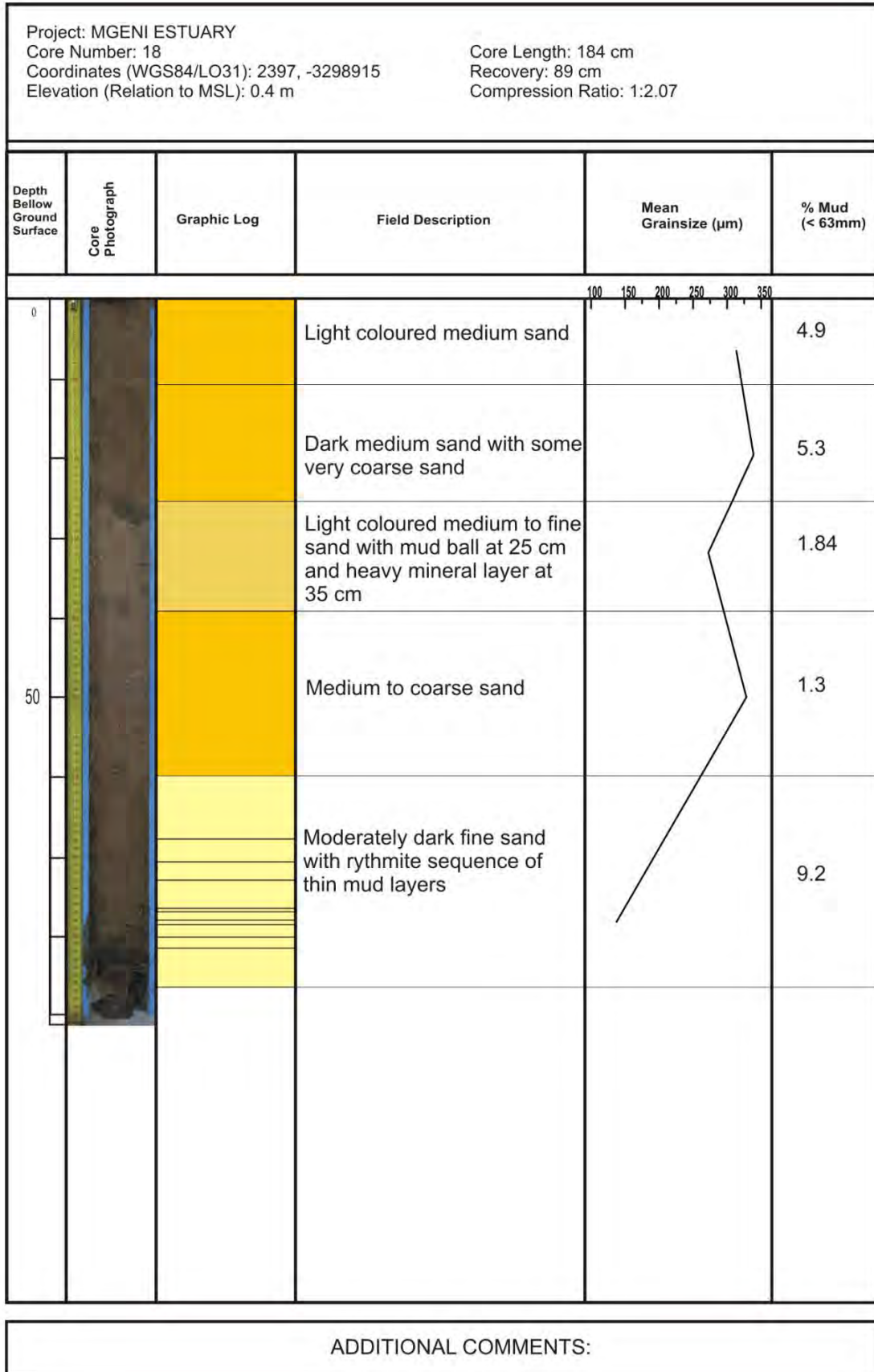


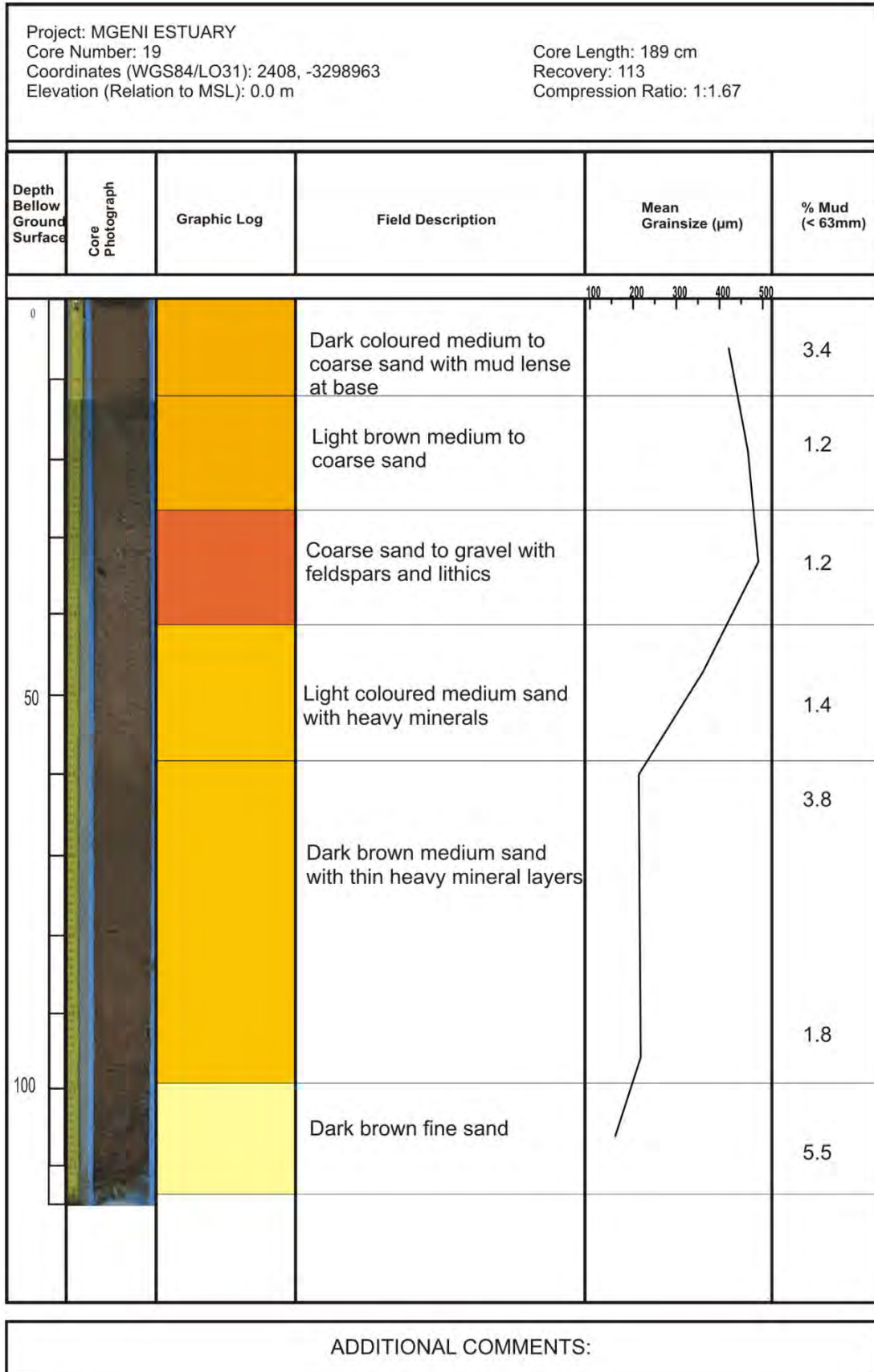


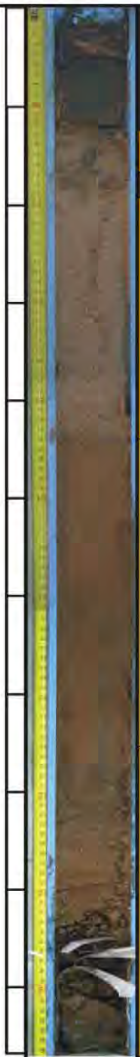
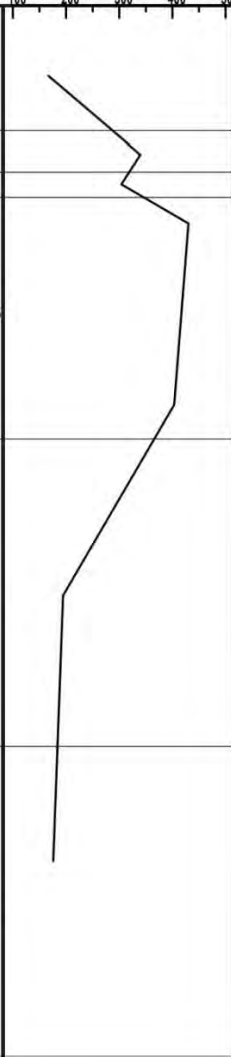




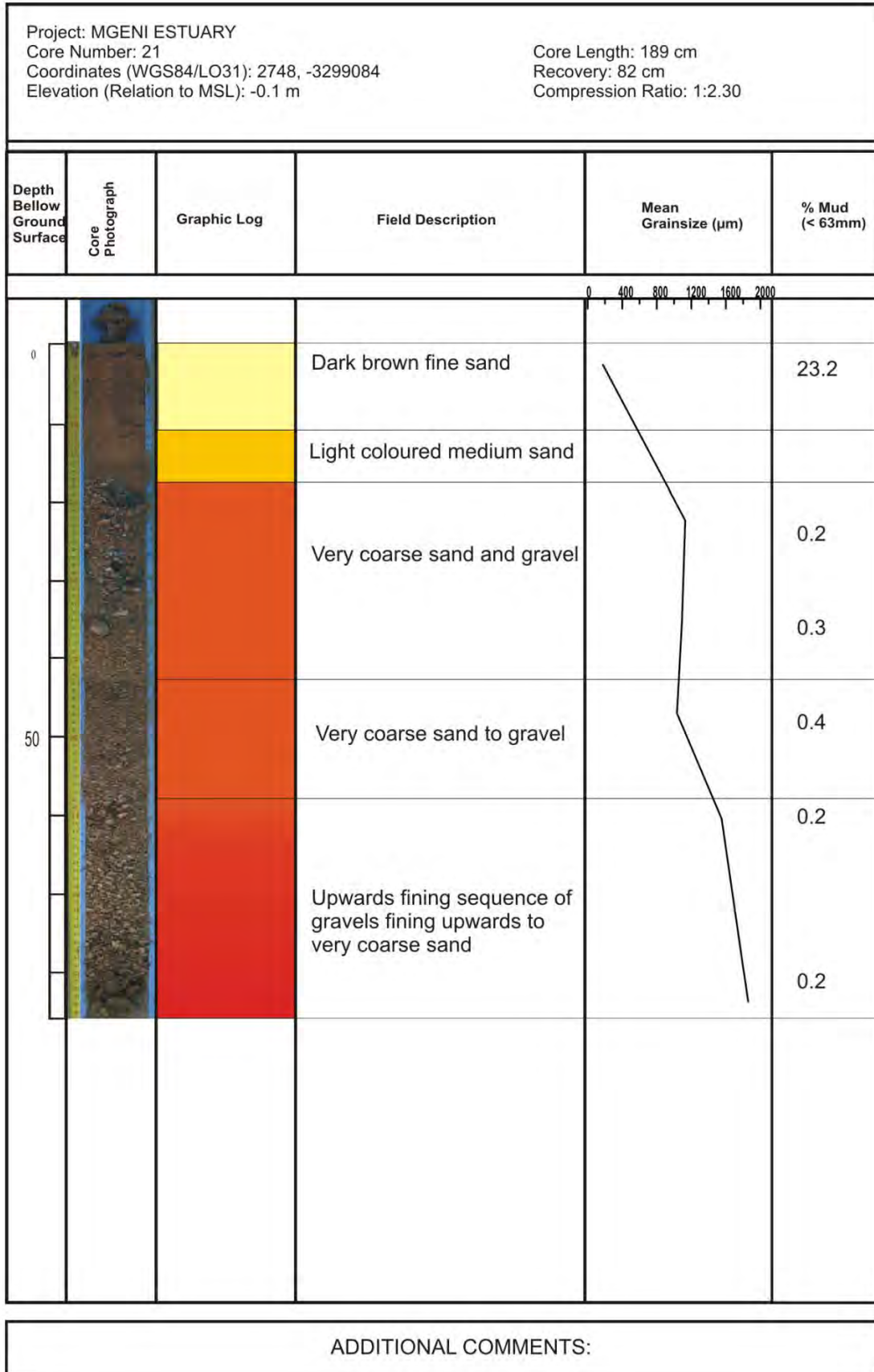


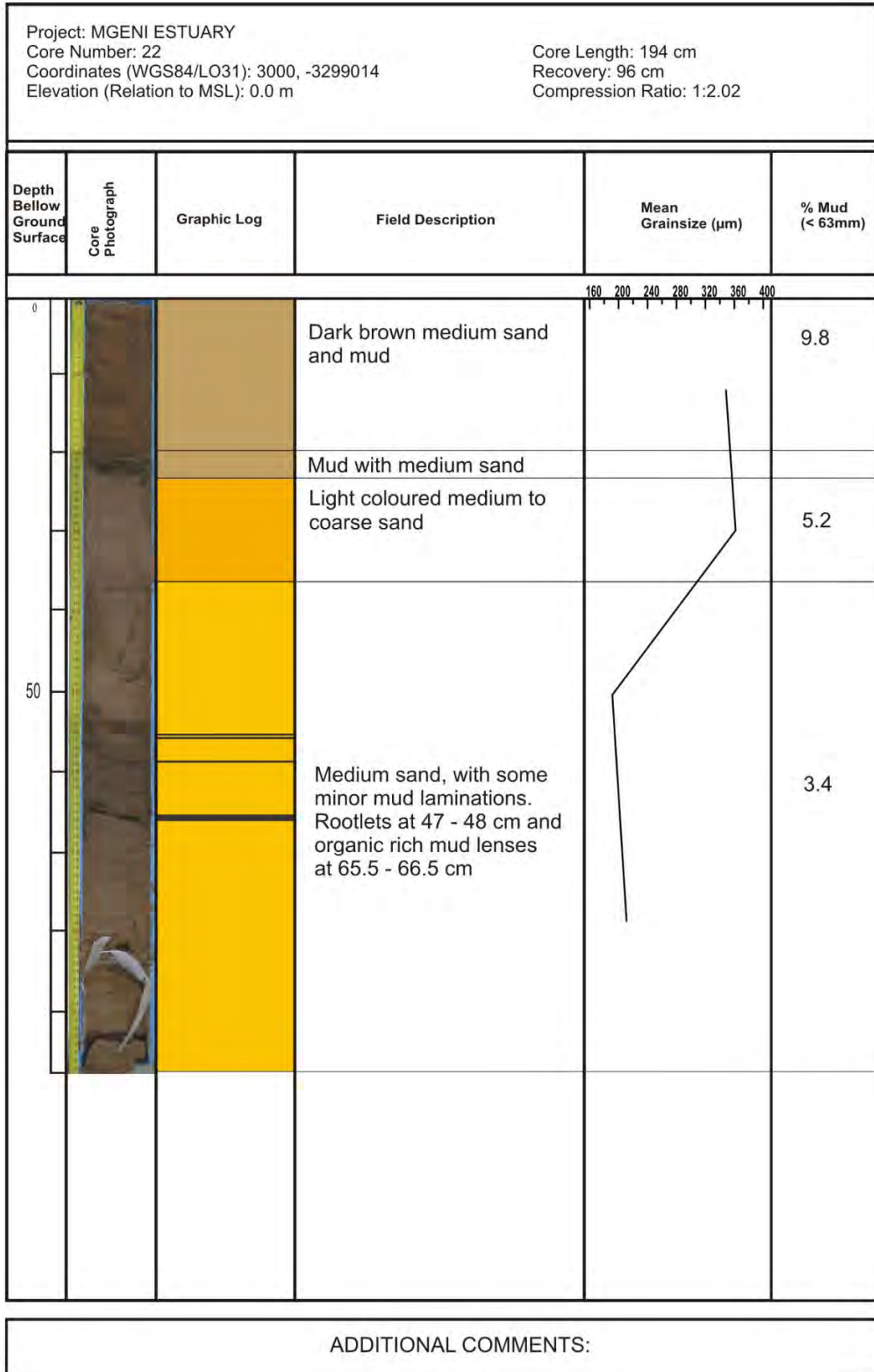


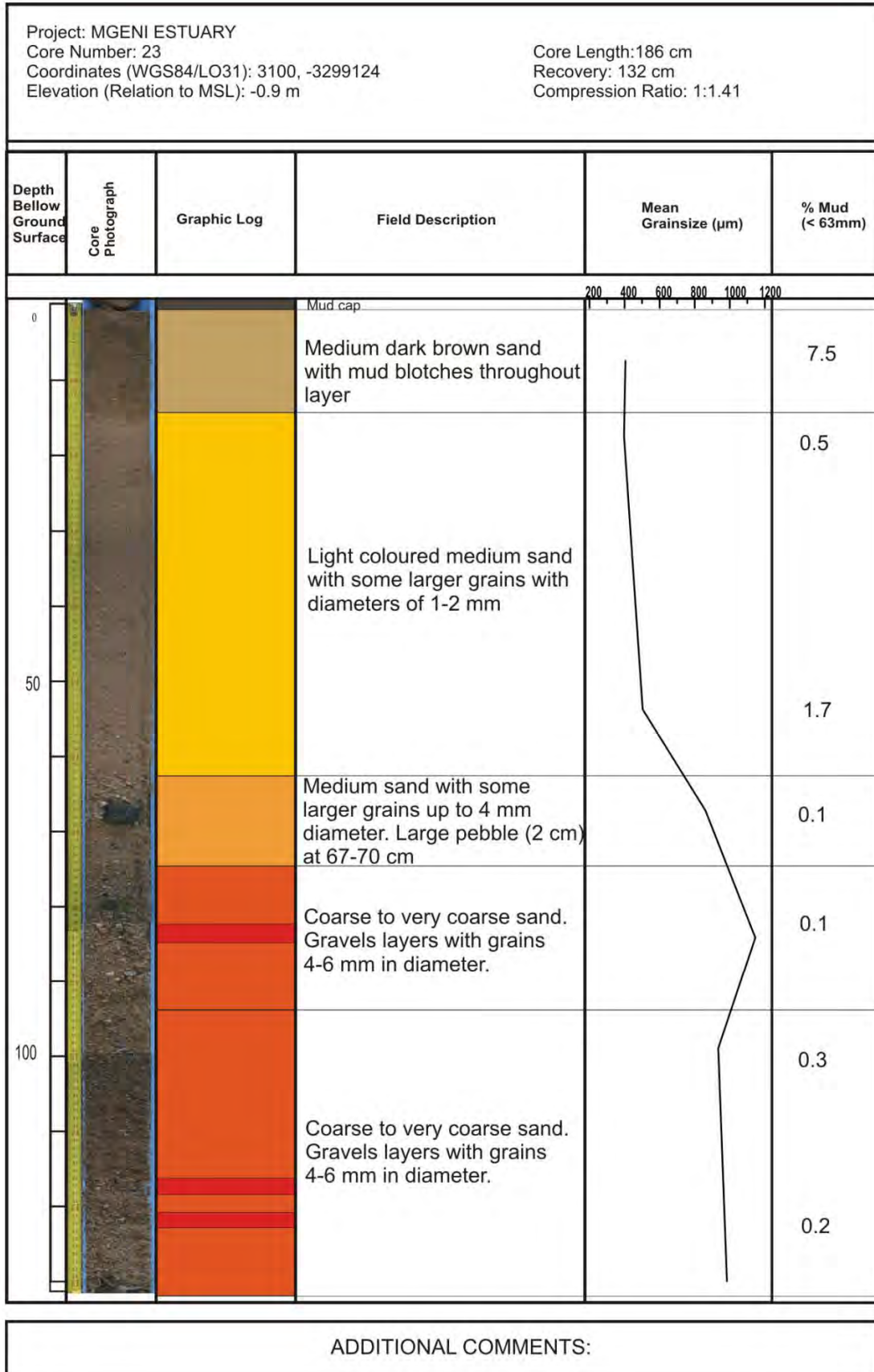


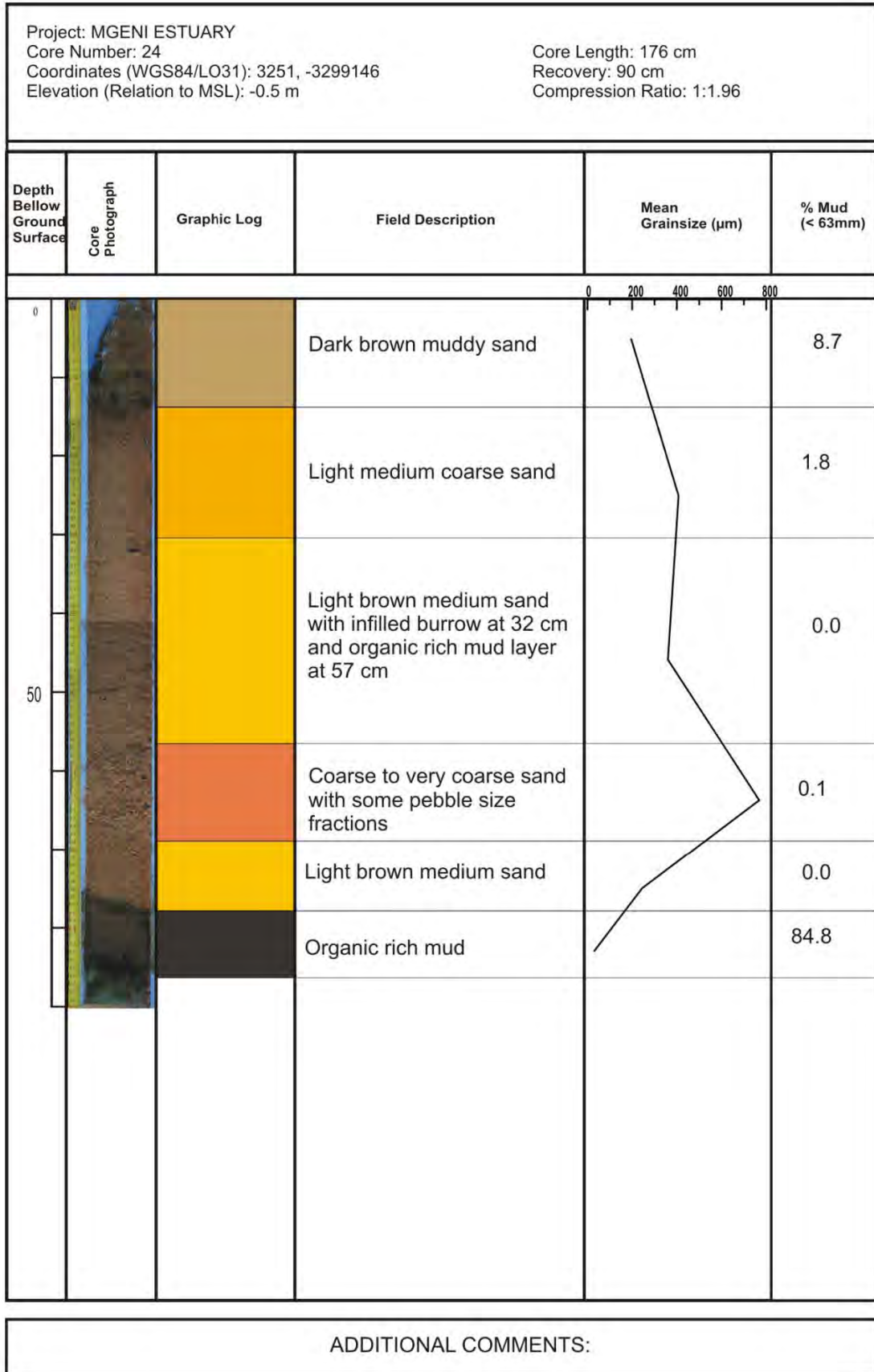
Project: MGENI ESTUARY Core Number: 20 Coordinates (WGS84/LO31): 2404, -3299014 Elevation (Relation to MSL): 0.0 m Core Length: 193 cm Recovery: 108 cm Compression Ratio: 1:1.79						
Depth Below Ground Surface	Core Photograph	Graphic Log	Field Description	Mean Grainsize (µm)	% Mud (< 63mm)	
0			Dark brown organic rich mud		41.4	
			Light coloured medium sand		5.3	
			Mud lense		24.1	
			Light coloured medium sand with some gravel sized grains		1.7	
50					Brown fine to medium sand	3.7
100					Dark brown medium to fine sand	2.5

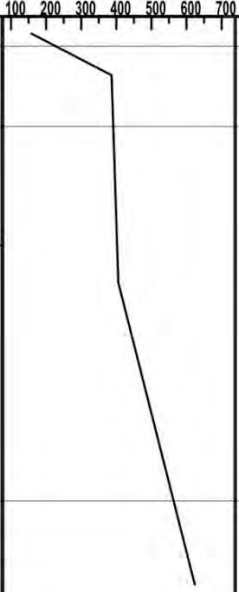
ADDITIONAL COMMENTS:









Project: MGENI ESTUARY Core Number: 25 Coordinates (WGS84/LO31): 3511, -3299180 Elevation (Relation to MSL): -1.1 m Core Length: not recorded Recovery: 55 cm Compression Ratio: n/a					
Depth Below Ground Surface	Core Photograph	Graphic Log	Field Description	Mean Grainsize (µm)	% Mud (< 63mm)
0			Dark brown Mud		43.9%
			Light coloured medium sand		3.3%
			Medium sand with some gravel up to 4mm in diameter. Thin mud lense at 48 cm		1.9%
50			Medium to very coarse sand Coarse to very coarse sand with some gravel		0.3%
ADDITIONAL COMMENTS:					

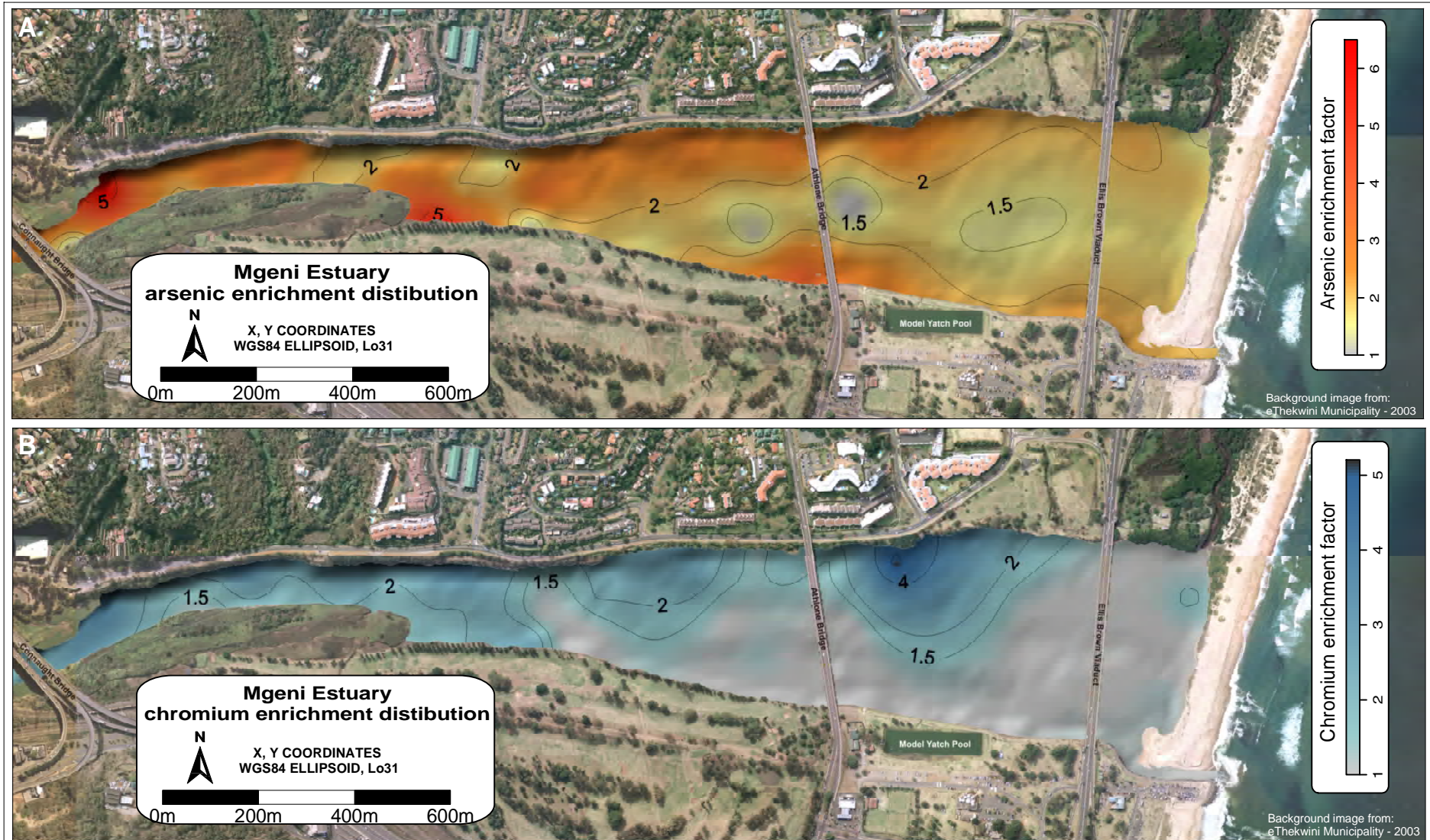


Figure 7. A) The distribution of arsenic enrichment in the Mgeni Estuary. The enrichment distribution of arsenic closely follows that of finer grained sediments, with high enrichment towards the northern side-attached bar, main channel and in the organic rich muds close to Connaught Bridge. B) The distribution of Chromium enrichment. With high enrichment around the storm water drain on the northern bank, and the organic rich muds towards Connaught Bridge.

Appendix C

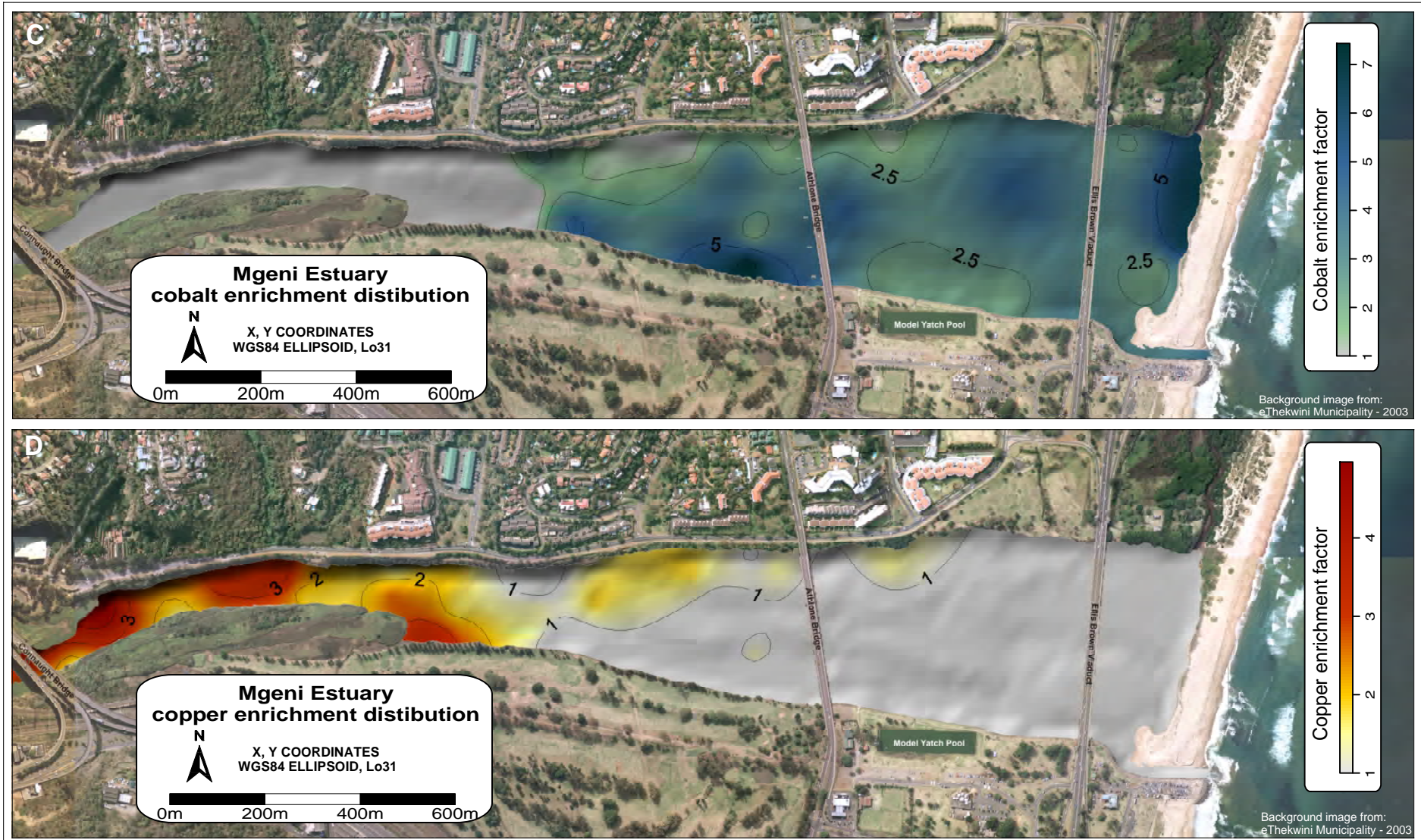


Figure 7. C) The cobalt enrichment within the Mgeni Estuary. The enrichment distribution differs to other elements round the supratidal barrier and the storm water drain on the southern bank. D) Distribution of copper enrichment. Enrichment is limited to the head of the estuary especially in the organic rich mud around Connaught Bridge.

Sample	lat	long	Mud	mean	mode	organics	SiO2	Al2O3	Fe2O3	MnO	MgO	CaO	Na2O	K2O	TiO2	P2O5	Zn	Cu	Nb	Y	Rb	Zr	Sr	U	Th	Ni	Cr	V	La	Pb	Ga	Co	Ce	Nd	As	Sn	Cd	S	Total	LOI
3	6700650.47	309355.4	11.02	346.61	1.60	0.63	87.41	6.16	1.08	0.0289	0	0.63	1.54	2.52	0.2141	0.07	45.8	0.6	3.4	10.9	62.8	117.7	112.1	1.1	0.8	0.1	11.4	16.9	0	30	6	72	10	0	11	12	7	400	99.65	1.28
11	6700607.13	309509.07	24.03	283.73	1.69	1.28	84.41	7.55	2	0.0255	0.16	0.71	2.01	2.53	0.3643	0.09	112.1	6.5	5.5	13.9	72.4	229.5	118	0.5	9.1	4.4	57.2	35.6	0	21	6	45	11	2	10	11	13	2683	99.85	3
15	6700581.88	309610.46	12.64	348.91	1.55	0.64	86.04	6.74	1.25	0.0224	0.04	0.7	1.65	2.59	0.2238	0.06	58.7	0.4	4	9.2	66.7	94.2	121	0.1	3.7	2.8	36.9	25	0	34	8	76	19	5	13	11	7	3425	99.32	1.8
20	6700628.7	309729.22	69.38	83.91	5.25	1.54	79.35	10.02	3.58	0.0321	0.39	0.91	2.19	2.47	0.5417	0.17	262.7	24.1	9.3	21.1	81	267.8	122.8	0	11.9	13.4	79.6	61.9	0	20	6	25	27	10	9	12	2	4880	99.65	5.36
24	6700548.93	309815.5	15.03	355.14	1.50	0.81	85.18	6.9	1.94	0.0309	0.12	0.79	1.79	2.46	0.4386	0.07	82.1	3.7	7.3	13.8	71.2	266.1	118	0.8	8	4.5	34.9	36.6	0	62	11	70	72	26	24	11	4	1505	99.72	2.37
33	6700486.27	310382.88	4.79	278.43	2.01	0.46	79.9	5.42	1.45	0.0291	0.53	9.08	1.38	1.84	0.2477	0.08	16.5	0.4	4.1	13.6	49	145.5	434.9	0	3.1	2	35.3	25.8	0	32	7	39	26	10	11	11	1	1835	99.96	7.96
40	6700585.26	310582.69	14.21	172.50	2.67	1.08	74.56	7.06	2.46	0.0386	0.74	9.3	2.1	2.15	0.5181	0.12	51.1	0	6.2	17	58.7	422.4	426.3	0	3.7	4.4	50.5	31.4	0	21	5	25	18	3	11	10	2	5561	99.05	7.82
43	6700783.41	309278.21	15.23	349.34	1.55	0.30	86.01	6.11	2.12	0.0473	0.05	0.63	1.45	2.33	0.6199	0.08	57.6	0.8	7.8	14.8	61.9	315.6	105.9	0	4.7	2.1	47.9	33.9	0	20	8	38	29	8	14	10	2	3774	99.45	3.01
60	6700829.87	309894.97	53.12	119.81	4.46	1.03	84.03	7.57	2.94	0.0335	0.19	0.8	1.49	2.31	0.6647	0.15	143	10.8	7.8	23.5	66.1	491.7	115.9	1	4.3	6.7	65	55.3	0	34	6	33	36	11	15	12	5	3695	100.18	1.66
M25	6700777.91	309696.17	42.53	171.74	3.24	3.79	81.94	9.27	3.28	0.0543	0.25	0.68	1.39	2.43	0.6559	0.14	83.9	17.6	9.9	24.4	81	523.3	108.4	0	11	10.3	78	70.9	1.1	47	9	78	82	31	20	11	8	532	100.09	3.86
M21	6700833.23	309728.42	39.49	191.10	2.49	1.05	84.11	7.54	2.68	0.0315	0.2	0.72	1.43	2.33	0.6172	0.15	129	10.8	8	18.1	65.5	374.1	111.3	0.4	7.9	8.1	52.2	55.3	0	32	10	28	46	15	16	11	6	3008	99.81	2.95
M38	6700794.64	309593.9	64.10	100.96	5.02	1.71	70.83	15.61	6.74	0.134	0.77	0.57	1.29	2.46	1.1253	0.35	259.1	49.5	15.9	40	102.3	339.9	93.8	0	18.4	31.7	248.9	129.7	11.9	90	16	34	141	59	40	10	6	966	99.88	10.2
M18	6700810.57	309776.94	59.08	91.55	4.80	0.77	73.56	13.22	6.28	0.2539	0.72	0.79	1.52	2.43	0.8807	0.42	186.3	32.7	12.6	33.4	92.9	496.6	125.1	0.3	15.8	27	145.5	112.5	3.2	81	16	33	108	47	37	9	6	7017	100.07	7.6
N10	6700818.58	310008.07	56.99	86.97	4.54	1.37	75.51	10.96	4.85	0.0711	0.54	0.76	2.4	2.48	0.87	0.26	151.7	28.1	11.9	30.8	84.5	530.5	122.5	0.3	10.8	19.5	332.7	92	0	63	13	24	75	23	28	12	5	12965	98.7	6.61
A70	6700631.42	310612.65	6.53	421.99	1.57	0.22	84.77	5.93	1.53	0.0257	0.24	2.92	1.69	2.32	0.3597	0.07	27.8	0	6.7	13.2	59	276.4	184.7	0.3	4.3	0.2	14.5	21	0	21	8	78	8	0	8	11	3	7527	99.86	3.29
A64	6700567.54	309994.09	94.71	17.91	6.18	0.14	81.62	8.7	2.75	0.0282	0.34	0.96	2.07	2.56	0.4903	0.1	157.5	10.4	7.8	18.2	73.8	308.4	127.2	0.3	4	8.2	44.3	38.5	0	36	10	33	36	11	19	11	3	8694	99.62	4.12
A77	6700746.01	310263.99	24.62	156.01	2.64	0.44	82.49	8.26	2.28	0.0291	0.23	0.91	1.98	2.66	0.5637	0.09	52.1	6.2	8.8	22.5	73.9	604.4	134.6	0.7	7.4	5.6	57.6	39.7	0	27	7	85	46	12	12	11	1	6107	99.49	2.29
A57	6700586.37	309725.08	24.45	282.37	1.73	0.37	85.79	7.07	1.61	0.0235	0.04	0.71	1.68	2.61	0.3243	0.08	71.5	1.9	5.2	13.7	68.5	207.4	123.7	0	6.5	2.8	42.1	21.5	0	26	7	107	34	8	13	11	4	3946	99.94	2.46
A47	6700712.09	309275.34	72.56	56.68	5.46	7.32	62.27	15.98	7.71	0.0853	1.4	0.88	5.26	2.03	0.975	0.57	640.2	43.9	11.4	32.5	82.9	241.3	105.5	0	12.9	21.5	89.1	35.3	0	112	12	15	41	15	50	11	7	10449	97.16	17.01
A41	6700733.66	309394.3	79.64	34.49	5.97	17.42	69.3	15.9	7.16	0.2224	0.81	0.68	2.17	2.22	1.0598	0.4	384.1	52.7	15	39.9	93.6	296.1	93.7	0	15.9	34.5	185.7	134.4	9.3	71	15	38	119	41	36	10	5	7034	99.92	12.64
A05	6700703.19	309669.79	39.21	205.92	2.41	0.75	86.02	6.47	1.65	0.0221	0	0.68	1.5	2.24	0.3594	0.07	62.5	0	5	14	64.7	302.7	120.2	0	6.9	1.5	31.3	23.3	0	30	7	54	24	8	9	10	4	6316	99.01	1.71
B70	6700692.78	309920.41	17.77	239.46	1.93	0.40	86.92	6.24	1.56	0.0279	0.06	0.72	1.64	2.39	0.4098	0.06	39.6	0	5.4	11.3	61.2	344.8	115.2	0.6	2.5	1.4	26	26.5	0	25	8	66	24	6	4	11	7	4111	100.03	1.23
B65	6700527.4	310274.92	58.45	78.12	4.71	0.49	77.51	8.76	2.76	0.034	0.57	3.42	2.06	2.67	0.4819	0.11	121	6.9	8	19.4	76.9	450.6	244.4	0	6.6	7.4	51.2	36	0	38	11	34	24	11	14	12	7	6787	98.38	5.99
B61	6700635.68	310174.59	27.22	198.87	2.23	0.23	84.64	6.69	2.15	0.0322	0.17	0.85	1.68	2.32	0.5108	0.08	62.3	0	7.7	18.4	61.7	553.8	121.4	1.4	6.5	4.1	50.9	33.4	0	25	7	38	24	5	8	10	3	4520	99.12	1.81
B57	6700677.62	310329.15	22.99	182.64	2.36	0.12	84.7	6.6	2.27	0.0389	0.12	0.95	1.67	2.45	0.6891	0.07	34.1	0	9.7	24.1	64.7	1062	130	0.8	6.8	0.4	24.3	31.3	0	23	7	55	27	8	8	11	3	3414	99.56	1.48
B50	6700829.03	310523.9	35.09	138.05	2.95	0.25	83.47	7.64	2.54	0.0323	0.28	0.96	1.72	2.43	0.5738	0.12	73.5	3.1	8.8	21.8	68.6	545.5	130.7	0	8.1	4.7	40.7	35.2	0	34	8	34	27	4	15	11	0	7123	99.77	2.83
B37	6700846.15	310633.62	0.08	418.70	1.55	0.10	84.49	5.12	1.38	0.0353	0.19	3.19	1.5	2.29	0.4637	0.05	7.4	0	6.3	12.2	54.2	203.1	182.2	1.5	4.9	0	26.3	15.1	0	16	5	62	24	6	6	10	6	4679	98.71	2.92
B36	6700758.44	310619.89	23.57	218.21	2.35	0.37	84.4	6.24	2.11	0.033	0.27	1.71	1.9	2.23	0.5038	0.1	37.7	0	8.3	17.1	59.6	447	142.8	0	10	2.4	60.8	29.7	0	22	6	82	13	5	11	11	2	11281	99.5	2.83
B31	6700671.51	310481.21	16.17	167.69	2.63	0.29	80.91	7.81	2.4	0.0366	0.24	1.46	1.95	2.67	0.6533	0.09	43.6	0	9.1	24	72.1	924.9	161.9	0	9.1	3.6	31.1	39.3	0	25	11	45	50	20	11	10	7	8368	98.22	2.14
3	6700535.09	308185.15	78.465993	59.80	4.36278128	3.288797533	63.62	16.7	9.22	0.1159	1.21	0.81	1.53	2.18	1.0679	0.73	1009.3	89.2	13928	41.1	96.4	300.2	111.8	3.1	15.7	464	178.6	130.3	40.3	122	13	19	505	274	47	34	3	13928	97.21	14.25
7	6700618.81	308257.29	67.11124	67.20	4.25496832	5.058365759	60.45	19.45	10.26	0.2675	1.32	0.77	1.7	2.22	1.1285	0.87	1085.9	102.6	6714	46.8	113.2	196.2	105.7	7.2	24.6	1088	218.1	161	59.3	115	14	28	682	442	44	34	3	6714	98.47	16.48
11	6700588.36	308319.04	17.715656	150.75	2.53276203	0.413436693	85.58	6.53	1.54	0.0178	0.12	0.67	1.25	2.51	0.2293	0.0038	68.5	15.4	5.1	11.9	69.1	145.9	119	2.9	6.8	128	109.4	21.8	1.6	24	6	1	0	0	5	39	2	1848	98.5	1.44
23	6700693.86	308378.82	63.543271	72.00	4.21313462	4.021937843	69.42	13.98	7.9	0.053	1.09	1.12	1.14	2	1.0371	0.0367	1454.7	124.6																						

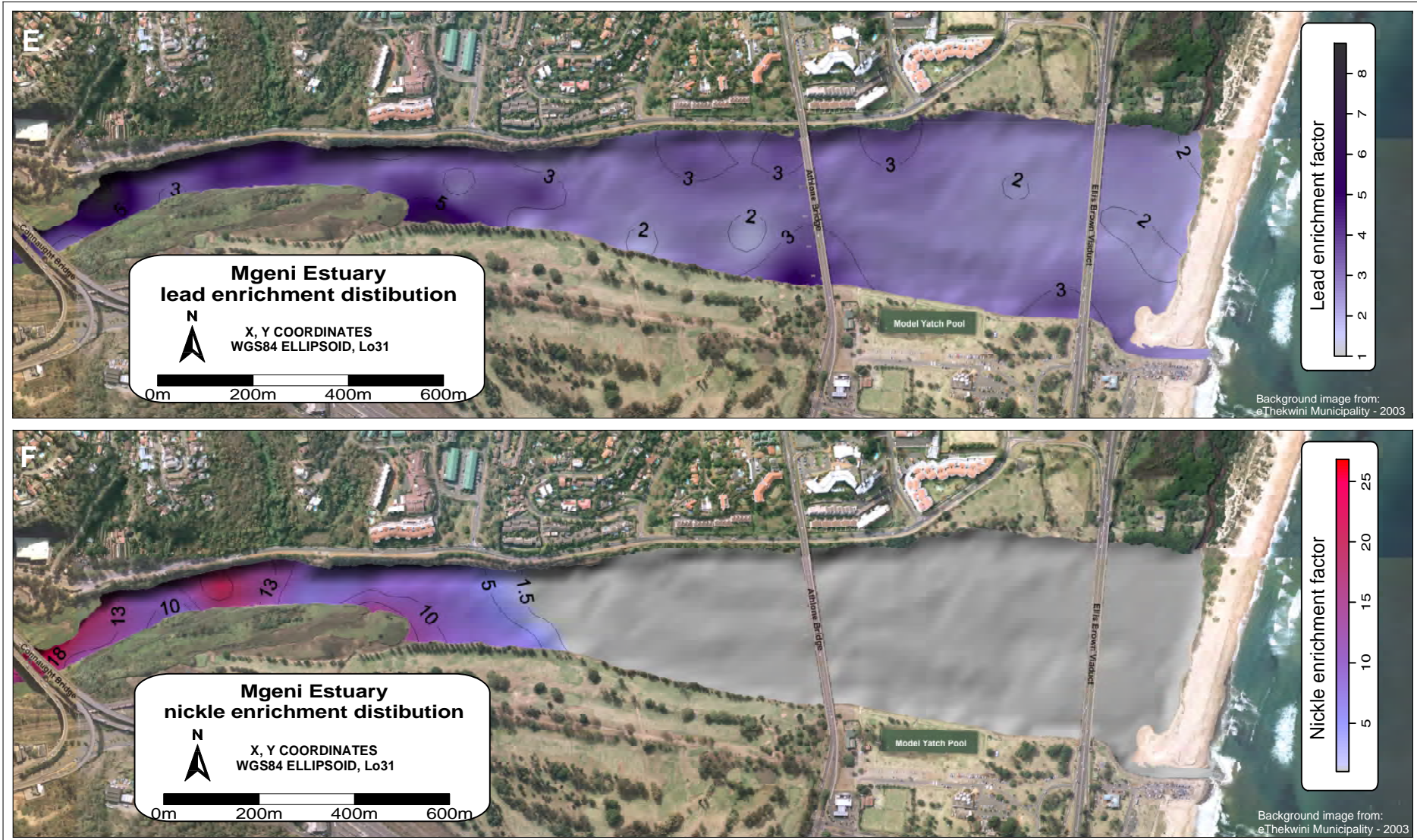


Figure 7. E) The distribution of lead enrichment in the Mgeni Estuary. Lead enrichment is found throughout the estuary, with the highest concentrations being found towards the head of the estuary and in the areas adjacent to storm water drains. F) The Nickel distribution. Nickel enrichment occurs only at the head of the estuary where enrichment factors are as high as 18.

Sample	lat (UTM36s)	long (UTM36s)	ZN	Cu	Cr	V	As	Sn	Pb	Co	Ni
B37	6700846	310634	0.27	0.00	0.90	0.33	1.33	3.81	1.86	6.05	0.00
3	6700650	309355	1.39	0.06	0.32	0.30	2.03	3.80	2.89	5.84	0.01
A70	6700631	310613	0.87	0.00	0.43	0.39	1.54	3.62	2.10	6.58	0.02
B57	6700678	310329	0.96	0.00	0.65	0.52	1.38	3.25	2.07	4.17	0.03
B70	6700693	309920	1.18	0.00	0.73	0.47	0.73	3.44	2.38	5.29	0.11
A05	6700703	309670	1.80	0.00	0.85	0.40	1.58	3.02	2.76	4.17	0.11
43	6700783	309278	1.76	0.08	1.37	0.61	2.61	3.20	1.95	3.11	0.17
33	6700486	310383	0.57	0.04	1.14	0.52	2.31	3.96	3.51	3.60	0.18
B36	6700758	310620	1.13	0.00	1.71	0.52	2.01	3.44	2.09	6.57	0.19
A57	6700586	309725	1.88	0.16	1.04	0.34	2.09	3.04	2.19	7.57	0.20
15	6700582	309610	1.62	0.04	0.96	0.41	2.20	3.19	3.00	5.64	0.21
B31	6700672	310481	1.04	0.00	0.70	0.55	1.60	2.50	1.90	2.88	0.23
11	6700607	309509	2.77	0.51	1.33	0.52	1.51	2.84	1.65	2.98	0.29
B61	6700636	310175	1.74	0.00	1.33	0.55	1.36	2.92	2.22	2.84	0.30
B50	6700829	310524	1.79	0.24	0.93	0.51	2.24	2.81	2.64	2.23	0.30
40	6700585	310583	1.35	0.00	1.25	0.49	1.77	2.77	1.77	1.77	0.31
24	6700549	309816	2.22	0.32	0.89	0.58	3.96	3.11	5.34	5.07	0.32
A77	6700746	310264	1.18	0.45	1.22	0.53	1.65	2.60	1.94	5.15	0.33
B65	6700527	310275	2.57	0.47	1.02	0.45	1.82	2.67	2.58	1.94	0.42
60	6700830	309895	3.52	0.85	1.50	0.81	2.26	3.09	2.67	2.18	0.44
A64	6700568	309994	3.37	0.71	0.89	0.49	2.49	2.47	2.46	1.90	0.47
M21	6700833	309728	3.19	0.85	1.21	0.81	2.42	2.85	2.52	1.86	0.53
M25	6700778	309696	1.69	1.13	1.47	0.84	2.46	2.32	3.01	4.21	0.55
20	6700629	309729	4.89	1.43	1.39	0.68	1.02	2.34	1.19	1.25	0.66
A47	6700712	309275	7.47	1.63	0.98	0.24	3.56	1.34	4.16	0.47	0.66
N10	6700819	310008	2.58	1.52	5.32	0.93	2.91	2.14	3.42	1.09	0.88
M38	6700795	309594	3.09	1.88	2.79	0.92	2.92	1.25	3.43	1.09	1.00
M18	6700811	309777	2.63	1.47	1.93	0.94	3.19	1.33	3.64	1.25	1.01
A41	6700734	309394	4.50	1.97	2.05	0.93	2.58	1.23	2.65	1.19	1.07
117_(03/02/06)	6700768	309198	1.50	1.09	2.29	0.39	1.39	12.61	3.32	0.52	4.14
137_(03/02/06)	6700688	308538	1.64	1.37	0.99	0.64	1.75	7.23	2.73	0.26	5.55
125_(03/02/06)	6700741	308785	4.82	1.85	1.81	0.68	2.07	9.14	3.48	0.39	6.17
128	6700757	308886	4.14	1.77	2.61	0.57	1.72	8.56	3.17	0.21	7.04
149	6700792	309108	4.07	1.98	3.67	0.73	2.49	6.27	3.66	0.32	7.61
114_(03/02/06)	6700642	309261	1.38	1.25	2.83	0.34	1.03	10.59	1.83	0.09	7.86
121_(03/02/06)	6700709	309106	4.36	1.67	1.90	0.60	1.98	10.45	2.24	0.29	8.01
123_(03/02/06)	6700739	308977	8.19	2.78	1.70	0.82	2.97	7.73	3.73	0.48	9.16
147	6700791	308983	3.07	1.40	2.39	0.59	1.51	7.77	2.46	0.25	9.18
142_(03/02/06)	6700651	308755	2.87	2.41	1.55	0.93	2.29	5.70	3.08	0.29	9.49
27	6700736	308439	8.09	2.76	2.16	0.83	3.01	5.01	3.74	0.43	9.53
11	6700588	308319	1.95	1.40	2.94	0.37	0.87	11.66	2.18	0.08	9.68
130_(03/02/06)	6700692	308491	3.08	2.08	1.70	0.88	2.40	4.25	3.04	0.54	10.37
148_(03/02/06)	6700644	309075	5.75	4.14	1.87	0.94	6.14	8.01	8.50	0.47	10.66
135_(03/02/06)	6700595	308420	3.21	2.29	1.67	0.91	1.99	3.42	2.70	0.58	11.28
119	6700771	308748	10.62	3.61	1.92	0.79	3.59	4.82	4.92	0.40	12.45
3	6700535	308185	9.67	2.73	1.61	0.74	2.75	3.41	3.73	0.49	13.72
38	6700787	308653	5.90	3.26	3.81	1.14	2.32	6.06	3.59	0.75	14.38
23	6700694	308379	19.39	5.30	3.57	1.03	6.68	8.66	8.97	0.57	16.40
144_(03/02/06)	6700681	308940	3.11	1.97	1.50	0.91	2.38	7.71	3.17	0.58	19.28
109	6700750	308617	7.41	3.22	1.77	0.76	3.27	6.41	4.63	0.46	22.29
7	6700619	308257	12.12	3.65	2.29	1.06	3.00	3.97	4.09	0.84	27.63

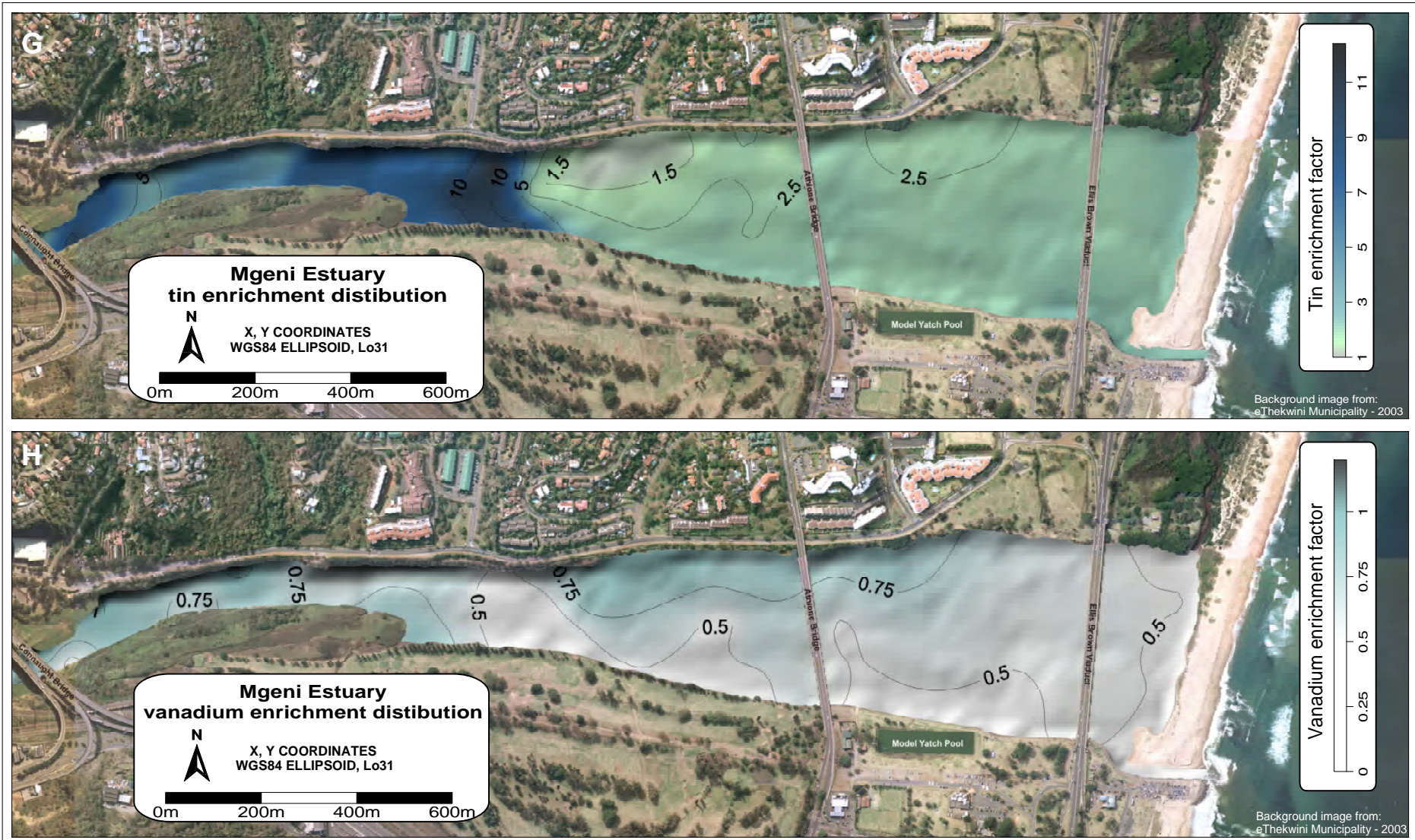
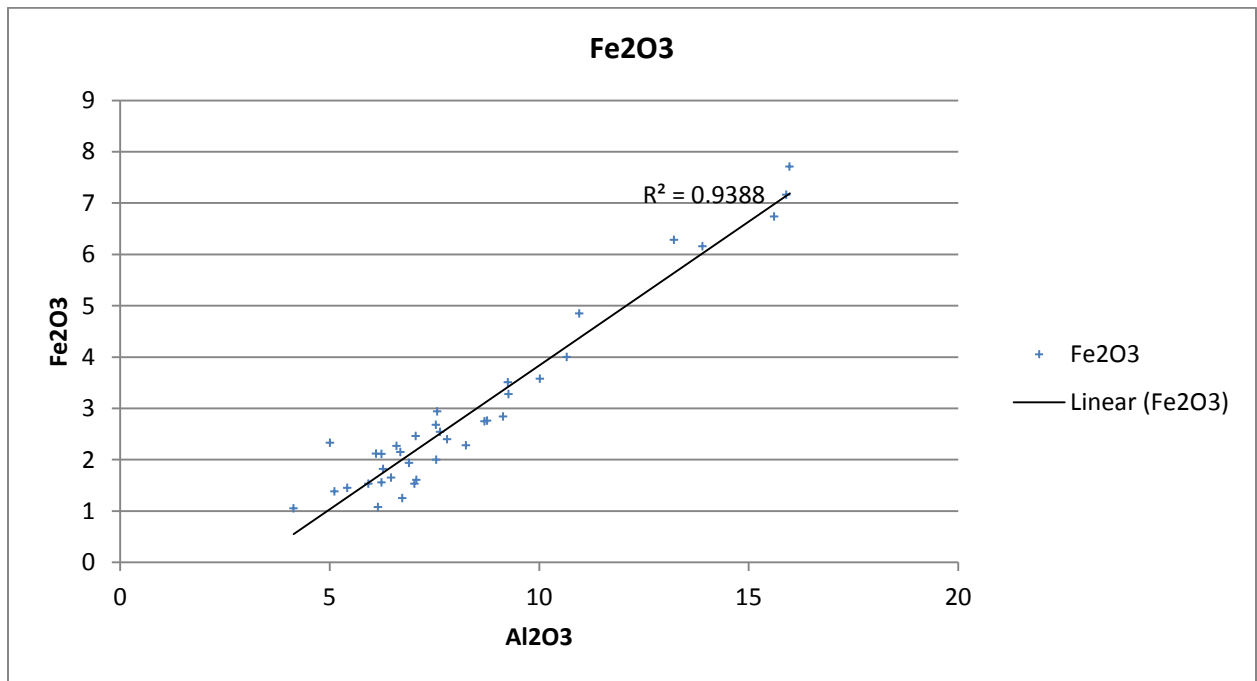
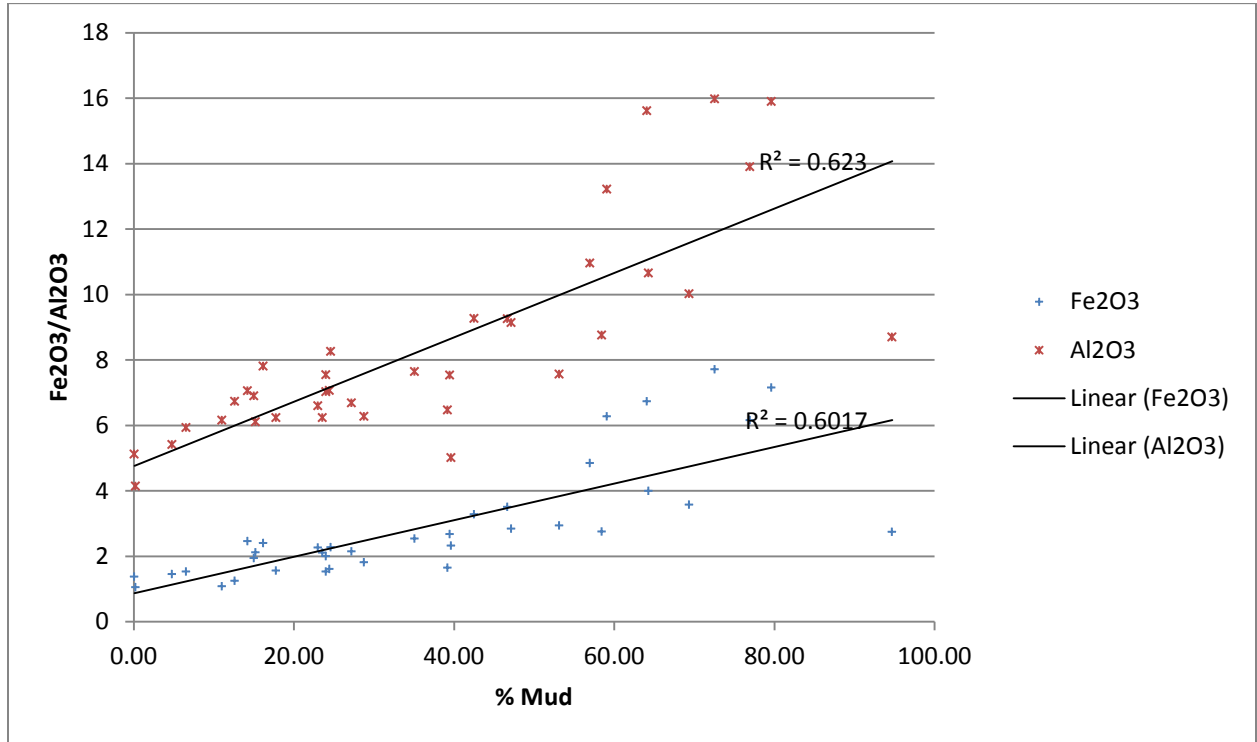
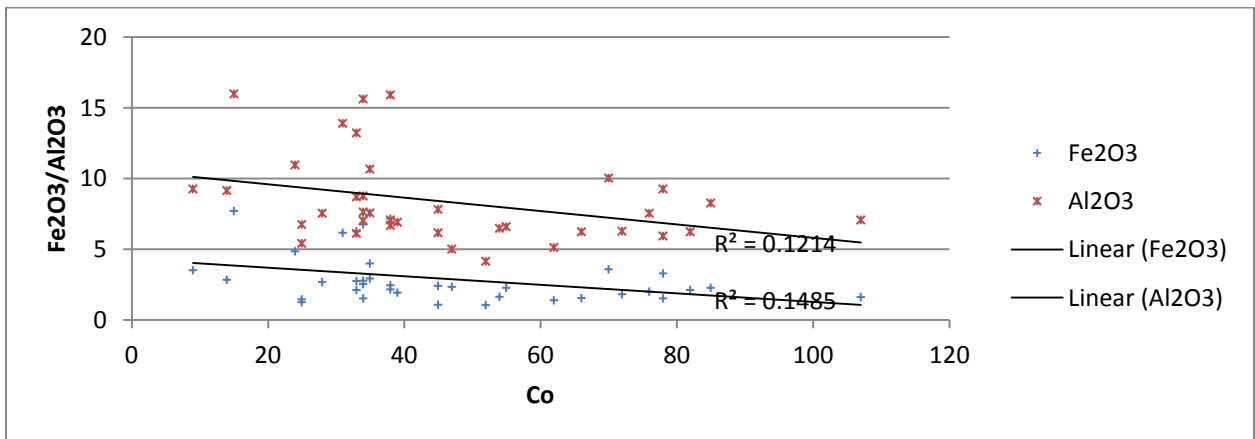
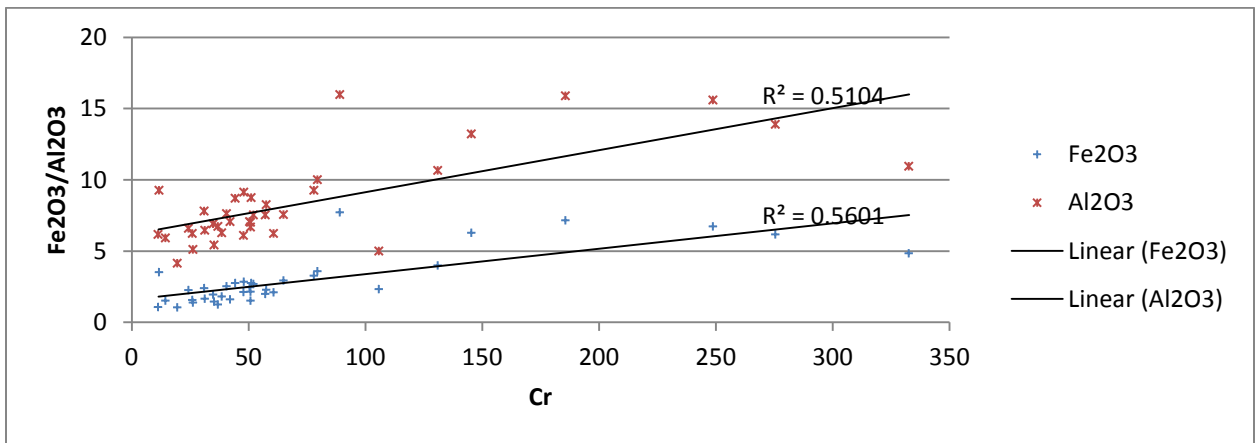
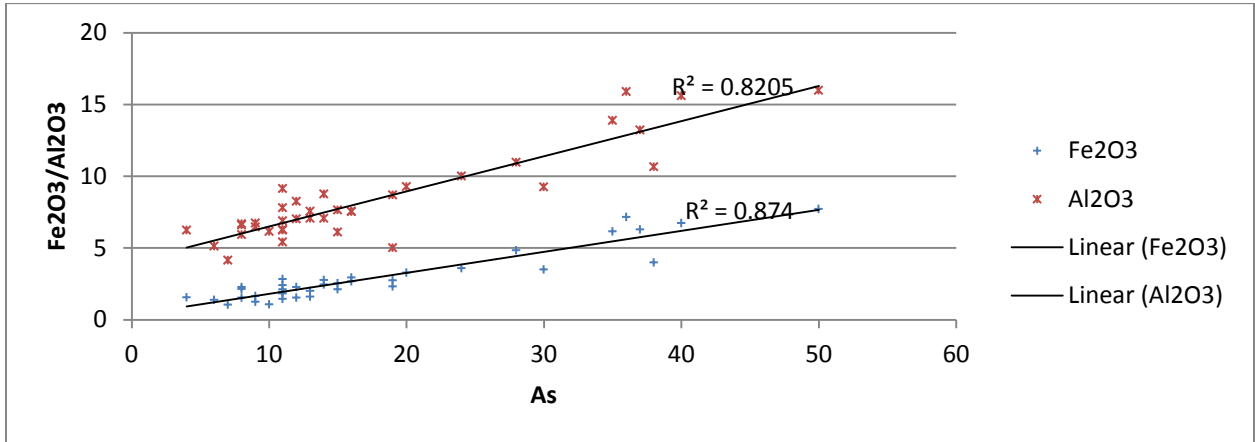
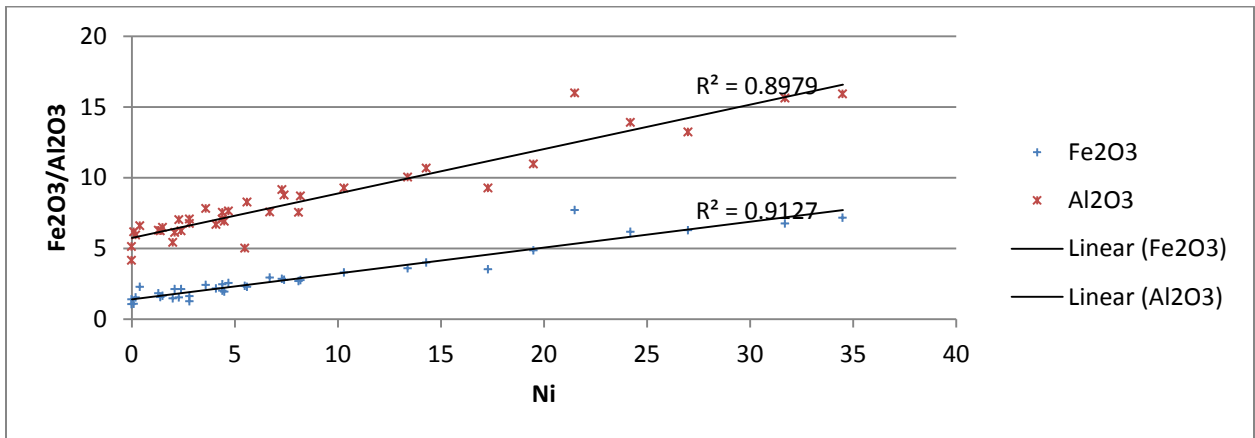
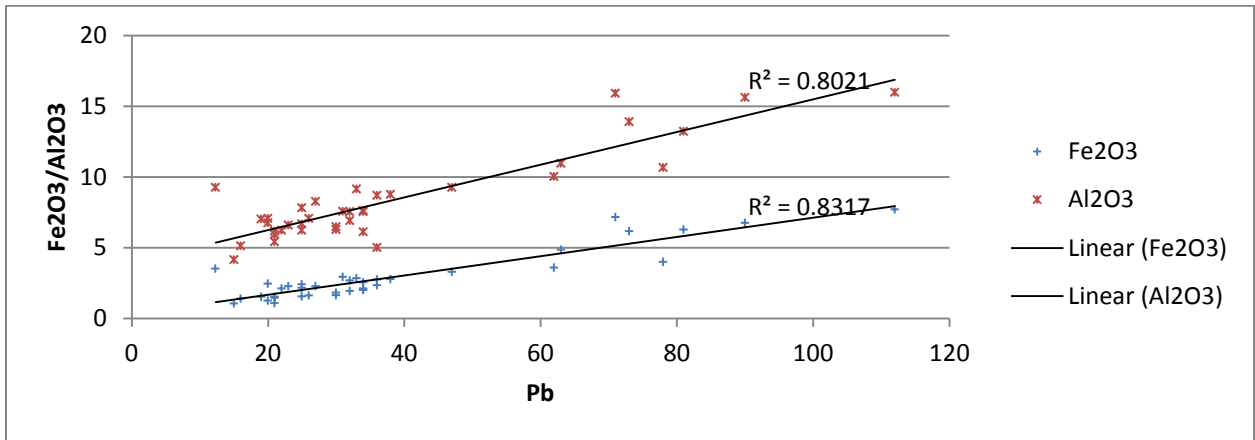
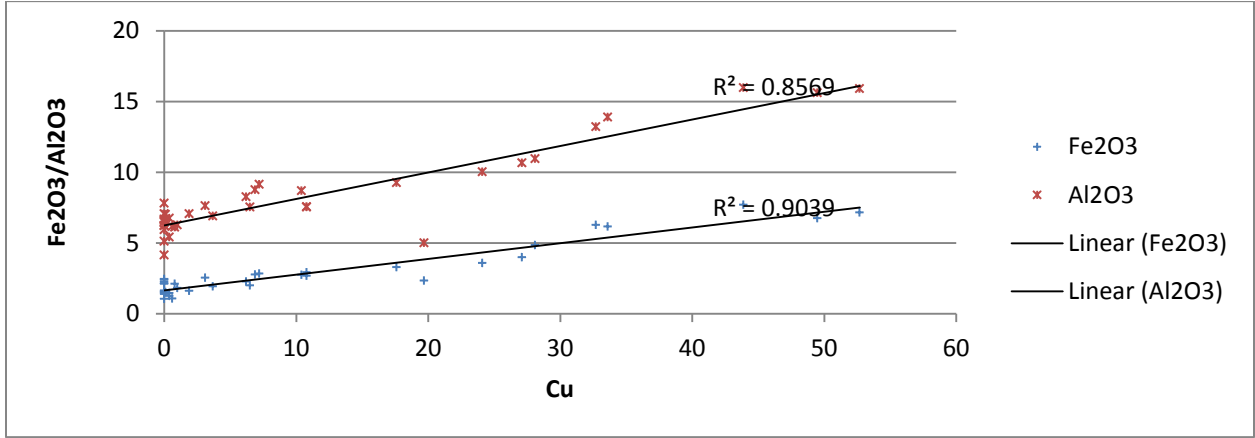
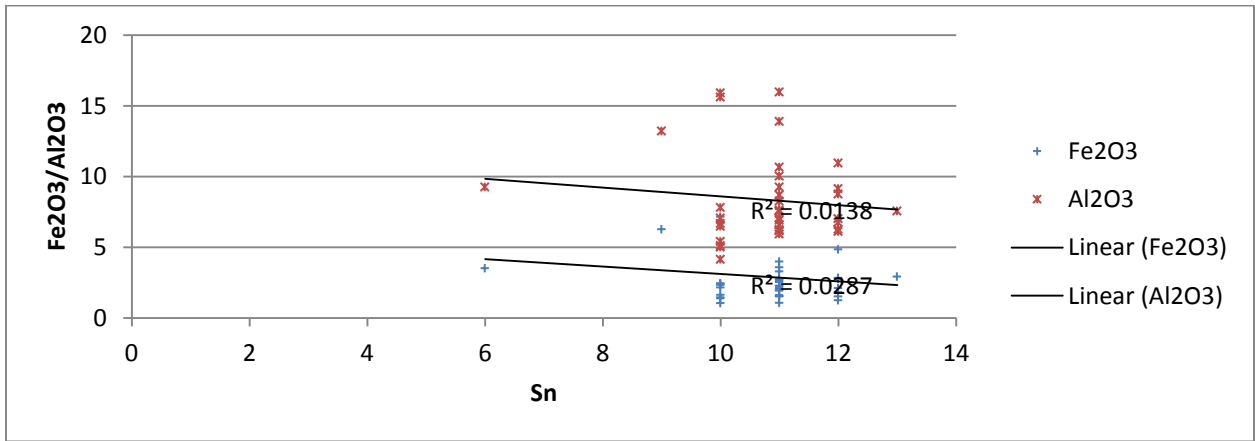
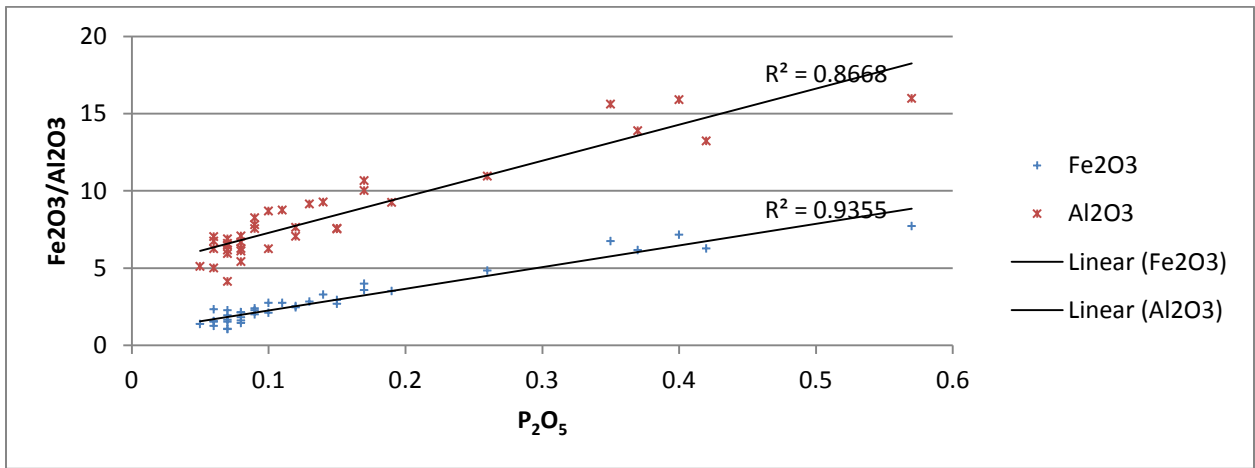
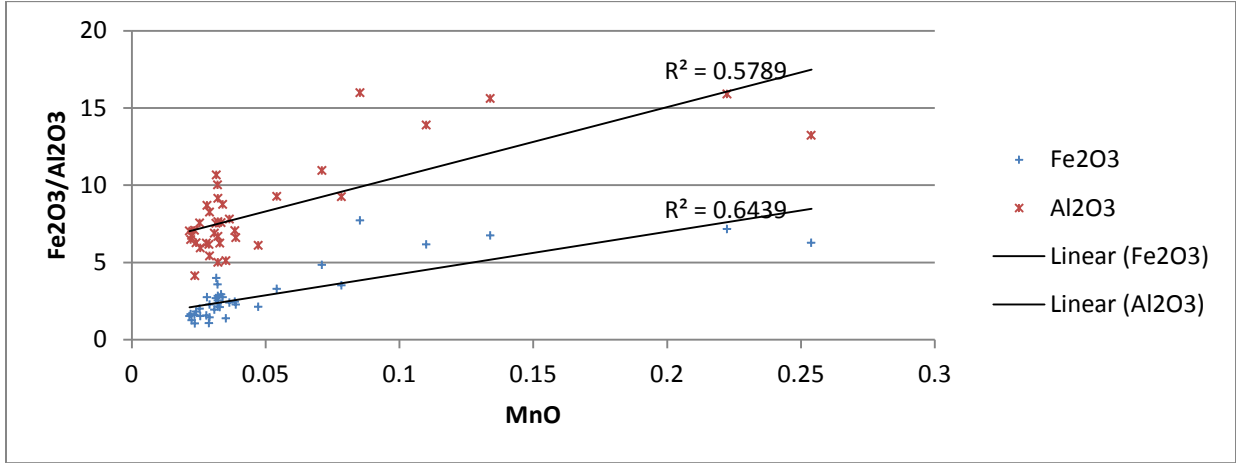


Figure 7. G) The enrichment distribution of tin throughout the estuary. The highest concentration of tin is found towards the head of the estuary. There is an isolated pocket of no concentration against the northern bank. H) The vanadium enrichment within the estuary. There is little to no vanadium enrichment within the Mgeni Estuary.









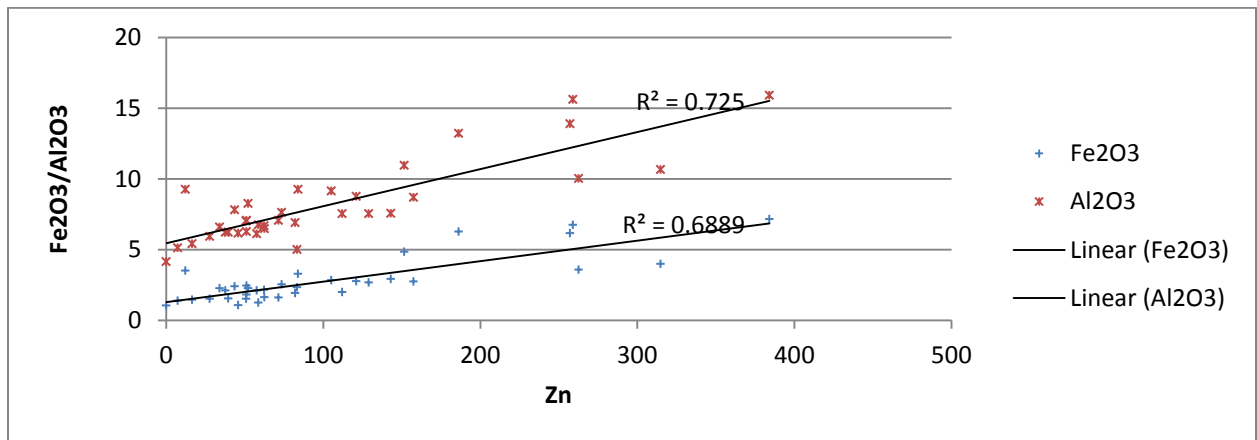
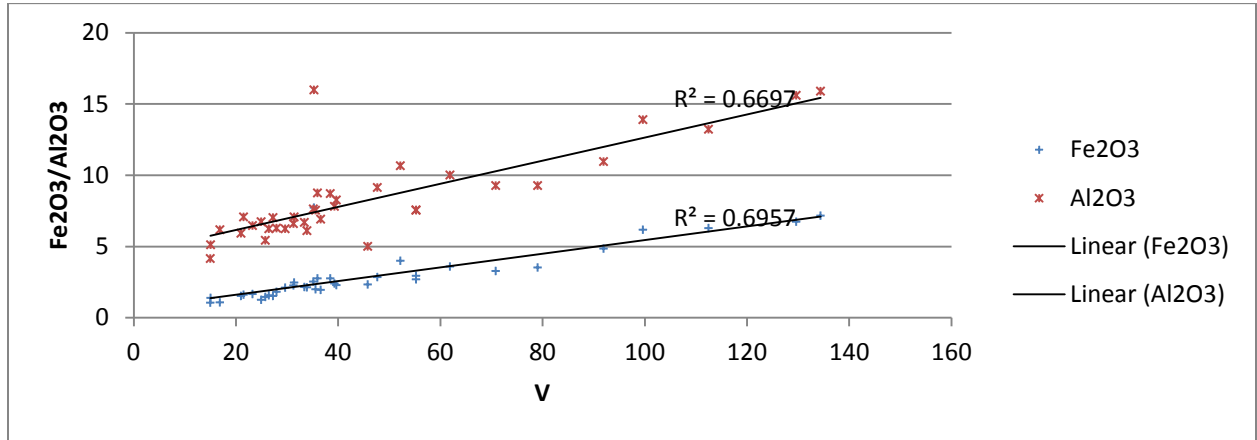
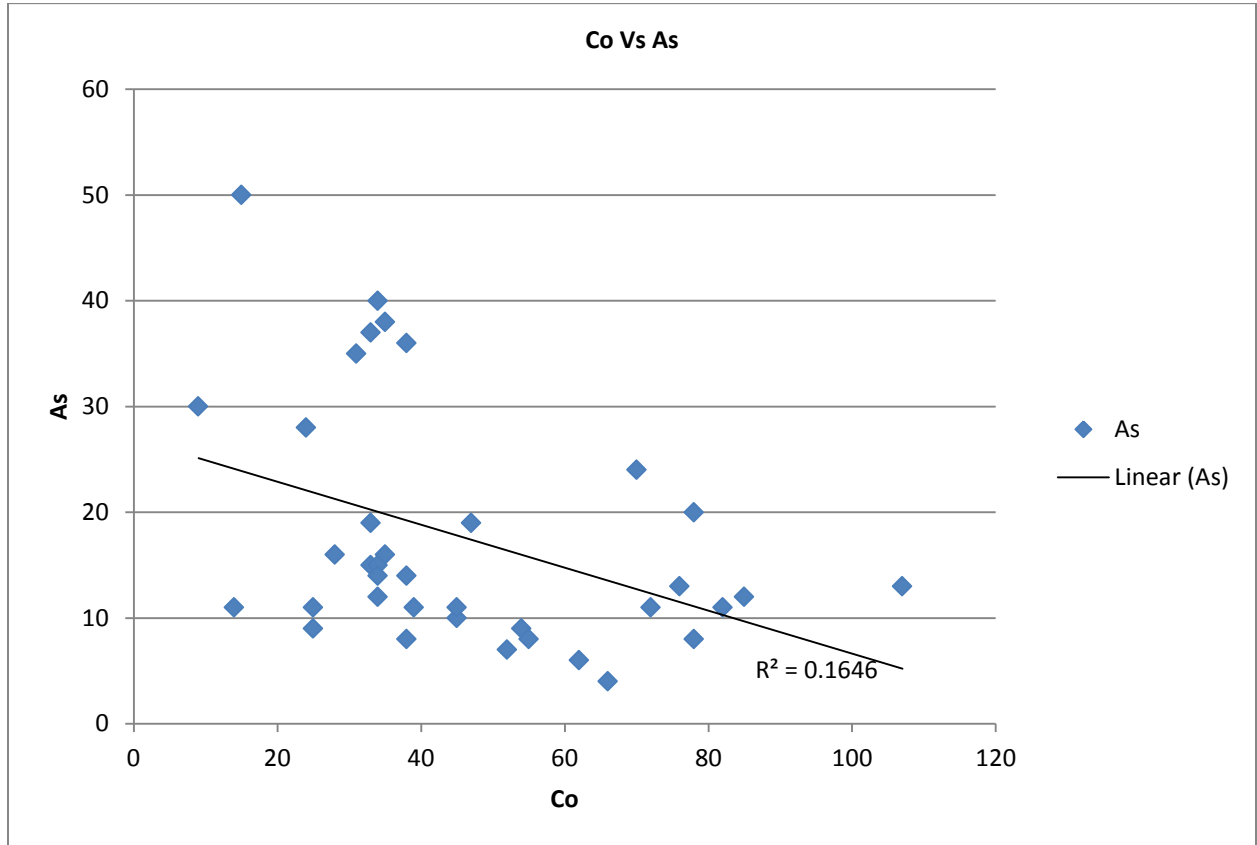
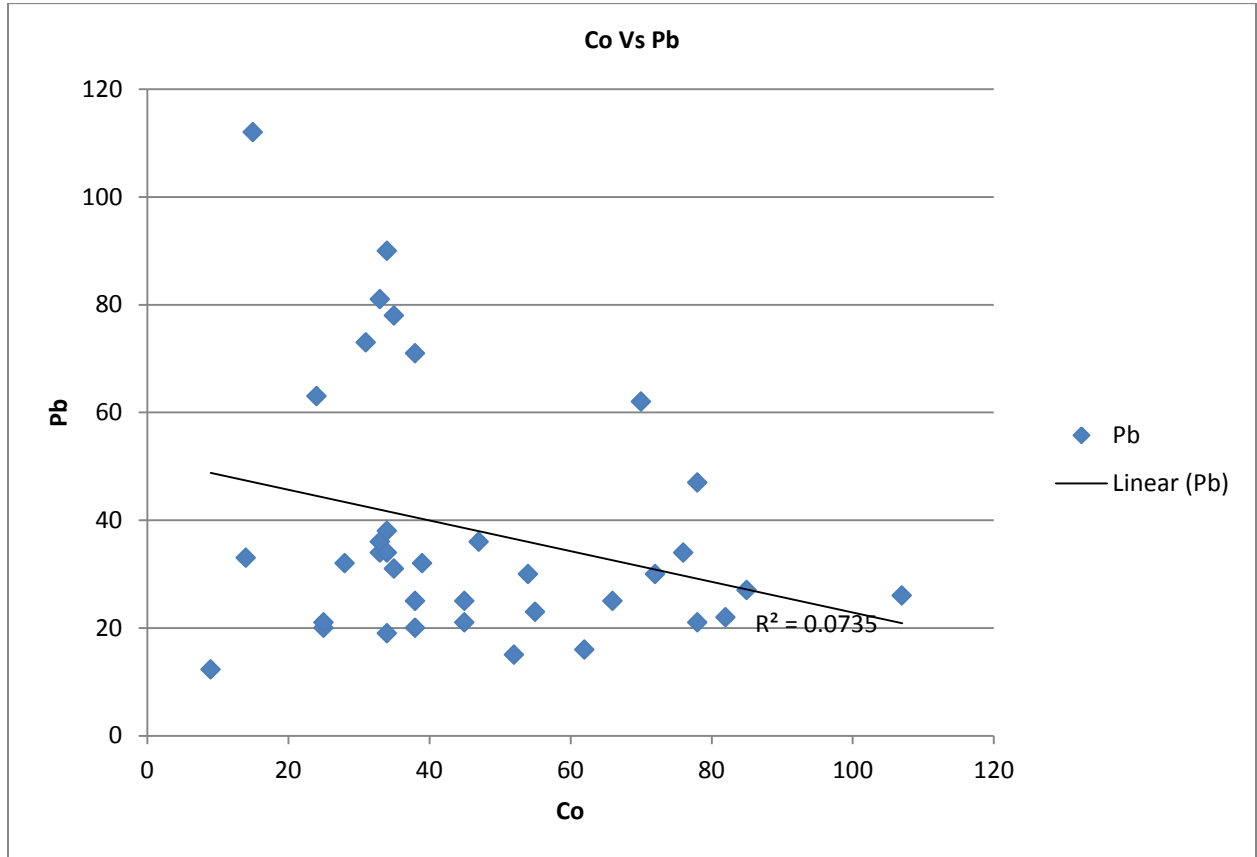
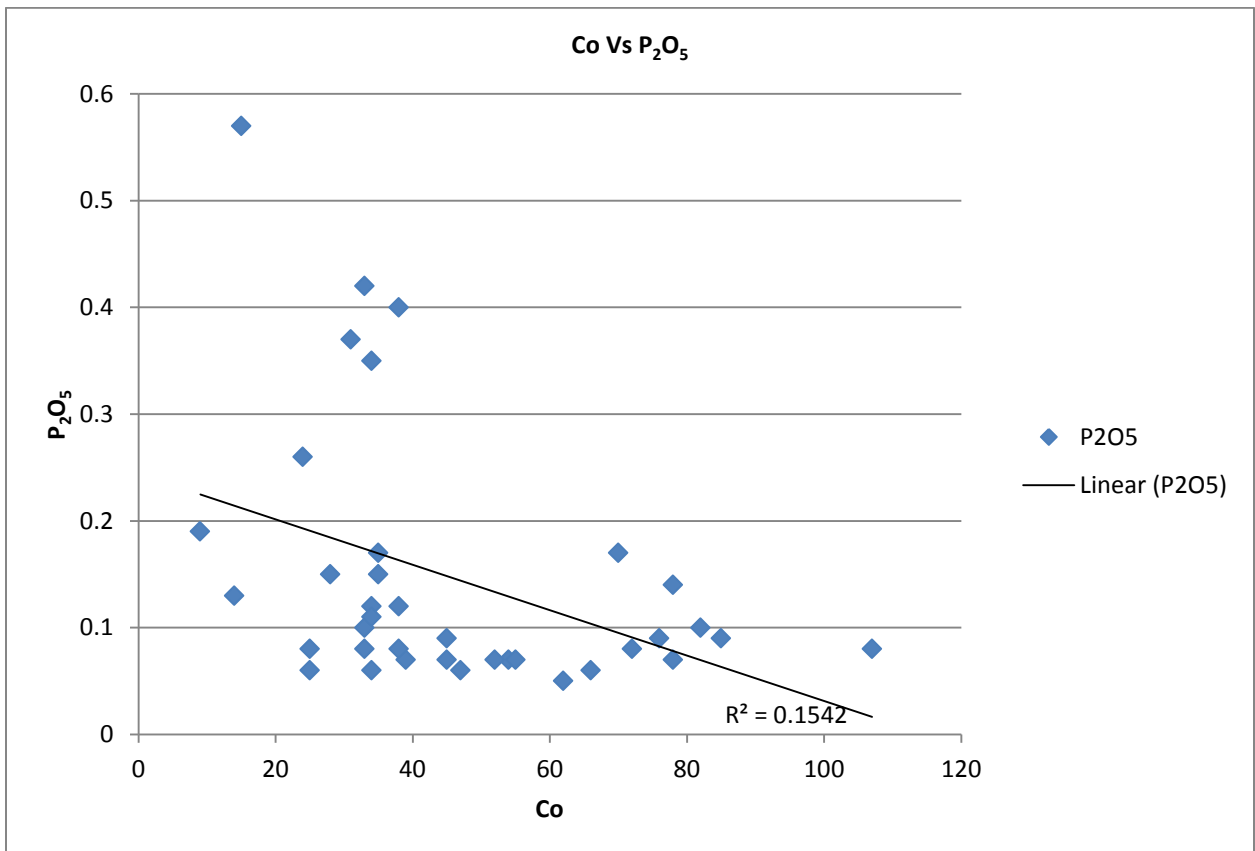
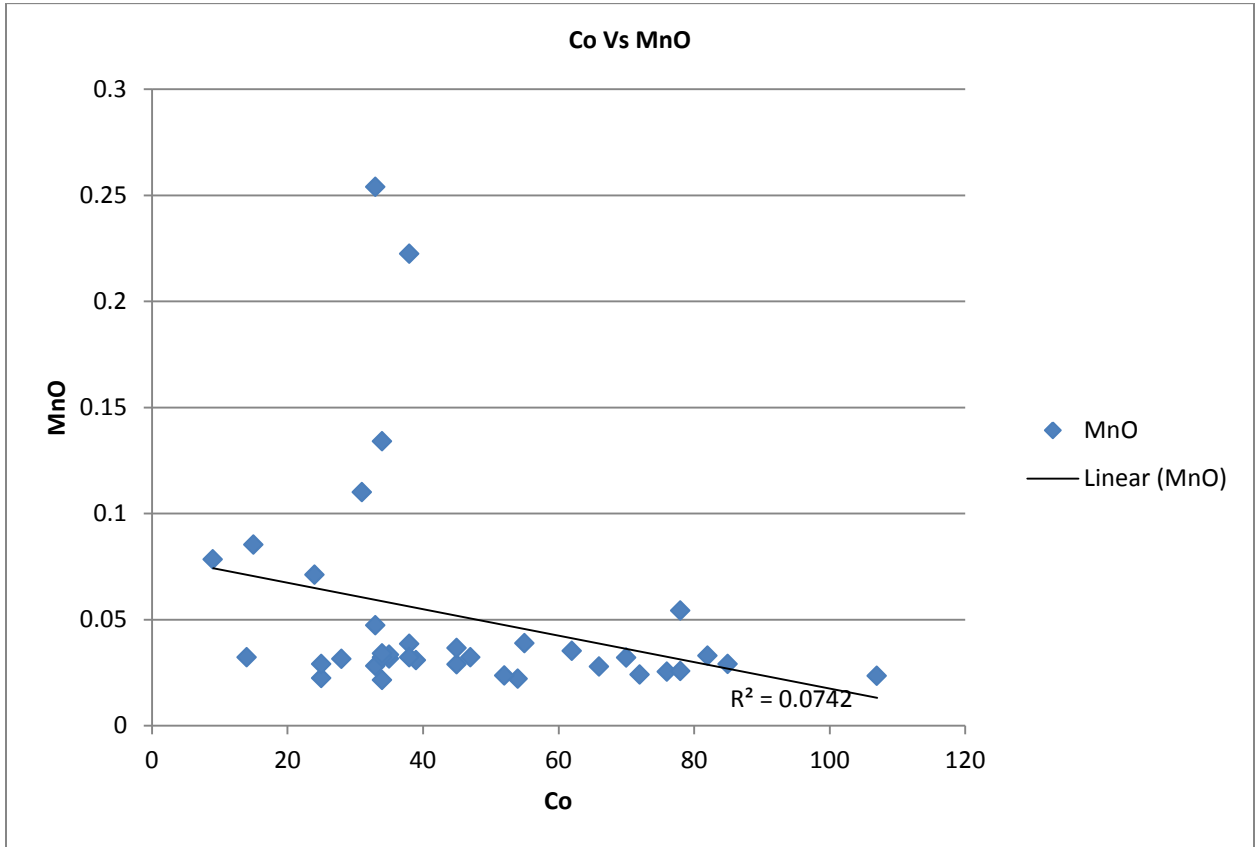


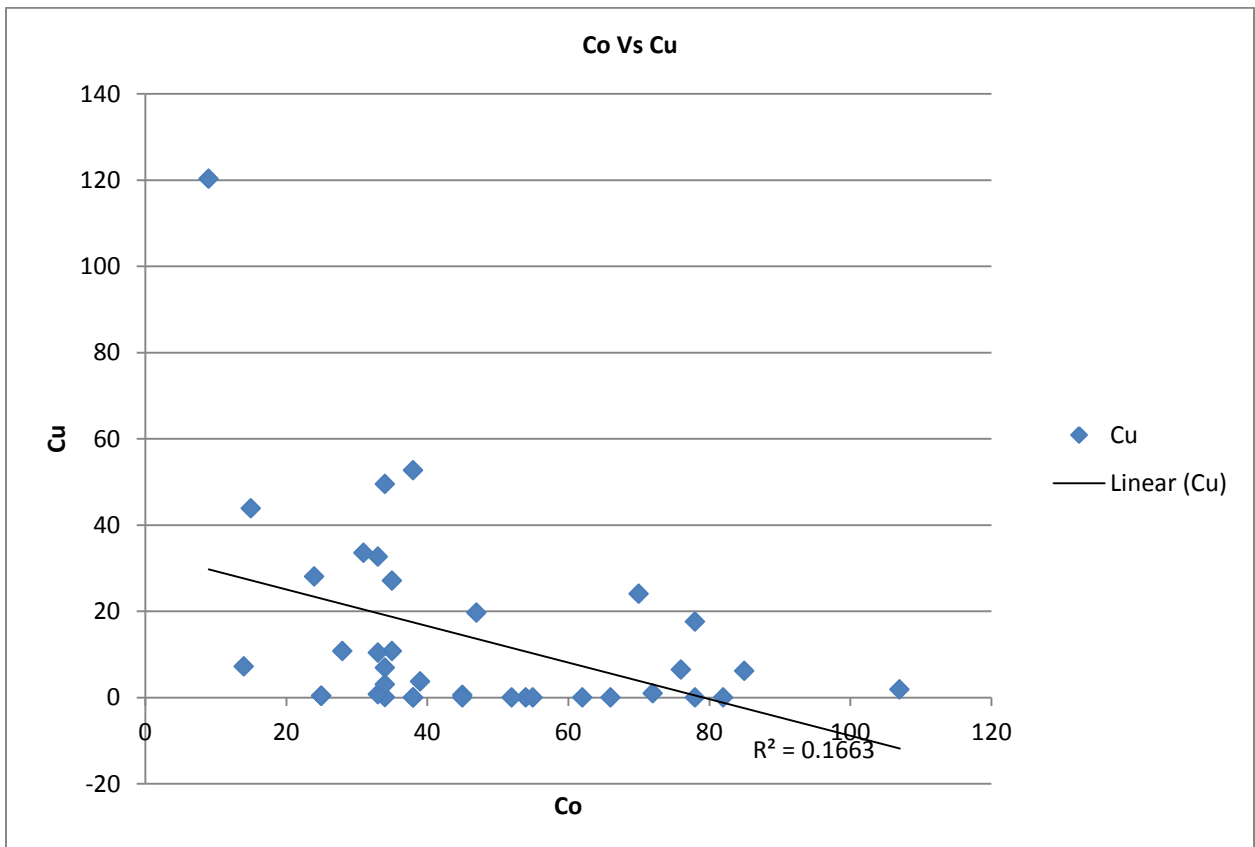
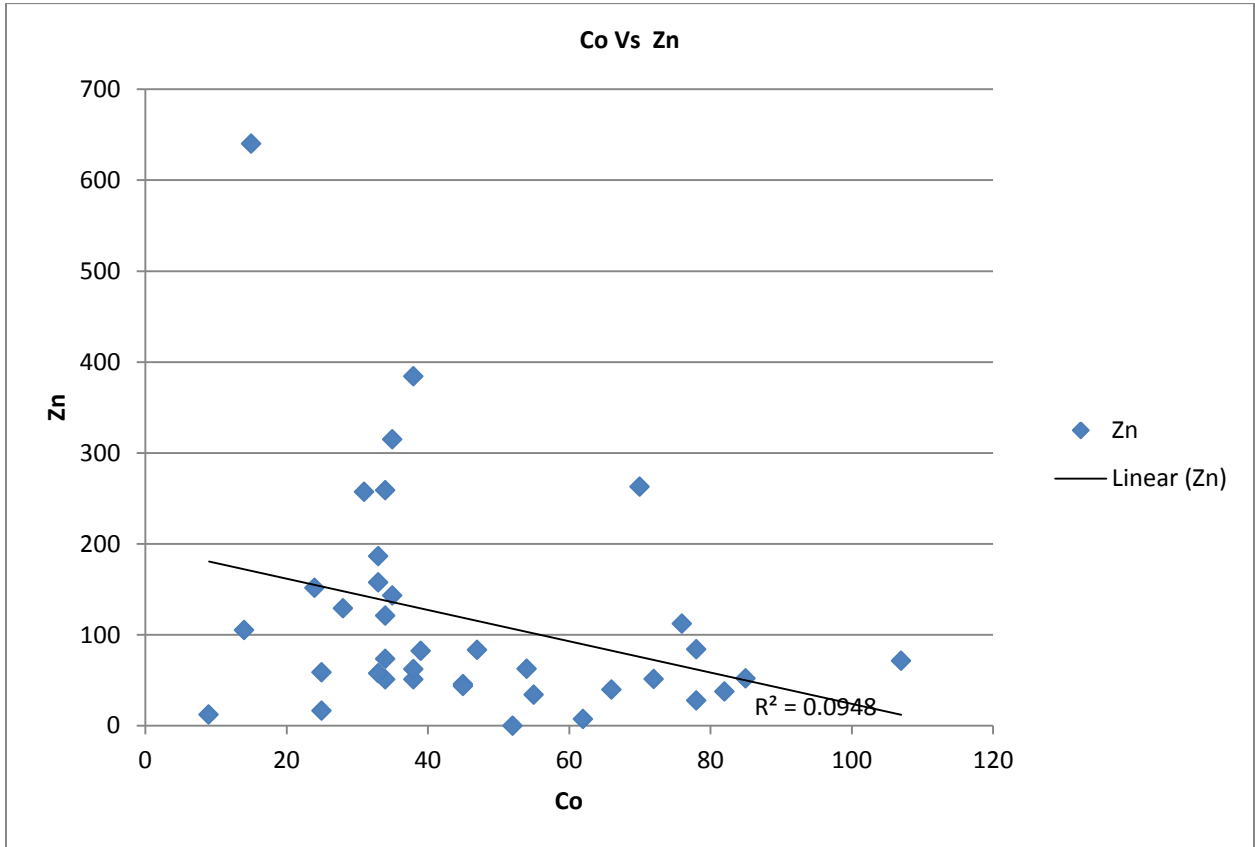


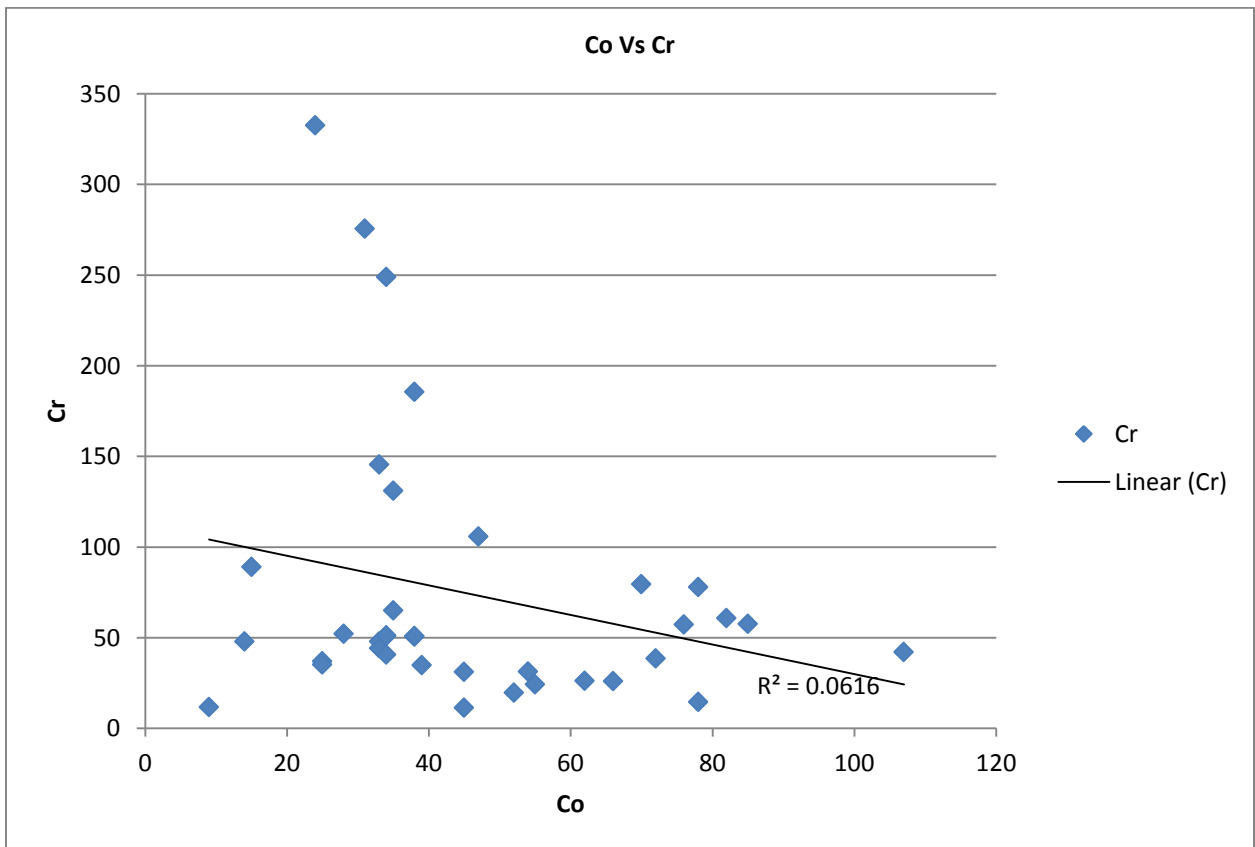
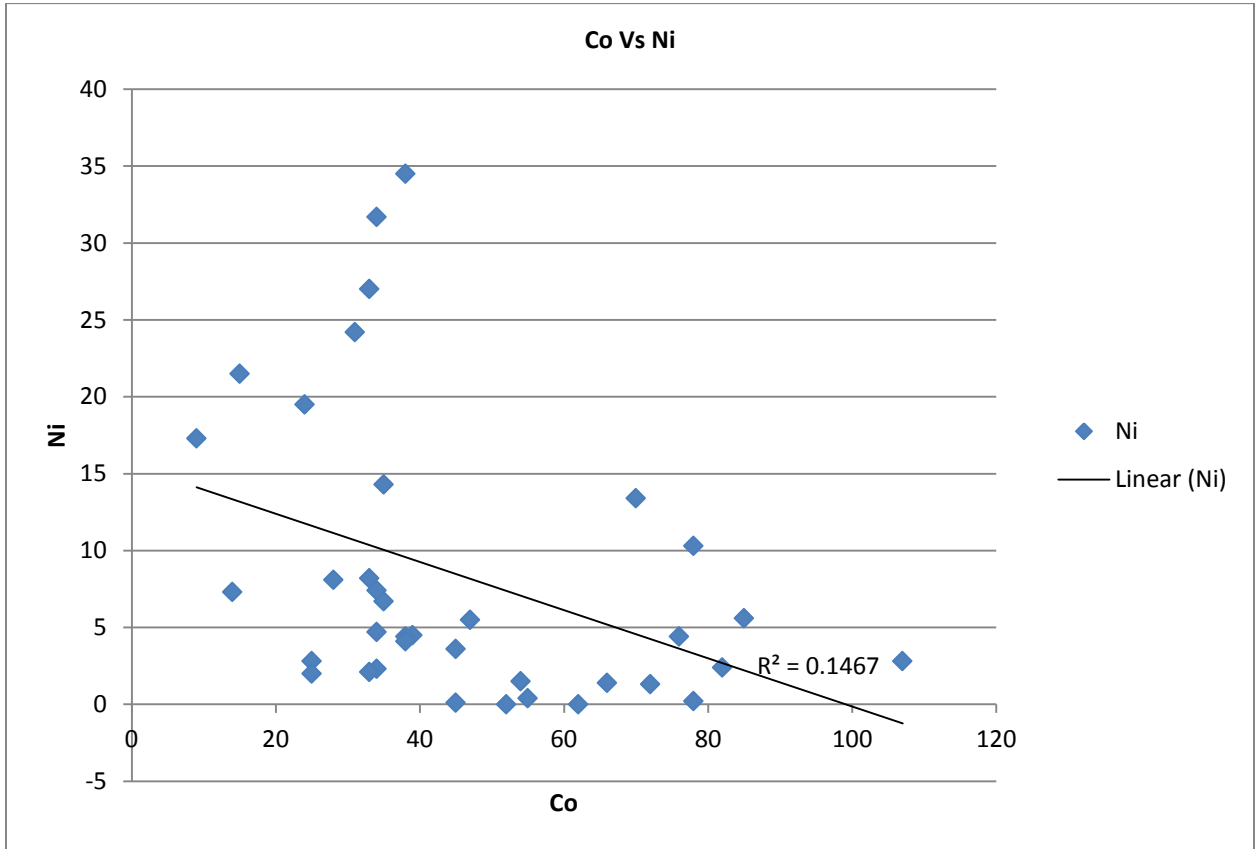
Figure 7. 1) Zinc enrichment distribution in the Mgeni Estuary. The highest concentrations of zinc are found in the organic rich muds towards Connaught Bridge depleting east-wards towards the tidal inlet, where the enrichment is diluted with cleaner and coarser marine sediments. Zinc pollution is derived predominantly from the galvanizing of iron and steel.

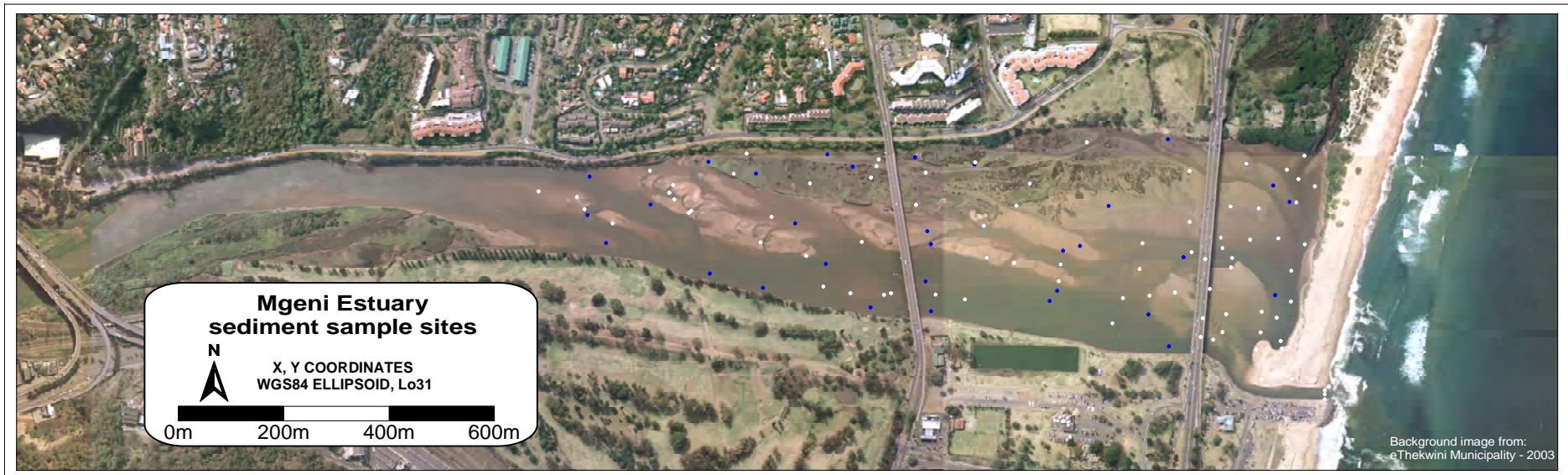












Appendix A3. Shows the distribution of sediment samples tested for carbonate (white) and organics (blue).